

**INHIBITION OF GALVANIC CORROSION BY  
PHENYLTHIOUREA UNDER FLOWING  
CONDITIONS IN HYDROCHLORIC ACID  
SOLUTION**

**A Thesis**

**Submitted to the College of Engineering  
of Nahrain University in Partial Fulfillment of the  
Requirements for the Degree of Doctor of Philosophy in  
Chemical Engineering**

**by  
SHAKER SALEH BAHAR AL-KELABY**

**(B.Sc. 2000)**

**(M.Sc 2003)**

Rabii Al-awal  
April

1428  
2007

## Certification

I certify that this thesis entitled "INHIBITION OF GALVANIC CORROSION BY PHENYLTHIOUREA UNDER FLOWING CONDITIONS IN HYDROCHLORIC ACID SOLUTION" was prepared by **SHAKER SALEH BAHAR**, under my supervision at Al-Nahrain University, College of Engineering, in partial fulfillment of the requirements for the degree of Doctor of Philosophy in the Chemical Engineering.

Signature:

Name: Prof. Dr. Q. J.M. Slaiman

(Supervisor)

Date: 12 / 7 / 2007

Signature:

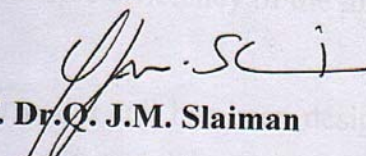
Name: Prof. Dr. Q. J.M. Slaiman

(Head of Department)

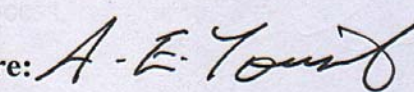
Date: 12 / 7 / 2007

# Certificate

We certify, as an examining committee, that we have read the thesis entitled "INHIBITION OF GALVANIC CORROSION BY PHENYLTHIOUREA UNDER FLOWING CONDITIONS IN HYDROCHLORIC ACID SOLUTION " and examined the student **SHAKER SALEH BAHAR**, and found that the thesis meets the standard for the degree of Doctor of Philosophy in the Chemical Engineering.

Signature:   
Name: Prof. Dr. Q. J.M. Slaiman  
(Supervisor)


Date: 12/7/2007

Signature:   
Name : Prof. Dr. Albert E. Yousif  
(Chairman)

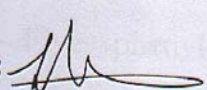
Date 12/7/2007

Signature:  
Name: Dr. Muslat H. Shaaban  
(Member)

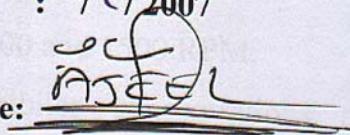
Date: / / 2007

Signature:   
Name : Dr. A. S. Yaro  
(Member)

Date : 12/7/2007

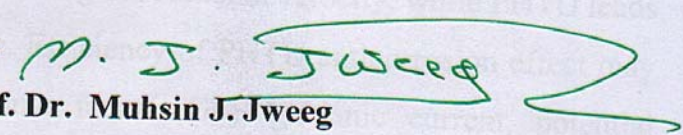
Signature:   
Name: Dr. Shatha A. Samh  
(Member)

Date: 17/7/2007

Signature:   
Name : Dr. Sami A. Ajeel  
(Member)

Date : 17/7/2007

Approval of the College of Engineering

Signature:   
Name: Prof. Dr. Muhsin J. Jweeg  
(Acting Dean)

Date: 6/8/2007

## Abstract

Because of the practical importance of galvanic corrosion arises the need to study the effect of corrosion inhibitors, area ratio of cathode to anode ( $A_c/A_a$ ), rotational velocities of specimens on galvanic corrosion of several industrially important metals and also to follow the behavior of corrosion rate. The use of weight loss technique is adopted as indicator for performance efficiency of the inhibition process.

Corrosion cell has been designed to measure current and potential versus time for the coupled metal.

The performance of galvanic corrosion process has been tested for four major factors that affect the process.

- 1- Type of metals, copper, carbon steel, and zinc has been chosen.
- 2- Four area ratios of more noble to less noble metal (Cu/Fe, Cu/Zn and Fe/Zn) are (0.25, 0.5, 1 and 2).
- 3- Four rotational velocities, 0, 500, 1000 and 1500 RPM.
- 4- Five phenylthiourea (PHTU) inhibitor concentrations are selected to be 0, 0.001, 0.05, 0.1 and 0.15g/L in air-saturated 0.1N HCl solution at 40 °C.

In this study we found that corrosion rate increased in correspondence to the increasing of rotational velocity, while PHTU leads to very low corrosion rate. Efficiency of PHTU anticorrosion effect may approach to 99%. Galvanic factor (GF), galvanic current, potential difference and dissolution current ( $I_d$ ) have been studied in most of the cases.

Current and potential have been checked out for copper / carbon steel couple together. We found that the potential of either one of them approach the value of the other, which is in range of their values, when they are separated.

Current value has been calculated, in condition of zero ammeter resistance for certain parameters. This value was very small in comparison with practical results.

Generally, results showed that corrosion potential is more negative with increasing rotational velocities (U) and area ratio (AR), while it is shifted to less negative with increasing PHTU concentration (C).

The occurrence of the galvanic corrosion was efficiently verified during the experiments using the following equation given by West:

$$\frac{i_d^B}{i_d^N} = \frac{A_c}{A_a} \left[ \frac{|i_c^N|}{i_d^N} - 1 \right] + \frac{|i_c^B|}{i_d^N}$$

and for each case at  $E_{\text{coupling}}$ ,  $\sum I^c = \sum I^a$  and  $\sum I_g = 0$

The experimental results were quantified using the non-linear curve fitting technique by Hooke - Jeeves and quasi - Newton method by using statistical program package to find equations expressing the galvanic current and potential difference at steady state of each investigated couple which is affected by rotational velocities (U), area ratio (AR) and PHTU concentration (C) as follows:

### **For Fe-Zn**

$$E = -862.914 + 383.606(C) - 38.737(U) - 0.058(AR).$$

$$I_g = 10.726 - 71.41(C) + 0.006(U) + 2.032(AR) - 9.208 \left[ \frac{U}{U + C + AR} \right]^{5740.76}$$

### **For Cu-Fe**

$$E = -418.464 + 276.631(C) - 28.12(U) - 0.087(AR).$$

$$I_g = 4.373 - 32.092(C) + 0.005(U) + 0.553(AR) - 7.517 \left[ \frac{U}{U + C + AR} \right]^{2026.289}$$

### **For Cu-Zn**

$$E = -831.346 + 376.643(C) - 30.549(U) - 0.055(AR).$$

$$I_g = 9.049 - 65.121(C) + 0.006(U) + 0.633(AR) - 13.457 \left[ \frac{U}{U + C + AR} \right]^{3159.814}$$

Depending on weight loss and single metal polarization experiments, metals were sorted according to their corrosion resistivity in the environment of air-saturated 0.1N HCl solution, and follows:

$$Cu > C.S. > Zn$$

# List of Contents

	<b>Page</b>
Abstract	I
List of contents	IV
Nomenclature	VII
<b>CHAPTEER ONE</b>	
<b>INTRODUCTION</b>	
1.1 Corrosion	1
1.2 Corrosion Prevention:	2
1.3 Addition of inhibitors	2
1.4 The Scope of Present Work	3
<b>CHAPTER TWO</b>	
<b>CORROSION</b>	
2.1 Introduction	4
2.2 Definition of corrosion	4
2.3 Classification of Corrosion	6
2.4 Polarization	8
2.4.1 Activation Polarization $\eta_A$	9
2.4.2 Concentration Polarization $\eta_c$	11
2.4.3 Combined Polarization	13
2.5 Cathodic Reactions in Corrosion	15
2.6 Factors Influence Corrosion Reaction	16
2.6.1 Solution pH	16
2.6.2 Oxidizing agents	17
2.6.3 Temperature	19
2.6.4 Fluid velocity	19
2.6.5 Suspended Solids	21
2.7 Limiting Current Density	21
2.8 Nernst Diffusion Layer	22
<b>CHAPTER THREE</b>	
<b>GALVANIC CORROSION AND EFFECT OF ENVIRONMENT CONDUTIONS</b>	
3.1 Introduction	24
3.2 Fundamental of Galvanic Corrosion	26
3.3 Theory of galvanic corrosion	26
3.4 Factors affecting galvanic corrosion	34
3.4.1 Electrode Potentials	34
3.4.2 Reaction kinetics	34
3.4.3 Alloy Composition	34
3.4.4 Protective film characteristics	35

3.4.5	Mass Transport	35
3.4.6	Bulk Solution Environment	35
3.4.7	Bulk Solution properties	35
3.4.8	Total Geometry	35
3.5	Corrosion inhibitor	36
3.5.1	Introduction	36
3.5.2	Classification of Inhibitors	37
3.6	Application of Inhibitors for Acid Media	42
3.6.1	Hydrochloric acid	42
3.6	Phenylthiourea	44
3.7	Corrosion Inhibition Mechanism	44
3.8	Types of corrosion inhibitor	45
3.8.1	Anodic Inhibitor	47
3.8.2	Cathodic inhibitor	48
3.8.3	Mixed inhibitor	49
3.9	Oxygen Reductions and Transport	49
3.10	Electrochemical Measurements in Flowing Solutions	51
3.10.1	The Rotating Cylinder Electrode	52
3.10.2	The Rotating Disk Electrode	54

## **CHAPTER FOUR EXPERIMENTAL WORK**

4.1	Introduction	56
4.2	System specifications	57
4.3	The electrolyte	58
4.4	Solvents Used	59
4.5	The electrical circuit	59
4.6	Description of corrosion cell	62
4.7	Experimental procedure	62
4.7.1	Specimen preparation	62
4.7.2	Corrosion rate measurements by weight loss of single metals (free corrosion)	63
4.7.3	Measuring the current, potential difference and corrosion rate of couple metals	63
4.7.4	Measuring the voltage and current simultaneously in galvanic corrosion.	64
4.7.5	Polarization investigation procedure	65
4.7.6	Cell resistance measurement procedure	69



**CHAPTER FIVE  
RESULTS AND INTERPRETATION**

5.1	Introduction	70
5.2	Weight loss of individual metals	71
5.3	Galvanic coupling	74
5.3.1	Copper and carbon steel coupling	74
5.3.3	Carbon steel and zinc coupling	107
5.4	Measuring the potential and current to gather for copper and carbon steel couple	124
5.5	Free Corrosion	140
5.6	Polarization Curves	147
5.7	Results of cell resistance measurement	154

**CHAPTER SIX  
DISCUSSION**

6.1	Introduction	154
6.2	Parameters that affect single metal (Free corrosion)	154
6.2.1	Rotational velocity	154
6.2.2	Inhibitor concentration	157
6.3	Parameters that affect galvanic corrosion	159
6.3.1	Rotational velocity	159
6.3.2	Inhibitor concentration	160
6.3.3	Area ratio	160
6.4	Parameters that affect galvanic corrosion current	169
6.5	Measuring the potential and current together for copper and carbon steel couple	183
6.6	Effect of rotational velocity and PHTU concentration on polarization curves behavior	184
6.7	Effect of rotational velocities and PHTU concentration on potential and current density at regions close to the corrosion potential value	186
6.8	Galvanic cell resistance measurement	188
6.9	Statistical Relationships	190

**CHAPTER SEVEN  
CONCLUTIONS AND RECOMMENDATIONS  
FOR FUTURE WORK**

7.1	Conclusions	192
7.3	Recommendations for Future Work	194
	<b>REFERENCES</b>	195
	<b>APPENDICES</b>	-

# Nomenclature

<b><i>SYMBOL</i></b>	<b><i>MEANING</i></b>	<b><i>UNIT</i></b>
<i>A</i>	Surface area	m <sup>2</sup>
<i>AR</i>	Area ratio	-
<i>A<sub>a</sub>, A<sub>c</sub></i>	Anodic and cathodic area	m <sup>2</sup>
<i>β<sub>A</sub></i>	Anodic Tafel slope=[2.3RT/αzF]	V
<i>β<sub>c</sub></i>	Cathodic Tafel slope =[2.3RT/(1- α)zF]	V
<i>C</i>	PHTU concentration	g/lit
<i>C<sub>B</sub></i>	Bulk concentration of reacting species	g/lit
<i>Cu</i>	Copper	-
<i>CR</i>	Corrosion rate	-
<i>CS</i>	Carbon Steel	-
<i>D</i>	Diffusion coefficient of reaction ion	m <sup>2</sup> /s
<i>E</i>	Potential difference	mV
<i>E<sub>eq.</sub></i>	Equilibrium potential	mV
<i>E<sub>coupl.</sub></i>	Coupling potential	mV
<i>E<sub>g</sub></i>	Galvanic potential	mV
<i>E<sub>a</sub></i>	Anodic potential	mV
<i>E<sub>c</sub></i>	Cathodic potential	mV
<i>E<sub>corr.</sub></i>	Corrosion potential	mV
<i>F</i>	Faraday constant 96487	Coulomb/equiv.
<i>Fe</i>	Iron	-
<i>GF</i>	Galvanic factor	-
<i>i</i>	Current density	μA/cm <sup>2</sup>
<i>i<sub>d</sub></i>	Dissolution current density	μA/cm <sup>2</sup>
<i>i<sub>a</sub></i>	Anodic current density	μA/cm <sup>2</sup>
<i>i<sub>app.</sub></i>	Applied current	μA/cm <sup>2</sup>
<i>i<sub>c</sub></i>	Cathodic current density	μA/cm <sup>2</sup>
<i>i<sub>corr.</sub></i>	Corrosion current	μA/cm <sup>2</sup>
<i>i<sub>cp.</sub></i>	Cathodic protection current density	μA/cm <sup>2</sup>
<i>i<sub>L</sub></i>	Limiting current density	μA/cm <sup>2</sup>
<i>i<sub>o</sub></i>	Exchange current density	μA/cm <sup>2</sup>
<i>i<sub>net</sub>, Δi</i>	Net current density	μA/cm <sup>2</sup>
<i>I</i>	Current	mA
<i>I<sub>g</sub></i>	Average galvanic current	mA
<i>I<sub>1</sub></i>	Cathodic galvanic current	mA
<i>I<sub>2</sub></i>	Anodic galvanic current	mA
<i>I<sub>3</sub></i>	I <sub>2</sub> - I <sub>1</sub>	mA

$I_4$	$I_2 - \bar{I}_g$	mA
$k$	Mass transfer coefficient	m/s
$L$	Metal specimen length	cm
$mm/y$	Millimeter penetration per year	-
$mpy$	Millinch penetration per year	-
$Mt$	Molecular weight of metal	g/mol
$n, z$	Number of electrons transferred	-
$OD$	Outside diameter	cm
$R$	Resistance	$\Omega$
$Re$	Reynolds number	-
$R_f$	Film resistance	$\Omega$
$R_o$	Resistance of the electrolyte solution	$\Omega$
$R_{soln.}$	Electrical resistance of solution	$\Omega$
$Sc$	Schmidt number	-
$SCE$	Saturated Calomel Electrode	V
$Sh$	Sherwood number	-
$q$	Electric charge	Coulomb
$t$	Exposure time	s
$T$	Temperature	$^{\circ}C$
$U$	Rotational velocity	RPM
$\Delta W$	Weight loss	g
$\Delta W_a$	Anodic weight loss	g
$\Delta W_c$	Cathodic weight loss	g
$\eta_A$	Activation polarization	V
$\eta_C$	Concentration polarization	V
$\eta_R$	Resistance Polarization	V
$\delta$	Thickness of the diffusion layer.	cm
$\delta_d$	Diffusion layer thickness	$\mu m$
$\rho$	Density	$Kg/m^3$
$\alpha$	Symmetry factor $\sim 0.5$	-
$\varepsilon_D$	Eddy diffusivity for mass transfer	$m^2/s$

# Chapter One

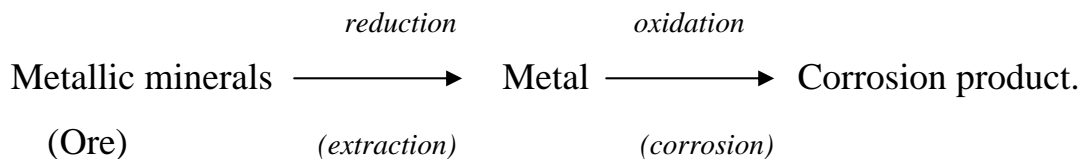
## Introduction

### 1.1 Corrosion

The cost of corrosion has been estimated at \$300 billion per year in the United States <sup>[1]</sup>. The corrosion-related cost to the transmission pipeline industry is approximately \$5.4 to \$8.6 billion annually<sup>[2,3]</sup>. This can be divided into the cost of failures, capital, and operations and maintenance (O&M) at 10, 38, and 52 percent, respectively<sup>[1]</sup>.

Corrosion is a serious problem because it definitely contributes to the depletion of natural resources, for example, steel is made from iron ore ,that has been dwindled. Another important factor concerns the world's supply of metal resources<sup>[4,5]</sup>. The rapid industrialization of many countries indicates that the competition for and the price of metal resources will increase<sup>[5,6]</sup>.

Many corrosion products are chemically similar to the corresponding metallic minerals as shown in the following simple corrosion cycle<sup>[5,7]</sup>:



An excellent example of this cycle is shown by the behavior of iron. Many iron ores contain iron in the oxidized form (oxides, carbonates) which are reduced by carbon in the smelting process to metallic iron .In the presence of moisture, the iron, so obtained will then oxidize to rust as a corrosion product. If the rust is analyzed it will be found to be an iron

oxide of similar composition to the mineral hematite, though it must be emphasized that rust is a far more complex substance than  $\text{Fe}_2\text{O}_3\text{-H}_2\text{O}$ <sup>[5,8]</sup>.

At ordinary temperatures, in aqueous solution, the essential step in the transformation of a metal atom into a mineral molecule is that the metal passes into solution, during this process the atom loses one or more electrons and becomes an ion<sup>[5,9]</sup>. This reaction can occur only if an electron acceptor is present in the solution, so corrosion must always involve two simultaneous processes at the metal surface<sup>[10,11]</sup>. For example in acid solutions:



Then after combining(1&2), the following equation obtained.



## 1.2 Corrosion Prevention

There are many methods for corrosion prevention illustrated as follows<sup>[12,13,14]</sup>.

- 1- *Addition of inhibitors*
- 2- *Anodic Protection.*
- 3- *Protective Coatings such as paint.*
- 4- *Corrosion –resistant alloys.*
- 5- *Cathodic Protection*
- 6- *Very pure metals.*
- 7- *Etc.*

## 1.3 Addition of inhibitors

Very low concentrations of solutes with particular characteristics can intervene with corrosion kinetics and there by protect metals from

corrosion and are described by the general term, *inhibitors*. Some occur naturally and others are introduced artificially as a strategy for corrosion control<sup>[15,16]</sup>.

Inhibitors intervene in corrosion kinetics in various ways. Some inhibit cathodic reactions, others inhibit anodic reactions and yet others, *mixed inhibitors*, do both<sup>[6,16]</sup>.

### **1.3The Scope of Present Work**

The purpose of present work is to construct Inhibition of Galvanic Corrosion under Flowing Condition in Acid Solution System to study the effect of multivariable on galvanic corrosion. The structure chosen during the present work is copper, carbon steel (CS), and zinc metal specimens. The variables investigated experimentally are area ratio (AR), inhibitor concentration (C), rotational velocity (U) at a constant temperature (T). This is monitored by weight loss and polarization technique.

# Chapter Two

## Corrosion

### 2.1 Introduction

Almost all metals except noble metals like gold, silver and, rarely, copper are found in nature in chemical combination with non-metals, that is, they have transferred to or shared electrons with other elements. The minerals so formed through chemical combination are often different from each other, but under the geological conditions in which they are found, they are in a stable and preferred state<sup>[17,18]</sup>.

Corrosion is the undesirable combination of processes by which metals tend to chemically bind with other materials by losing or sharing electrons to or with other elements<sup>[17,19]</sup>.

The chemical tendency for metals to form compounds by chemical reaction is not always undesirable. For example, as will be discussed below, carbon (mild) steel can react with oxygen to form the mineral magnetite, which protects the steel from corrosion<sup>[17,20]</sup>

### 2.2 Definition of corrosion

*Corrosion* may be defined as a destruction or deterioration of a material because of reaction with its environment<sup>[21,22]</sup>. Deterioration by physical causes is not called corrosion, but is described as erosion, galling, or wear. In some instances, chemical attack accompanies physical deterioration as described by the terms<sup>[21,23]</sup> : corrosion-erosion, corrosive wear, or fretting corrosion. Nonmetals are not included in the present definition<sup>[24,25]</sup>.

In nature, most metals are found in a chemically combined state known as ores. Ores may be oxides, sulfides, carbonates or other more

complex compounds, and because many have been found in earth's crust since it was formed, their chemical condition is somehow preferred by nature. Ores and other such compounds are in low energy states. In order to separate a metal from one of its ores, it is necessary to supply a large amount of energy<sup>[24,26,27]</sup>. Therefore metals in their uncombined condition are usually of high-energy states. It is this tendency of metals to recombine with components of environment that leads to phenomenon known as corrosion. So it is simply a problem caused by nature that affects materials and is governed by energy changes. A fundamental definition of corrosion is the degradation of a metal by an electrochemical reaction with its environment<sup>[28,29]</sup>.

Corrosion is related to metals. This means that only a half-reaction can be a true corrosion reaction. The second half –reaction, though it describes a process essential for corrosion, is not itself a corrosion reaction. By using the word degradation in the definition, we assume the corrosion is an undesirable process. There are circumstances in which this is not true. In which case the process is not referred to as corrosion. The degradation involves not just a chemical but an electrochemical reaction, electron transfer occurs between the participants. Electrons are negatively charged species, and their transport constitutes an electrical current, so electrical reactions are influenced by electrical potential. The environment is a convenient name to describe all species adjacent to the corroding metal at time of the reaction. Environments that cause corrosion are called corrosive. A metal that suffers corrosion is called corrodible<sup>[29,30]</sup>.

Corrosion is an extractive metallurgy in reverse. Fig.2-1.shows that most iron ores contain oxides of iron and rusting of steel by water and



oxygen results in a hydrated iron oxide. Rusting is a term reserved for steel and iron corrosion, although many other metals form their oxides when corrosion occurs<sup>[21,31]</sup>.

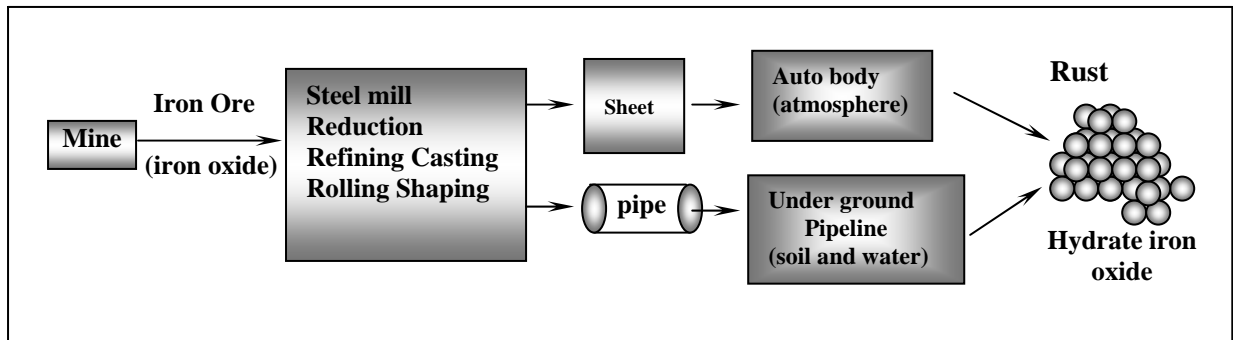


Figure2-1. Metallurgy in reverse<sup>[21]</sup>.

## 2.3 Classification of Corrosion

For the mechanism of the corrosion process, we may distinguish two types of corrosion<sup>[32]</sup>.

### a) Chemical corrosion

Chemical corrosion can be classified to:

1. Gaseous corrosion : Is corrosion of metals in the complete absence of moisture on the surface . Ordinary ,this term refers to corrosion of metals at elevated temperature.
2. Corrosion in non-electrolytes refers to action on a metal by aggressive organic substance that does not possess significant electrical conductivity<sup>[32]</sup>.

### b) Electrochemical corrosion

Electrochemical corrosion can be classified to:

1. Corrosion in electrolytes is a widespread type corrosion that includes the action of natural waters and most aqueous solutions on metal structures .Depending on the chemical nature of the medium there may be acid, alkali, salt, or marine corrosion<sup>[7,31]</sup> .

2. Atmospheric corrosion is the corrosion of metals in the atmosphere by moist gases and it is most prevalent type of corrosion because most metal structures are exposed to atmospheric conditions.
3. Electrocorrosion or corrosion by an external current refers for example to the corrosion of underground pipelines by stray currents.
4. Contact corrosion is type of electrochemical corrosion caused by contact of two or more metals of different electrochemical potentials.
5. Stress corrosion is caused by simultaneous action of the corrosive medium and mechanical stress.
6. Corrosion with simultaneous action of impingement or abrasion (corrosion due to impingement is also known as cavitation corrosion).
7. Biocorrosion refers to those cases of underground corrosion or corrosion in electrolytes that are sharply accelerated by products formed by microorganisms.
8. Stain corrosion is initiated at isolated spots and it spreads superficially with the result coverage of relatively large areas.
9. Pitting corrosion is characterized by deep local pits in limited areas.
10. Pinpoint corrosion is characterized by small pinpoint pits randomly distributed over the surface of the metal.

## 2.4 Polarization

The rate of an electrochemical reaction is limited by various physical and chemical factors. Hence, electrochemical reaction is said to be polarized or retarded by these environmental factors. Polarization can be conveniently divided into two different types, activation polarization and concentration polarization<sup>[24,33,34]</sup>. In analysis of rates of reaction there is an important principle, i.e., the rate of reaction is determined by the slowest step. When small currents are involved, the transport of cathode reactant, e.g. dissolved oxygen, through the solution is relatively easy and the activation process is the rate determining step. However, when large current flows, the cell demands a greater charge transfer than can be accommodated by the electrolyte. The speed of passage of dissolved oxygen species becomes the slowest step and is thus rate determining. Under these conditions we refer to the process as diffusion controlled<sup>[29,36,37]</sup>.

As the degree of the polarization increases, the rate of corrosion decreases. The polarization of anode may be less than, or greater than, that on the cathode<sup>[37,38,39]</sup>. The corrosion reaction is said to be cathodically controlled if polarization occurs at the cathodes where the corrosion potential is close to the open circuit potential of the anode as shown in **Fig.2-2a**<sup>[36,40]</sup>. The corrosion reaction is said to be anodically controlled if polarization occurs at the anode where the corrosion potential is then near the open circuit of cathode potential **Fig.2-2b**. Mixed control occurs when polarization occurs in some degree at both anodes and cathodes **Fig.2-2c**. When electrolyte resistance is so high that the resultant current is not sufficient to appreciably polarize anodes or cathodes, resistance control occurs. The corrosion is then controlled by the IR drop through the electrolyte **Fig.2-2d**. A reaction with a higher thermodynamic tendency may result in a smaller corrosion rate than with

a lower thermodynamic tendency **Fig.2-2e**. The corrosion potential  $E_{\text{corr}}$  gives no indication of corrosion rate as shown in Fig.2.2f<sup>[39,41]</sup>.

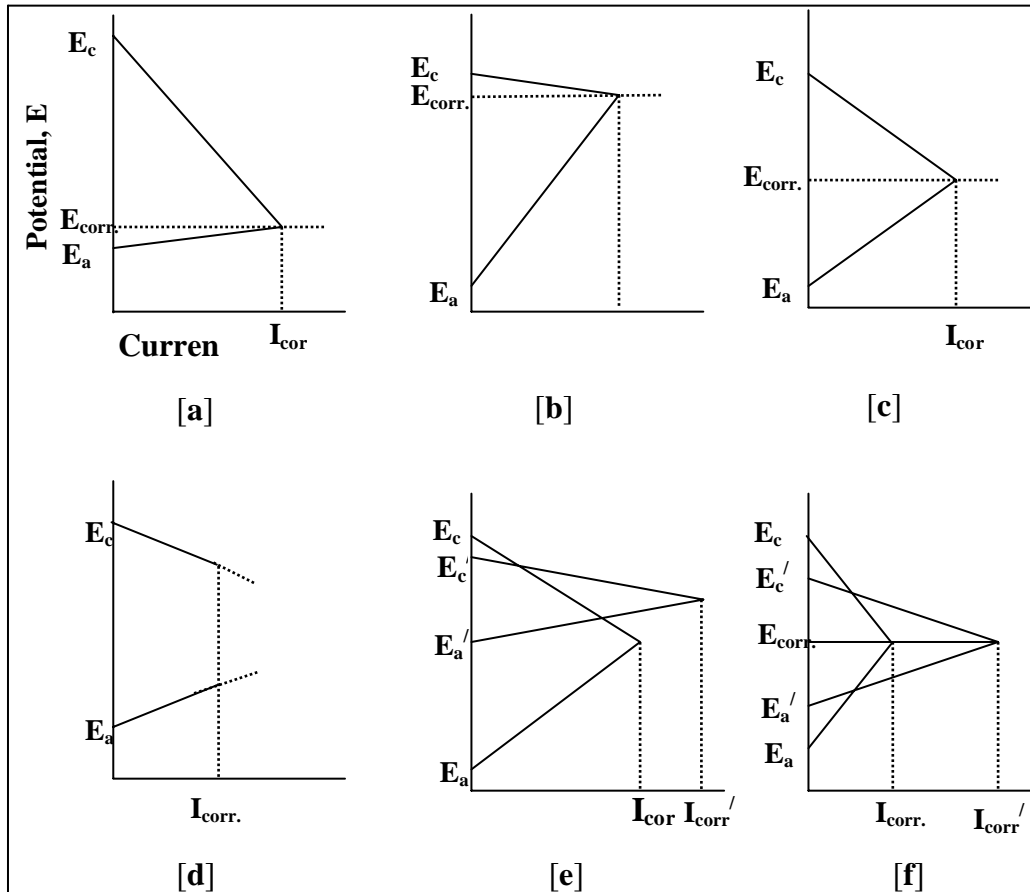


**Figure.2-2**<sup>[41]</sup>Evans diagrams illustrating [a] cathodic control, [b] anodic control, [c] mixed control, [d] resistance control, [e] how a reaction with a higher thermodynamic tendency ( $E_{r,\text{cell}}$ ) may result in a smaller corrosion rate than one with a lower thermodynamic tendency and [f] how  $E_{\text{corr}}$  gives no indication of the corrosion rate.

### 2.4.1 Activation Polarization $\eta_A$

The most important example is that of hydrogen ion reduction at a cathode<sup>[21]</sup>:



The corresponding polarization term being called hydrogen overvoltage<sup>[41]</sup>.



where ( $H_{ads}$ ) represents hydrogen atoms adsorbed on the metal surface. This relatively rapid reaction is followed by a combination of adsorbed hydrogen atoms to form hydrogen molecules and bubbles of gaseous hydrogen<sup>[32]</sup>.



This reaction is relatively slow, and its rate determines the value of hydrogen overvoltage on platinum. The controlling slow step of  $H^+$  discharge is not always the same but varies with metal current density and environment<sup>[42]</sup>.

Pronounced activation polarization also occurs with discharge of  $OH^-$  at an anode accompanied by oxygen evolution:



This is known as oxygen overvoltage. The activation polarization  $\eta_A$  of any kind increases with anodic and cathodic current density in accord with the Tafel equation<sup>[21]</sup>:

$$\eta_A = \frac{2.303RT}{\alpha zF} \log\left(\frac{i_a}{i_o}\right) \quad \text{For anodic reaction} \quad \dots (2-9)$$

$$\eta_A = \frac{2.303RT}{\alpha zF} \log\left(\frac{i_c}{i_o}\right) \quad \text{For cathodic reaction} \quad \dots (2-10)$$

These equation may be simplified to:

$$\eta_A = \beta_A \log\left(\frac{i_a}{i_o}\right) \quad \dots (2-11)$$

$$\eta_C = \beta_C \log\left(\frac{i_c}{i_o}\right) \quad \dots \quad \dots (2-12)$$

where  $\beta_A$ ,  $\beta_C$  &  $i_o$  are constants of a given metal and environment and are both dependent on temperature. The exchange current density  $i_o$  represents the current density equivalent to the equal forward and reverse reactions at the electrode at equilibrium. The larger the the value of  $i_o$  and

the smaller the value of  $\beta_A$  &  $\beta_c$ , the smaller is the corresponding overvoltage.

Activation polarization refers to electrochemical reactions which are controlled by a slow step in the reaction sequence. The species must first be adsorbed or attached to the surface before the reaction can proceed according to step1. Following this, electron transfer (step2) must occur, resulting in a reduction of the species. As shown in step3, two hydrogen molecules then combine to form a bubble of hydrogen gas (step4) as shown in **Fig.2-3**. The speed of reduction of the hydrogen ions will be controlled by the slowest of these steps<sup>[21,31]</sup>.

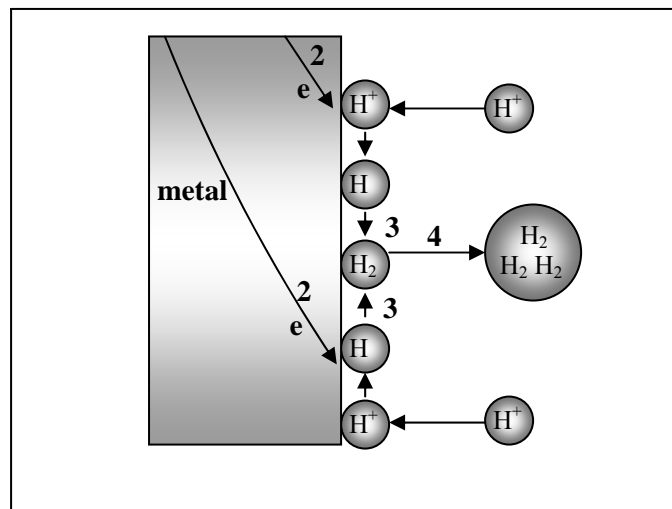


**Figure 2-3**<sup>[21]</sup> Hydrogen-reduction reaction under activation control (simplified)

## 2.4.2 Concentration Polarization $\eta_c$

Concentration polarization refers to electrochemical reactions which are controlled by the diffusion in the electrolyte. It is the slowing down of a reaction due to an insufficiency of the desired species or an excess of the unwanted species at the electrode. This type of polarization occurs at the cathode when reaction rate or the cathode current is so large that the substance being reduced cannot reach the cathode at a sufficiently rapid rate. Since the rate of reaction is determined by the slowest step, the diffusion rate will be the rate determining step.

At very high reduction rates, the region adjacent to the electrode surface will become depleted of ions. If the reduction rate is increased further, a limiting rate will be reached which is determined by the diffusion rate of ions to the electrode surface. This limiting rate is the limiting diffusion current density  $i_L$ . It represents the maximum rate of reduction possible for a given system; the expressing of this parameter is<sup>[21,24]</sup>:

$$i_L = \frac{DnFC_B}{\delta} \quad \dots (2-13)$$

where  $i_L$  is the limiting diffusion current density,  $D$  is the diffusion coefficient of the reacting ions,  $C_B$  is the concentration of the reacting ions in the bulk solution, and  $\delta$  is the thickness of the diffusion layer.

By combining the laws governing diffusion with Nernst equation<sup>[21]</sup>:

$$E = E_o + 2.3 \frac{RT}{nF} \log \frac{a_{oxid}}{a_{red}} \quad \dots (2-14)$$

the following expression can be developed<sup>[7,8]</sup>:

$$E_i - E = \eta_c = \frac{2.303RT}{nF} \log \left( 1 - \frac{i}{i_L} \right) \quad \dots (2-15)$$

This equation is shown in **Fig.2-4**. For the case of hydrogen evolution any change in the system which increases the diffusion rate will decrease the effects of concentration polarization and hence increases reaction rate. Thus, increasing the velocity or agitation of the corrosive medium will increase rate only if the cathodic process is controlled by concentration polarization, agitation will have no influence on corrosion rate<sup>[21,43]</sup> (**Fig.2-5**).

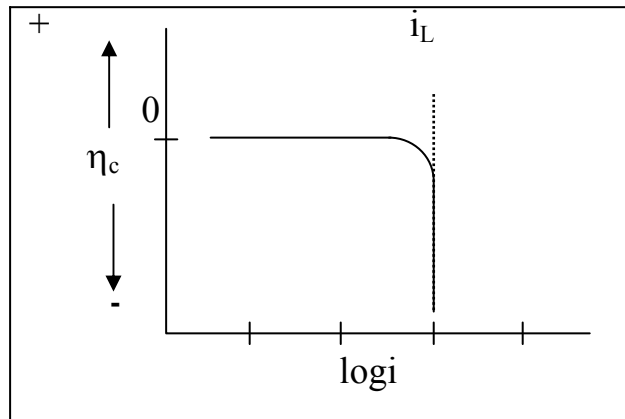


**Figure 2-4**<sup>[21]</sup>. Concentration polarization curve (reduction process).

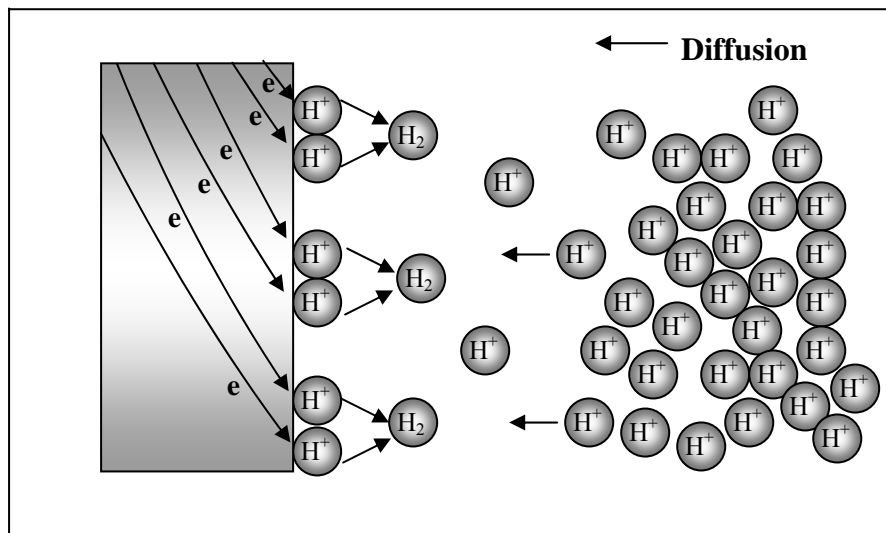


**Figure 2-5**<sup>[21]</sup>. Concentration polarization during hydrogen reduction.

### 2.4.3 Combined Polarization

Both activation and concentration polarization usually occur at an electrode. At low reaction rates activation polarization usually controls, while at higher reaction rates concentration polarization becomes controlling<sup>[12,44]</sup>. The total polarization of an electrode is the sum of the contribution of activation polarization and concentration polarization<sup>[7,8]</sup>:

$$\eta_t = \eta_A + \eta_C \quad \dots (2-16)$$

During reduction process such as hydrogen evolution or oxygen reduction, concentration polarization is important as the reduction rate



approaches the limiting diffusion current density. The overall reaction for activation process is given by<sup>[21,24]</sup>:

$$\eta_{red} = -\beta_c \log \frac{i}{i_o} + \frac{2.303RT}{nF} \log \left( 1 - \frac{i}{i_L} \right) \quad \dots (2-17)$$

this case can be shown in **Fig.2-8**<sup>[21]</sup>.

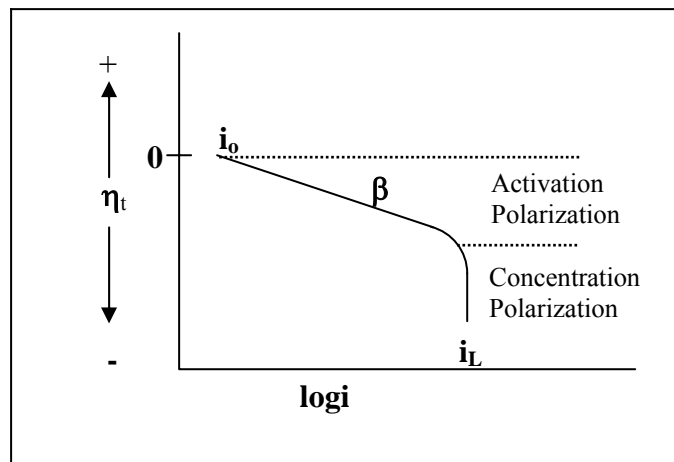


**Figure 2-6**<sup>[21]</sup> Combined Polarization curve.

In corrosion, the resistance of the metallic path for charge transfer is negligible. Resistance overpotential  $\eta_R$  is determined by factors associated with the solution or with the metal surface<sup>[45]</sup>. Resistance polarization  $\eta_R$  is only important at higher current densities or in higher resistance solution<sup>[45,46]</sup>. It may be defined as<sup>[21,24,41]</sup>:

$$\eta_R = I(R_{soln} + R_f) \quad \dots (2-18)$$

where  $R_{soln}$  is the electrical resistance of solution, which is dependent on the electrical resistivity ( $\Omega$  cm) of the solution and the geometry of the corroding system, and  $R_f$  is the resistance produced by films or coatings formed on the surface of the sites, which block contact between the metal and the solution, and increase the resistance overpotential.

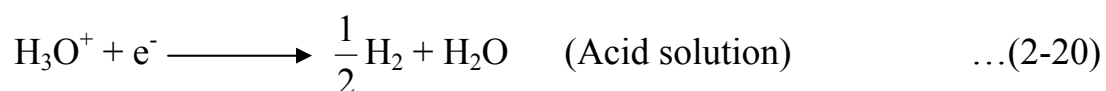
The total polarization at a metal electrode then becomes as the algebraic sum of the three types described above<sup>[21,24,41]</sup>.

$$\eta = \eta_A + \eta_C + \eta_R \quad \dots (2-19)$$

## 2.5 Cathodic Reactions in Corrosion

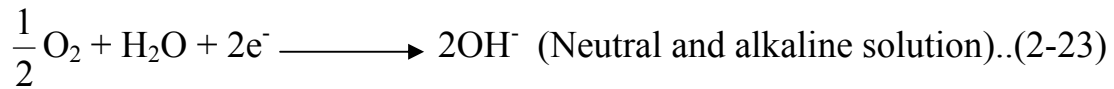
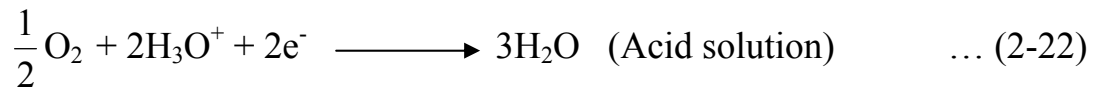
The hydrogen evolution reaction (h.e.r) and the oxygen reduction reaction are the two most important cathodic processes in the corrosion of metals, and this is due to the fact that the hydrogen ions and water molecules are invariably present in aqueous solution, and since most aqueous solutions are in contact with the atmosphere, dissolved oxygen molecules will normally be present<sup>[41,47]</sup>.

In the complete absence of oxygen, or any other oxidizing species, the h.e.r will be the only cathodic process possible, and if the anodic reaction is only slightly polarized the rate will be determined by the kinetics of the h.e.r on the particular metal under consideration (cathode control). However, when dissolved oxygen is present, both cathodic reactions will be possible, and the rate of the corrosion reaction will depend upon a variety of factors such as the reversible potential of the metal /metal ion system, the pH of the solution, the concentration of oxygen reduction reaction on the metal under consideration, and temperature,...etc.<sup>[14]</sup> In general, the contribution made by the h.e.r will increase in significance with decrease of pH, but this too will depend upon the nature of the metal and the metal oxide. It should be noted that in neutral or alkaline solutions the activity of  $H_3O^+$  is too low for it to participate in the h.e.r, and under these circumstances, the water molecules will act as the electron acceptor<sup>[41,45]</sup>.





and for the oxygen reduction reaction



It should be noticed that both reactions will result in an increase in pH in the diffusion layer<sup>[41]</sup>.

## 2.6 Factors Influence Corrosion

### 2.6.1 Solution pH<sup>[48]</sup>:

The relationship between pH and corrosion rates tends to follow one of three general patterns:

1. Acid-soluble metals such as iron have a relationship as shown in **Fig.2-7**. In the middle pH range ( $\approx 4$  to 10), the corrosion rate is controlled by the rate of transport of oxidizer (usually dissolved O<sub>2</sub>) to the metal surface. At very high temperature such as those encountered in boilers, the corrosion rate increases with increasing basicity as shown by the dashed line.

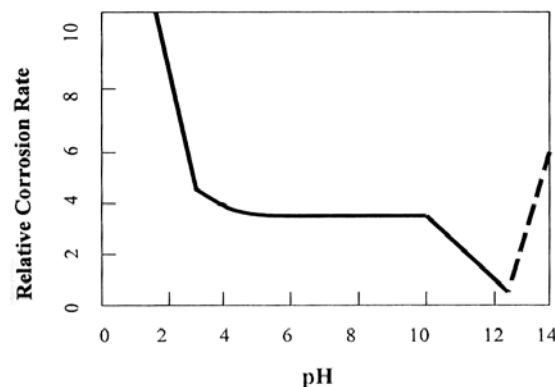


**Figure 2-7<sup>[48]</sup>** Effect of pH on Corrosion Rate of Iron

Amphoteric metals such as aluminum and zinc have a relationship as shown in **Fig.2-8**. These metals dissolve rapidly in either acidic or basic solutions.

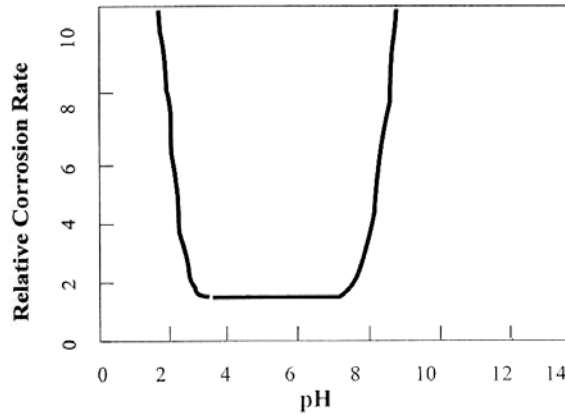


Figure 2-8<sup>[48]</sup> Effect of pH on the Corrosion Rate of Amphoteric Metals (Al and Zn)

3. Noble metals such as gold and platinum are not appreciably affected by pH as shown in **Fig.2-9**.

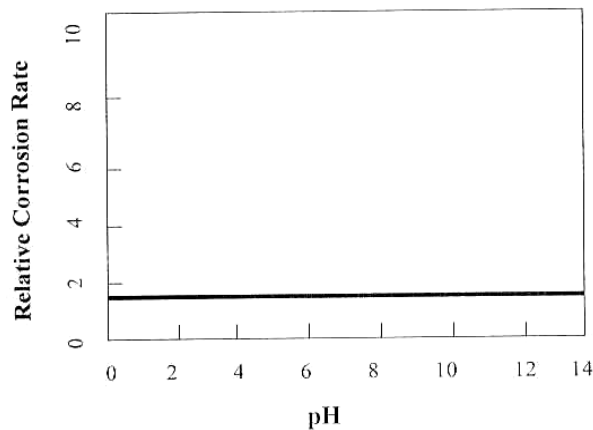
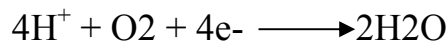


Figure 2-9<sup>[48]</sup> Effect of pH on the Corrosion Rate of Noble Metals

### 2.6.2 Oxidizing agents

In some corrosion processes<sup>[48]</sup>, such as the dissolution of zinc in hydrochloric acid, hydrogen may evolve as a gas. In others such as the relatively slow dissolution of copper in sodium chloride, the removal of hydrogen, which must occur so that corrosion may proceed, is effected by a reaction between hydrogen ion and some

oxidizing chemical such as oxygen to form water. Because of the high rates of corrosion that usually accompany hydrogen evolution, metals are rarely used in solution from which they evolve hydrogen at an appreciable rate<sup>[48,49]</sup>. Most of the corrosion observed in practice occurs under conditions in which the oxidation of hydrogen to form water is a necessary part of the corrosion process. For this reason, oxidizing agents are often powerful accelerators of corrosion and in many cases the oxidizing power of a solution is most important property in so far as corrosion is concerned.



Oxidizing agents that accelerate the corrosion of some materials may also retard corrosion of other through the formation on their surface of oxides or layers of adsorbed oxygen which make them more resistant to chemical attack<sup>[48,50]</sup>. It follows then, oxidizing substances, such as dissolved air, may accelerate the corrosion of one class of materials and retard the corrosion of another class. In the latter case, the behavior of the material usually represents a balance between the power of oxidizing compounds to preserve a protective film and their tendency to accelerate corrosion when the agencies responsible for protective-film breakdown are able to destroy the films.

For diffusion-controlled process, an increase in concentration of the diffusing species in the bulk of the environment increases the concentration gradient at the metal interface. The concentration gradient provides the driving force for the diffusion process. Thus the maximum rate at which oxygen can be diffused to the surface (the limiting diffusion current) would be essentially directly proportional to the concentration in solution. **Fig. 2-10** is example of the cathodic polarization diagram which is operative for this system<sup>[51]</sup>.

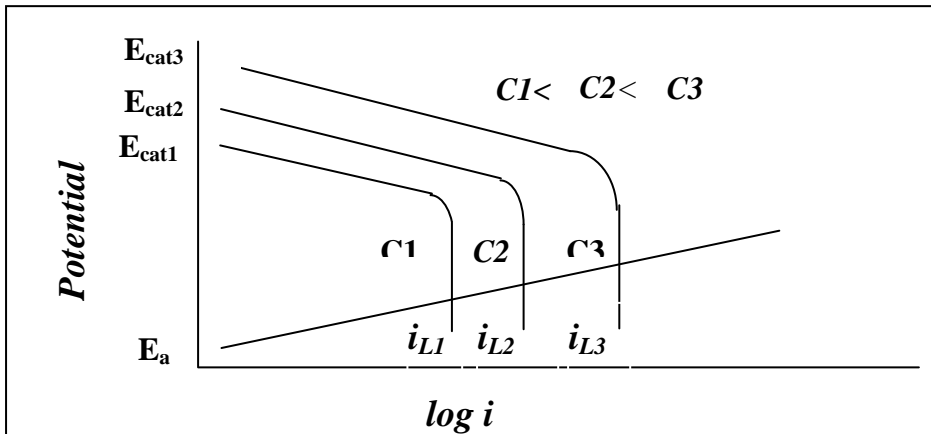


**Figure 2-10** Effect of Concentration on  $i_L$  <sup>(51)</sup>

### 2.6.3 Temperature

As a general rule<sup>[52]</sup>, increasing temperature increases corrosion rates. This is due to a combination of factors- first, the common effect of temperature on the reaction kinetics themselves and the higher diffusion rate of many corrosive by-products at increased temperatures. This latter action delivers these by-products to the surface more efficiently. Occasionally, the corrosion rates in a system will decrease with increasing temperature. This can occur because of certain solubility considerations. Many gases have lower solubility in open systems at higher temperatures. As temperatures increase, the resulting decrease in solubility of the gas causes corrosion rates to go down.

### 2.6.4 Fluid velocity

Velocity primarily affects corrosion rate through its influence on diffusion phenomena. It has no effect on activation controlled processes. The manner in which velocity affects the limiting diffusion current is a marked function of the physical geometry of the system. In addition the diffusion process is affected differently by velocity when the flow conditions are laminar as compared to a situation where turbulence exists.. For most conditions the limiting diffusion current can be expressed by the equation:  $i_L = k u^n$  ... (2.24)

where  $k$  is a constant,  $u$  is the velocity of the environment relative to the surface and  $n$  is a constant for a particular system. Values of  $n$  vary from 0.2 to 1<sup>[53,54]</sup>. **Fig.2-11** shows the effect of velocity on the limiting current density.

The effect of velocity on corrosion rate, like the effect of oxidizer addition, complex and depends on the characteristics of the metal and the environment to which it is exposed. **Fig.2-12** shows the typical observations when agitation or solution velocity is increased<sup>[7]</sup>. For corrosion processes which are controlled by activation polarization, agitation and velocity have no effect on the corrosion rate as illustrated in curve B. If the corrosion process is under cathodic control, then agitation or velocity increases the corrosion rate as shown in curve A, section 1. This effect generally occurs when an oxidizer present in very small amounts as in the case of dissolved oxygen in acids or water. If the process is under diffusion control and the metal is readily passivated, then the behavior corresponding to curve A, section 1 and 2, will be observed. Some metals owe their corrosion resistance in certain medium to the formation of massive bulk protective films on their surface. When materials such as these are exposed to extremely high corrosive velocities, mechanical damage or removal of these films can occur, resulting in accelerated attack as shown in curve C. This is called erosion corrosion<sup>[54]</sup>.

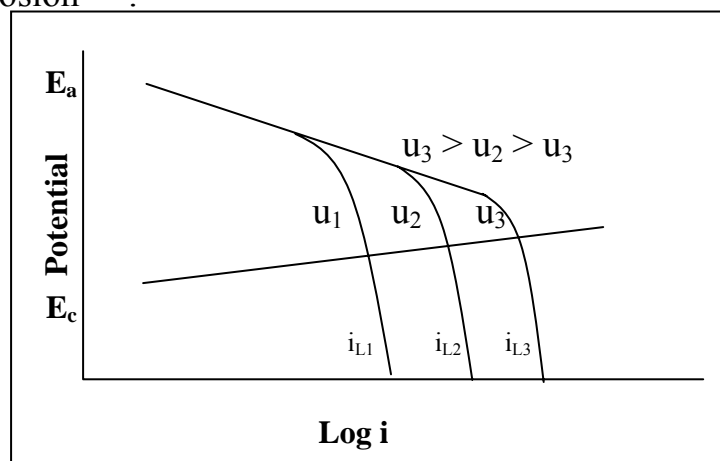


**Figure 2-11**<sup>[54]</sup> Effect of velocity on  $I_L$ .

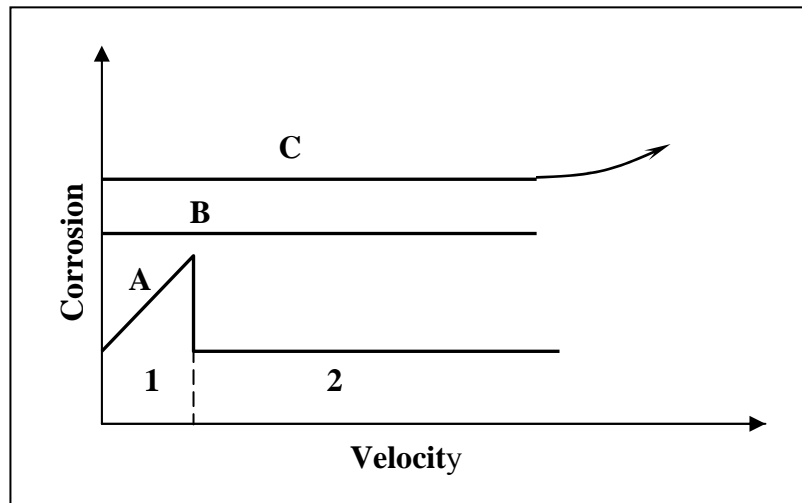


**Figure. 2-12**<sup>[21]</sup> Effect of Velocity on the Corrosion Rate.

### 2.6.5 Suspended Solids

An increase in suspended solids levels will accelerate corrosion rates. These solids include any inorganic or organic contaminants present in the fluid. Examples of these contaminants include clay, sand, silt or biomass <sup>[52]</sup>.

### 2.7 Limiting Current Density

The limiting current is defined as the maximum current that can be generated by a given electrochemical reaction, at a given reactant concentration, under well-established hydrodynamic conditions, in the steady state. This definition implies that the limiting rate is determined by the composition and transport properties of electrolytic solution and by the hydrodynamic conditions at the electrode surface.

In the mass transfer boundary layer (or diffusion layer), whose thickness is indicated by ( $\delta_d$ ), the reactant concentration varies from the bulk value to practically zero at the electrode, this is the limiting-current condition. Determination of mass transfer coefficient involves the measuring of limiting currents in the cathodic reaction process.



Measurement of limiting currents is an experimental technique that has been quit widely employed in mass transfer experiment. Its relative simplicity and flexibility make limiting current method a powerful tool in experimental studies of forced and free convection. At the limiting current the rate of transport of reactant to the interface is smaller than the rate at which it can be potentially be consumed by the charge transfer reaction; as a result, at the interface the concentration of this species approaches zero <sup>[55]</sup>. The flux of reacting species is given by:

$$N_A = \frac{i_L}{Z \times F \times (1 - t_+)} \quad \dots (2.25)$$

When concentration of the reacting species relative to the total ionic concentration of the electrolyte is small,  $t_+ \ll 1$ , Eq.(2.25) becomes;

$$N_A = \frac{i_L}{Z \times F} \quad \dots (2.26)$$

from the measured current, a mass transfer coefficient,  $k$ , defined by;

$$N_A = K \times (C_b - C_s) \quad \dots (2.27)$$

may be calculated. Since at the limiting current we set  $C_s = 0$ , hence

$$K = \frac{i_L}{Z \times F \times \Delta C} \quad \dots (2.29)$$

## 2.8 Nernst Diffusion Layer

One of the first approaches to mass transfer in electrode processes was given by Nernst in 1904<sup>[55]</sup>. He assumed a stationary thin layer of solution in contact with electrode. Within this layer it was postulated that diffusion alone controlled the transfer of substances to the electrode. Outside the layer, diffusion was negligible and concentration of electro-active material was maintained at the value of bulk concentration by convection. This hypothetical layer has become known as “Nernst diffusion layer ( $\delta_d$ )”.

**Fig. 2-13** gives a schematic diagram of this layer. Nernst assumed that the concentration varied linearly with distance through layer. The thickness of this layer is given by:

$$\delta_d = \frac{D}{K} \quad \dots (2.30)$$

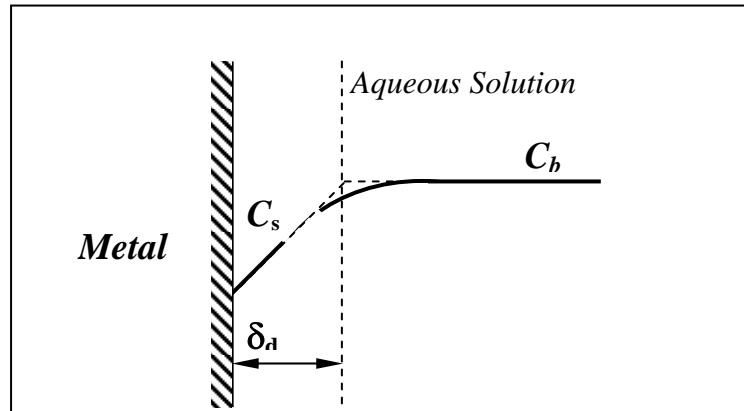


**Figure 2-13** Nernst Diffusion Layer <sup>(55)</sup>.

The diffusion layer thickness is dependent on the velocity of the solution past the electrode surface. As the velocity increases,  $\delta_d$  decreases and the limiting current density increases <sup>[56]</sup>. The time interval required to set up the diffusion layer varies with the current density and limiting diffusion rate, but it is usually of the order of 1 second while it is  $10^{-4}$  second needed to establish the electrical double layer, which makes it possible to distinguish between  $\eta^A$  and  $\eta^c$  experimentally. The diffusion layer may reach a thickness of 100-500  $\mu\text{m}$ , depending upon concentration, agitation (or velocity), and temperature <sup>[45, 57, 58, 59]</sup>.

# Chapter Three

## Galvanic Corrosion and Effect of Environmental Conditions

### 3.1 Introduction

A huge problem that manufacturers have had to put up with for hundreds of years is the problem of corrosion. When in contact with polar compounds such as water, metals will give up electrons, resulting in metal oxide formation. This compromises the integrity of the metal and thus is undesirable to use in some conditions. A general definition for corrosion is the process by which a metal forms ions in solution or an ionic compound of the metal <sup>[60,61]</sup>. The corroding metal gives up electrons to the other metal, providing the other metal has ions in solution.



**Figure 3-1** Automobile door with significant corrosion damage<sup>[60]</sup>

The purpose of this experiment is to explore the electrochemical nature of corrosion and corrosion control. Concepts such as current strength and polarity are discussed, as well as the characteristics of the metals during the corrosion process. Galvanic Corrosion is the type of corrosion being dealt with. It involves two metals electrically connected in a liquid electrolyte where one metal acts as the anode (corrodes) and the other is the cathode<sup>[60]</sup>.

Galvanic corrosion occurs when two different metals are connected in the presence of an electrolyte<sup>[62,63]</sup>. Because corrosion is an electrochemical process involving the flow of electric current, corrosion can be generated by a galvanic effect, which arises from the contact of dissimilar metals in an electrolyte (an electrolyte is an electrically conductive liquid). In fact, three conditions are required for galvanic corrosion to proceed, the two metals must be widely separated in the galvanic series, and they must be in electrical contact and their surfaces bridged by an electrically conducting fluid. Removal of any of these three conditions will prevent galvanic corrosion<sup>[63]</sup>.

When two different metals are in a corrosive environment, they corrode at different rates, according to their specific corrosion resistances to that environment, however, if the two metals are in contact, the more corrosion prone (metal 1) corrodes faster and the less corrosion prone (metal 2 the more noble one) corrodes slower than originally, i.e. when no contact existed. The accelerated damage to the less resistant metal is called galvanic corrosion, and is heavily dependent on the relative surface areas of the metals. In galvanic corrosion, the added anodic currents (on metals 1 and 2) equal the

added cathodic currents (on metals 1 and 2) <sup>[62]</sup> so that

$$I_{a.1} + I_{a.2} = |I_{c.1}| + |I_{c.2}| \quad \dots(3.1)$$

or .in terms of current densities and areas

$$i_{a.1} A_1 + i_{a.2} A_2 = |i_{c.1} A_1| + |i_{c.2} A_2| \quad \dots(3.2)$$

If  $I_{a.1} \gg I_{a.2}$

This equation is reduced to

$$i_{a.1} A_1 = |i_{c.1} A_1| + |i_{c.2} A_2| \quad \dots(3.3)$$

### 3.2 Fundamental of Galvanic Corrosion

The more active metals (base metal), anode, is corroded more rapidly than it would if it was uncoupled in the same medium. The less active (noble metal), a cathode, generally corrodes less than would be the case if it was uncoupled in the same medium or it could be made resistant to corrosion. This effect is referred to as galvanic cathodic protection <sup>[64]</sup>.

### 3.3 Theory of galvanic corrosion:

The galvanic couple between dissimilar metals can be treated by application of mixed potential theory <sup>[21,65]</sup>. Consider a galvanic couple between a corroding and an inert metal. If a piece of platinum is coupled to zinc corroding in an air-free acid solution, vigorous hydrogen evolution occurs on the platinum surface and the rate of hydrogen evolution on the zinc sample is decreased. Also, the corrosion rate of zinc is greater when coupled to platinum. The electrochemical characteristics of this system are schematically illustrated in **Fig. 3-2** <sup>[66,67]</sup>.

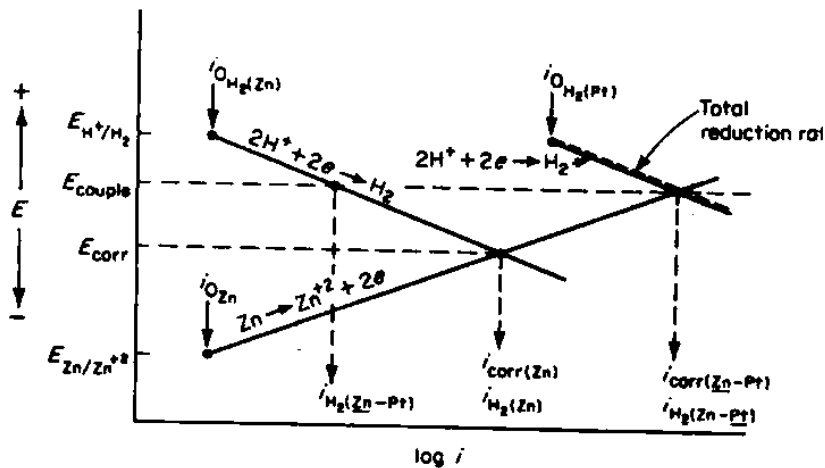


**Figure 3-2** Effect of galvanically coupling zinc to platinum<sup>[66]</sup>.

The corrosion rate of zinc in an air-free acid is determined by the interaction between the polarization curves corresponding to the hydrogen evolution and zinc-dissolution reaction, yielding a corrosion rate equal to  $i_{\text{corr.}(Zn)}$ . When equal areas of platinum and zinc are coupled, the total rate of hydrogen evolution is equal to the sum of the rates of this reaction on both the zinc and platinum surfaces. Since the hydrogen-hydrogen ion exchange current density is very high on platinum and very low on zinc, the total rate of hydrogen evolution is effectively equal to the rate of hydrogen evolution on the platinum surface, as shown in **Fig.3-2**. **Fig.3-2** shows that coupling zinc to platinum shifts the mixed potential from  $E_{\text{corr.}}$  to  $E_{\text{couple}}$ , increases corrosion rate from  $(i)_{\text{corr.}(Zn)}$  to  $i_{\text{corr.}(Zn-pt)}$  and increases the rate of hydrogen evolution on the zinc from  $i_{H_2(Zn)}$  to  $i_{H_2(Zn-pt)}$ . The rate of hydrogen ion reduction on the platinum is  $i_{H_2(Zn-pt)}$ . As mentioned above, the increase in corrosion rate of zinc observed when this metal is coupled to platinum is the result of the higher exchange current density for hydrogen evolution on platinum surface. It is not due to the noble reversible potential of the platinum-platinum-ion electrode, as frequently stated in the literature. To illustrate this point, consider the

relative positions of platinum and gold in the emf and galvanic series. The reversible potential of the gold electrode is more positive than that of platinum in the emf series, where as in most galvanic series tabulations the position of the platinum is below gold. The effect of coupling zinc to gold and to platinum is compared. As mentioned before, the exchange current density for the rate of hydrogen reaction on the zinc metal surface is very low, and as a consequence the rate of hydrogen evolved in a galvanic couple can be assumed to be almost equal to the rate of hydrogen evolution on either gold or platinum.

If equal areas of gold and zinc are coupled, the corrosion rate increase is less than that observed if equal areas of platinum and zinc are coupled. The reason why gold produces a less severe galvanic effect is not related to its reversible potential but rather to the fact that it has a lower hydrogen exchange current density than platinum<sup>[68,69]</sup>.

A couple between a corroding and an inert material represents the simplest example of galvanic corrosion. A couple between two corroding metals may also be examined by application of mixed potential principles, as shown in **Fig.3-3**.

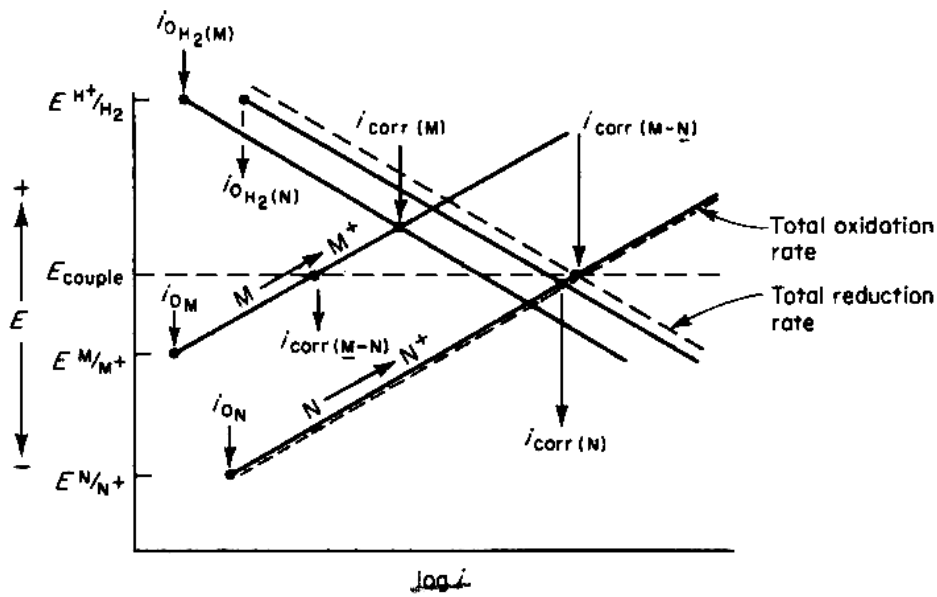
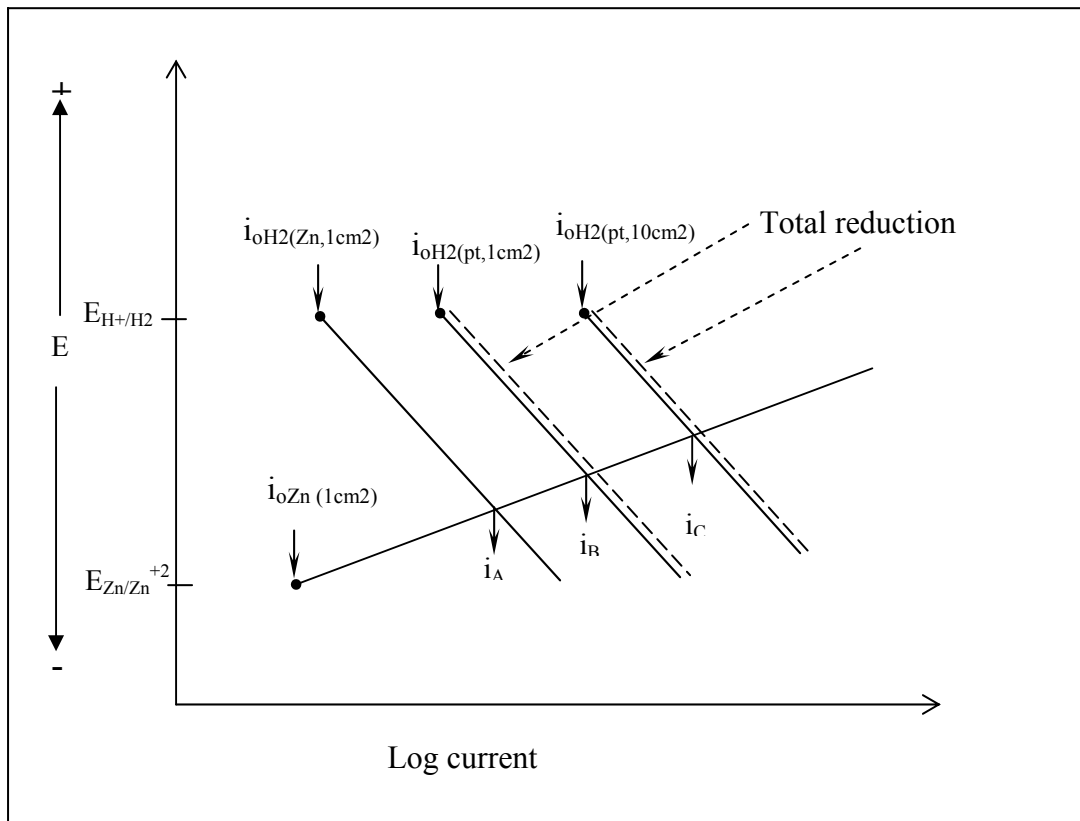


Figure 3-3 Galvanic couple between two corroding metals<sup>[68]</sup>.

The Figure shows the corrosion rate of two metals before and after coupling. Metal M has a relatively noble corrosion potential and a low corrosion rate  $i_{corr(M)}$ , while metal N corrodes at a high rate  $i_{corr(N)}$  at an active corrosion potential. If equal areas of these two metals are coupled, the resultant mixed potential of this system occurs at the point where the total oxidation rate equals total reduction rate. The rates of the individual partial processes are determined by the mixed potential. As shown in **Fig.3-3**, coupling equal areas of these two metals decreases the corrosion rate of metal M to  $i_{corr(M-N)}$  and increases the corrosion rate of metal N to  $i_{corr(M-N)}$ <sup>[68]</sup>.

The relative areas of the two electrodes in a galvanic couple also influence galvanic behavior. Figure 3.4 illustrates the effect of cathode area on the behavior of a galvanic couple of zinc and platinum. Current rather than current density is used in this figure. If a piece of zinc  $1 \text{ cm}^2$  in area is exposed to the acid solution, it will corrode with a rate equal to  $i_A$ . Note that since  $1 \text{ cm}^2$  of zinc is considered, current and current density  $i_A$





**Figure 3-4** Effect of cathode - anode ratio on galvanic corrosion of zinc-platinum couples<sup>[68]</sup>.

are equal. If this zinc specimen is coupled to a platinum electrode of 1 cm<sup>2</sup> area, the zinc corrosion rate is equal to  $i_B$ . Again, since electrodes with 1 cm<sup>2</sup> areas are used, current and current density are equal. However, if a platinum electrode with an area of 10 cm<sup>2</sup> and its behavior in terms of current is plotted, it has an exchange current  $i_0^*$ , which is 10 times greater than 1 cm<sup>2</sup> of an electrode. Thus, increasing the area of an electrode increases its exchange current density, which is directly proportional to specimen area. This is illustrated in **Fig.3-4**. As shown the corrosion rate of the couple is increased as the area of platinum is increased. As the size of the cathode in a galvanic couple is increased, the

corrosion rate of the anode is increased. If the relative area of the anode electrode in a galvanic couple is increased, its overall corrosion rate is reduced <sup>[68]</sup>.

So the situation often arises where: (a) components of several different metals are in electrical contact and/or (b) more than one cathodic reactant is present. In these circumstances, several anodic and/or cathodic processes may take place simultaneously: the corroding system is then called a polyelectrode <sup>[68,70]</sup>.

Because the current density  $i$ , and hence the current  $I$ , at any given electrode is a function of the potential it follows that, for a given potential, the total anodic current of polyelectrode system is the sum of the corresponding anodic currents of the individual electrodes. If the total area of the system is  $S$ , made up of fractions  $f^A$ ,  $f^B$ , ...etc for the various components  $A$ ,  $B$ , ..., then the anodic current from the  $j^{\text{th}}$  component is <sup>[66,71]</sup>.

$$I_a^{\text{system}} = \sum_j J_a^j = S \sum_j f^j i_a^j \quad \dots (3-4)$$

Similarly, the total cathodic current is:

$$I_c^{\text{system}} = \sum_j J_c^j = S \sum_j f^j i_c^j \quad \dots (3-5)$$

At the corrosion potential adopted by the polyelectrode, the total anodic and cathodic currents are equal, so that:

$$I_{\text{corr.}}^{\text{system}} = I_a^{\text{system}} = |I_c^{\text{system}}| \quad \dots (3.6)$$

And

$$\sum_j f^j i_a^j = \sum_j f^j |i_c^j| \quad \dots (3.7)$$

where the current densities on the various components are those corresponding to  $E = E_{\text{corr.}}$ . It should be noted that the anodic and cathodic current densities on any particular component might be very different. That is, attack of a component is intensified if it is connected to large cathode. The combination of large cathode/small anode is all too frequently encountered in corrosion process. This conclusion regarding the intensifying effect of large cathode/small anode upon corrosion rate is a general one that is elegantly formulated by equation (3.8) <sup>[26]</sup>:

$$\frac{i_a^B}{i_c^N} = \frac{f^N}{f^B} \left[ \frac{|i_c^N|}{i_a^N} - 1 \right] + \left[ \frac{|i_c^N|}{i_a^N} \right] \quad \dots (3.8)$$

For instance<sup>[26]</sup> if a metal is placed in an aqueous solution containing cations of a more noble metal, i.e. one which is above it in the electrochemical series, then it will displace the more noble ions from solution and itself dissolves. Such a spontaneous reaction is called galvanic displacement and is presented by Fig 3.5. Displacement continues until the baser metal is with a “flash” porous coating of the more noble one, possibly 1 μm or so in thickness, where upon further reaction substantially ceases. Iron dipped into a copper solution rapidly develops a flash coating of copper, whilst copper dipped into silver nitrate acquires a black deposit of finely divided silver within seconds. The structures of these coatings correspond closely to these obtained at high  $i/i_L$  values. They are therefore frequently non-adherent or only loosely so. In these instances the reaction is soon over but, when two different solid metals are in contact with one another, the consequences can be more

disastrous. For a noble<sup>[5,69]</sup> metal N and a base metal B immersed in a corrodent, the corrosion of the resulting polyelectrode can be represented by equation (3.8) given previously. If the cathodic process takes place readily on the noble metal, i.e. the term in brackets is positive, a small area of B connected to a large one of N ( $f^B \ll f^N$ ) results in an intense attack of B such might occur. For example, if a small area of steel or cast iron, in electrical contact with a much larger area of bronze, were immersed in seawater, the cathodic reactant being dissolved oxygen. Or again, if aluminum rivets were used in a steel structure exposed to weather, the rivets would corrode preferentially whenever the structure got wet. Both are examples of galvanic attack (bimetallic corrosion). The intensification of attack of the baser metal depends on:

- a. The relative area ( $f^N/f^B$ ) and
- b. The relative electrochemical activities of the metals concerned.

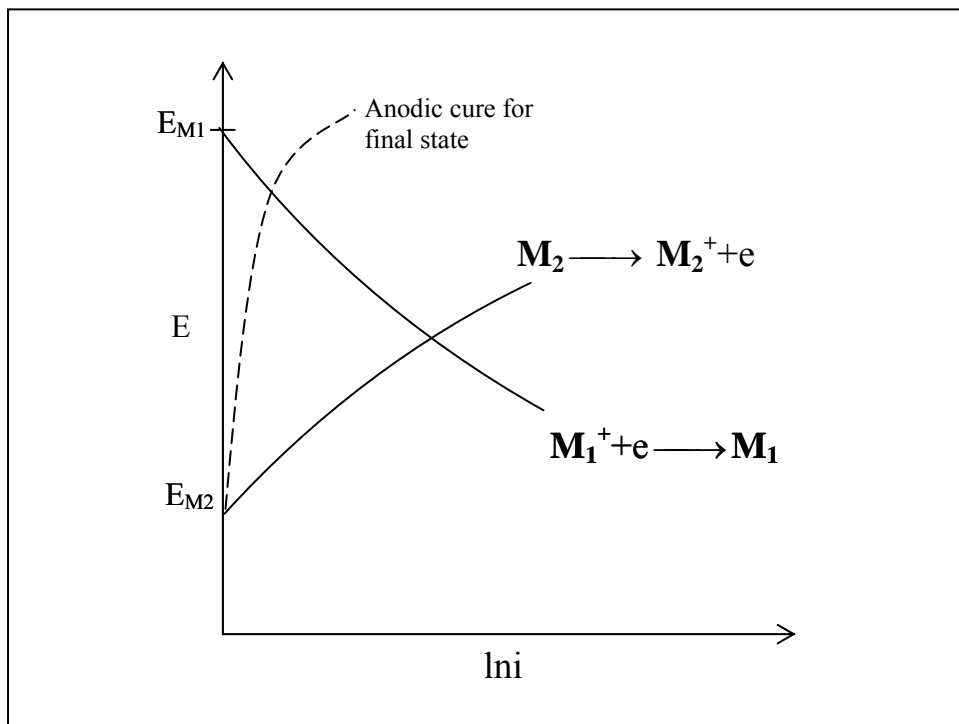


**Figure3-5** Galvanic Displacement <sup>[21]</sup>.

### **3.4 Factors affecting galvanic corrosion** <sup>[6,71,72]</sup>

Many factors including the electrochemical ones determine whether or not galvanic corrosion will occur, as follows:

#### **3.4.1 Electrode Potentials** <sup>[62]:</sup>

The standard electrode potential of a metal in a solution of its ions gives a rough guide to the position of the metal in a galvanic series. In practice however we usually concerned with alloys rather than pure metals and in environments that do not contain the metal ions. To check the best method of obtaining a “galvanic series” of potentials is to actually measure these potentials in the environment under consideration.

#### **3.4.2 Reaction kinetics** <sup>[69]:</sup>

Electrode Potential data will indicate whether or not galvanic corrosion can occur. The reaction kinetic data indicate how quickly corrosion can take place. The metal dissolution kinetics give information on the rate of the anodic reaction in the corrosion cell; the oxygen reduction or hydrogen evolution overpotentials on the metals or alloys involved, or both, give information on the rate of cathodic reactions and whether they will occur on one or both materials.

#### **3.4.3 Alloy Composition** <sup>[63]:</sup>

The composition of an alloy affects galvanic corrosion by directly affecting the alloys corrosion resistance. In addition the constituents affect the corrosion potential and the kinetics of the cathodic processes involved, minor constituents can play an important role in this respect.

#### **3.4.4 Protective film characteristics <sup>[22]</sup>:**

The characteristics of the protective film, which exists on most metals and alloys, are important in determining whether or not galvanic corrosion will occur and what form it will take, for example, general or localized, in a particular environment. In particular the potential dependence and resistance to various solution constituents are important.

#### **3.4.5 Mass Transport <sup>[71]</sup>:**

Depending on the particular system being considered, one, two, or all of the three forms of mass transport, migration, diffusion, and convective can play an important role in galvanic corrosion.

#### **3.4.6 Bulk Solution Environment <sup>[63]</sup>:**

Included in this group are factors such as the solution temperature, volume, height above the couple, and the flow rate across the surface. All these can affect whether or not galvanic corrosion can occur to any great extent.

#### **3.4.7 Bulk Solution properties <sup>[62]</sup>:**

This group of factors is one of the most important; the oxygen level, and pH. The corrosivity of the solution determines whether corrosion can occur, and the conductivity determines the geometric extent to which it can occur.

#### **3.4.8 Total Geometry <sup>[72,73]</sup>:**

One of the most important parameters in galvanic corrosion is the “area ratio”. A high cathode to anode ratio usually resulting in rapid corrosion or high anode (base) to cathode noble ratio giving lower corrosion <sup>[28]</sup>. If the area of the less noble material is large compared to

that of more noble (cathodic) the corrosive effect is greatly reduced, and may in fact become negligible. Conversely a large area of noble (base) metal in contact with a small area of less noble (base) will accelerate the galvanic corrosion rate<sup>[71]</sup>. Distribution of the area is obviously important as is surface shape and condition. The number of galvanic cells in a given system is also important<sup>[63]</sup>.

### 3.5 Corrosion inhibitor:

#### 3.5.1 Introduction

The use of chemical inhibitors to decrease the rate of corrosion processes is quite varied. In the oil extraction and processing industries, inhibitors have always been considered to be the first line of defense against corrosion. A great number of scientific studies have been devoted to the subject of corrosion inhibitors. However, most of what is known has grown from trial and error experiments, both in the laboratories and in the field. Rules, equations, and theories to guide inhibitor development or use are very limited<sup>[74,75,76]</sup>.

By definition, a corrosion inhibitor is a chemical substance that, when added in small concentration to an environment, effectively decreases the corrosion rate. The efficiency of an inhibitor can be expressed by a measure of this improvement<sup>[24,74]</sup>:

$$\text{Inhibitor efficiency (\%)} = 100 \frac{CR_{\text{uninhibited}} - CR_{\text{inhibited}}}{CR_{\text{uninhibited}}} \quad \dots (3.9)$$

where  $CR_{\text{uninhibited}}$  corrosion rate of the uninhibited system

$CR_{\text{inhibited}}$  corrosion rate of the inhibited system

In general, the efficiency of an inhibitor increases with an increase in inhibitor concentration (e.g., a typically good inhibitor would give 95% inhibition at a concentration of 0.008% and 90% at a concentration of 0.004%). A synergism, or cooperation, is often present between different inhibitors and the environment being controlled, and mixtures are the usual choice in commercial formulations. The scientific and technical corrosion literature has descriptions and lists of numerous chemical compounds that exhibit inhibitive properties. Of these, only very few are actually used in practice. This is partly because the desirable properties of an inhibitor usually extend beyond those simply related to metal protection. Considerations of cost, toxicity, availability, and environmental friendliness are of considerable importance. Commercial inhibitors are available under various trade names and labels that usually provide little or no information about their chemical composition. It is sometimes very difficult to distinguish between products from different sources because they may contain the same basic anticorrosion agent<sup>[74,77,78]</sup>. Commercial formulations generally consist of one or more inhibitor compounds with other additives such as surfactants, film enhancers, de-emulsifiers, oxygen scavengers, and so forth. The inhibitor solvent package used can be critical in respect to the solubility/ dispersibility characteristics and hence the application and performance of the products<sup>[74,79]</sup>.

### **3.5.2 Classification of Inhibitors**

Inhibitors are chemicals that react with a metallic surface, or the environment this surface is exposed to, giving the surface a certain level of protection. Inhibitors often work by adsorbing themselves on



the metallic surface, protecting the metallic surface by forming a film. Inhibitors are normally distributed from a solution or dispersion. Some are included in a protective coating formulation. Inhibitors slow corrosion processes by increasing the anodic or cathodic polarization behavior (Tafel slopes), reducing the movement or diffusion of ions to the metallic surface. Increasing the electrical resistance of the metallic surface inhibitors have been classified differently by various authors. Some authors prefer to group inhibitors by their chemical functionality, as follows<sup>[74,80,81]</sup>:

*Inorganic inhibitors.* Usually crystalline salts such as sodium chromate, phosphate, or molybdate. Only the negative anions of these compounds are involved in reducing metal corrosion. When zinc is used instead of sodium, the zinc cation can add some beneficial effect. These zinc-added compounds are called mixed-charge inhibitors<sup>[81]</sup>.

*Organic anionic.* Sodium sulfonates, phosphonates, or mercapto-benzotriazole (MBT) are used commonly in cooling water and antifreeze solutions.

*Organic cationic.* In their concentrated forms, these are either liquids or waxlike solids. Their active portions are generally large aliphatic or aromatic compounds with positively charged amine groups.

However, by far the most popular organization scheme consists of regrouping corrosion inhibitors in a functionality scheme as follows<sup>[73]</sup>.

### **a. Passivating (anodic)**

Passivating inhibitors cause a large anodic shift of the corrosion potential, forcing the metallic surface into the passivation range. There are two types of passivating inhibitors: oxidizing anions, such as chromate, nitrite, and nitrate, that can passivate steel in the absence of oxygen and the nonoxidizing ions, such as phosphate, tungstate, and molybdate, that require the presence of oxygen to passivate steel<sup>[18,82]</sup>.

These inhibitors are the most effective and consequently the most widely used. Chromate-based inhibitors are the least-expensive inhibitors and were used until recently in a variety of applications (e.g., recirculation-cooling systems of internal combustion engines, rectifiers, refrigeration units, and cooling towers). Sodium chromate, typically at concentrations of 0.04 to 0.1%, was used for these applications. At higher temperatures or in fresh water with chloride concentrations above 10 ppm higher concentrations are required. If necessary, sodium hydroxide is added to adjust the pH to a range of 7.5 to 9.5. If the concentration of chromate falls below a concentration of 0.016%, corrosion will be accelerated. Therefore, it is essential that periodic colorimetric analysis be conducted to prevent this from occurring. In general, passivation inhibitors can actually cause pitting and accelerate corrosion when concentrations fall below minimum limits. For this reason it is essential that monitoring of the inhibitor concentration be performed<sup>[24,74,82,83]</sup>.

### **b. Cathodic**

Cathodic inhibitors either slow the cathodic reaction itself or selectively precipitate on cathodic areas to increase the surface impedance and limit the diffusion of reducible species to these areas. Other cathodic inhibitors, ions such as calcium, zinc, or magnesium,

may be precipitated as oxides to form a protective layer on the metal. Oxygen scavengers help to inhibit corrosion by preventing the cathodic depolarization caused by oxygen. The most commonly used oxygen scavenger at ambient temperature is probably sodium sulfite ( $\text{Na}_2\text{SO}_3$ ).

### **c. Organic**

Both anodic and cathodic effects are sometimes observed in the presence of organic inhibitors, but as a general rule, organic inhibitors affect the entire surface of a corroding metal when present in sufficient concentration. Organic inhibitors, usually designated as *film-forming*, protect the metal by forming a hydrophobic film on the metal surface. Their effectiveness depends on the chemical composition, their molecular structure, and their affinities for the metal surface. Because film formation is an adsorption process, the temperature and pressure in the system are important factors. Organic inhibitors will be adsorbed according to the ionic charge of the inhibitor and the charge on the surface. Cationic inhibitors, such as amines, or anionic inhibitors, such as sulfonates, will be adsorbed preferentially depending on whether the metal is charged negatively or positively. The strength of the adsorption bond is the dominant factor for soluble organic inhibitors<sup>[21,24,83,84]</sup>.

### **d. Precipitation inhibitors**

Precipitation-inducing inhibitors are film-forming compounds that have a general action over the metal surface, blocking both anodic and cathodic sites indirectly. Precipitation inhibitors are compounds that cause the formation of precipitates on the surface of the metal, thereby providing a protective film. Hard water that is high in

calcium and magnesium is less corrosive than soft water because of the tendency of the salts in the hard water to precipitate on the surface of the metal and form a protective film<sup>[81,85,86]</sup>.

The most common inhibitors of this category are the silicates and the phosphates. Sodium silicate, for example, is used in many domestic water softeners to prevent the occurrence of *rust water*. In aerated hot water systems, sodium silicate protects steel, copper, and brass. However, protection is not always reliable and depends heavily on pH and a saturation index that depends on water composition and temperature. Phosphates also require oxygen for effective inhibition. Silicates and phosphates do not afford the degree of protection provided by chromates and nitrites; however, they are very useful in situations where nontoxic additives are required<sup>[74]</sup>.

#### **e. Volatile corrosion inhibitors**

Volatile corrosion inhibitors (VCIs), also called vapor phase inhibitors (VPIs), are compounds transported in a closed environment to the site of corrosion by volatilization from a source. In boilers, volatile basic compounds, such as morpholine or hydrazine, are transported with steam to prevent corrosion in condenser tubes by neutralizing acidic carbon dioxide or by shifting surface pH toward less acidic and corrosive values. In closed vapor spaces, such as shipping containers, volatile solids such as salts of dicyclohexylamine, cyclohexylamine, and hexamethylenamine are used. On contact with the metal surface, the vapor of these salts condenses and is hydrolyzed by any moisture to liberate protective ions. It is desirable, for an efficient VCI, to provide inhibition rapidly and to last for long periods. Both qualities depend on the volatility of these compounds, fast action wanting high volatility, whereas enduring protection requires low

volatility<sup>[74, 81]</sup>. *Phenylthiourea* is best example as organic inhibitor. It has been used as inhibitor in the present work.

### **3.6 Application of Inhibitors for Acid Media**

Acid solutions are widely used in industry, the most important fields of application being acid pickling, industrial acid cleaning, acid descaling and oil well acidizing. Because of general aggressivity of acid solutions the practice of inhibition is commonly used to reduce the corrosive attack on metallic materials. The selection of appropriate inhibitors mainly depends on the type of acid, its concentration, temperature, and velocity of flow, the presence of dissolved inorganic and/or organic substances even in minor amount and, of course, on the type of metallic material exposed to the action of the acidic solutions. Among the commercially available acids and the most frequently used are hydrochloric, sulphuric, nitric, hydrofluoric, citric, formic and acetic acid<sup>[88]</sup>.

At present time hydrochloric acid is the most important pickling acid. Large scale continuous treatment such as metal strip and wire pickling, as well as economic advantages in the regeneration of depleted pickling solutions- a factor of increasing economic and ecological importance- were the main reasons why hydrochloric acid gradually replaced sulphuric acid in its former leading role as a pickling acid. Other acids, such as nitric, phosphoric, sulphamic, oxalic, tartaric, citric, acetic and formic acid are used only for special applications<sup>[88]</sup>.

#### **3.6.1 Hydrochloric acid**

Effective inhibitors in the corrosion prevention of iron and steel on treatment with HCl mainly belong to the group of nitrogen-containing

compounds, such as alkyl and aryl amines, saturated and unsaturated nitrogen ring compounds, condensation products of amines (mainly aryl amines like aniline toluidines, etc.) with aldehydes (mainly formaldehyde) and ketones (e.g., cyclohexanone), nitriles, aldoximes and ketoximes, thiourea, phenylthiourea and imidazolin derivatives.

In the case of n-alkylammonium salts, n-alkyl-trimethylammonium salts as well as other quaternary alkyl-acid corrosion of steel generally increases with increasing n-alkyl chain-length, with a maximum efficiency at C<sub>10</sub>-C<sub>12</sub>.

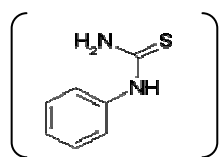
Highly effective nitrogen-containing inhibitor compounds include alkylamines, benzylquinolinium and alkylbenzylquinolinium halides, n-alkyltrimethylammonium, n-alkylpyridinium and n-alkylisoquinolinium halides with chain length of the alkyl part usually C<sub>8</sub>-C<sub>12</sub>. These inhibitors are applied in concentration of 10<sup>-4</sup>-5\*10<sup>-3</sup> mol/L<sup>[88]</sup>.

The outstanding characteristics of the above mentioned acetylenic compounds are their excellent efficiency at temperature up to 100 °C. Therefore, in commercial inhibitors recommended for use in hydrochloric acid at elevated or high temperatures acetylenic compounds very often will be present. The excellent high temperature efficiency of propargyl derivatives is explained by Fe-complex catalysed formation of protective polymer films, a reaction which is favored with increasing temperature<sup>[88,89]</sup>.

The dissolution of copper and brass in hydrochloric acid can be effectively inhibited using sulphur- containing compounds. Good results are obtained with thiourea and its derivatives, benzimidazoles, and 2-mercaptobenzothiazole, phenylthiourea being the most effective for both copper and brass in HCl solution up to 7M.

Effective inhibitors for aluminum in hydrochloric acid exhibit even better efficiency for zinc in the same solution<sup>[88]</sup>.

### 3.6.2 Phenylthiourea



Synonyms: phenylthiocarbamide, N-phenylthiourea, 1-phenyl-2-thiourea, **PHTU**, TU, PTC, alpha- phenylthiourea and 1- phenylthiourea. Molecular formula: C<sub>7</sub>H<sub>8</sub>N<sub>2</sub>S [Structural: C<sub>6</sub>H<sub>5</sub>NHCSNH<sub>2</sub>] and its physical data: melting point is 150 °C, specific gravity is 1.3 and stable<sup>[89,90]</sup>.

### 3.7 Corrosion Inhibition Mechanism

**1. Adsorption theory:** the adsorption theory of protective activity has been proposed by most of investigators, which say that inhibitors are adsorbed on the metal surface forming protective layer. The adsorption was considered either as physical adsorption or chemisorptions.

The physical adsorption may be due to adsorbed species and the electric charge on the metal at the metal/solution interface, that is, on the so called "null –charge potential" ( $E_{\text{corr.}} - E_q = 0$ ) on the surface of the anodic or the cathodic section of the corroding metal. Physical adsorption does not involve the bonding on the electrode but require electrical variables viz., potential or charge on the electrode. Thus, if under corrosion conditions the metal surface is (-ve.) charge, the adsorption of cations is favored, and if the surface carries (+ve.) charge, the adsorption of anion takes place. At a surface charge close to zero relative to solution, adsorption of both molecules and ions is possible. The deciding factor in choosing an adsorption inhibitor is, therefore the potential of the metal with respect to the solution, and this depends on ( $E_{\text{corr}}$ ) and ( $E_q$ ) for the metal and electrolyte under consideration. Besides electrostatics

interaction, inhibitors can bond to metal surface by electron transfer to the metal to form a coordinate type of link. This process is favored by the presence in the metal of vacant electron orbital of low energy, such as occurs in the transition metals; and by availability for relatively loosely bound electrons, such as may be found in anions, and natural organic molecules containing lone pair electrons or pi-electron systems with multiple, especially triple bond or aromatic rings.

This theory cannot explain mechanism of inhibitor action fully as many of the surface active substance<sup>[81,84]</sup>.

**2. Film theory:** This theory assumes that the effective protection of the metals by inhibitors is due to the formation on the metal surface of a layer of insoluble or slightly soluble corrosion products. However, in all cases, a preliminary stage of adsorption of the inhibitor can be envisaged and to the extent, the adsorption theory has fulfilled its purpose<sup>[74,81,93,94]</sup>.

**3. Hydrogen overvoltage theory:** This theory postulates that inhibitors that are adsorbed on the metal retard either anodic or cathodic or in some cases both reactions. This leads to rapid polarization of anodic or cathodic sites and thus overall corrosion rate is retarded<sup>[21]</sup>. Many known inhibitors are however, cathodic polarizer having no direct action on the anodic reaction. They block the cathodic regions on the metal surface and suppress the hydrogen evolution reaction correspondingly, the anodic reaction is reduced, and hence there is inhibition of corrosion<sup>[84]</sup>.

### **3.8 Types of corrosion inhibitor**

In corrosion inhibition addition, of a certain chemicals in small quantity are made to the corrosive environment which causes a substantial reduction in the rate of corrosion of a metal either by reducing



the probability of its occurrence or by reducing the rate of attack or by doing both. It should, however, be noted that the environment can in some cases, be made less aggressive by other methods, removal of dissolved oxygen, or adjustment of PH, while using a corrosion inhibitor for a specific problem. It is essential to make proper selection of corrosion inhibitor, as no universal corrosion inhibitor exists. Moreover, inhibitors that are valuable for some corrosion problems can be harmful to other under certain situation. In low concentration, inhibitors are often found to function as corrosion stimulators. However when various methods of protecting metals are inapplicable, corrosion inhibitors can sometimes be employed to advantage<sup>[35]</sup>.

It is well known that corrosion is an electrochemical phenomenon, hence inhibitor may be defined as a decrease of the velocity of electrochemical electrode reaction, from kinetic point of view, and inhibitor may be defined more accurately by corresponding decrease of the velocity of partial steps of electrode reactions. For convenience all kinds of substances which cause inhibition could be called inhibitor<sup>[81]</sup>.

Depending on the mechanism of their inhibiting action on the electrochemical corrosion, inhibitor can be classified as (i) anodic type (ii) cathodic type and (iii) mixed type as shown in **Fig.3-8** according to their nature. Inhibitors can be differentiated as soluble and insoluble, acidic, basic and natural, volatile and nonvolatile, organic and inorganic etc.

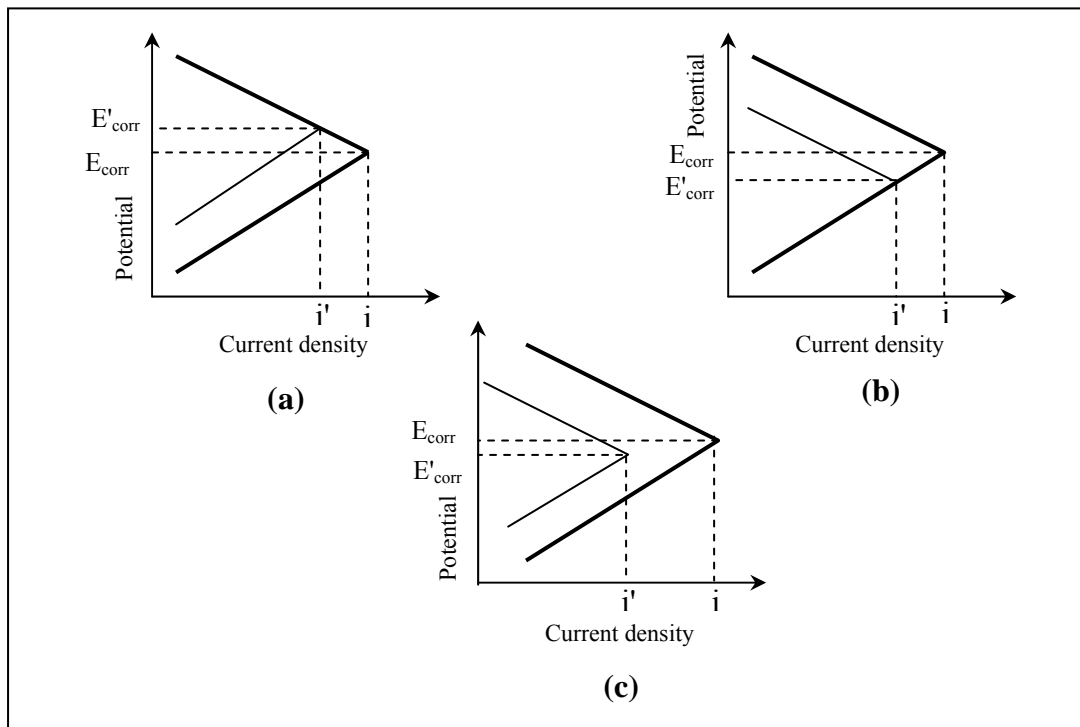


**Figure 3-6** Mechanism of action of corrosion inhibitors based on polarization effects (a) Anodic inhibitors. (b) Cathodic inhibitors. (c) Mixed inhibitors<sup>[84]</sup>.

### 3.8.1 Anodic Inhibitor

Those substances, which reduce the anode area by acting on the anodic sites and polarize the anodic reaction, are called anodic inhibitors. They displace the corrosion potential ( $E_{\text{corr}}$ ) in the positive direction and reduce corrosion current ( $i_{\text{corr}}$ ), thereby retard anodic reaction and suppress the corrosion rate. Anodic inhibitors are primarily inhibitors (inorganic) of oxidizing action. As oxidants they have a twofold nature, viz. (i) they act as good depolarizers and therefore, accelerate the cathodic process (corrosion simulators), and (ii) they also lead to the formation of protective film on the anode (chemical passivators). In other words, they function either as cathodic simulators or anodic inhibitor. Their resulting action can therefore be different depending on condition<sup>[21]</sup>.

### 3.8.2 Cathodic inhibitor

Those substances which reduce the cathodic area by acting on the cathodic sites and polarize the cathodic reaction are called cathodic inhibitors. They displace the corrosion potential ( $E_{\text{corr.}}$ ) in the negative direction and reduce the corrosion current ( $i_{\text{corr.}}$ ), thereby retard cathodic reaction and suppress the corrosion rate<sup>[21,81]</sup>.

Cathodic inhibitors may be divided into three categories, viz

(i) Those which absorb oxygen (deaerators or oxygen scavengers), examples of this type of inhibitor are sodium sulphite and hydrazine which remove dissolved oxygen from aqueous solution according to the reaction :



(ii) Those which reduce the area of the cathode. Examples of this type of inhibitor include  $\text{Ca}(\text{HCO}_3)_2$ ,  $\text{ZnSO}_4$  and some other compounds with cations that migrate toward the cathode surface and react with cathodically formed alkali(mild) to produce insoluble protective film.



(iii) Those which increase hydrogen overpotential of the cathodic process (hydrogen-evolution poison). Examples of this type include arsenic, bismuth and antimony ions which specially retard the hydrogen evolution reaction<sup>[21,24]</sup>.

### 3.8.3 Mixed inhibitor

Those substances, which affect both the cathodic and anodic reactions, are called mixed inhibitors. Such mixed inhibitors include the commercially available polyphosphates. Potential change in such a case is smaller and its direction is determined by the relative size of the anodic and cathodic effects <sup>[21,24]</sup>.

## 3.9 Oxygen Reduction and Transport

Most aqueous solutions (ranging from bulk natural water and chemical solutions to thin condensed films of moisture) are in contact with the atmosphere and will contain dissolved oxygen, which can act as a cathode reactant. The solubility of oxygen in water decreases significantly with the increase in temperature and slightly with concentration of dissolved salts. On the other hand, the concentration of  $H_3O^+$  in acid solution, which is given by the PH, is high, and since this ion has a high rate of diffusion; its rate of reduction is normally controlled by the activation energy for electron transfer. Furthermore, the vigorous evolution of hydrogen that occurs during corrosion facilitates transport, so that the diffusion is not a significant factor in controlling the rate of the reaction except at very high current densities. As PH in acid solution increases, the hydrogen evolution reaction becomes kinetically more difficult and requires a high overpotential. Oxygen reduction is more significant than hydrogen evolution in near-neutral solutions, and that in the case of the former, transport of oxygen to the metal surface will be more significant than activation-controlled electron transfer. A further important factor is that in near-neutral solutions solid corrosion product will be thermodynamically stable and will affect the corrosion rate either by passivating the metal or by forming barrier that hinders transport of oxygen to the metal surface <sup>[5,81]</sup>

The rate of corrosion processes with oxygen depolarization is determined mostly by the rate of oxygen diffusion to the metal surface. This kind of corrosion is extremely important, since it includes practically important process such as corrosion of iron and steel in neutral salts solutions, corrosion of zinc in several neutral solutions, various cases of copper corrosion. In the majority of practical cases, the concentration of oxygen in the solution corresponds to the oxygen solubility in particular electrolyte. If the solution has a certain amount of oxygen, but the system is closed so that no additional oxygen can enter the system, then the corrosion process with oxygen depolarization can proceed only until the oxygen supply is exhausted. When the metal is placed in open container, oxygen can reach the cathodic sections by means of diffusion from the air through the solution, and the corrosion process might cause complete destruction of the metal. The transport of oxygen from the atmosphere to the metal solution interface involves the following steps<sup>[81]</sup>.

1. Transport of oxygen across the atmosphere /solution interface.
2. Transport through the solution (by diffusion and by natural and forced convection) to the diffusion layer.
3. Transport across the static solution at the metal /solution interface (the diffusion layer  $\delta_d$ ) by diffusion.

The process involves the following reactions<sup>[5,81,95,96]</sup>:

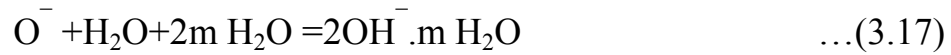
- 1) For the cathode polarization, diffusion of oxygen from the solution toward the cathode  $O_2 = O_2$  ... (3.14)

- 2) Adsorption of oxygen and dissociation of molecules into atoms:





Formation of hydroxyl ion:



4) Transfer of hydroxyl ions from the cathode into the bulk of the solution:



### 3.10 Electrochemical Measurements in Flowing Solutions

Electrochemical measurements are now widely used in most fields of corrosion. Detailed reviews are available which deal with the application of electrochemical techniques in general or specifically to pitting, galvanic corrosion, intergranular corrosion, crevice corrosion, stress corrosion cracking and high temperature high pressure situation. Electrochemical measurements in flowing solutions can provide data on (a) the rate of general corrosion and the possibility of other forms of attack, (b) mechanism by using the effect of flow as a diagnostic criterion, (c) the characteristic hydrodynamic parameters, e.g. the rate of mass transfer, the degree of turbulence or the surface shear stress, and (d) the composition of the solution by electro-analytically monitoring compositions or measuring redox potentials, pHs, etc<sup>[97]</sup>.

Apparatus for examining the effects of flow on corrosion is similar to that used in static tests except that either the specimen (rotating cylinders and discs) or the solution must be moved, and more thought must be given to the placement of reference and counter electrodes<sup>[98]</sup>.

### 3.10.1 The Rotating Cylinder Electrode

The rotating cylinder electrode is operated in the turbulent flow regime at  $Re > 200$ <sup>[99]</sup>, although flow can be complicated with vortexing until much higher  $Re$ , where true turbulence develops. A  $Re > 200$  is readily achieved at modest rotation rates and cylinder diameters. Therefore the cylinder can be readily utilized by the corrosion engineer to simulate corrosion conditions in turbulent pipes. For the smooth rotating cylinder electrode, the mass transport correlation is given by Eisenberg<sup>[100]</sup>. However, surface roughening increases mass transport.

$$Sh = 0.079 Re^{0.7} Sc^{0.36} \quad \dots(3.19)$$

This correlation is valid within the following range:  $1000 < Re < 100000$  and  $850 < Sc < 11490$ . Recalling that the limiting current density is given by:

$$i_L = nFK\Delta C \quad \dots(3.20)$$

and that  $K$  is given by

$$K = Sh \times \frac{D}{d} \quad \dots(3.21)$$

So that

$$i_L = \frac{nFD\Delta C}{d} Sh \quad \dots(3.22)$$

It is easy to show that the limiting current density can be expressed entirely in terms of very accessible parameters:  $D$ ,  $\Delta C$ ,  $d$ ,  $U$ , and  $\nu$ , again, assuming that  $C_s = 0$ :

$$i_L = 0.079 nFC_b (U)^{0.7} (D)^{0.64} (\nu)^{-0.34} (d)^{-0.3} \quad \dots(3.23)$$

If the characteristic dimension is taken as the radius of the cylinder,  $r$  ( $U=rw$ ), throughout the calculation where  $d=2r$  we have

$$i_L = 0.064 nFC_b (w)^{0.7} (D)^{0.64} (v)^{-0.34} (r)^{-0.4} \quad \dots(3.24)$$

Hence if the corrosion rate is determined by the mass transport of cathodic reactant to the cylinder surface, then the corrosion rate will increase as a function of the rotation rate raised to the 0.7 power and linearly with dissolved reactant concentration. Increasing the velocity by a factor of ten increases the corrosion rate by a factor of five. Silverman<sup>[101]</sup> has shown that the velocity of the rotating cylinder necessary to match the mass transport conditions for pipe flow, assuming the Eisenberg correlation applies, is given by:

$$U_{cyl} = 0.11845 \left( \left( \frac{\rho}{\nu} \right)^{0.25} \left( \frac{d_{cyl}^{0.429}}{d_{pipe}^{0.179}} \right) Sc^{-0.0857} \right) U_{pipe}^{1.25} \quad \dots(3.25)$$

Useful velocity conversions in order to have equality of mass transport conditions between the rotating cylinder and the annulus and impinging jet are also reported by Silverman.

The rotating cylinder electrode utilized a specimen with a fixed diameter. Consequently, all points on the surface are exposed to the same surface velocity (excluding surface roughness effects). The RCE can be used to simulate flowing conditions present in other geometries if flow in those geometries is tangential to the electrode surface by using in the appropriate rotation rate. The surface shear stress for the rotating cylinder is given as<sup>[98]</sup>:



$$\tau(\text{kg} / \text{m.s}^2) = \text{const.} \frac{f}{2} \rho \omega^2 r^2 \quad \dots(3.26)$$

where  $f$  is the friction factor. The Re number and the surface roughness are important factors in determining the surface shear stress. For a smooth cylinder,  $f/2$  is equal to  $0.079\text{Re}^{-0.3}$ <sup>[102]</sup>. Substitution of the relationship gives the following expression for shear stress:

$$\begin{aligned} \tau(\text{kg} / \text{m.s}^2) &= 0.079 \text{Re}^{-0.3} \rho \omega^2 r^2 \\ &= 0.079 \left( \frac{2r^2 \omega \rho}{\mu} \right)^{-0.3} \rho \omega^2 r^2 \end{aligned} \quad \dots(3.27)$$

Rearranging yields

$$\tau = 0.064(r^{1.4})(\rho^{0.7})(\omega^{1.7})(\mu^{0.3}) \quad \dots(3.28)$$

where the shear stress is given in terms of the fluid density,  $\rho$ , the angular velocity,  $\omega$ , the fluid viscosity,  $\mu$ , and the cylinder radius,  $r$ . Note that the shear stress will increase as a function of the rotation rate raised to the 1.7 power. In contrast, the limiting current density increases with velocity raised to the 0.7 power for the RCE.

### 3.10.2 The Rotating Disk Electrode

The rotating disk electrode (RDE) is an important system in electrochemistry. Axial followed by radial flow across the disk brings fresh solution to all points across the disk. The surface is therefore uniformly accessible to reacting species. The RDE operates under laminar flow for  $\text{Re} < 1.7 \times 10^5$ . Flow is turbulent above  $3.5 \times 10^5$  and is transitional in between<sup>[99]</sup>. Thus the system is less practical for the study of corrosion under turbulent conditions but enjoys widespread use in research electrochemistry. For the rotating disk electrode, the laminar

mass transport correlation obtained in the literature is given by Levich<sup>[103]</sup>:

$$\text{Sh} = 0.621 \text{Re}^{0.5} \text{Sc}^{0.33} \quad \dots (3.29)$$

or that

$$i_L = 0.621 \frac{nFd\Delta C}{d} \text{Re}^{0.5} \text{Sc}^{0.33} \quad \dots(3.30)$$

Moreover, it is easy to show that the limiting current density is expressed entirely in terms of readily obtained parameters:  $D$ ,  $\Delta C = C_b - C_s$ ,  $\omega$ , and  $\nu$ . Recall that  $C_s = 0$  when the limiting c.d. is reached, yielding

$$i_L = 0.621(nF)(D^{2/3})(C_b) (\nu^{-1/6}) (\omega)^{1/2} \quad \dots(3.31)$$

Flow is not uniform across the RDE. At high speeds the edges may be in turbulent flow, and the shear stress should vary with radial position. An average velocity or Re number value must be used in order to characterize the flow. Consequently, the RDE is not favored for studying corrosion controlled by shear stresses<sup>[103, 104]</sup>.

# Chapter Four

## Experimental Work

### 4.1 Introduction

The present chapter illustrates the experimental work as well as the laboratory design of Galvanic Corrosion Inhibition system.

Experimental work was carried out to determine the corrosion rate of copper, carbon steel and zinc specimens under static and flow conditions for rpm = 0, 500, 1000, and 1500 with PHTU inhibitor concentration of (0, 0.001, 0.05 and 0.15) g/L, and area ratio of metal specimen of 2, 1, 0.5 and 0.25 using weight loss and electrochemical polarization methods then all the above tests were carried out in aerated 0.1N HCl. Turbulent flow was chosen because of its practical importance. The experimental work was divided into five main parts:

1. Weight loss measurements of single metals (free corrosion) to determine the average corrosion rates and corrosion potential under static, rotating without and with PHTU inhibitor at isothermal conditions.
2. Measuring the current, potential difference and corrosion rate of couple metals under available rotating velocity with and without PHTU inhibitor concentration at isothermal conditions.
- 3- Measuring the potential and current simultaneously in galvanic corrosion.
4. Electrochemical polarization measurements of the instantaneous potential corrosion under isothermal conditions for clean surfaces. Also anodic dissolution of copper, carbon steel and zinc specimen was

investigated at different values of rotational velocity, area ratio and PHTU concentration.

5- Measuring galvanic cell resistance.

## 4.2 System Specifications

### a) Working Electrode (cathode):

The working electrode was a tube specimen of copper, carbon steel or zinc the length of the cathode was placed vertically 2 cm and 2.55cm outside diameter .The metal specimen was in the water bath at a depth of 5cm below the solution. The tube specimen of carbon steel and copper is analyzed by Heavy Engineering Equipment Company as follows:

**Table 4-1** Composition of the studied carbon steel alloy

<i>C%</i>	<i>Si%</i>	<i>Mn%</i>	<i>P%</i>	<i>S%</i>	<i>Cr%</i>	<i>Mo%</i>	<i>Ni%</i>	<i>Cu%</i>	<i>V%</i>	<i>Fe%</i>
<i>0.1649</i>	<i>0.2559</i>	<i>0.5027</i>	<i>0.0020</i>	<i>0.0068</i>	<i>0.0251</i>	<i>0.0000</i>	<i>0.0088</i>	<i>0.1505</i>	<i>0.0033</i>	<i>Rem.</i>

**Table 4-2** Composition of the studied copper alloy

<i>Zn%</i>	<i>Fe%</i>	<i>Mn%</i>	<i>Ni%</i>	<i>Cr %</i>	<i>Cu%</i>
<i>0.055</i>	<i>0.01</i>	<i>Nil.</i>	<i>Nil.</i>	<i>Nil.</i>	<i>Rem.</i>

and pure zinc supplied by BDH.

### b) Auxiliary Electrode (anode):

In polarization experiments, the auxiliary electrode was a rod made of high conductivity graphite, 1cm outside diameter, the length of the anode was 8cm, and located vertically opposite to the cathode at the same level.

### c) Reference Electrode:

The cathodic potential was determined with respect to Saturated Calomel Electrode (SCE) .A lugging capillary bridge leading to the

reference electrode was mounted near the center along the cathode length to within ( $\cong 1\text{mm}$ ) from the side of the cathode. The opening of the capillary tube near the sample metal (cathode) was equal to ( $\cong 1\text{mm}$ ) in diameter.

**d) Glass Container:** A container was made of glass with the dimensions ID=22 and Height=30cm.

**e) Water Bath:** A bath was used with a temperature controller up to  $95^{\circ}\text{C}$ .

**f) pH-meter:** A digital pH-meter with three decimal points was used to read hydrogen ion concentration (pH). A calibration procedure was used to calibrate the meter before any measurement using standard buffer solution of pH 2, 7 and 10.

**g) Conductivity meter:** A digital conductivity meter, type *GLASSCO* with a range ( $0.01\mu\text{mho}$  to  $1000\text{mmho cm}^{-1}$  in 5 ranges) was used.

### 4.3 The Electrolyte

**2- Distilled Water.**

**3- Inhibiter:** Phenylthiourea is used as an inhibitor

**4- (a) Hydrochloric Acid:** HCl, Analar hydrochloric acid (33%) supplied by Fluka and Merck was used throughout the present work as a corrosive medium after dilution into 0.1 N solution.

**(b) Hydrochloric Acid:** HCl Technical Hydrochloric acid of concentration 30%, supplied by *Rayon State Establishment, Saddat AL-Hindiyah* as a cleaning electrolyte for the metal specimen (before each test) an HCl of 3% concentration was used, which had been prepared according to the dilution law:

$$C_1 V_1 = C_2 V_2 \quad \dots (4-1)$$

$C_1$  : the first concentration.

$V_1$  : the first volume.

$C_2$  : the second concentration.

$V_2$  : the second volume.

A 20% HCl is needed as a cleaning electrolyte for the metal specimen (after each test), which had been prepared using the same procedure in the above paragraph. Besides an amount of inhibitor (hexamine) was added to the 20% HCl to prevent the corrosion. The best amount of inhibitor added was 60g of hexamine per liter of 20% HCl, where the weight loss was almost zero<sup>[10]</sup>.

#### 4.4 Solvents Used

These are used to clean the metal specimens.

**1- Acetone** :  $C_3H_6O$  of concentration  $\cong 99\%$  supplied by FLUKA.

**2- Ethanol** :  $C_2H_4O$  of concentration  $\cong 99\%$  supplied by FLUKA.

#### 4.5 The Experiments types:

The types of experiments are:

**A-** Galvanic corrosion cell (**Fig.4-1**).

**B-** Potential and current measurements cell (**Fig. 4-2**).

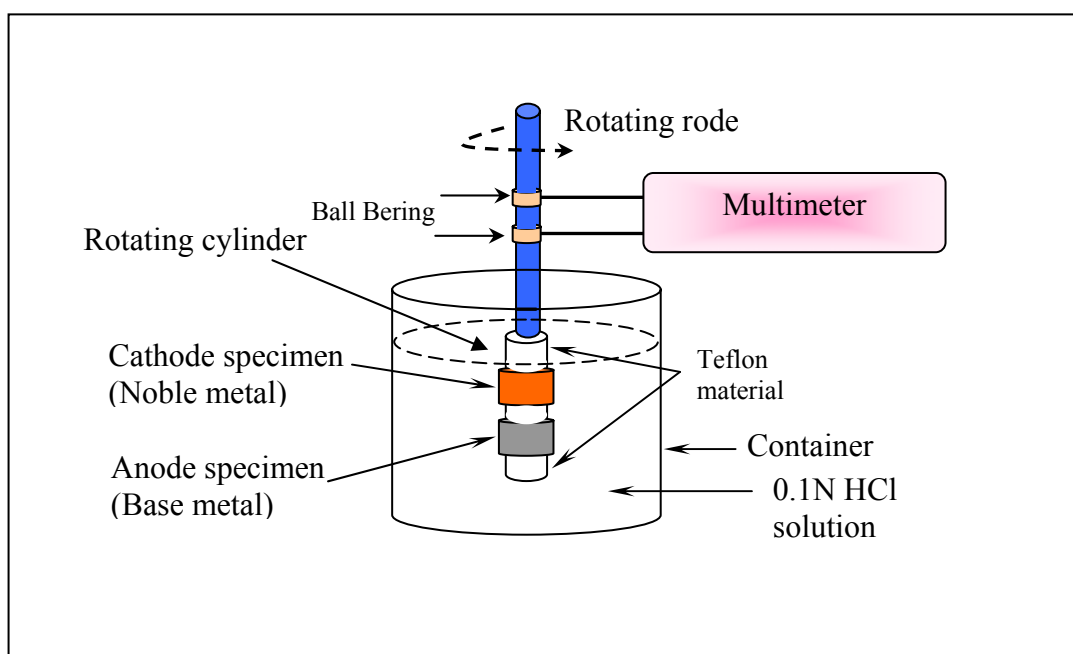


**Figure 4-1** Apparatus for measuring currents and potential between two metals immersed in 0.1N HCl solution

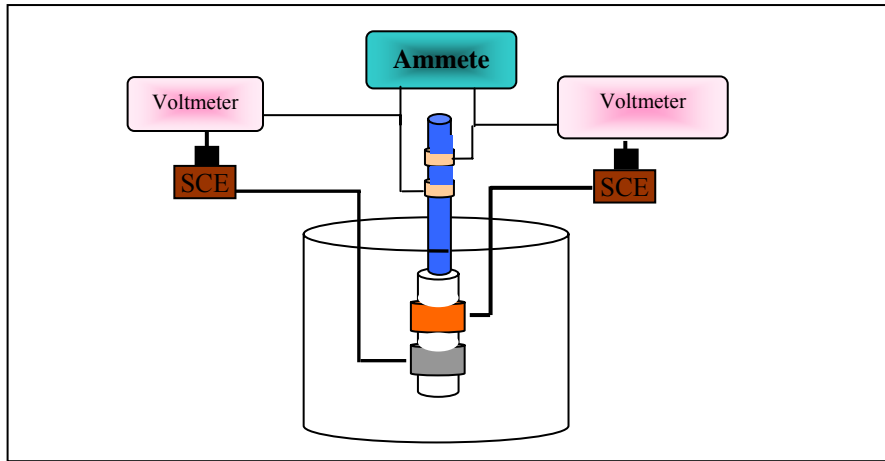


**Figure 4-2** The electrode potentials measured against the SCE and current measurement

**C- Free corrosion circuit**

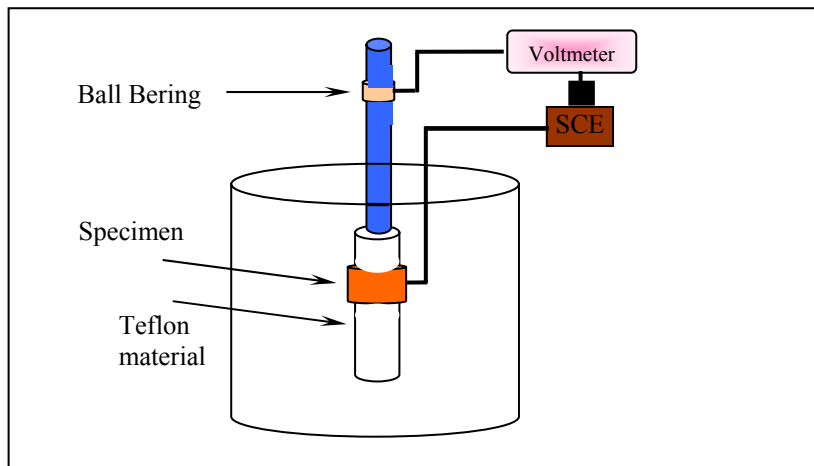


**Figure 4-3** Free corrosion circuit

**D- Polarization circuit:**

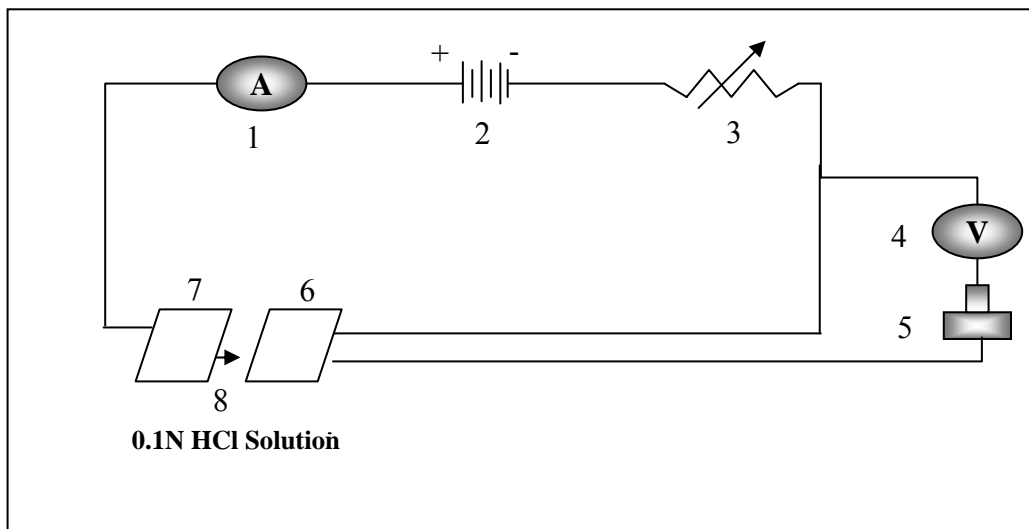


**Figure 4-4** The Electrical Circuit

**Table 4-3** Gives the item number with its details as illustrated in Fig.4.4.

Item No.	Details
1	<i>Multirange Ammeter.</i>
2	<i>D.C Power Supply.</i>
3	<i>Resistance Box.</i>
4	<i>Multirange Voltmeter.</i>
5	<i>Saturated Calomel Electrode (SCE)</i>
6	<i>Cathode</i>
7	<i>Anode</i>
8	<i>0.1N HCl Solution</i>

The following pieces of equipment are required to assemble the corrosion apparatus:

**1) Multirange Ammeter:** A digital Multirange ammeter ( $\approx 1\Omega$  resistor, type 1905 A Thurlby) was used to measure the current passing through the galvanic cell.

**2) Multirange Voltmeter:** Two types of Multirange voltmeter were used, one of these is to measure the potential difference between two metals (type 1905A Thurlby), and the other to measure working electrode/reference potential, type 2830 digital multimeter.

**3) Multirange Resistor (Resistance Box):** A variable resistance (Dambridge type, variable resistance (0-0.1 M $\Omega$ ) with accuracy of 0.1  $\Omega$  was used.

**4) D.C Power Supply:** A filtered D.C power supply which is often equipped with current and voltage limiters offers better stability and control and can be used for applying galvanostatic boundary condition. It is (type 6291 A, Hewlett Packard with a range 0-50V and 5A).



## 4.6 Description of corrosion cell

The description of the galvanic corrosion cell is shown in **Fig. 4-5**. The specimens had been fixed on the rotating and insulated shaft (Teflon material), which designed specially to pass the current to the circuit by two slip rings, then one of them is fixed and the other is rotated (Ball Bearing). The distance between the cathode and anode was 1cm, this has been fixed on insulated rode.

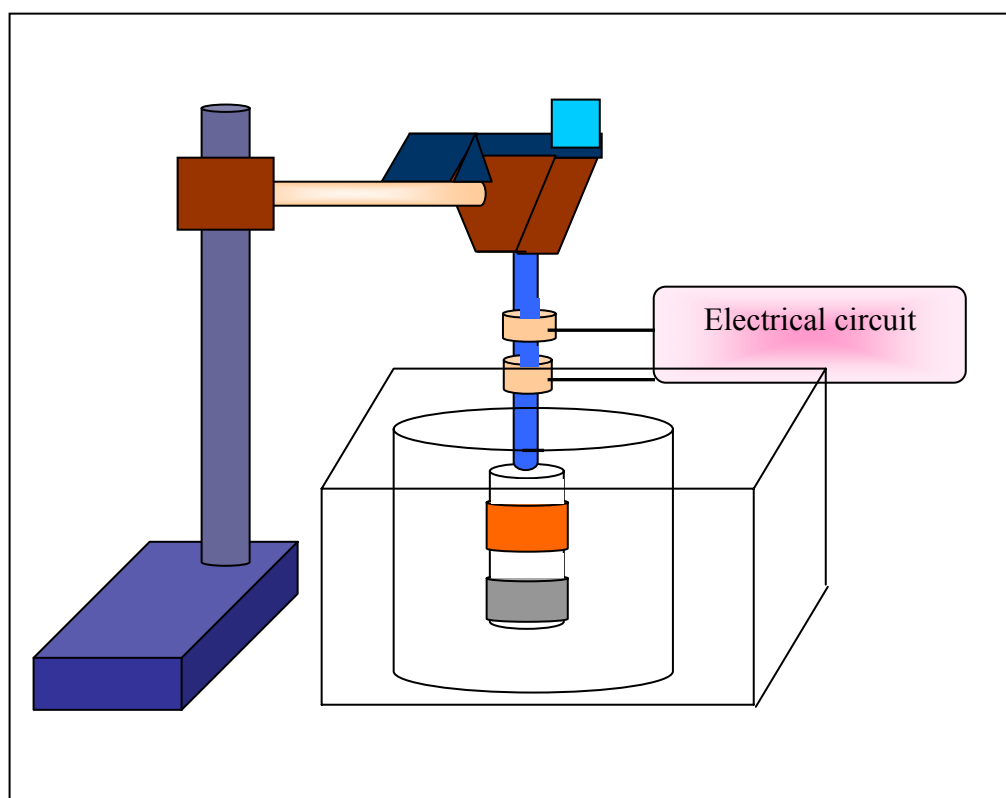


**Figure 4-5** galvanic corrosion cells.

## 4.7 Experimental procedure:

### 4.7.1 Specimen Preparation

Before each experiment, the metal specimen was immersed in 3% HCl for 30 minutes, then washed with distilled water, dried with paper tissue followed by immersing in analar methanol for two minutes, then

dried and immersed in analar acetone for two minutes, and finally left to dry for one hour in the dessicator over silica gel . Weighing the specimen was carried out using digital balance of 0.1 mg accuracy. (Analytical balance type AE260 Delta RANGE, mettler)<sup>[10]</sup>. 14.57ml from 33% HCl solution was diluted to prepare 1.5 L of 0.1NHCl according to the dilution law:  $C_1V_1=C_2V_2$

#### **4.7.2 Corrosion Rate Measurements by Weight Loss of single metals (free corrosion):**

To investigate the free corrosion for each metal for 2hrs and in the presence of different concentrations of PHTU inhibitor at different speeds, the circuit shown in **Fig. 4-3** was used.

The metal specimens were of outer diameter equal to 2.55cm with exact length of 2cm. They were cut from copper, carbon steel and zinc pipe, in order to use them in the weight loss experiments. After the specimen preparation, in the isothermal (T=40C) weight loss measurements the specimens were placed in the test section and the later was fixed by insulated rod to prevent the leakage of the solution to specimen inner. The test section was the specimen put in 0.1N HCl solution to read potential values each one minute for 2hrs, using five different PHTU concentrations (0, 0.001, 0.05, 0.1 and 0.15 g/L) and four rotational velocities 0, 500, 1000 and 1500rpm.

#### **4.7.3 Measuring the current, potential difference and corrosion rate of couple metals:**

The outer diameter of metal specimens was equal to 2.55cm with exact lengths of 4, 2, 1 and 0.5cm each which represent the cathode and 2cm to represent the anode electrode. They were cut from copper, carbon steel and zinc pipe, in order to use them in the weight loss experiments. Then the heater controller in the bath was set to the required temperature

of 40 °C to achieve thermal equilibrium before starting the experimental run. The experiment was carried out with 0.1N HCl and with (0.001, 0.05, 0.1, and 0.15 g/L PHTU added as an inhibitor at the following ratios AR=2, 1, 0.5, and 0.25.

At a certain value of (AR), rotational velocity and concentration of PHTU as inhibitor, the specimens were immersed in the solution, and then the current was read every one minute for 20 minutes by using the multimeter as a multirange ammeter (see **Fig.4-1**) with low resistance which depend on zero ammeter impedance principle and the weight loss was measured after this period (20 minutes) by using digital balance of 0.1 mg accuracy (Analytical balance type AE260 Delta RANGE, mettler) to calculate the corrosion rate as shown in **Fig.4-1**.

The experiments were repeated for different values of (AR) and concentration of PHTU inhibitor using four different speeds (0, 500, 1000, and 1500 rpm. All previous experiments were duplicated using different metal couples, i.e. Cu/Fe, Cu/Zn, and Fe/Zn.

Use the same apparatus as for above experiments but with the multimeter as a voltmeter as shown in **Fig.4-1**. The potential difference was measured every one minute for 20 minutes by using multirange voltmeter.

#### **4.7.4 Measuring the potential and current simultaneously in galvanic corrosion.**

All the previously mentioned experiments (copper and iron couple) were performed for a period of two hours in order to measure the galvanic current and potential simultaneously as shown in **Fig. 4-2**.

#### 4.7.5 Polarization Investigation Procedure

After the electrolyte (acid solution) preparation, the electrolyte was stirred by using a glass rod in order to obtain a homogenous solution, and then the heater controller in the bath was set to the required temperature of 40 °C to achieve thermal equilibrium before starting the experimental. The electrical circuit was connected to the reference electrode (SCE) after checking all the electrical connections. When the container reached the required temperature, the polarization electrical circuit was set to the (ON) position in order to draw the curve of any given condition (0, 0.001, 0.05 and 0.15 g/l concentration, 2, 1, 0.5 and 0.25 area ratio of metal specimen), a variable speed of metal specimens (0, 500, 1000 and 1500 rpm) and available of metal specimens type (Cu, Fe and Zn) by galvanostatic technique (making the voltage of the D.C power supply constant at 10V and changing the current by altering the resistance of the circuit). At each setting of the resistance two parameters were recorded (potential and cathodic and anodic current) by the voltmeter and the ammeter respectively, i.e, to measure the cathodic and anodic portion of the polarization curve. At least two minutes were allowed in order to record the steady state values of the polarization process (see **Fig.4-6**).

After reaching (  $E_{\text{corr.}}$  ) of the metal specimen used, the run was ended by switching the power off and the water bath emptied from the used electrolyte . The system was then washed entirely by using distilled water to make sure that there was no electrolyte left in the system.

The above procedure was repeated exactly for the other conditions of PHTU concentrations, area ratio of metal specimens, a variable rotational velocity of metal specimens and available metal specimen's types. Each run was repeated twice with a third run when reproducibility was in doubt.

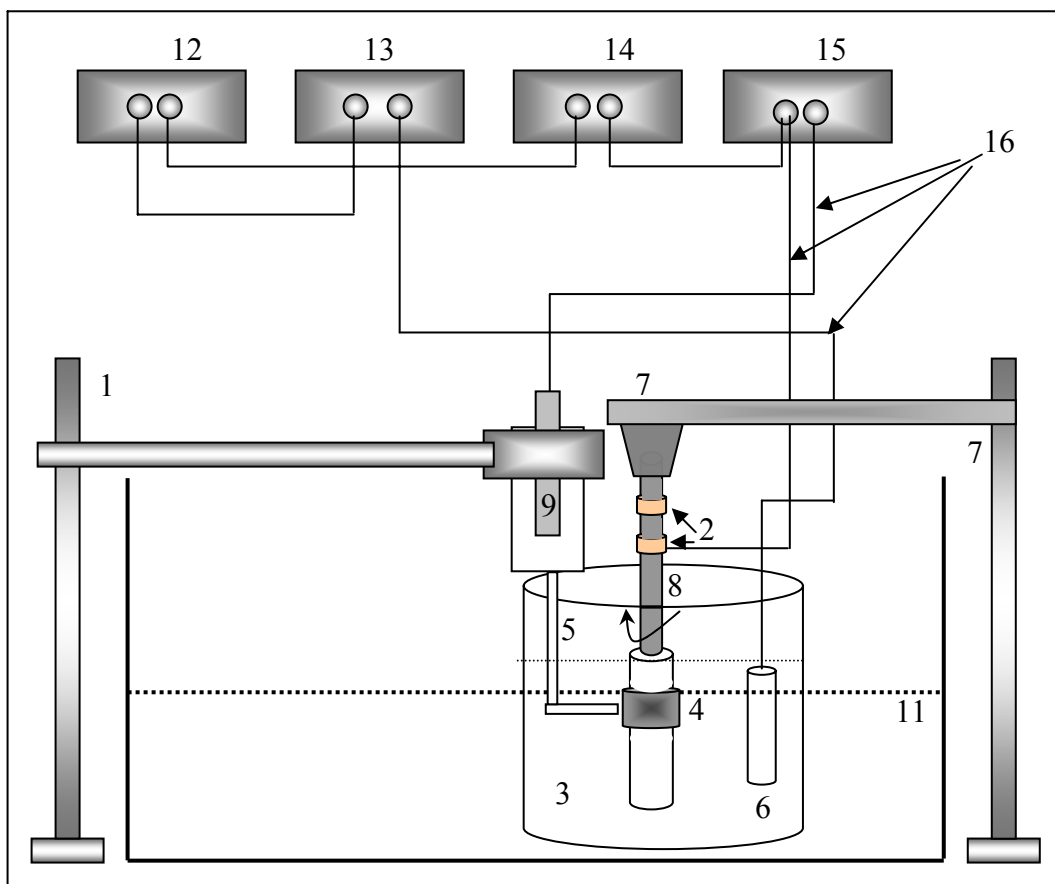


**Figure 4-6** A simple sketch showing the details of the laboratory polarization system and its identification is given in **Table 4-4**

**Table 4-4** gives the item number with its details as illustrated in **Fig.4.6**.

Item No.	Details
1	Stand
2	Ball bearing
3	Container (2L)
4	Cathode
5	Salt Bridge
6	Anode
7	Rotating device
8	Rotating shaft
9	Saturated Calomel Electrode(SCE)
10	Water Bath with temperature controller
11	stand
12	D.C Power supply
13	Multirange Ammeter
14	Resistance Box.
15	Multirange Voltmeter
16	Connecting Wires



**A**



**B**



**C**



**D**

**Figure 4-7 A, B, C and D Test Apparatus**

#### 4.7.6 Cell resistance measurement procedure<sup>[105]</sup>:

After the specimens cleaning, the circuit has been connected as shown in **Fig.4-8**. The variable resistance (1.3, 2.3, 3.3, 4.3 and 5.3 $\Omega$ ) between cathodic metal and anodic metal have been connected to measure potential values to each resistance value and for each minute for 20 minutes in static air-saturated 0.1N HCl solution, area ratio AR=1 and constant temperature of (T=40 °C).

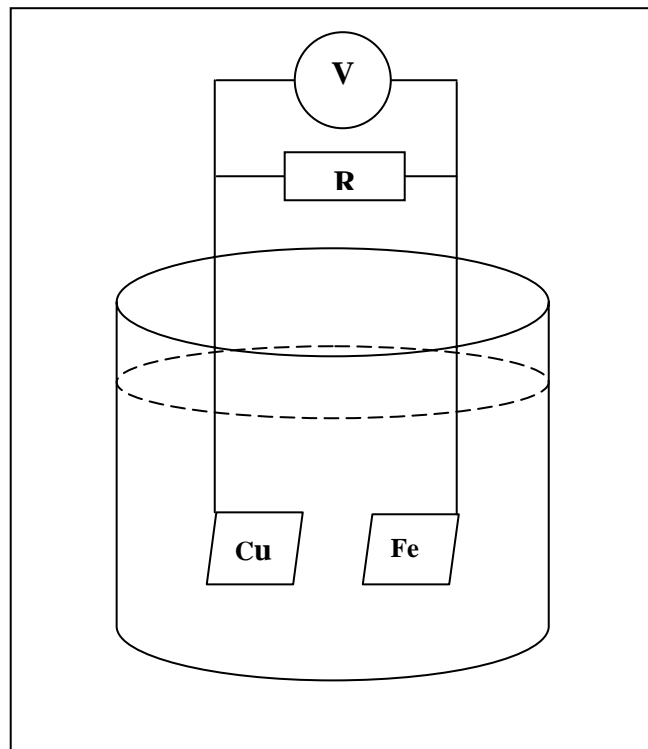


**Figure 4-8** Arrangement for cell resistance measurement<sup>[105]</sup>.



# Chapter Five

## Results

### 5.1 Introduction

As mentioned in chapter one, the aim of the present work is to study the galvanic action between several metals (copper, carbon steel and zinc), by coupling two metals at a time and compare the results with the results obtained from the weight loss and the polarization studies obtained for these metals in the single state. All the above experiments were carried out in aerated 0.1N HCl, a variable speed of metal specimens (0, 500, 1000 and 1500 rpm), with different PHTU inhibitor concentrations (0, 0.001, 0.05 and 0.15) g/l, and area ratios of metal specimen of 2, 1, 0.5 and 0.25. The reason behind aeration is to ensure that the corrosion reaction is activation and concentration controlled. Three operating conditions were taken into account during these experiments, inhibitor concentration, speed of rotating cylinder, and the geometry of the metal by altering the area ratio of the cathode to anode (AR=2, 1, 0.5, and 0.25). All the above techniques were used as a base to portray the facts of galvanic corrosion.

## 5.2 Weight loss of individual metals:

As mentioned in chapter four, specimens of OD=2.55cm and L=2cm, were cut from metal tubes of carbon steel, copper, and zinc using the cell shown in Fig.4-3. Tables 5-1 to 5-3 show the weight loss results, corrosion rate and PHTU efficiency on copper, carbon steel and zinc at T=40 °C in air-saturated 0.1N HCl solution, rotational velocities (RPM), PHTU concentration and t=2h.

**Table 5-1** Effect of inhibitor (PHTU) concentration and rotating cylinder speed on corrosion rate (by weight loss) of copper specimen in air-saturated 0.1N HCl solution, T=40C and t=120m .

RPM	C(g/L) PHTU	$\Delta W_a$ (g)	CR(gmd)	CR(mm/y)	CR(mpy)	$i_d$ ( $\mu A/cm^2$ )	$\eta\%$
0	0.000	0.0052	38.946	1.586	62.455	136.899	-
	0.001	0.0035	26.214	1.068	42.038	92.144	32.69
	0.050	0.0020	14.979	0.610	24.021	52.654	61.54
	0.100	0.0009	6.741	0.275	10.826	23.694	82.69
	0.150	0.0002	1.498	0.061	2.402	5.265	96.15
500	0.000	0.0081	60.666	2.471	97.287	213.248	-
	0.001	0.0053	39.695	1.617	63.657	139.532	34.57
	0.050	0.0032	23.967	0.976	38.435	84.246	60.49
	0.100	0.0016	11.983	0.488	19.216	42.123	80.25
	0.150	0.0005	3.745	0.153	6.006	13.163	93.83
1000	0.000	0.0098	73.399	2.989	117.706	258.003	-
	0.001	0.0072	53.925	2.197	86.476	189.553	26.53
	0.050	0.0048	35.950	1.464	57.651	126.369	51.01
	0.100	0.0022	16.477	0.671	26.423	57.919	77.55
	0.150	0.0008	5.992	0.244	9.609	21.061	91.84
1500	0.000	0.0111	83.135	2.386	133.319	292.228	-
	0.001	0.0075	56.172	2.288	90.079	197.451	32.43
	0.050	0.0052	38.946	1.586	62.455	136.899	53.15
	0.100	0.0025	18.724	0.763	30.027	65.817	77.48
	0.150	0.0009	6.741	0.275	10.810	23.694	91.89

**Table 5-2** Effect of inhibitor (PHTU) concentration and rotating cylinder speed on corrosion rate (by weight loss) of carbon steel specimen in air-saturated 0.1N HCl solution, T=40C and t=120m .

RPM	C(g/L) PHTU	$\Delta W_a$ (g)	CR(gmd)	CR(mm/y)	CR(mpy)	$i_d$ ( $\mu\text{A}/\text{cm}^2$ )	$\eta\%$
0	0.000	0.0162	121.332	5.627	221.522	485.245	-
	0.001	0.0135	101.110	4.689	184.601	404.371	16.67
	0.050	0.0099	74.147	3.438	135.374	296.539	38.89
	0.100	0.0032	23.967	1.111	43.758	95.851	80.25
	0.150	0.0005	3.745	0.174	6.837	14.977	96.91
500	0.000	0.0211	158.032	7.329	288.527	632.017	-
	0.001	0.0151	113.094	5.245	206.481	452.297	28.44
	0.050	0.0090	67.407	3.126	123.068	269.581	57.35
	0.100	0.0019	14.230	0.659	25.980	56.911	90.99
	0.150	0.0007	5.243	0.243	9.572	20.967	96.68
1000	0.000	0.0264	197.727	9.169	360.999	790.770	-
	0.001	0.0205	153.538	7.120	280.322	614.045	22.35
	0.050	0.0120	89.876	4.168	164.091	359.441	54.55
	0.100	0.0072	53.925	2.501	98.453	215.665	72.73
	0.150	0.0012	8.988	0.417	16.409	35.944	95.45
1500	0.000	0.0305	228.434	10.593	417.063	913.579	-
	0.001	0.0205	153.538	7.120	280.322	614.045	32.79
	0.050	0.0126	94.369	4.376	172.294	377.413	58.69
	0.100	0.0033	24.716	1.146	45.125	98.946	89.18
	0.150	0.0020	14.979	0.695	27.348	59.907	93.44

**Table 5-3** Effect of inhibitor (PHTU) concentration and rotating cylinder speed on corrosion rate (by weight loss) of zinc specimen in air-saturated 0.1N HCl solution, T=40C and t=120m .

RPM	C(g/L)PHTU	$\Delta W$ (g)	CR(gmd)	CR(mm/y)	CR(mpy)	$i_a(\mu A/cm^2)$	$\eta\%$
0	0.000	0.0437	327.298	16.753	659.583	1118.27	-
	0.001	0.0335	250.903	12.843	505.629	857.26	23.34
	0.050	0.0221	165.521	8.473	333.564	565.54	49.43
	0.100	0.0080	59.917	3.067	120.747	204.72	81.17
	0.150	0.0011	8.239	0.422	16.604	28.149	97.48
500	0.000	0.0511	382.721	19.590	771.274	1307.64	-
	0.001	0.0351	262.887	13.456	529.779	898.20	31.31
	0.050	0.0295	220.945	11.309	445.257	754.90	42.27
	0.100	0.0083	62.164	3.182	125.275	212.39	83.76
	0.150	0.0025	18.724	0.958	37.733	63.975	95.11
1000	0.000	0.0612	458.366	23.462	923.716	1566.09	-
	0.001	0.0365	273.372	13.993	550.909	934.03	40.36
	0.050	0.0285	213.455	10.926	430.162	729.31	53.43
	0.100	0.0120	89.876	4.600	181.121	307.08	80.39
	0.150	0.0029	21.719	1.112	43.769	74.211	95.26
1500	0.000	0.0677	507.049	25.954	1021.82	1732.4	-
	0.001	0.0495	370.737	18.977	747.123	1266.69	26.88
	0.050	0.0295	220.945	11.309	445.257	754.90	56.422
	0.100	0.0131	98.114	5.022	197.723	335.23	80.65
	0.150	0.0033	24.716	1.265	49.809	84.447	95.16

### **5.3 Galvanic coupling:**

The galvanic coupling experiments were conducted according to the conditions (rotating velocity=0, 500, 1000, and 1500rpm), (AR=2, 1, 0.5, and 0.25) and phenylthiourea concentration=0, 0.001, 0.05, 0.1, and 0.15g/l at 40 °C.

#### **5.3.1 Copper and carbon steel coupling:**

These experiments were divided into two main categories:

- a. Direct results of voltage difference between two metals against time for 20 minutes, experiments were carried out in aerated 0.1N HCl, a variable PHTU inhibitor concentration (0, 0.001, 0.05 and 0.15) g/l, with speed of metal specimens (0, 500, 1000 and 1500 rpm), and area ratio of metal couple as 2, 1, 0.5 and 0.25, **Figs.(5.1a-5.16a).**
- b. Direct results of current against time for 20 minutes and the same previously mentioned conditions, **Figs. (5.1b-5.16b).**

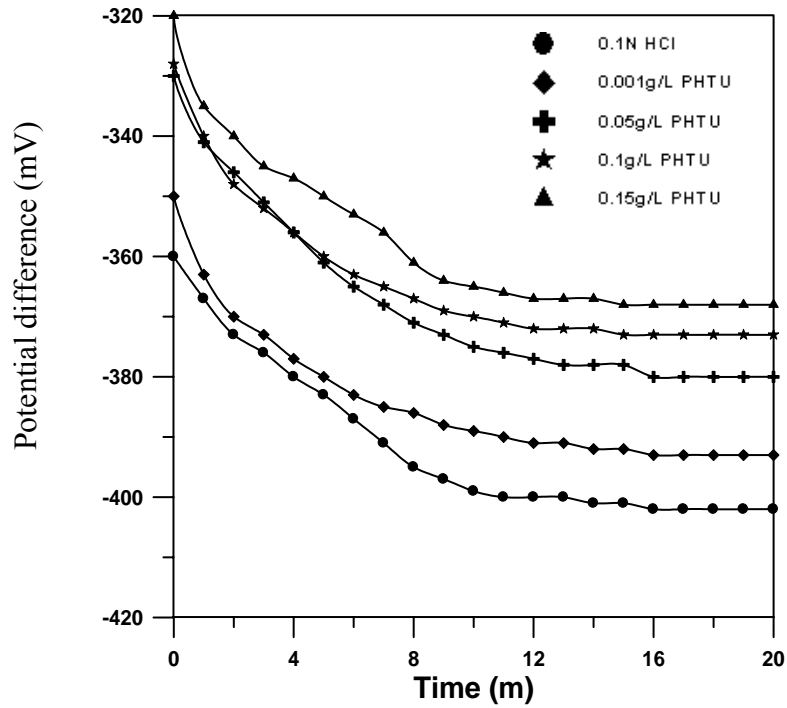


**Figure 5-1a** Potential difference vs. time for copper and iron metals in 0.1N HCl, AR(Cu/Fe)=0.25, T=40 °C, t=20m, and 0 RPM

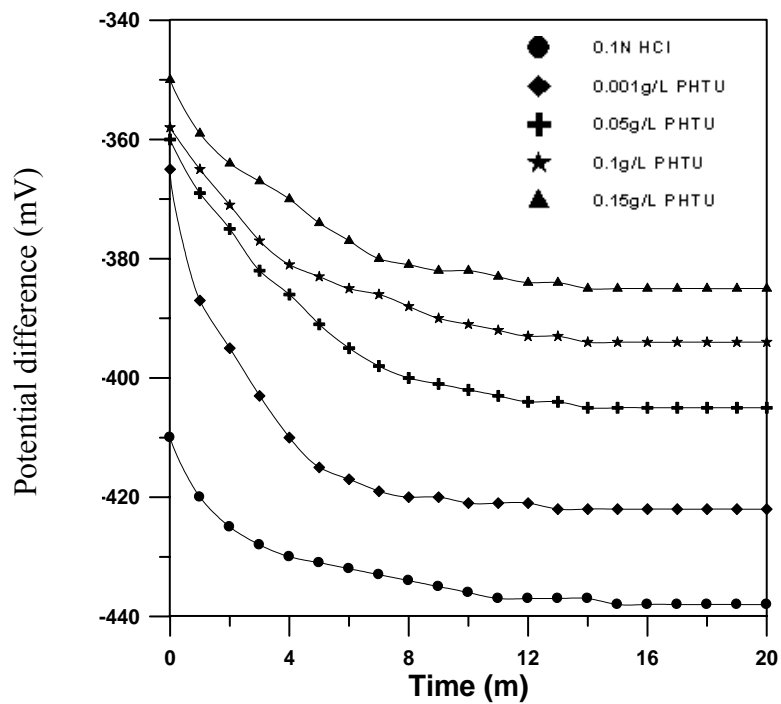


**Figure 5-2a** Potential difference vs. time for copper and iron metals in 0.1N HCl, AR(Cu/Fe)=0.5, T=40 °C, t=20m, and 0 RPM

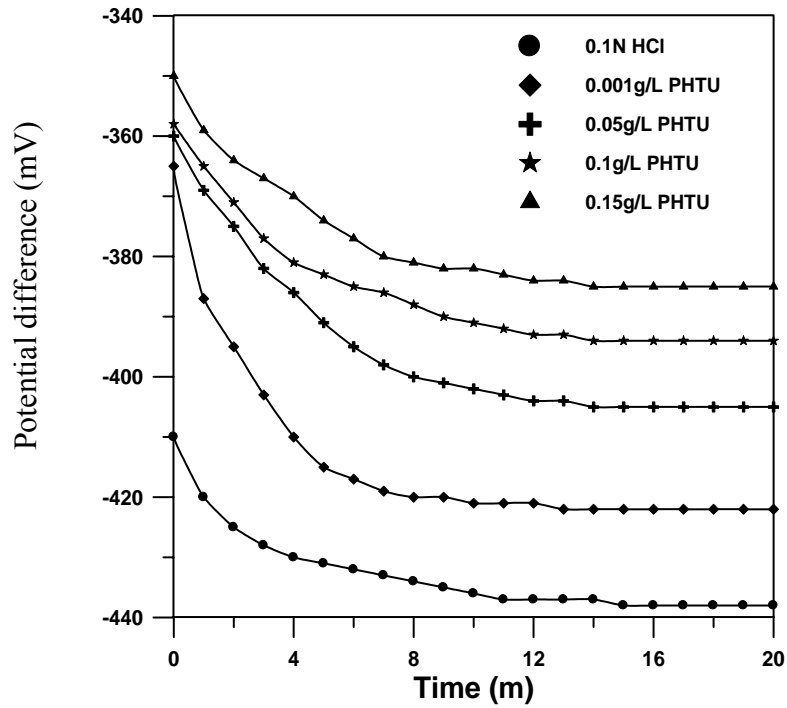


**Figure 5-3a** Potential difference vs. time for copper and iron metals in 0.1N HCl, AR(Cu/Fe)=1, T=40 °C, t=20m, and 0 RPM

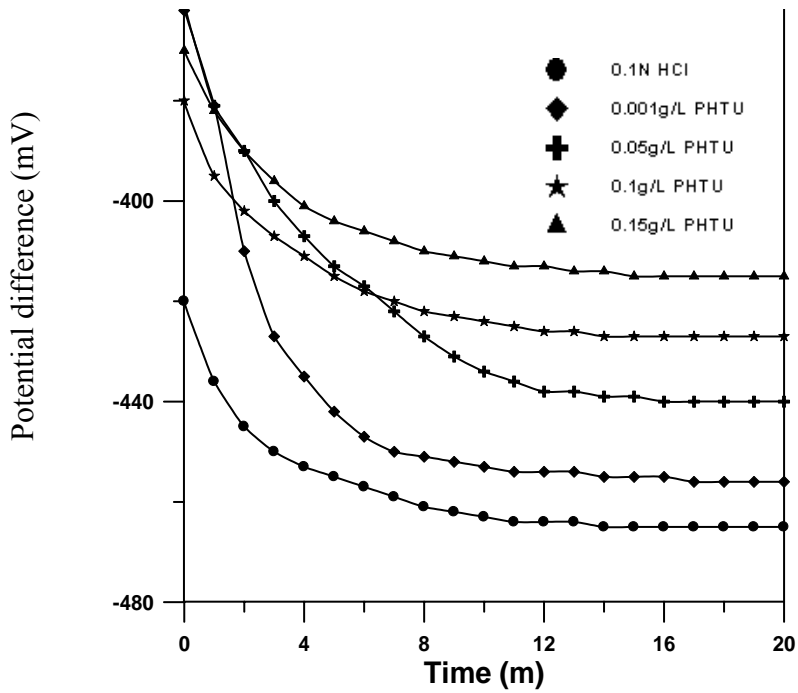


**Figure 5-4a** Potential difference vs. time for copper and iron metals in 0.1N HCl, AR(Cu/Fe)=2, T=40 °C, t=20m, and 0 RPM

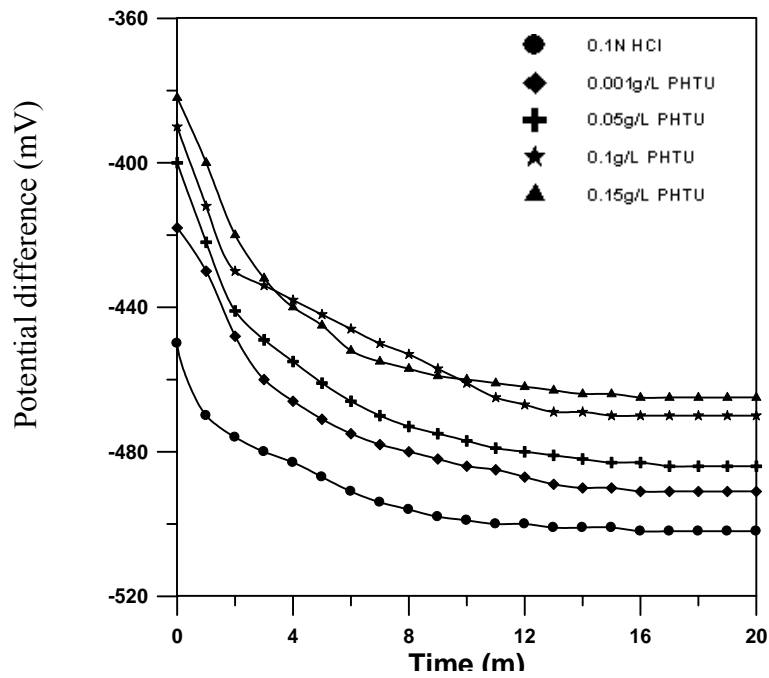


**Figure 5-5a** Potential difference vs. time for copper and iron metals in 0.1N HCl, AR(Cu/Fe)=0.25, T=40 °C, t=20m, and 500 RPM

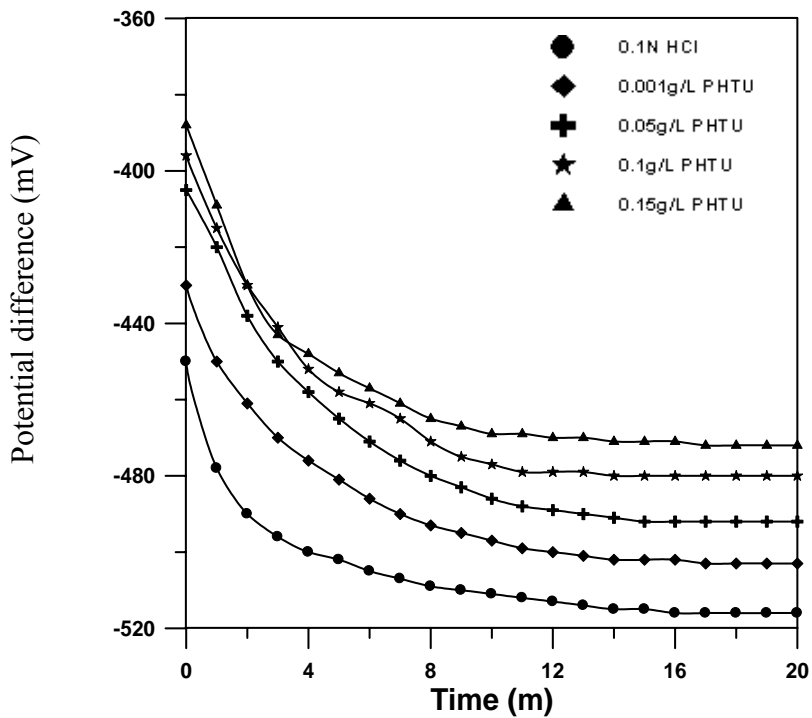


**Figure 5-6a** Potential difference vs. time for copper and iron metals in 0.1N HCl, AR(Cu/Fe)=0.5, T=40 °C, t=20m, and 500 RPM



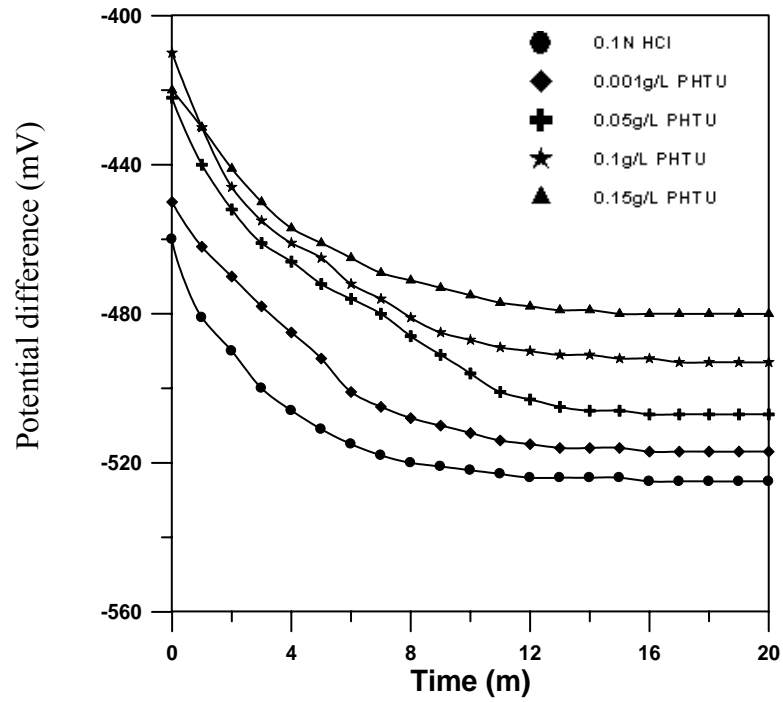


**Figure 5-7a** Potential difference vs. time for copper and iron metals in 0.1N HCl, AR(Cu/Fe)=1, T=40 °C, t=20m, and 500 RPM

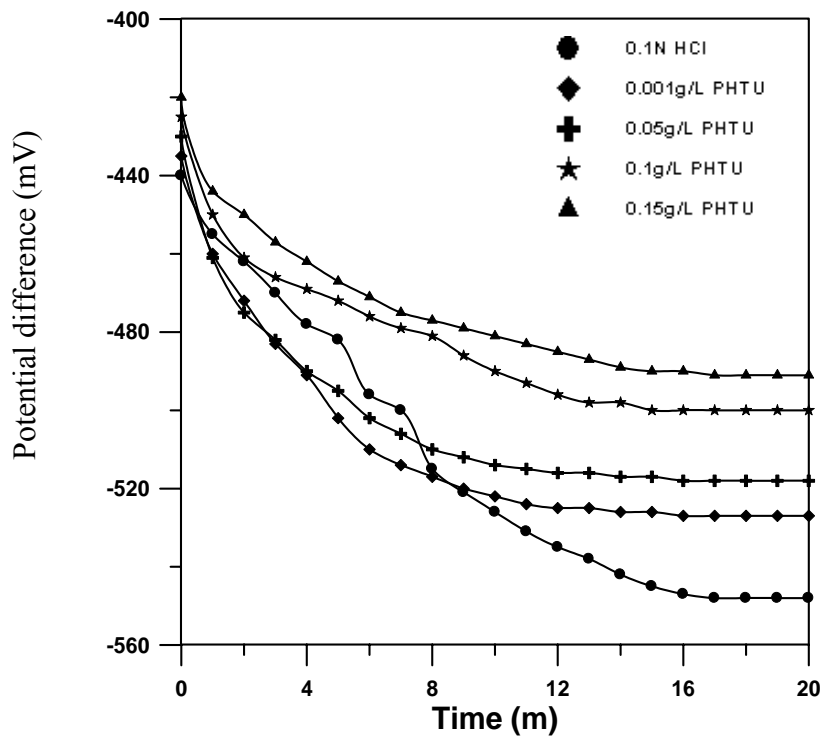


**Figure 5-8a** Potential difference vs. time for copper and iron metals in 0.1N HCl, AR(Cu/Fe)=2, T=40 °C, t=20m, and 500 RPM

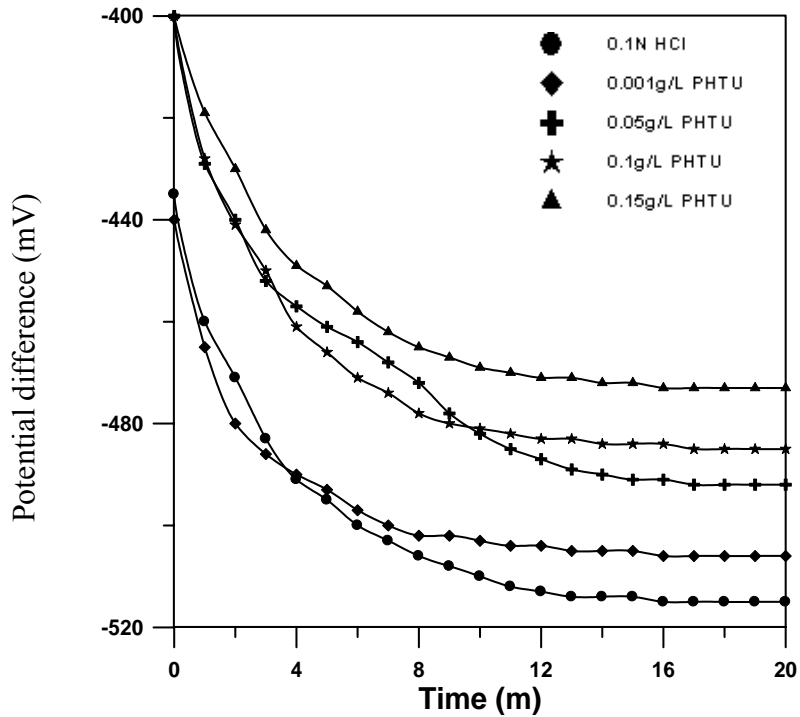


**Figure 5-9a** Potential difference vs. time for copper and iron metals in 0.1N HCl, AR(Cu/Fe)=0.25, T=40 °C, t=20m, and 1000 RPM

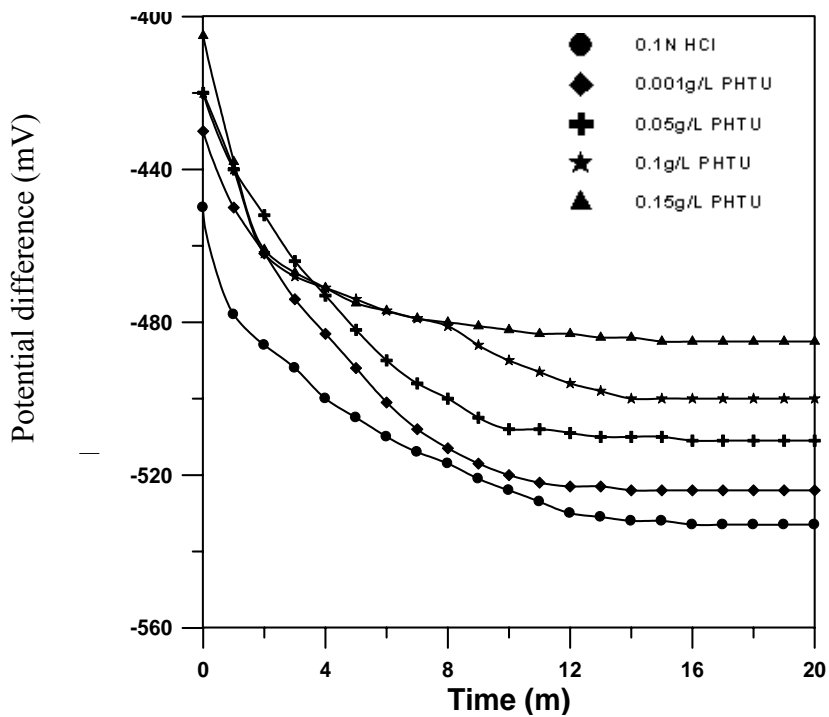


**Figure 5-10a** Potential difference vs. time for copper and iron metals in 0.1N HCl, AR(Cu/Fe)=0.5, T=40 °C, t=20m, and 1000 RPM

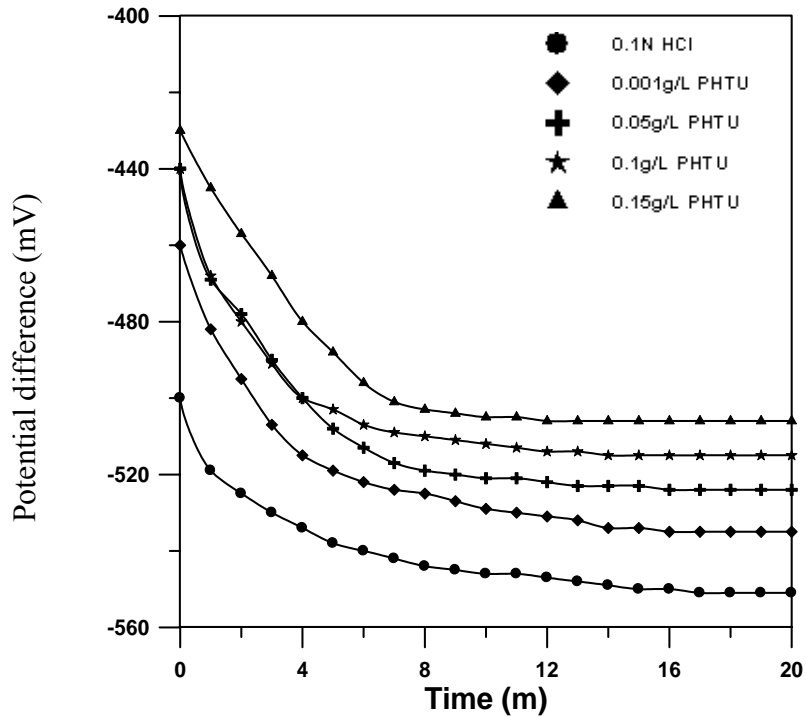


**Figure 5-11a** Potential difference vs. time for copper and iron metals in 0.1N HCl, AR(Cu/Fe)=1, T=40 °C, t=20m, and 1000 RPM

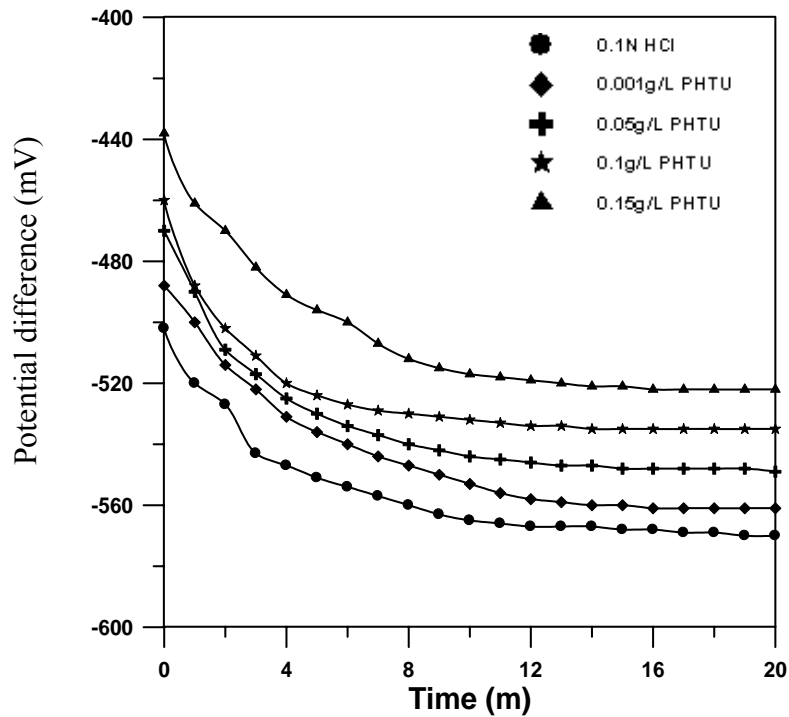


**Figure 5-12a** Potential difference vs. time for copper and iron metals in 0.1N HCl, AR(Cu/Fe)=2, T=40 °C, t=20m, and 1000 RPM

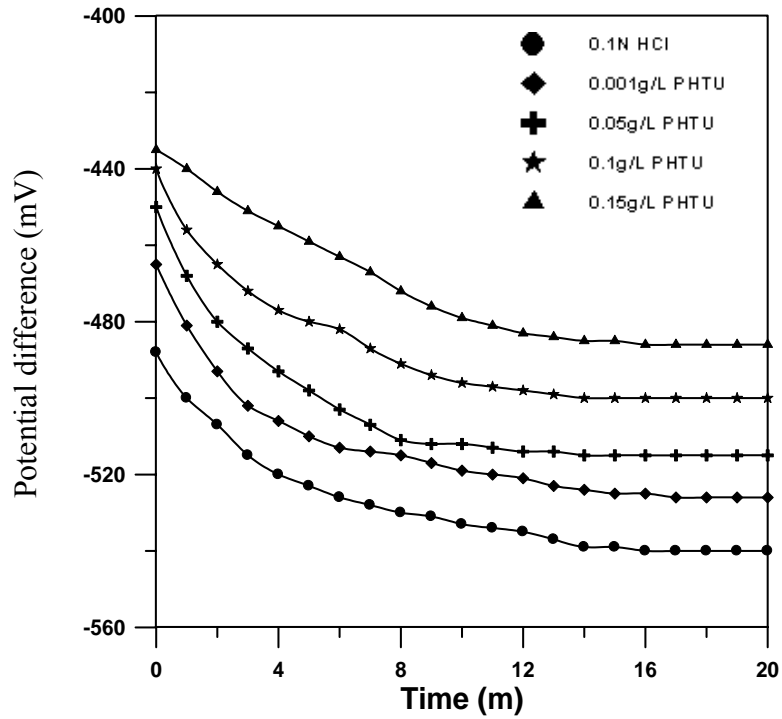


**Figure 5-13a** Potential difference vs. time for copper and iron metals in 0.1N HCl, AR(Cu/Fe)=0.25, T=40 °C, t=20m, and 1500 RPM

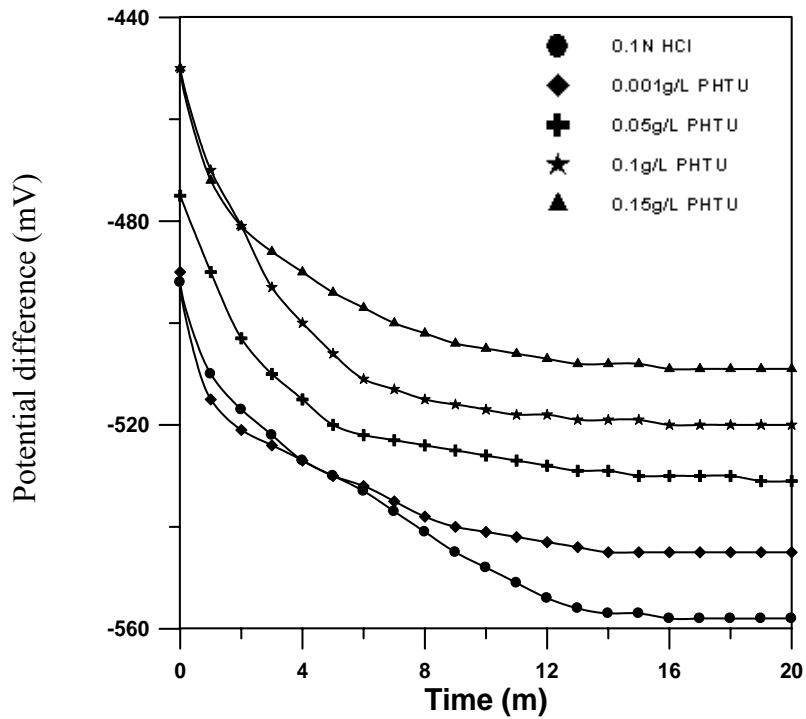


**Figure 5-14a** Potential difference vs. time for copper and iron metals in 0.1N HCl, AR(Cu/Fe)=0.5, T=40 °C, t=20m, and 1500 RPM

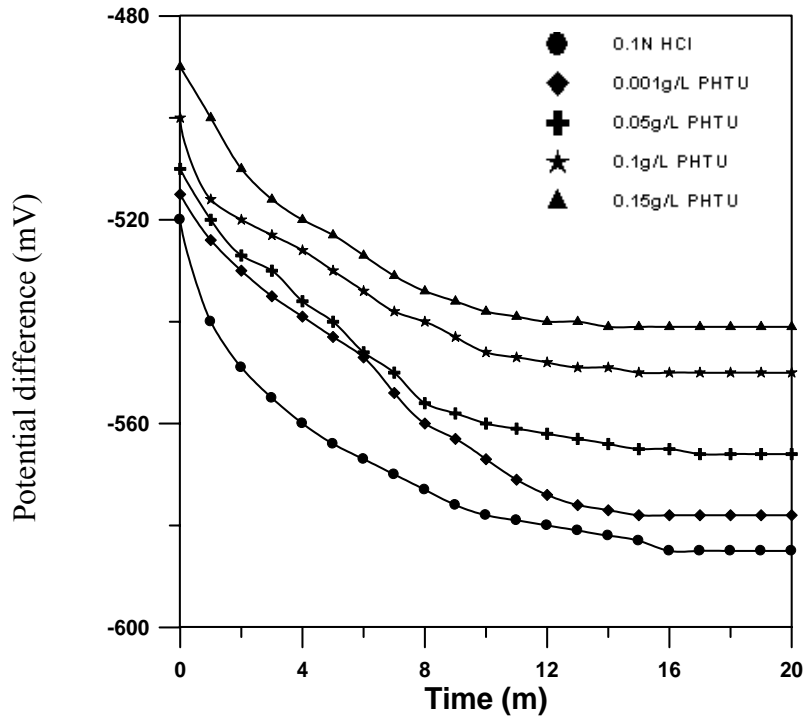


**Figure 5-15a** Potential difference vs. time for copper and iron metals in 0.1N HCl, AR(Cu/Fe)=1, T=40 °C, t=20m, and 1500 RPM

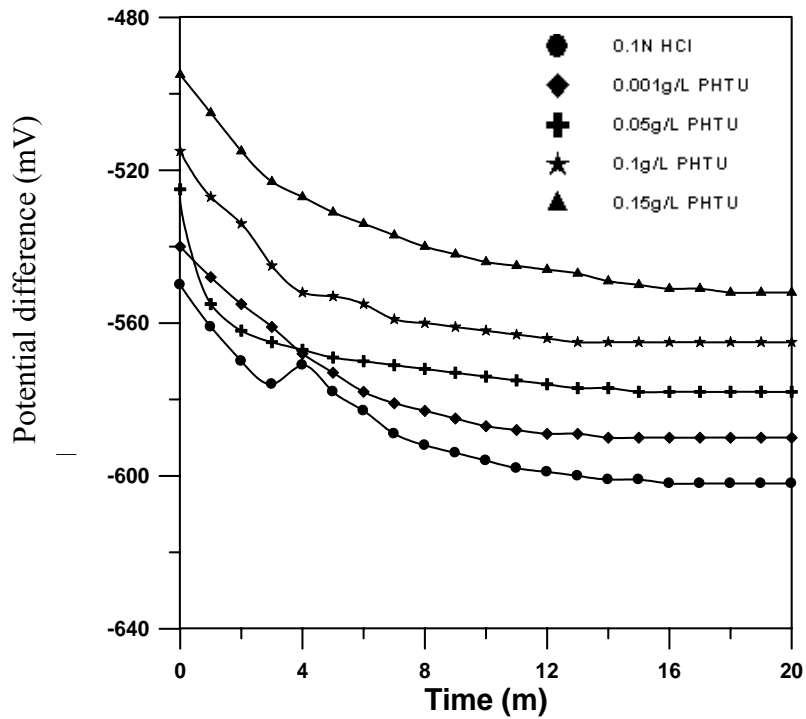


**Figure 5-16a** Potential difference vs. time for copper and iron metals in 0.1N HCl, AR(Cu/Fe)=2, T=40 °C, t=20m, and 1500 RPM

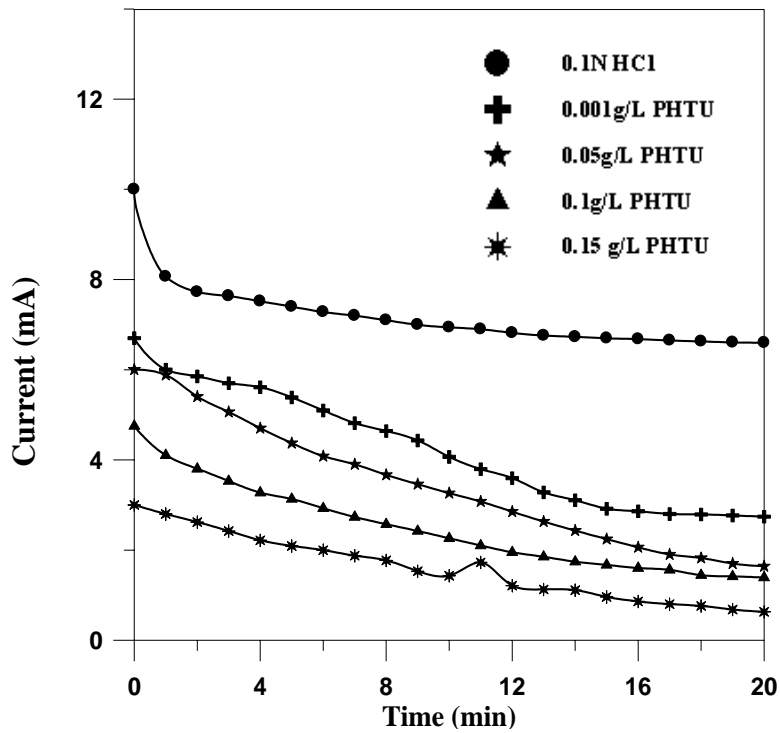


**Figure 5-1b** Current vs. time for a metal couple in 0.1N HCl, AR (Cu/Fe) = 0.25, T = 40 °C, t = 20m, and 0 RPM

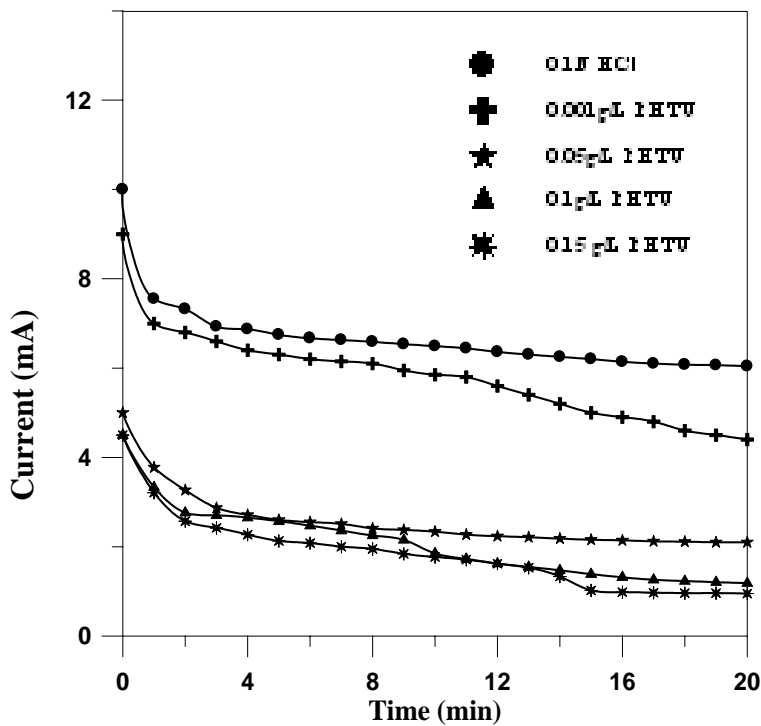


**Figure 5-2b** Current vs. time for a metal couple in 0.1N HCl, AR (Cu/Fe) = 0.5, T = 40 °C, t = 20m, and 0 RPM

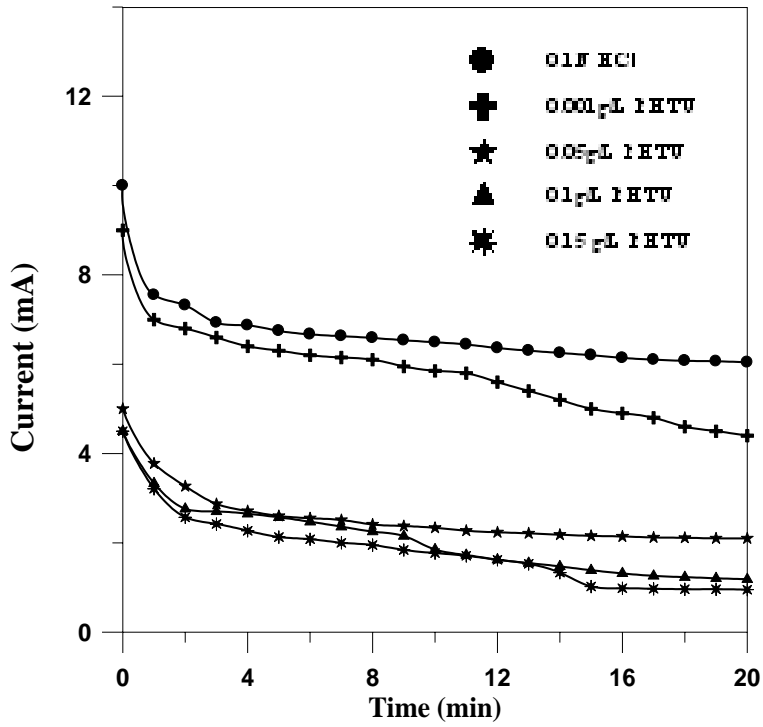


**Figure 5-3b** Current vs. time for a metal couple in 0.1N HCl, AR (Cu/Fe)=1, T=40 °C, t=20m, and 0 RPM

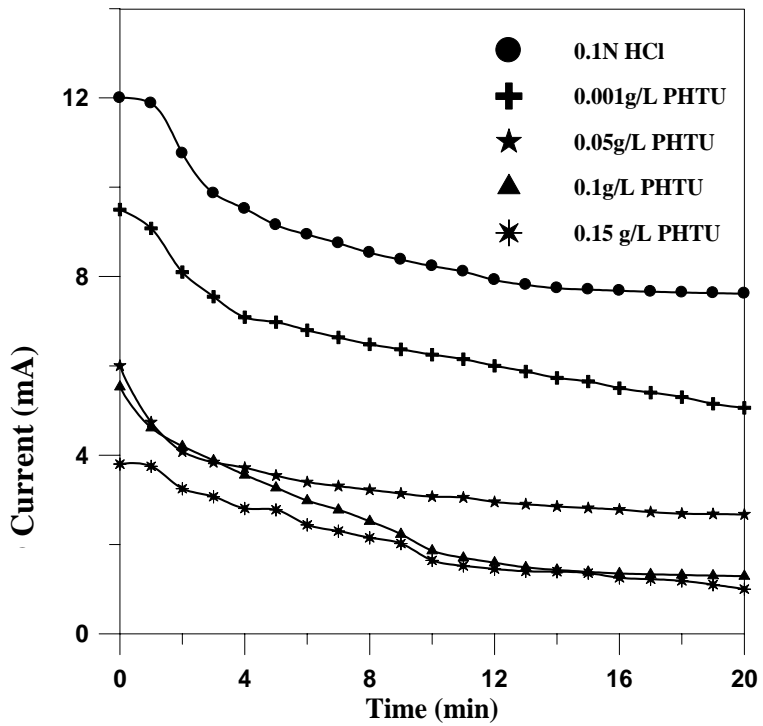


**Figure 5-4b** Current vs. time for a metal couple in 0.1N HCl, AR (Cu/Fe)=2, T=40 °C, t=20m, and 0 RPM

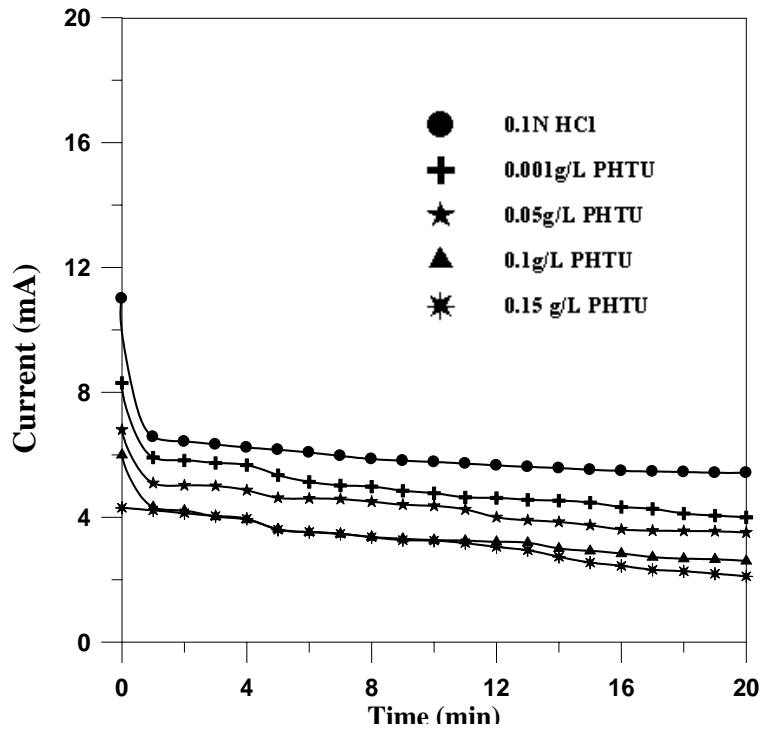


**Figure 5-5b** Current vs. time for a metal couple in 0.1N HCl, AR (Cu/Fe) = 0.25, T = 40 °C, t = 20m, and 500 RPM

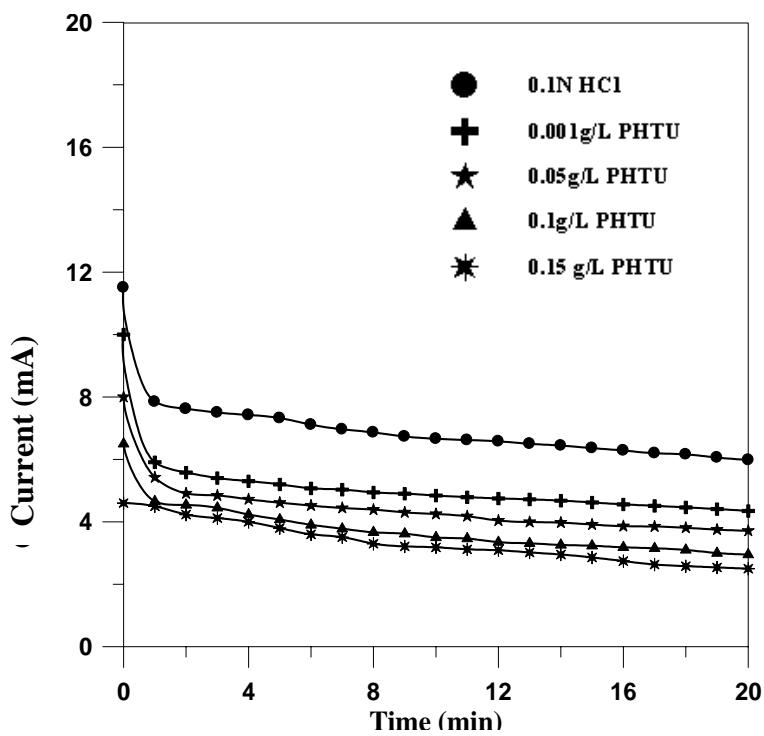


**Figure 5-6b** Current vs. time for a metal couple in 0.1N HCl, AR (Cu/Fe) = 0.5, T = 40 °C, t = 20m, and 500 RPM



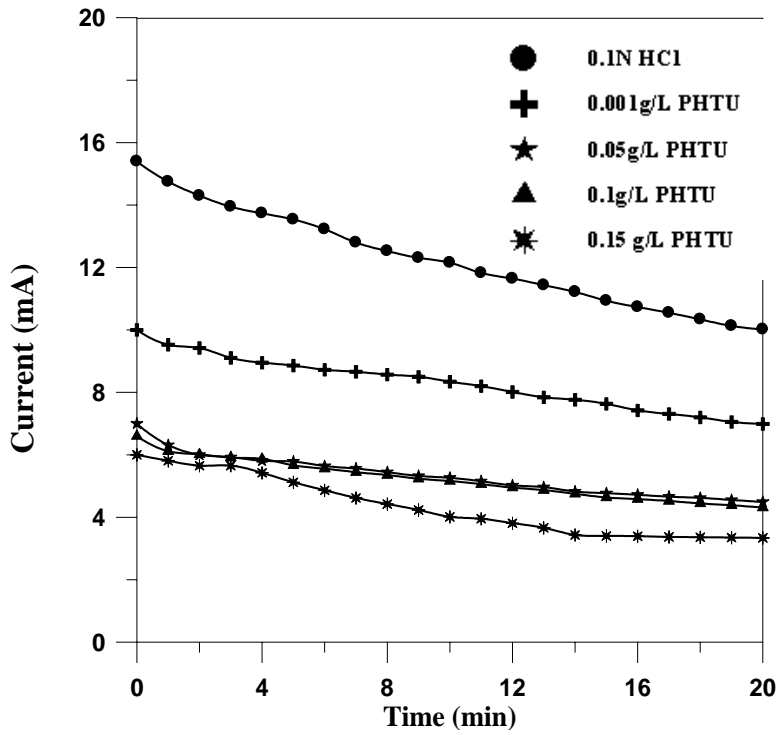


**Figure 5-7b** Current vs. time for a metal couple in 0.1N HCl, AR (Cu/Fe)=1, T=40 °C, t=20m, and 500 RPM

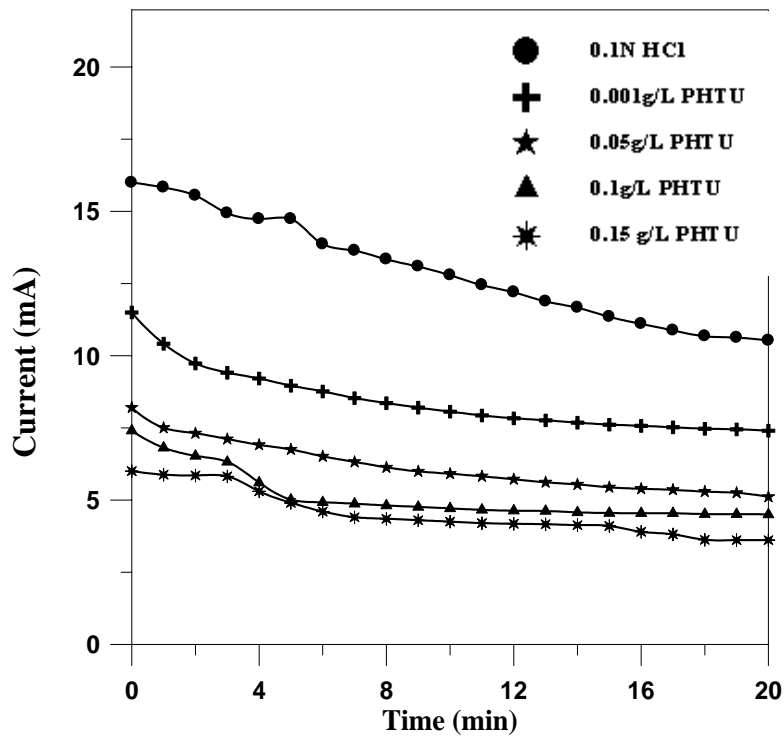


**Figure 5-8b** Current vs. time for a metal couple in 0.1N HCl, AR (Cu/Fe)=2, T=40 °C, t=20m, and 500 RPM

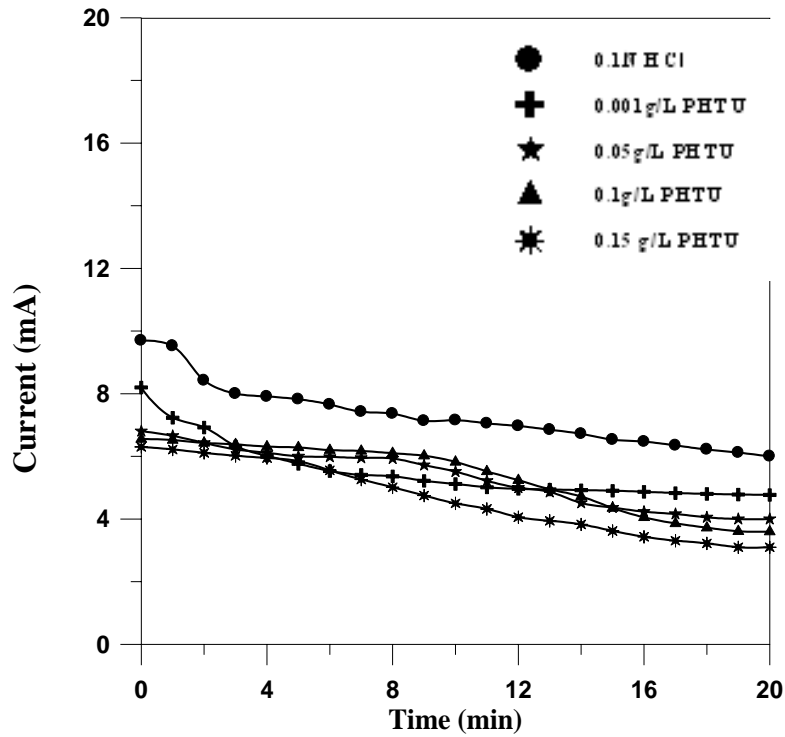


**Figure 5-9b** Current vs. time for a metal couple in 0.1N HCl, AR (Cu/Fe) = 0.25, T=40 °C, t=20m, and 1000 RPM

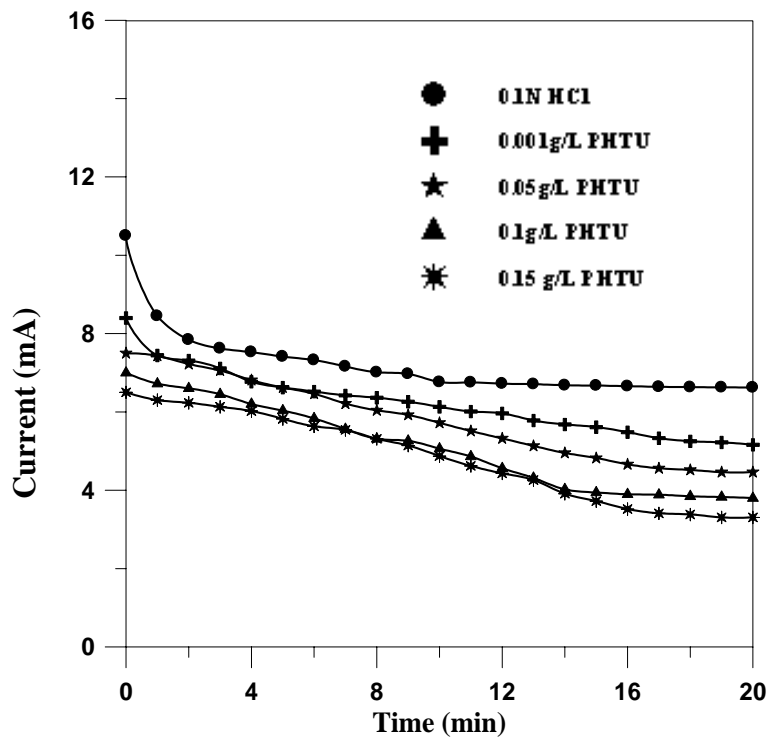


**Figure 5-10b** Current vs. time for a metal couple in 0.1N HCl, AR(Cu/Fe) = 0.5, T=40 °C, t=20m, and 1000 RPM

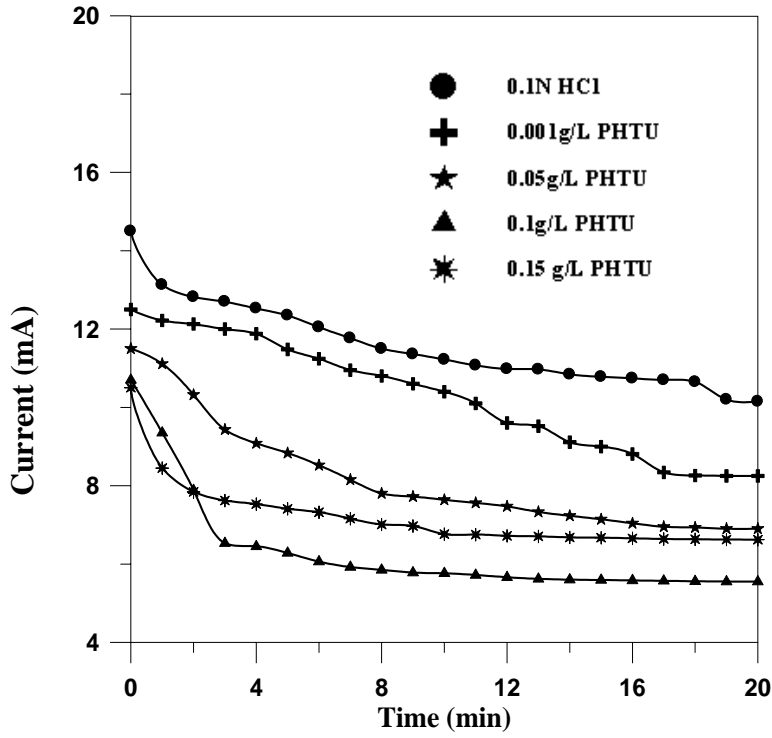


Figure 5-11b Current vs. time for a metal couple in 0.1N HCl, AR (Cu/Fe) =1, T=40 °C, t=20m, and 1000 RPM

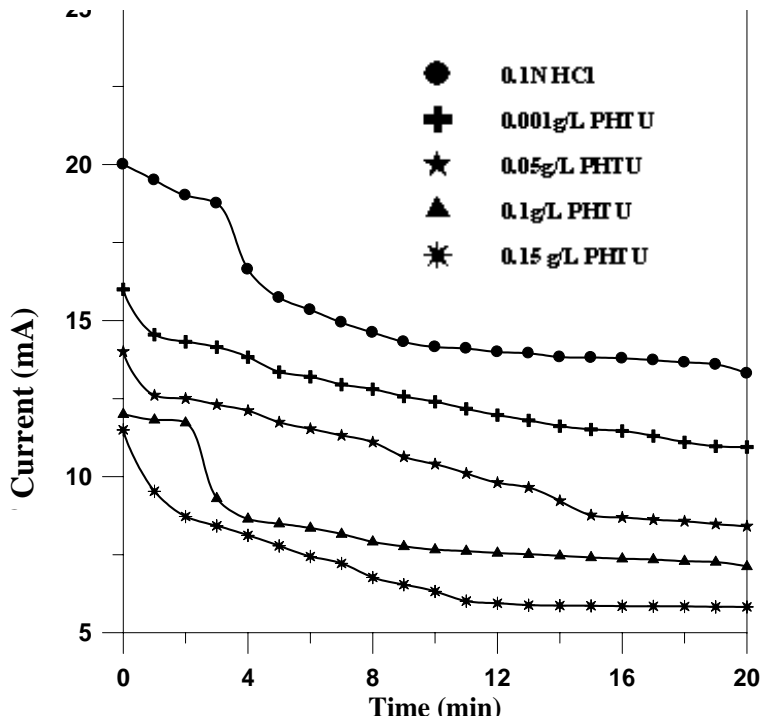
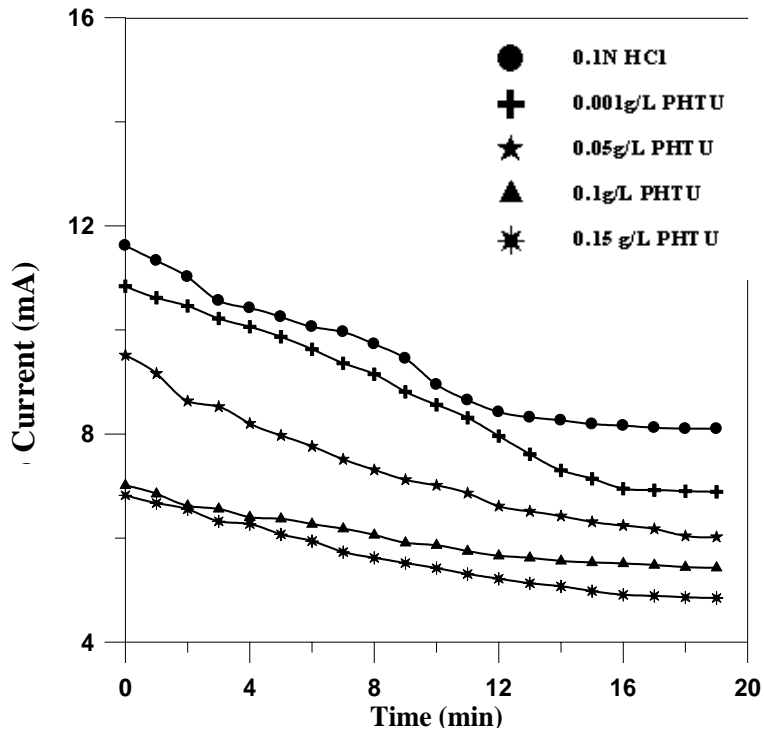
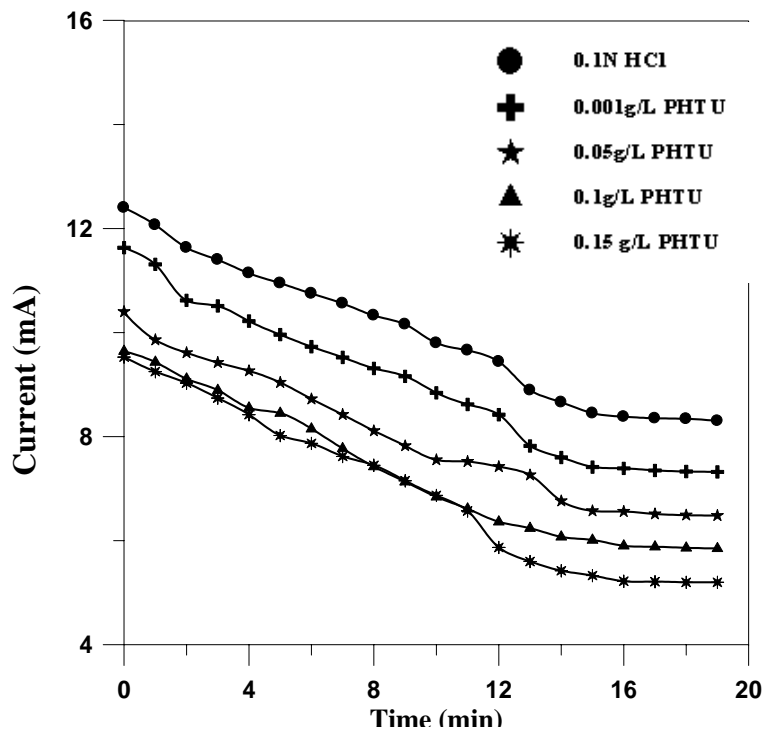


Figure 5-12b Current vs. time for a metal couple in 0.1N HCl, AR (Cu/Fe) =2, T=40 °C, t=20m, and 1000 RPM



**Figure 5-13b** Current vs. time for a metal couple in 0.1N HCl, AR (Cu/Fe) = 0.25, T = 40 °C, t = 20m, and 1500 RPM



**Figure 5-14b** Current vs. time for a metal couple in 0.1N HCl, AR (Cu/Fe) = 0.5, T = 40 °C, t = 20m, and 1500 RPM

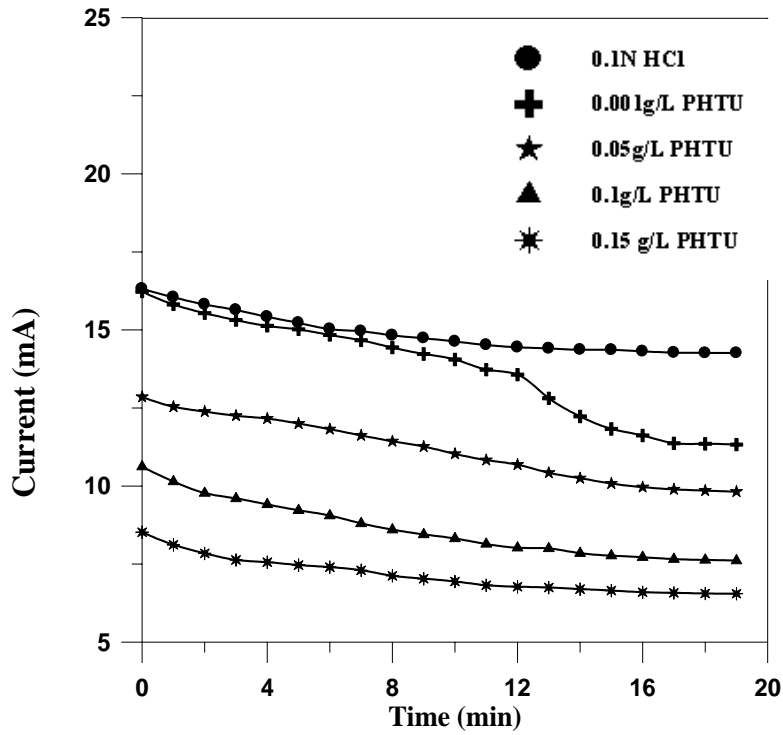


**Figure 5-15b** Current vs. time for a metal couple in 0.1N HCl, AR (Cu/Fe) =1, T=40 °C, t=20m, and 1500 RPM

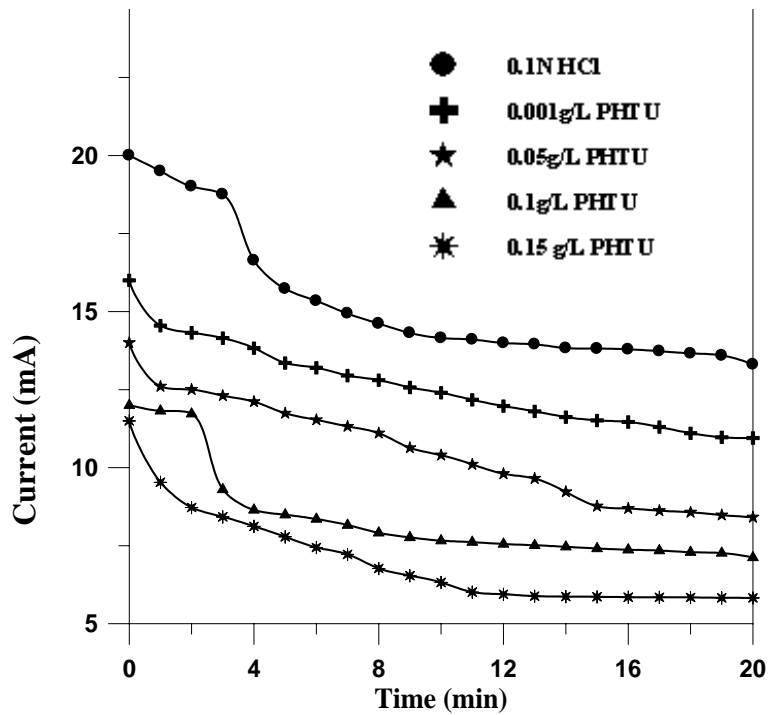


**Figure 5-16b** Current vs. time for a metal couple in 0.1N HCl, AR (Cu/Fe) =2, T=40 °C, t=20m, and 1500 RPM

### 5.3.2 Copper and Zinc coupling:

The experiments have been divided into two main departments:

- a. Direct results of potential difference against time for 20 minute, experiments were carried out in aerated 0.1N HCl as the same previous conditions of copper and carbon steel coupling, **Figs.(5.17a-5.32a)**.
- b. Direct results of current against time for 20 minute as shown in **Figs.(5.17b-5.32b)**.

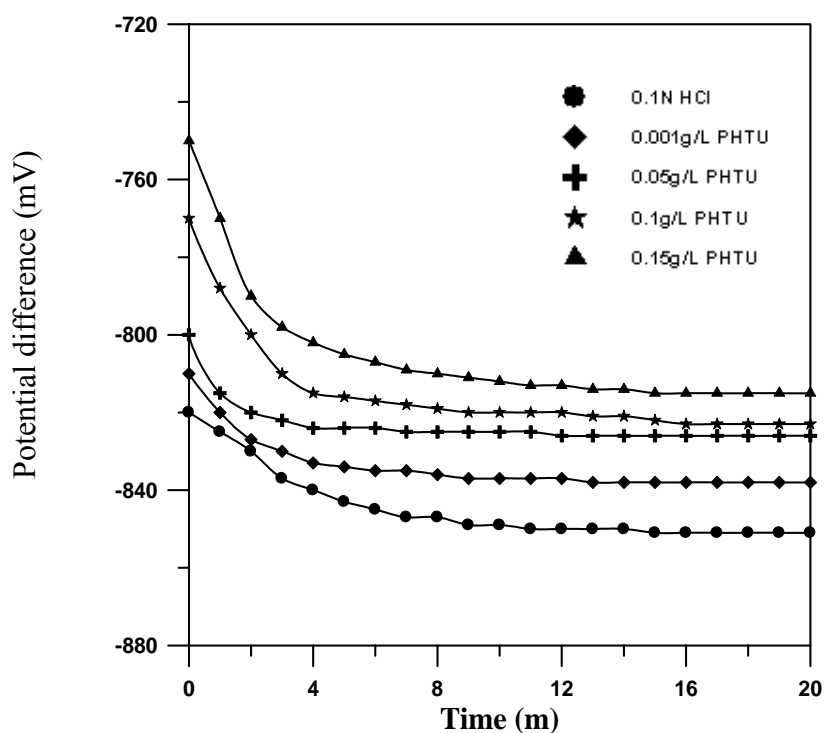


**Figure 5-17a** Potential difference vs. time for copper and zinc metals in 0.1NHCl, AR (Cu/Zn) =0.25, T=40 °C, t=20m, and 0 RPM

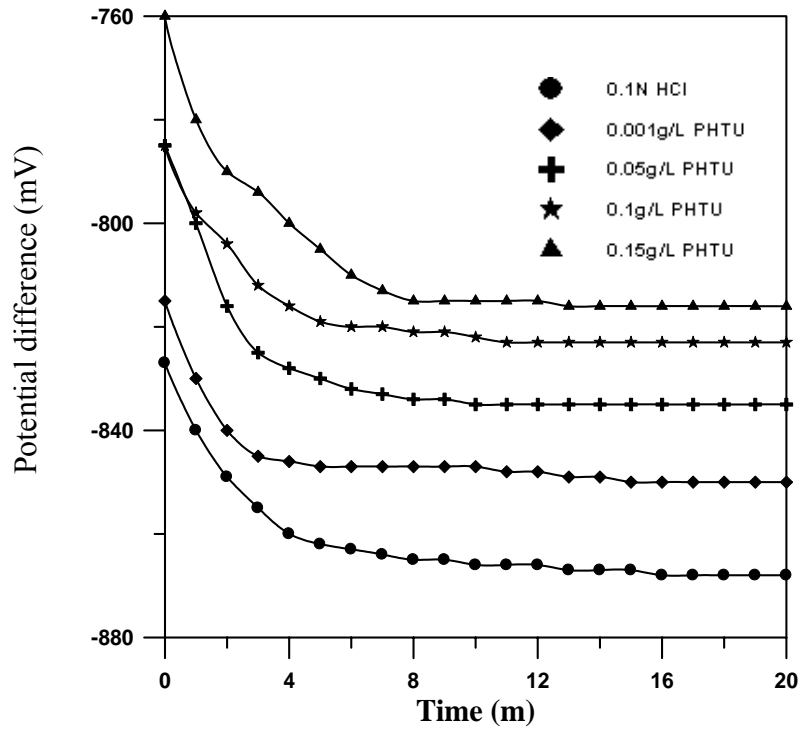


**Figure 5-18a** Potential difference vs. time for copper and zinc metals in 0.1N HCl, AR (Cu/Zn)=0.5, T=40 °C, t=20m, and 0 RPM

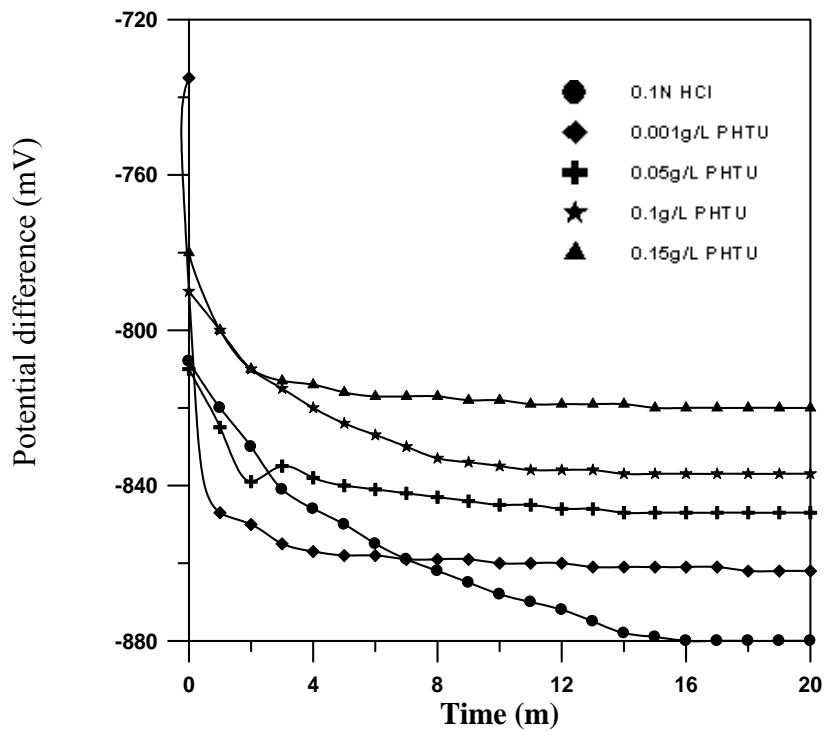


**Figure 5-19a** Potential difference vs. time for copper and zinc metals in 0.1N HCl, AR (Cu/Zn)=1, T=40 °C, t=20m, and 0 RPM

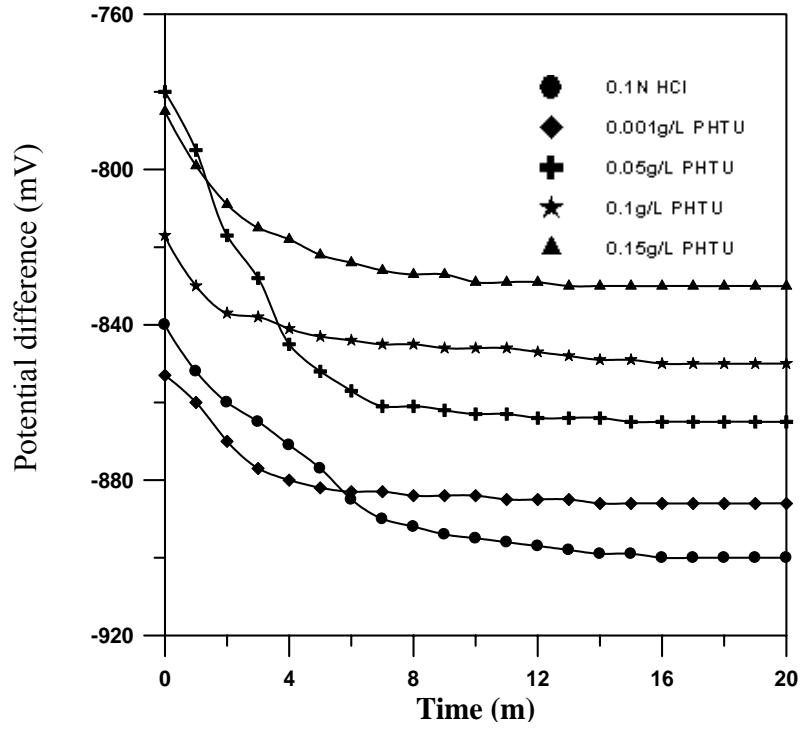


**Figure 5-20a** Potential difference vs. time for copper and zinc metals in 0.1N HCl, AR (Cu/Zn)=2, T=40 °C, t=20m, and 0 RPM

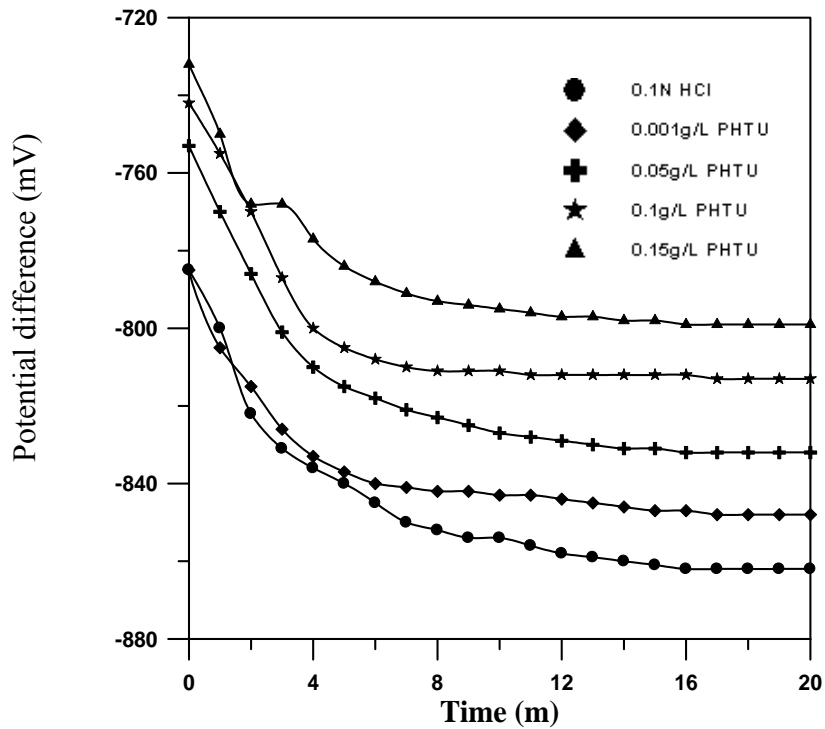


**Figure 5-21a** Potential difference vs. time for copper and zinc metals in 0.1N HCl, AR (Cu/Zn) =0.25, T=40 °C, t=20m, and 500 RPM



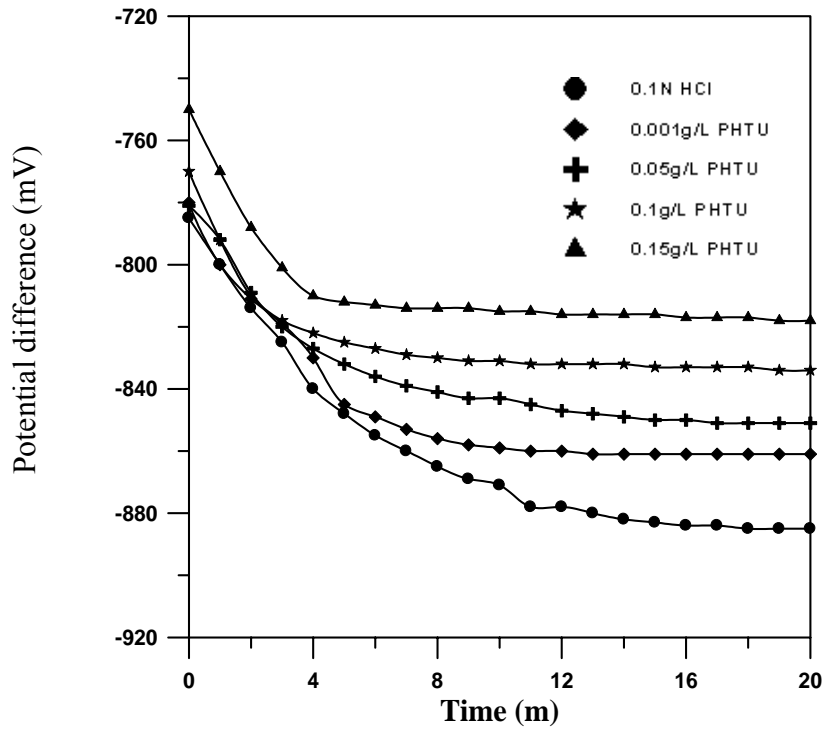


**Figure 5-22a** Potential difference vs. time for copper and zinc metals in 0.1N HCl, AR (Cu/Zn)=0.5, T=40 °C, t=20m, and 500 RPM

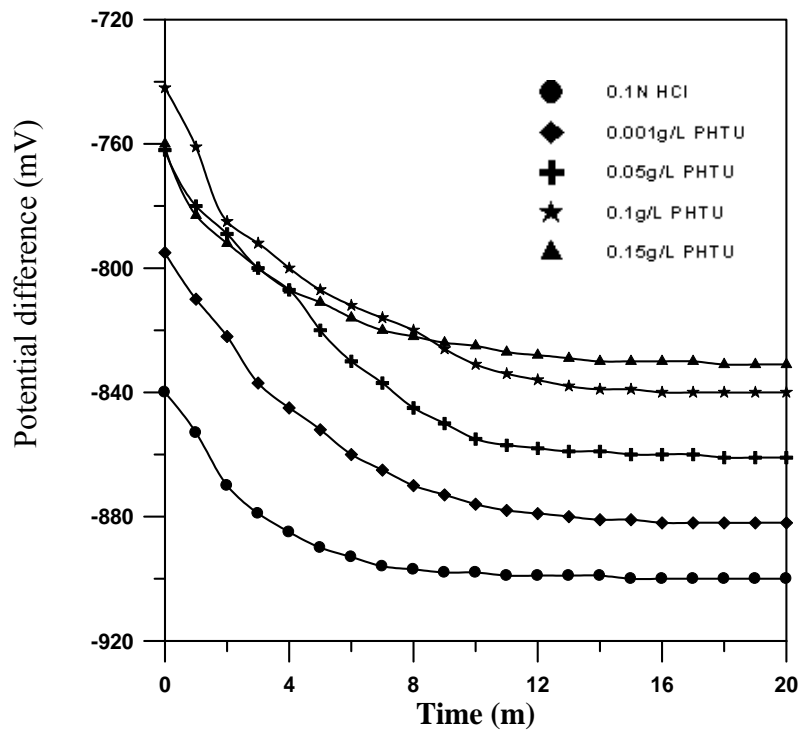


**Figure 5-23a** Potential difference vs. time for copper and zinc metals in 0.1N HCl, AR (Cu/Zn)=1, T=40 °C, t=20m, and 500 RPM

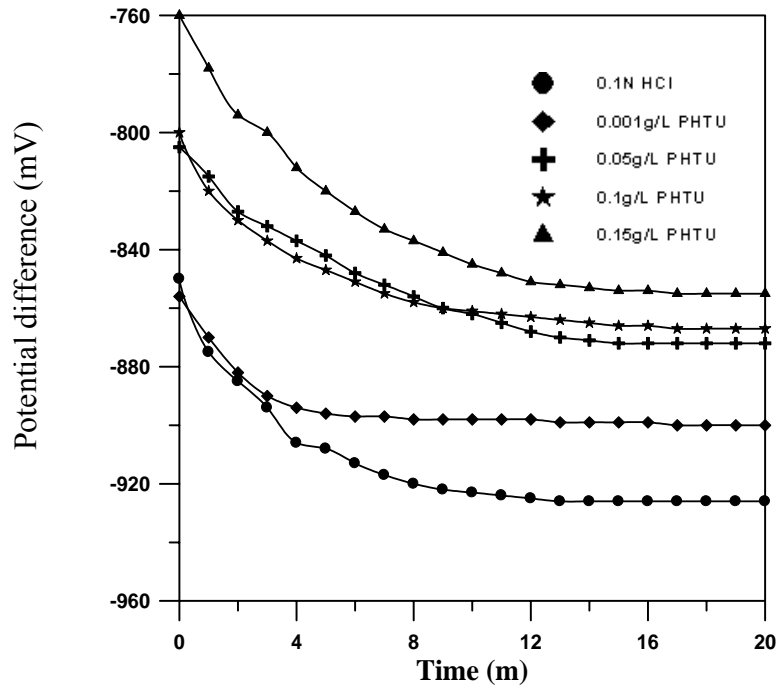


**Figure 5-24a** Potential difference vs. time for copper and zinc metals in 0.1N HCl, AR (Cu/Zn)=2, T=40 °C, t=20m, and 500 RPM

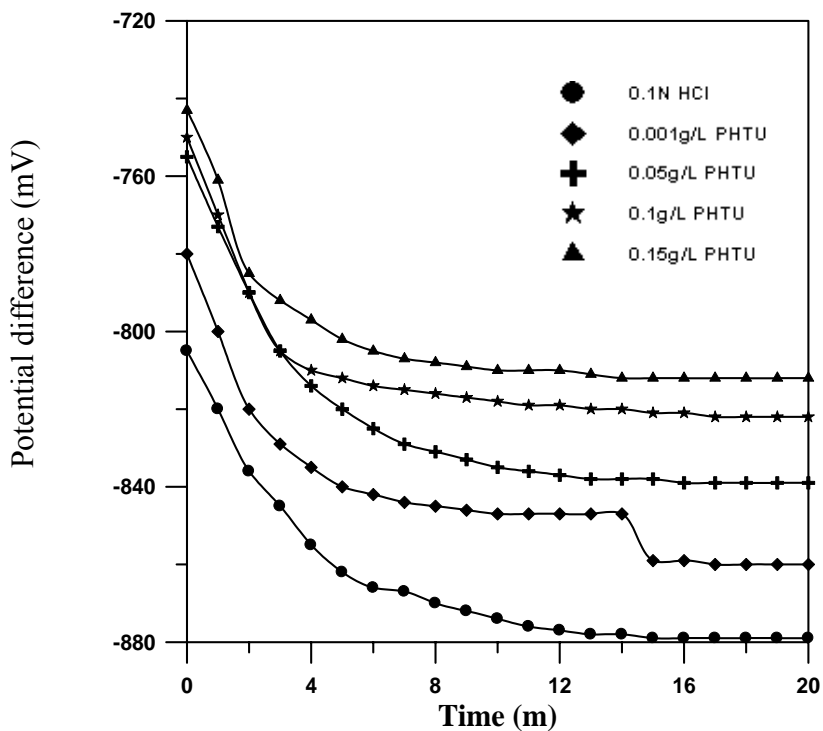


**Figure 5-25a** Potential difference vs. time for copper and zinc metals in 0.1N HCl, AR (Cu/Zn)=0.25, T=40 °C, t=20m, and 1000 RPM

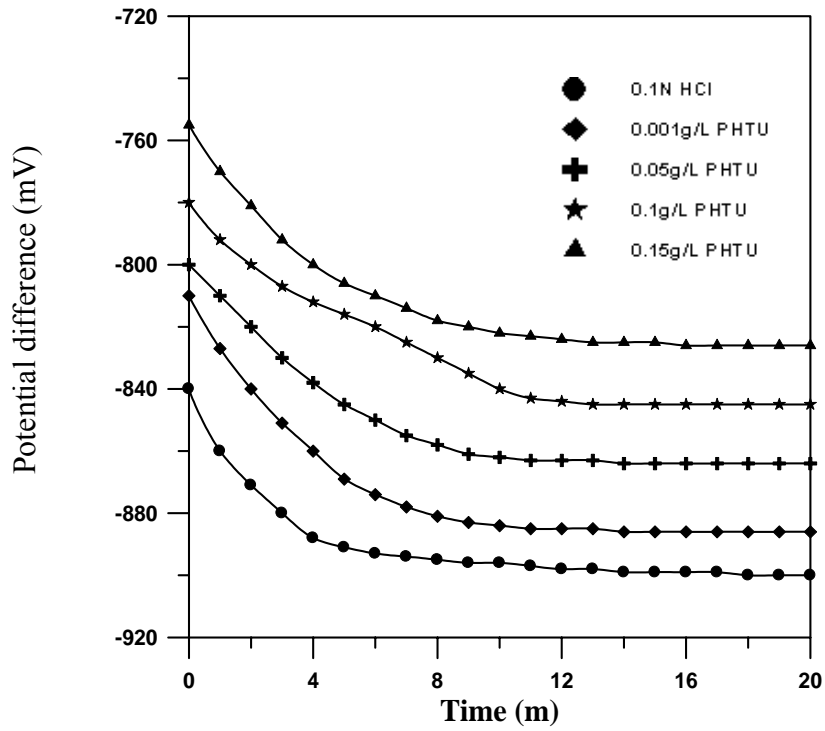


**Figure 5-26a** Potential difference vs. time for copper and zinc metals in 0.1N HCl, AR (Cu/Zn)=0.5, T=40 °C, t=20m, and 1000 RPM

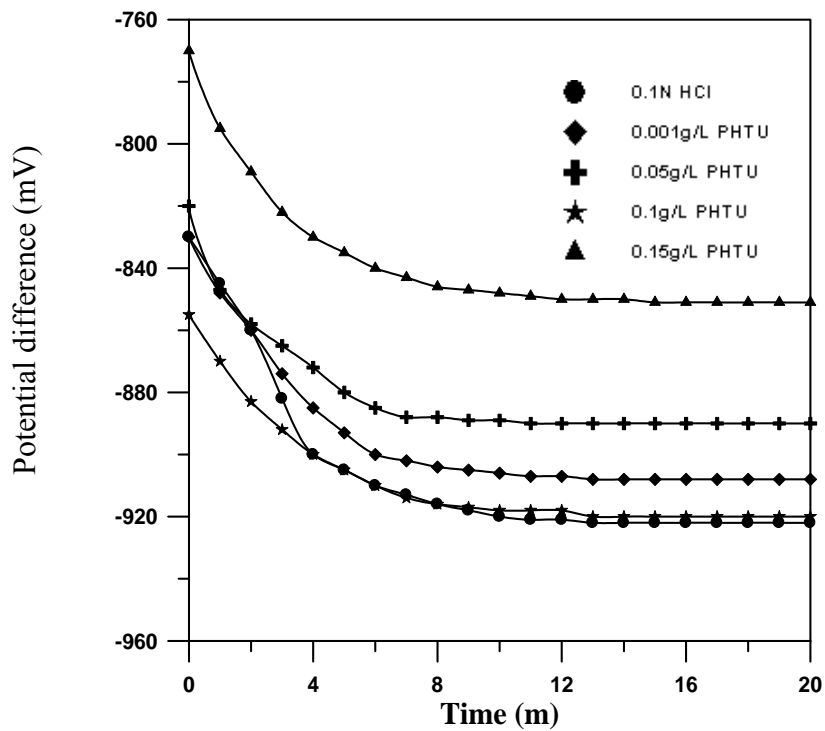


**Figure 5-27a** Potential difference vs. time for copper and zinc metals in 0.1N HCl, AR (Cu/Zn)=1, T=40 °C, t=20m, and 1000 RPM

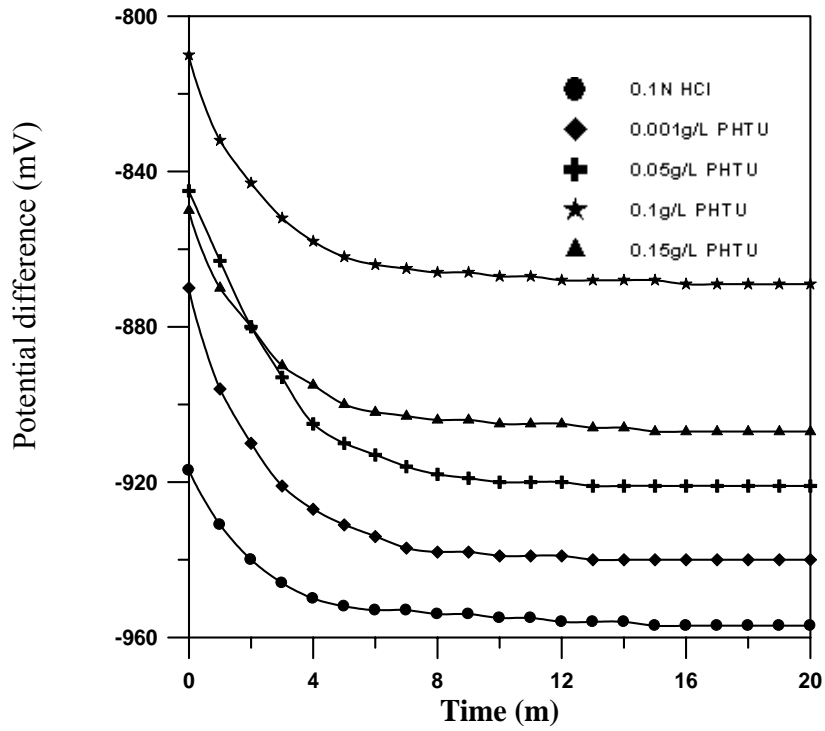


**Figure 5-28a** Potential difference vs. time for copper and zinc metals in 0.1N HCl, AR (Cu/Zn)=2, T=40 °C, t=20m, and 1000 RPM

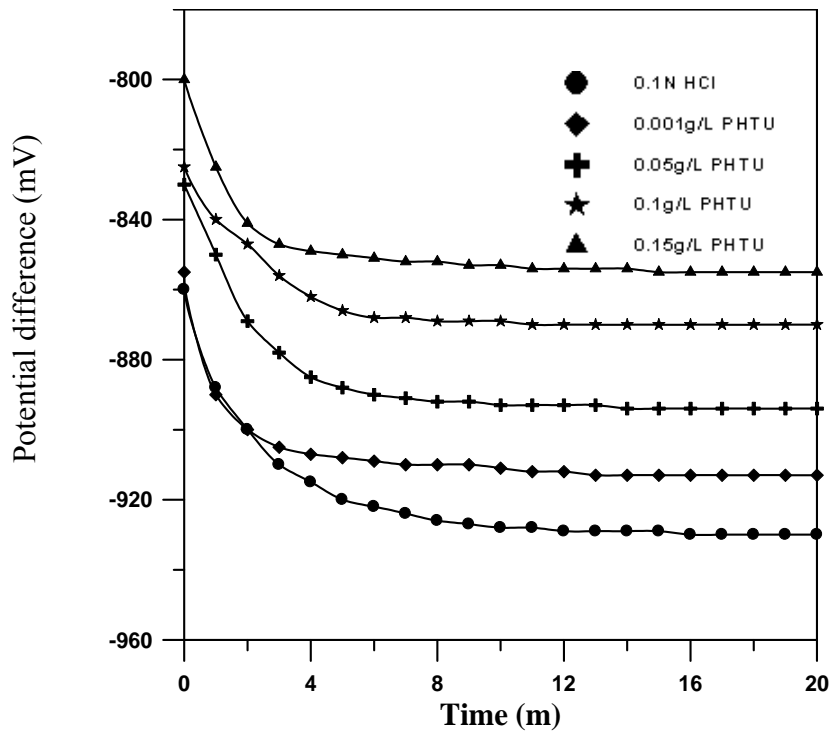


**Figure 5-29a** Potential difference vs. time for copper and zinc metals in 0.1N HCl, AR(Cu/Zn)=0.25, T=40 °C, t=20m, and 1500 RPM

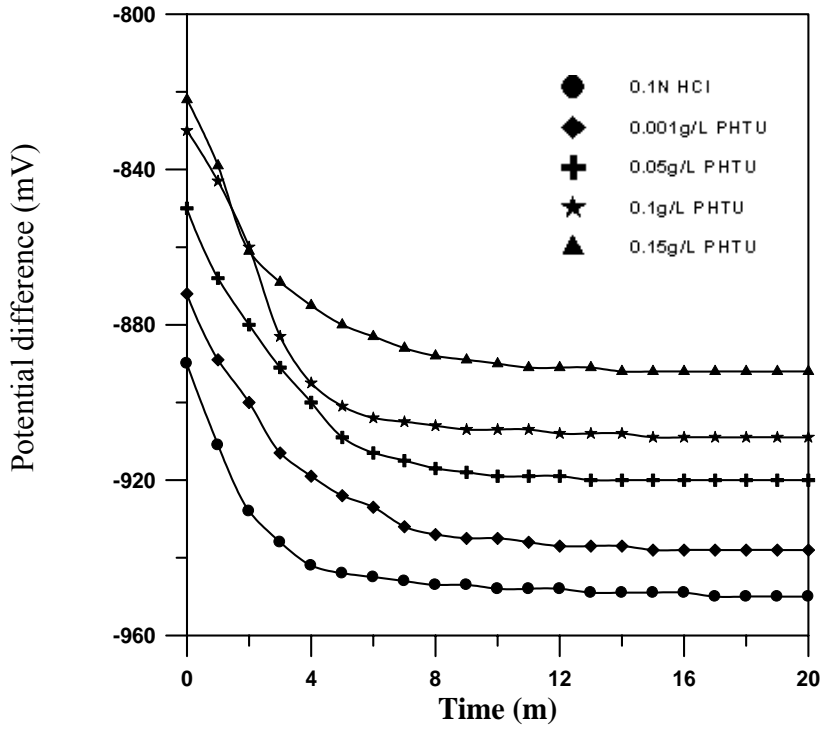


**Figure 5-30a** Potential difference vs. time for copper and zinc metals in 0.1N HCl, AR (Cu/Zn) = 0.5, T=40 °C, t=20m, and 1500 RPM

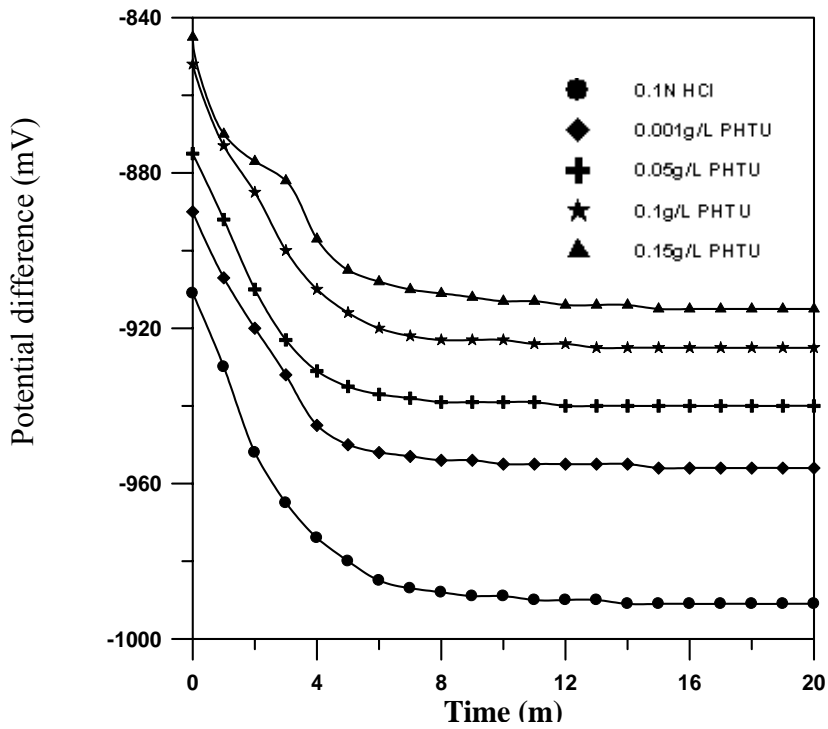


**Figure 5-31a** Potential difference vs. time for copper and zinc metals in 0.1N HCl, AR (Cu/Zn) = 1, T=40 °C, t=20m, and 1500 RPM

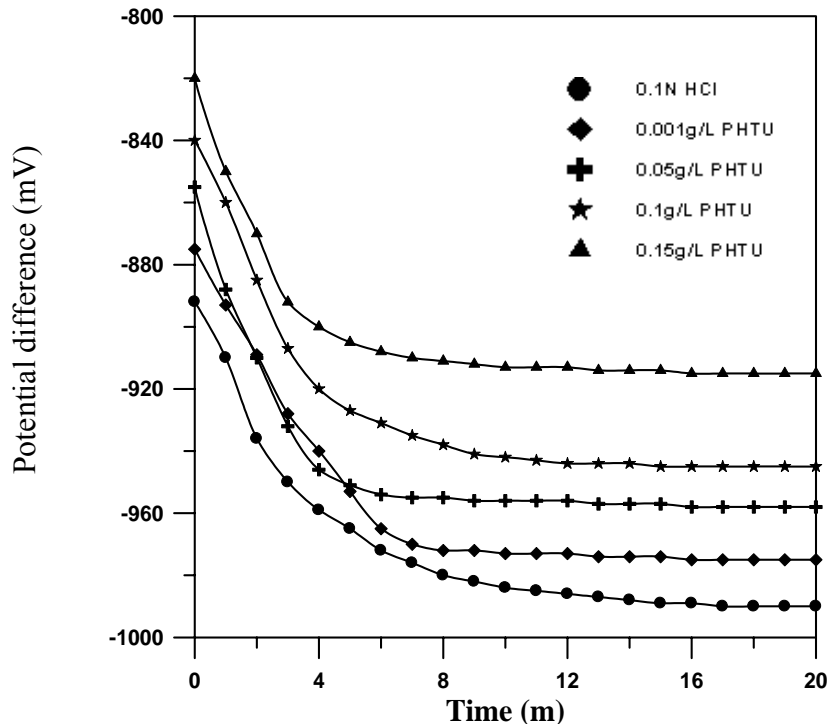


**Figure 5-32a** Potential difference vs. time for copper and zinc metals in 0.1N HCl, AR (Cu/Zn) =2, T=40 °C, t=20m, and 1500 RPM

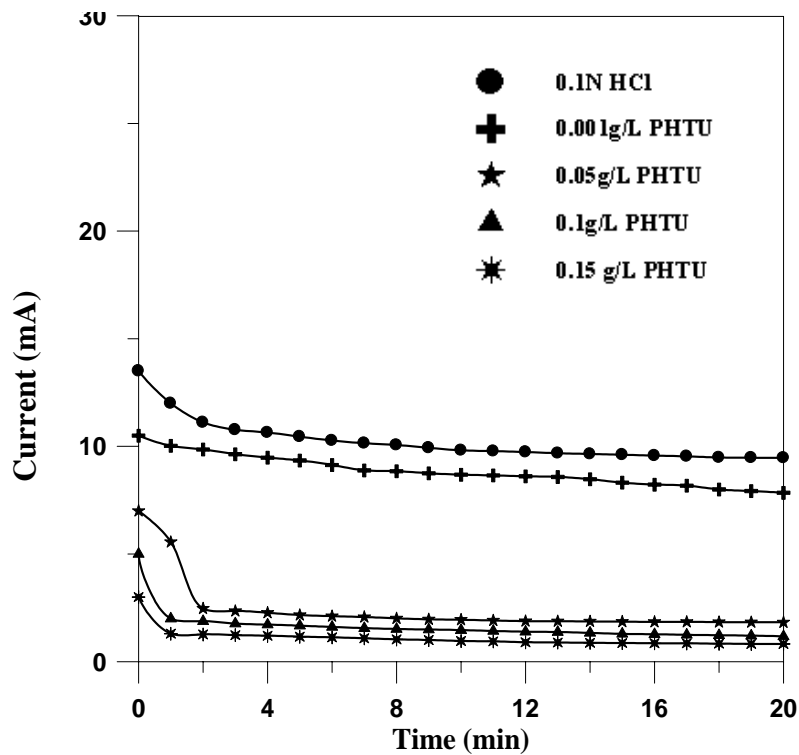


**Figure 5-17b** Current vs. time for a metal couple in 0.1N HCl, AR (Cu/Zn) =0.25, T=40 °C, t=20m, and 0 RPM

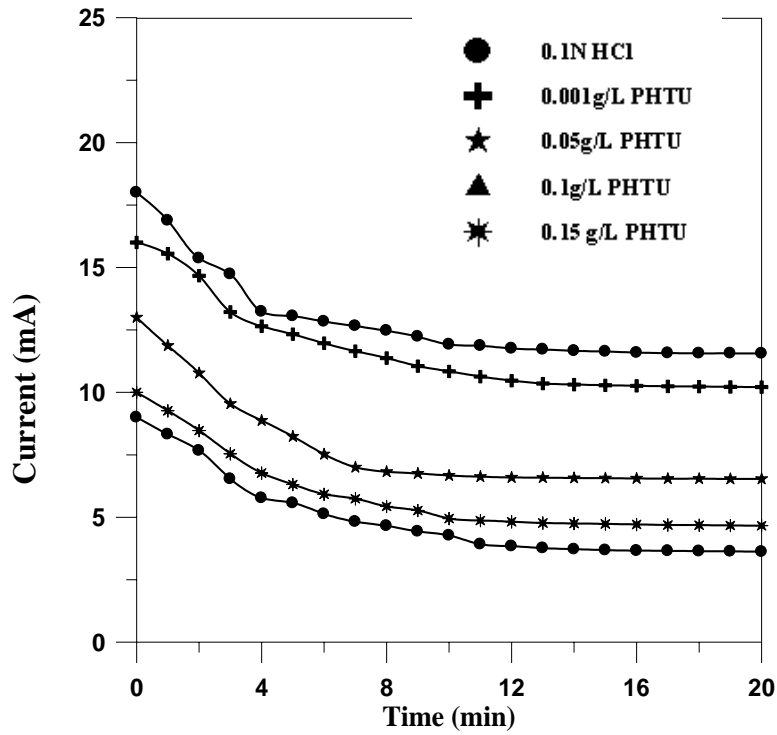


**Figure 5-18b** Current vs. time for a metal couple in 0.1N HCl, AR (Cu/Zn)=0.5, T=40 °C, t=20m, and 0 RPM

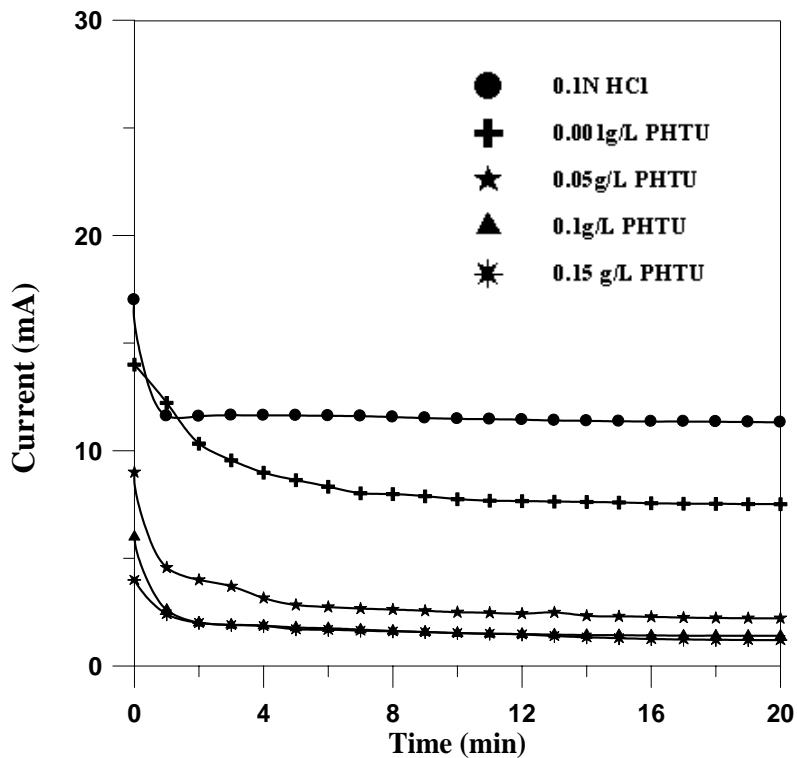


**Figure 5-19b** Current vs. time for a metal couple in 0.1N HCl, AR (Cu/Zn) = 1, T=40 °C, t=20m, and 0 RPM

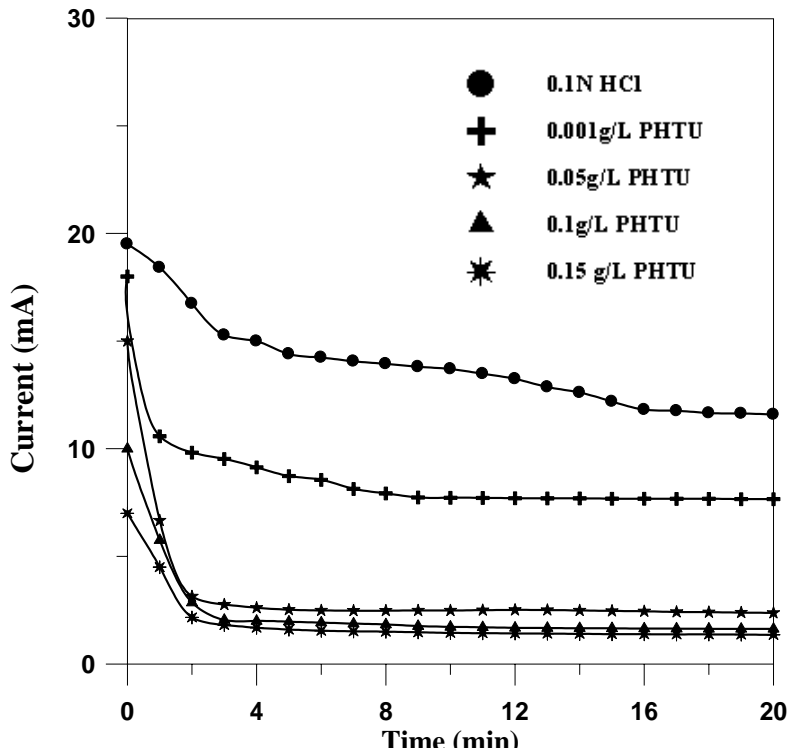


**Figure 5-20b** Current vs. time for a metal couple in 0.1N HCl, AR (Cu/Zn) =2, T=40 °C, t=20m, and 0 RPM

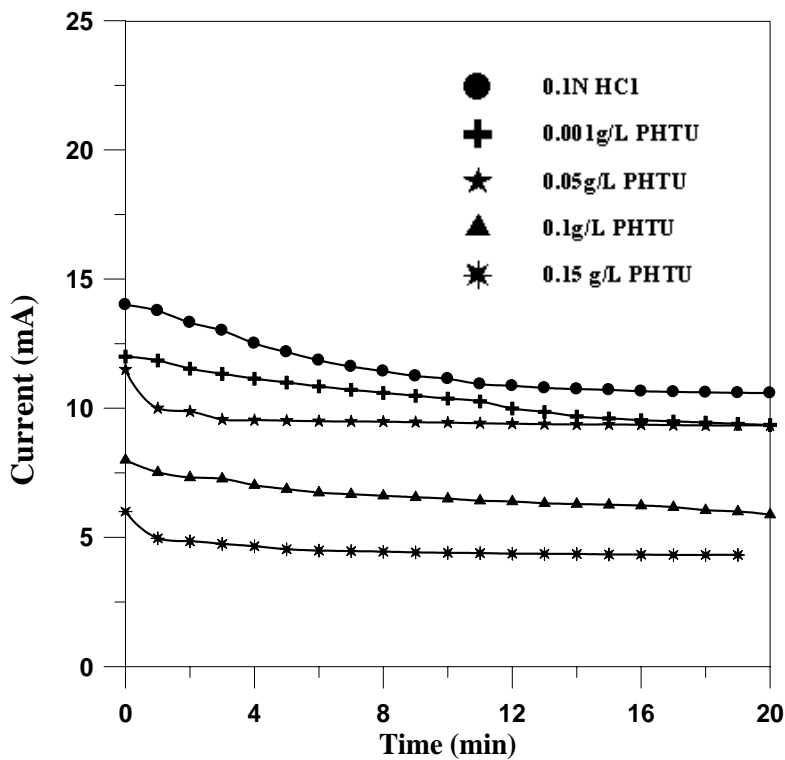


**Figure 5-21b** Current vs. time for a metal couple in 0.1N HCl, AR (Cu/Zn) =0.25, T=40 °C, t=20m, and 500 RPM



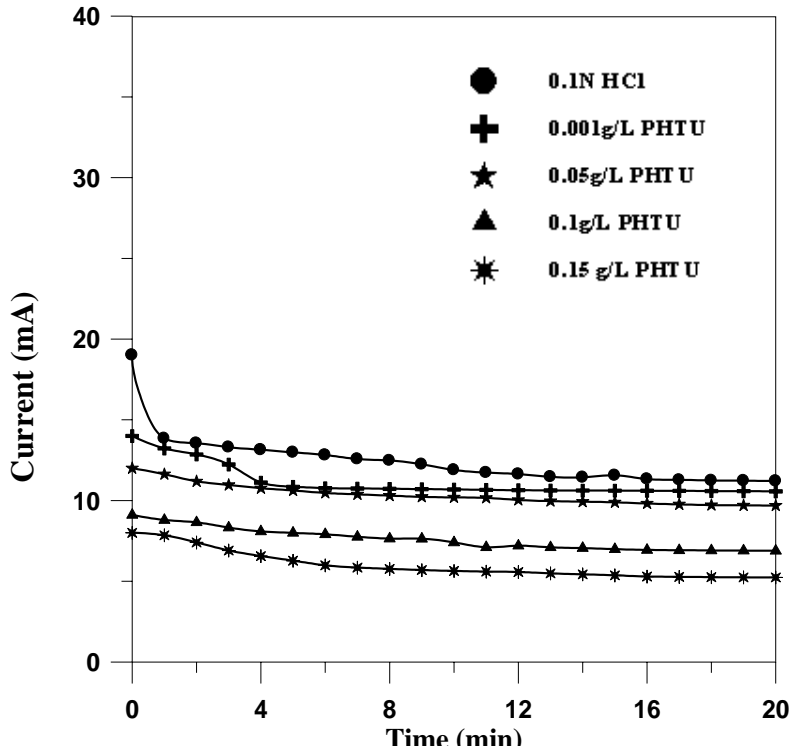


**Figure 5-22b** Current vs. time for a metal couple in 0.1N HCl, AR(Cu/Zn) =0.5, T=40 °C, t=20m, and 500 RPM

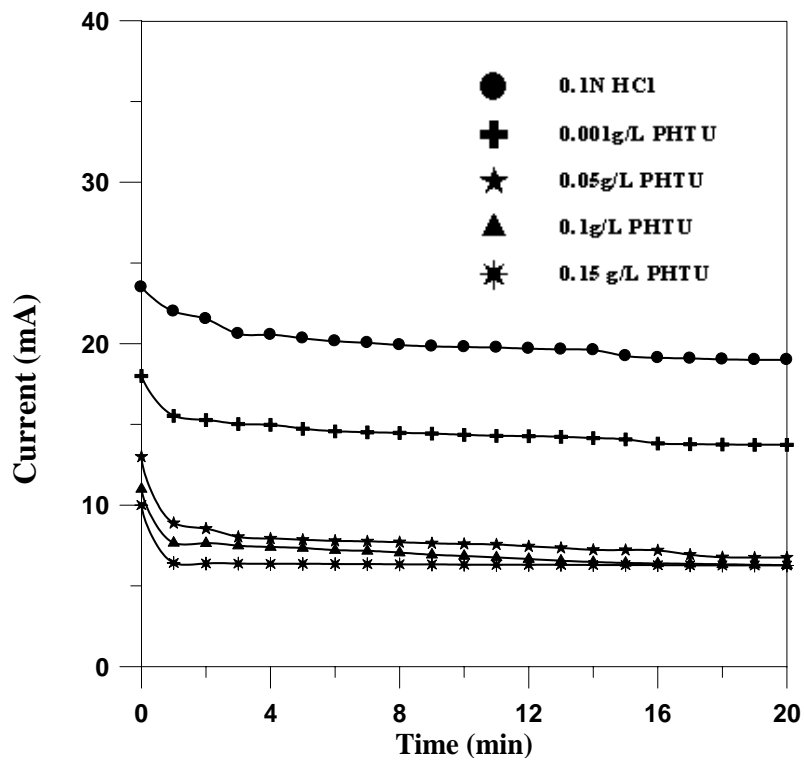


**Figure 5-23b** Current vs. time for a metal couple in 0.1N HCl, AR (Cu/Zn) =1, T=40 °C, t=20m, and 500 RPM

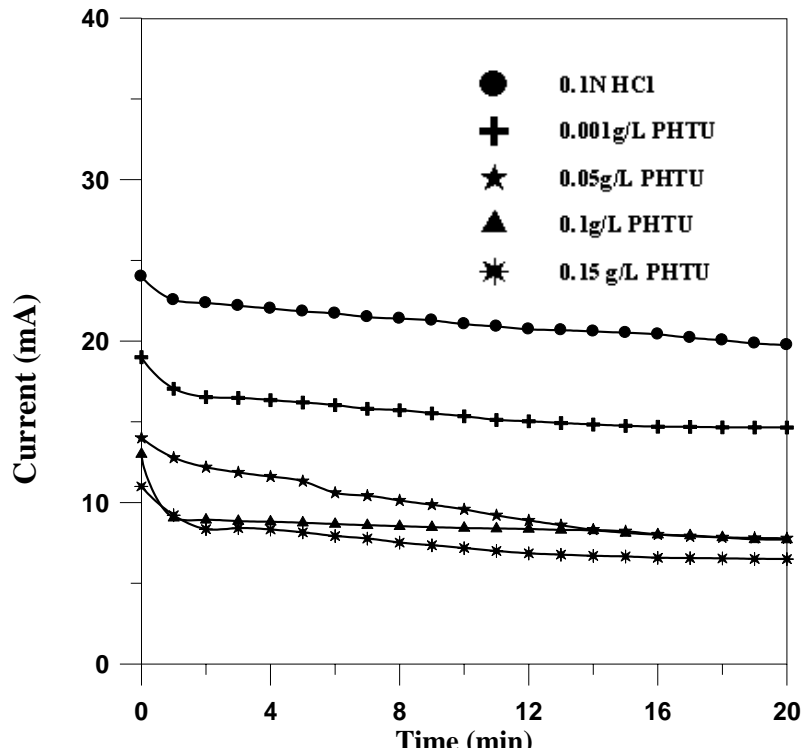


**Figure 5-24b** Current vs. time for a metal couple in 0.1N HCl, AR (Cu/Zn)=2, T=40 °C, t=20m, and 500 RPM

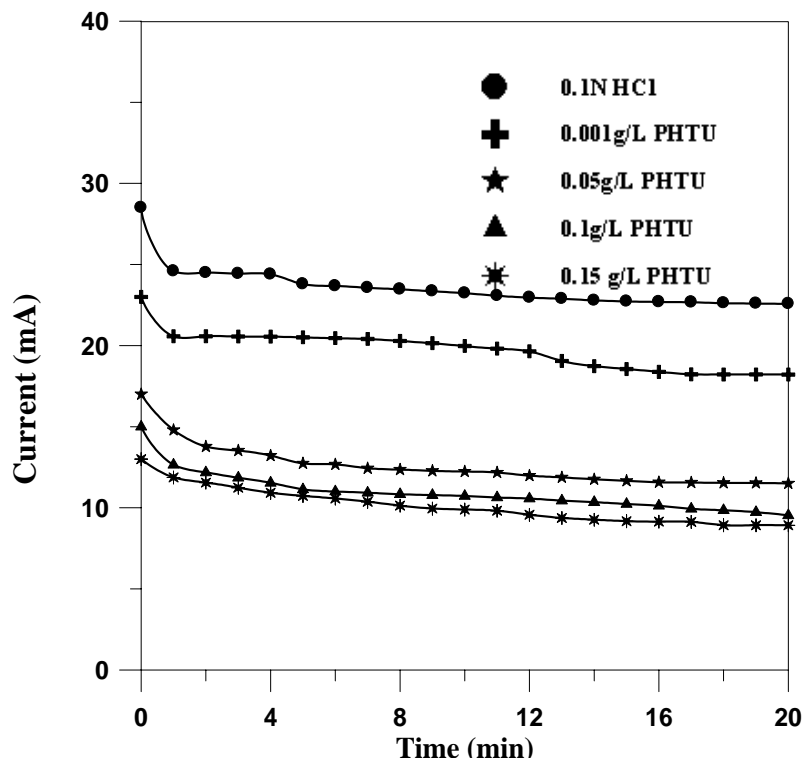


**Figure 5-25b** Current vs. time for a metal couple in 0.1N HCl, AR(Cu/Zn)=0.25, T=40 °C, t=20m, and 1000 RPM

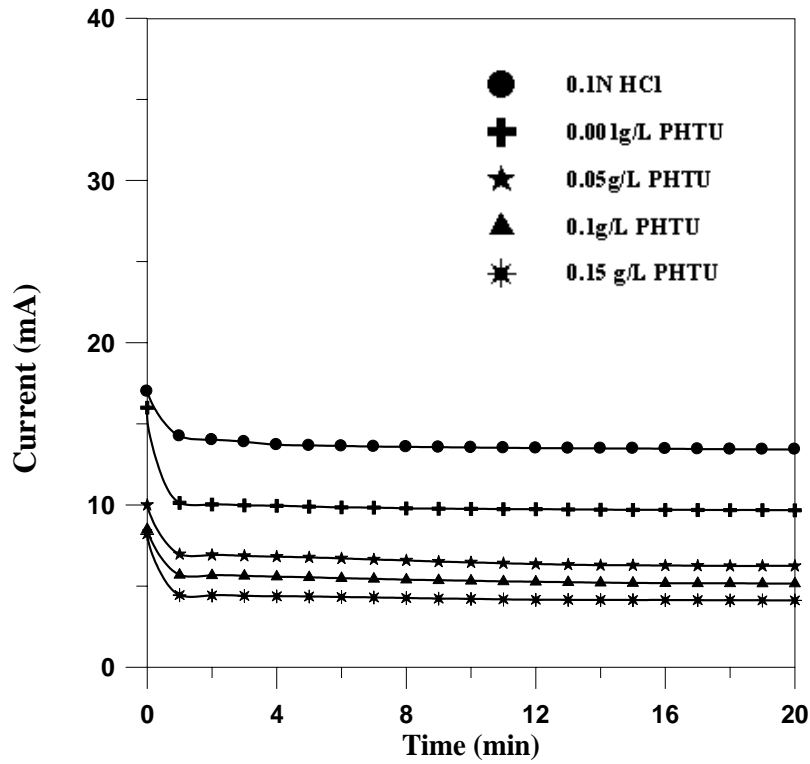


Figure 5-26b Current vs. time for a metal couple in 0.1N HCl, AR (Cu/Zn)=0.5, T=40 °C, t=20m, and 1000 RPM

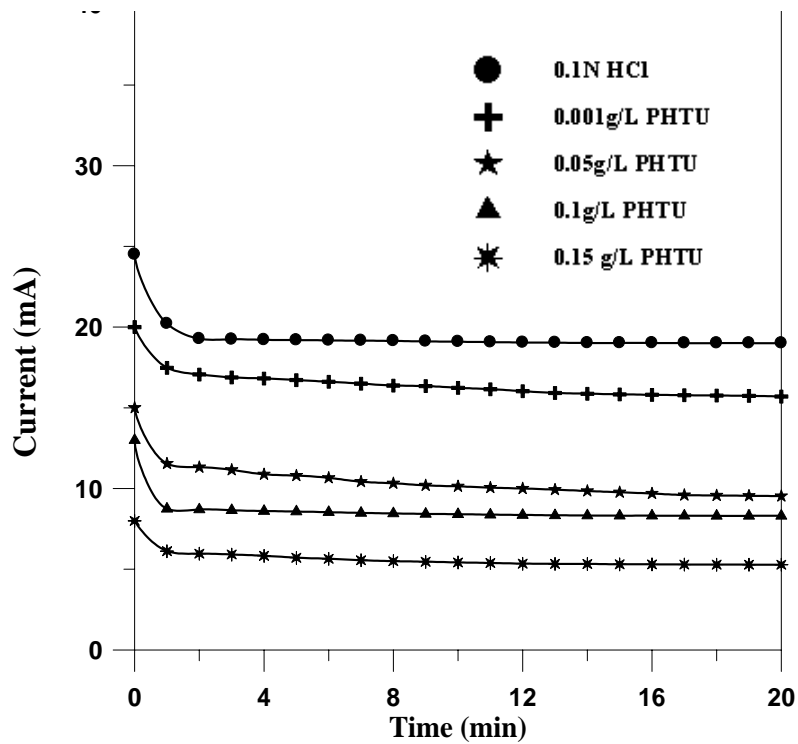
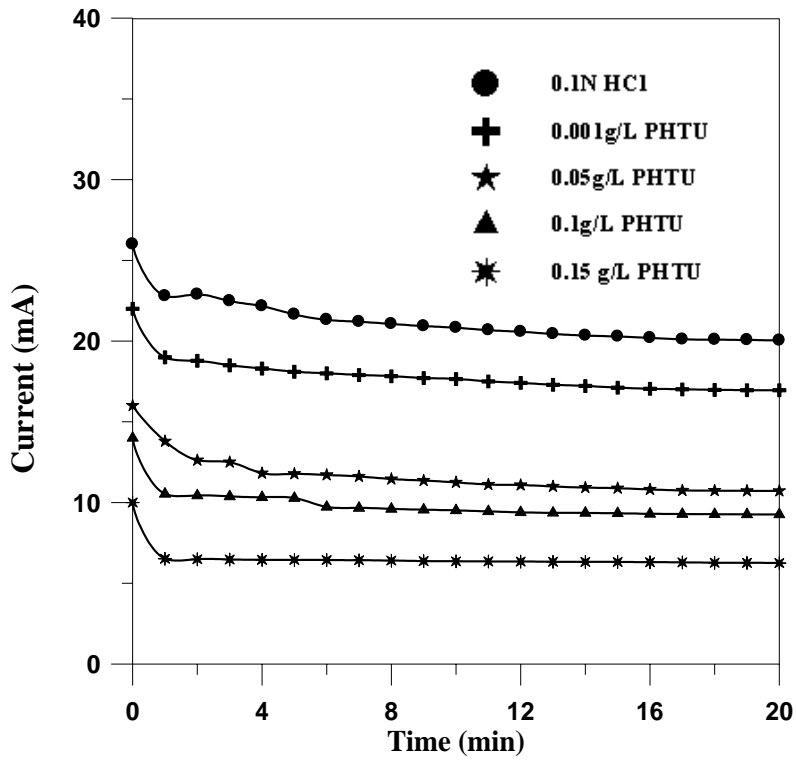
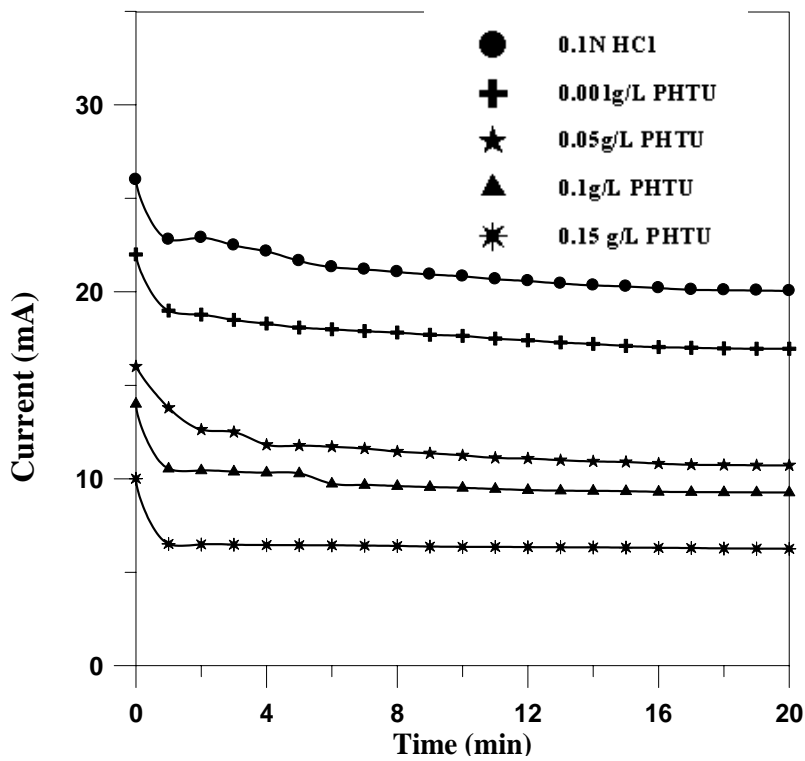


Figure 5-27b Current vs. time for a metal couple in 0.1N HCl, AR(Cu/Zn) =1, T=40 °C, t=20m, and 1000 RPM



**Figure 5-28b** Current vs. time for a metal couple in 0.1N HCl, AR (Cu/Zn)=2, T=40 °C, t=20m, and 1000 RPM



**Figure 5-29b** Current vs. time for a metal couple in 0.1N HCl, AR (Cu/Zn)=0.25, T=40 °C, t=20m, and 1500 RPM

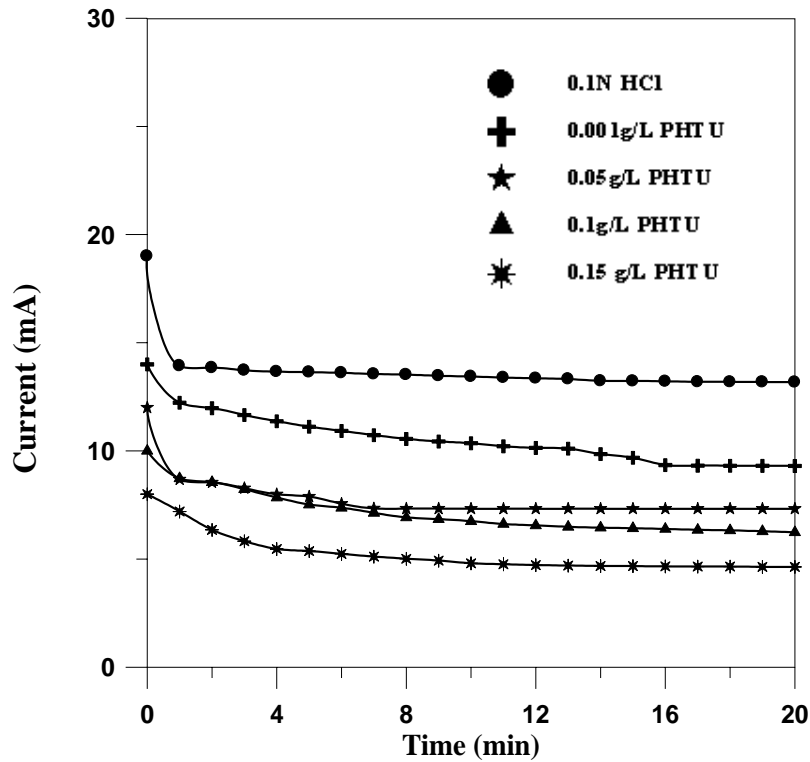


**Figure 5-30b** Current vs. time for a metal couple in 0.1N HCl, AR (Cu/Zn) = 0.5, T=40 °C, t=20m, and 1500 RPM

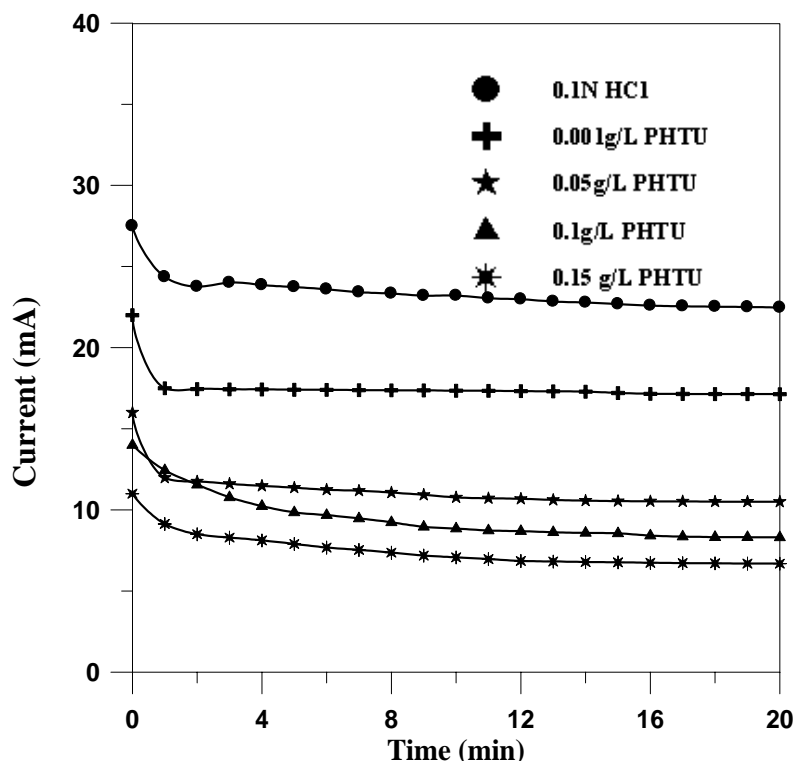


**Figure 5-31b** Current vs. time for a metal couple in 0.1N HCl, AR (Cu/Zn) = 1, T=40 °C, t=20m, and 1500 RPM

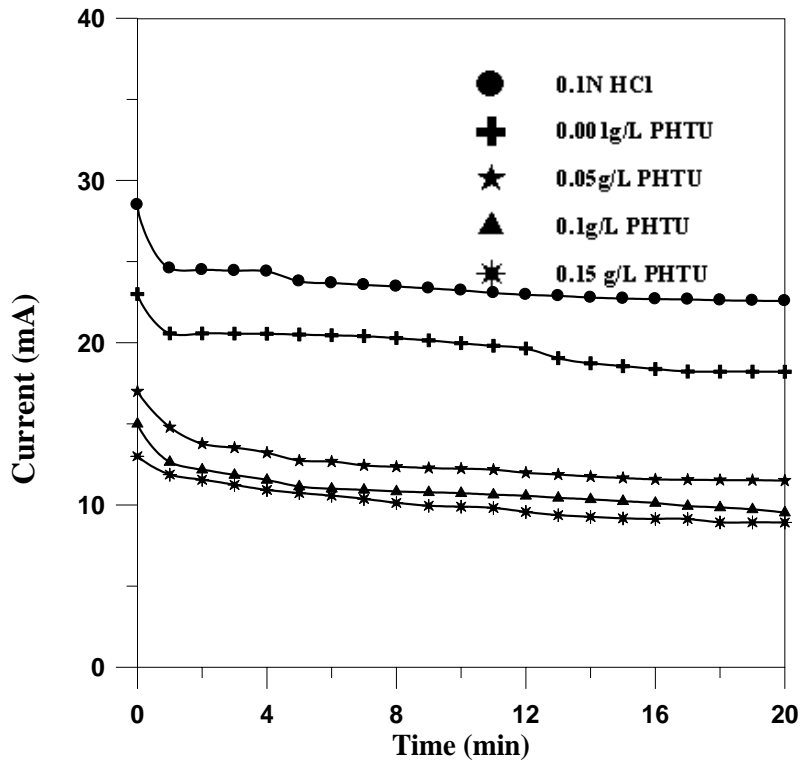


**Figure 5-32b** Current vs. time for a metal couple in 0.1N HCl, AR (Cu/Zn) =2, T=40 °C, t=20m, and 1500 RPM

### 5.3.3 Carbon Steel and Zinc coupling:

There are two main categories of these experiments:

- a. Direct results of voltage difference against time for 20 minutes, experiments were carried out in aerated 0.1N HCl under the same previous conditions of copper and carbon steel coupling above, **Figs.(5.33a-5.48a).**
- b. Direct results of current against time for 20 minutes as shown in **Figs.(5.33b-5.48b).**

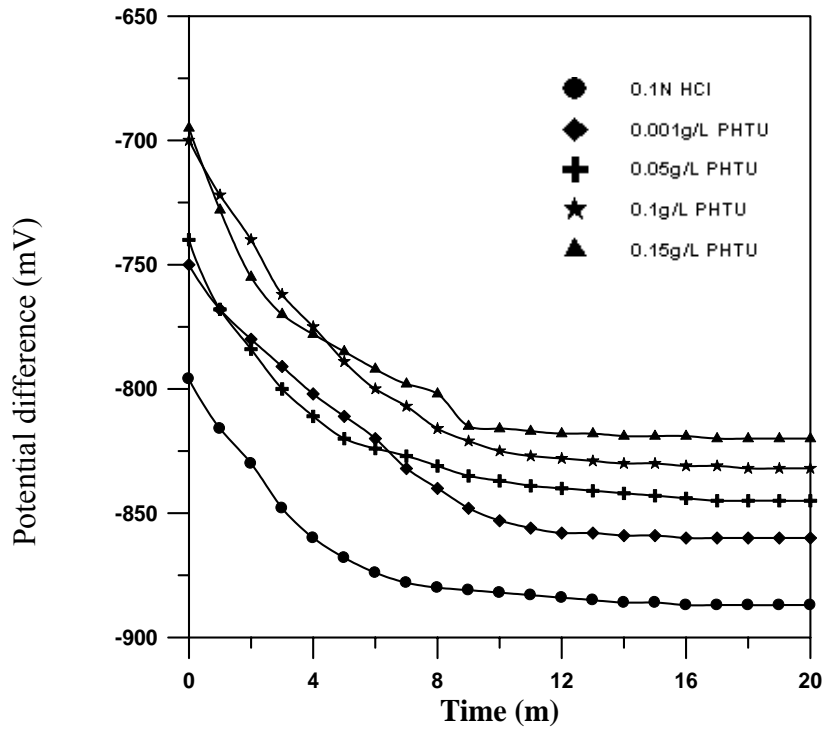


**Figure 5-33a** Potential difference vs. time for iron and zinc metals in 0.1N HCl, AR (Fe/Zn)=0.25, T=40 °C, t=20m, and 0 RPM

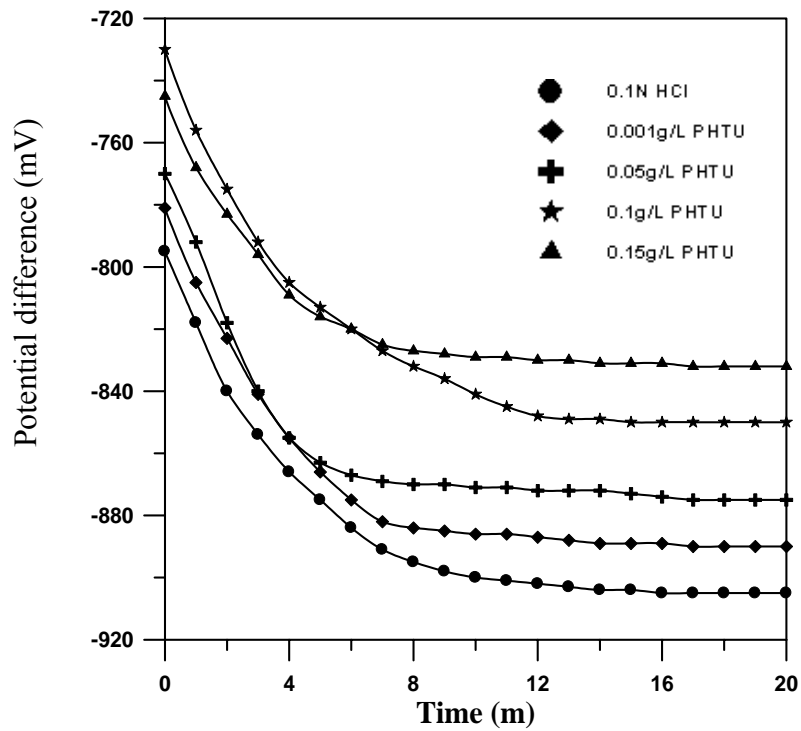


**Figure 5-34a** Potential difference vs. time for iron and zinc metals in 0.1N HCl, AR (Fe/Zn)=0.5, T=40 °C, t=20m, and 0 RPM

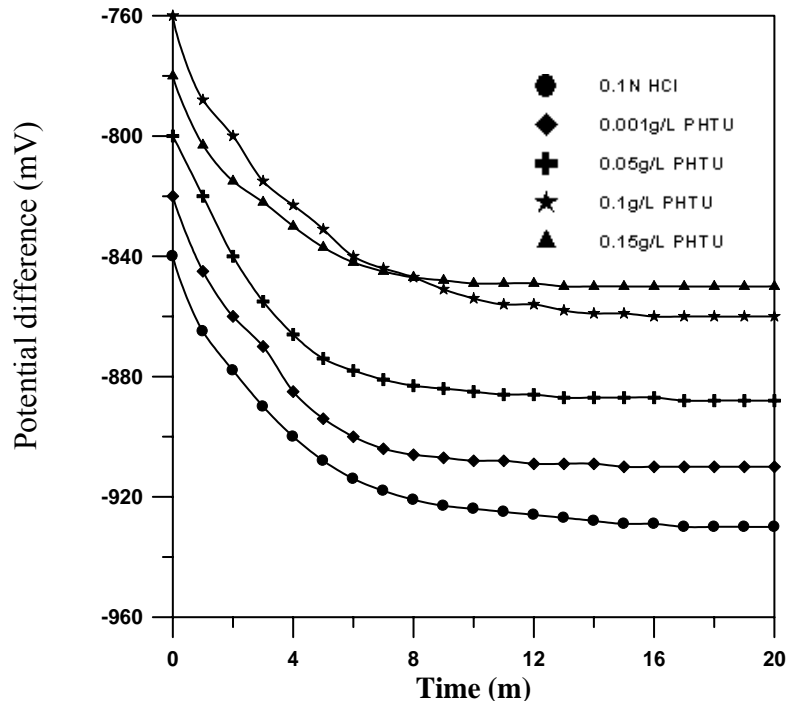


**Figure 5-35a** Potential difference vs. time for iron and zinc metals in 0.1N HCl, AR (Fe/Zn)=1, T=40 °C, t=20m, and 0 RPM

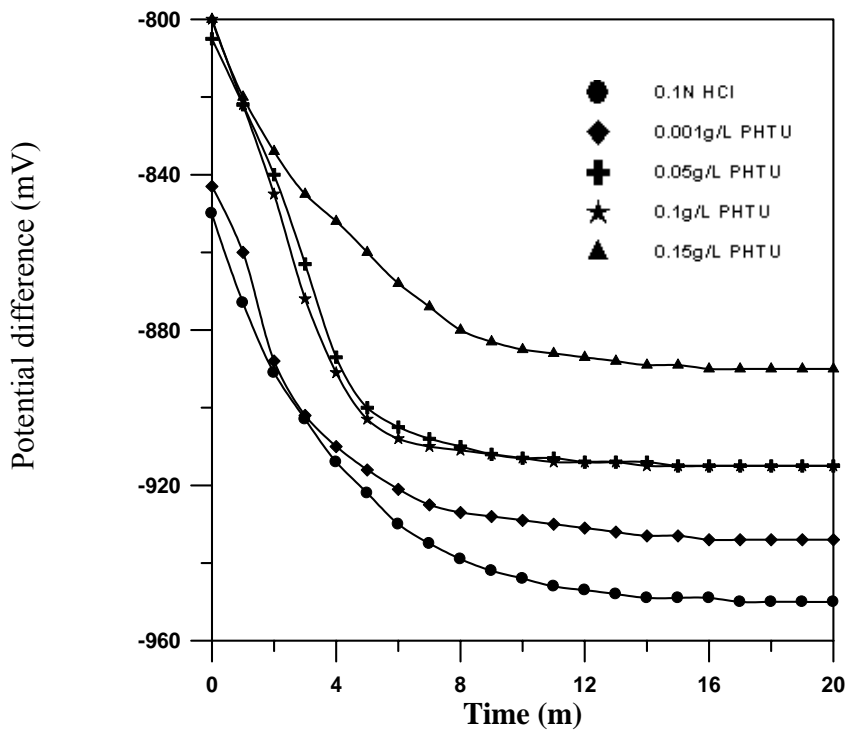


**Figure 5-36a** Potential difference vs. time for iron and zinc metals in 0.1N HCl, AR (Fe/Zn)=2, T=40 °C, t=20m, and 0 RPM



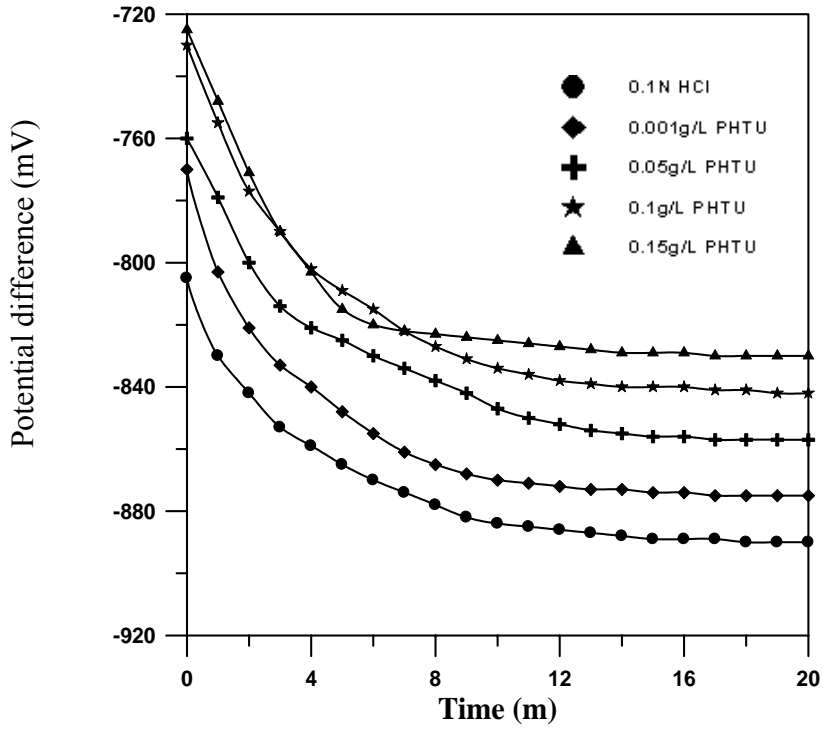


**Figure 5-37a** Potential difference vs. time for iron and zinc metals in 0.1N HCl, AR (Fe/Zn) = 0.25, T = 40 °C, t = 20m, and 500 RPM

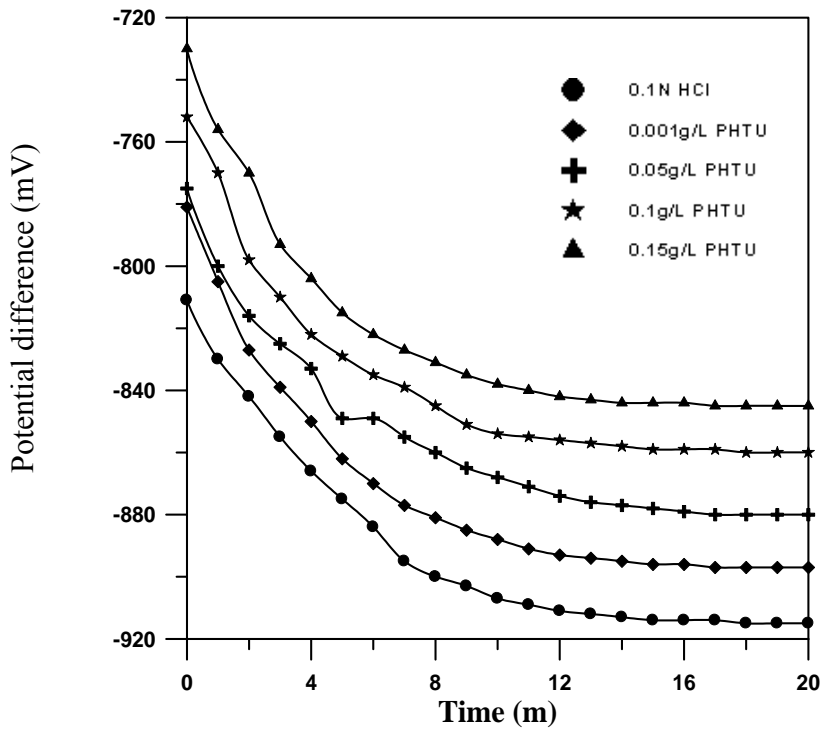


**Figure 5-38a** Potential difference vs. time for iron and zinc metals in 0.1N HCl, AR (Fe/Zn) = 0.5, T = 40 °C, t = 20m, and 500 RPM

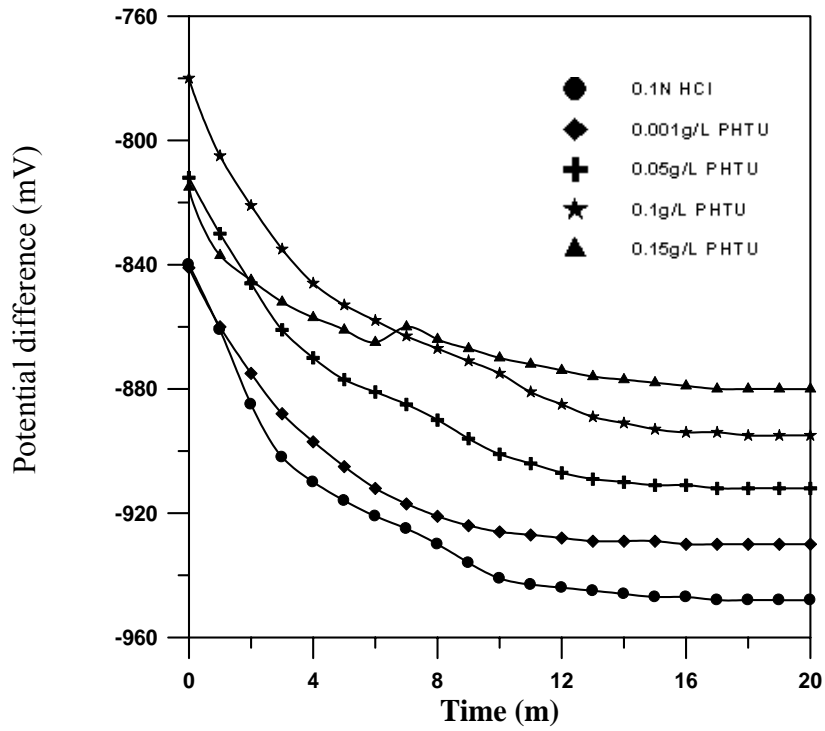


**Figure 5-39a** Potential difference vs. time for iron and zinc metals in 0.1N HCl, AR (Fe/Zn) =1, T=40 °C, t=20m, and 500 RPM

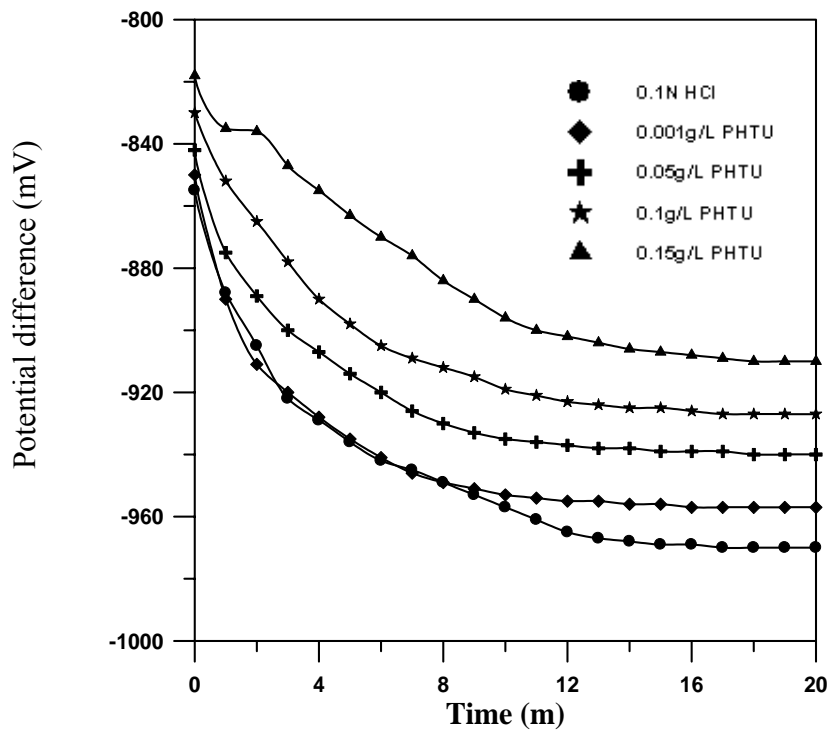


**Figure 5-40a** Potential difference vs. time for iron and zinc metals in 0.1N HCl, AR(Fe/Zn) =2, T=40 °C, t=20m, and 500 RPM

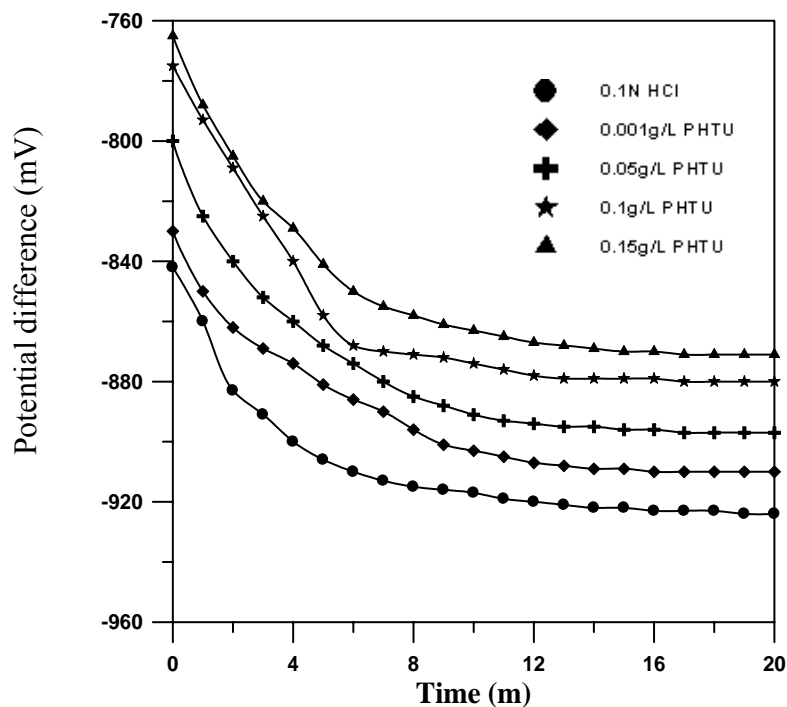


**Figure 5-41a** Potential difference vs. time for iron and zinc metals in 0.1N HCl, AR (Fe/Zn) = 0.25, T=40 °C, t=20m, and 1000 RPM

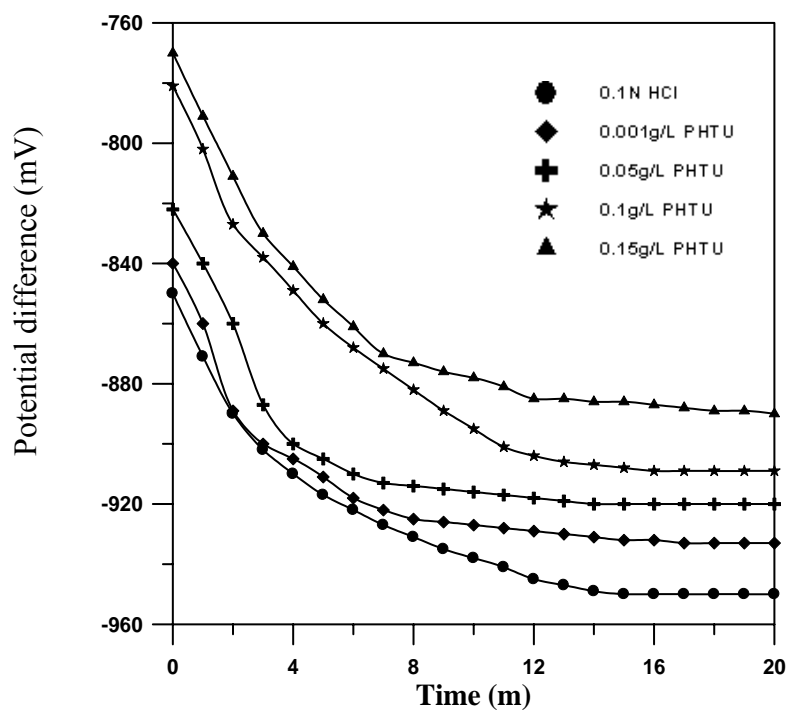


**Figure 5-42a** Potential difference I vs. time for iron and zinc metals in 0.1N HCl, AR (Fe/Zn) = 0.5, T=40 °C, t=20m, and 1000 RPM

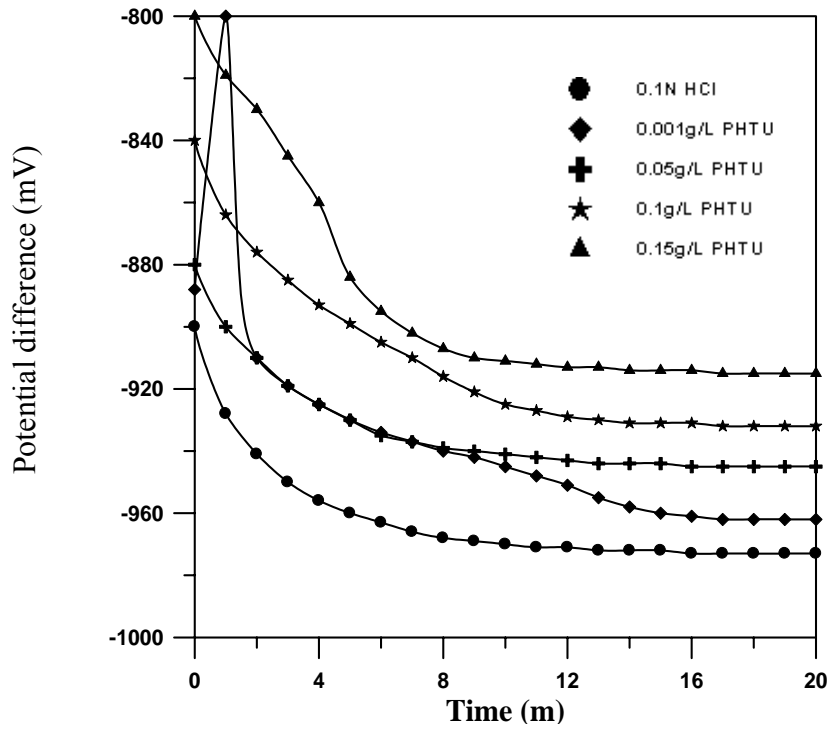


**Figure 5-43a** Potential difference vs. time for iron and zinc metals in 0.1N HCl, AR (Fe/Zn) = 1, T=40 °C, t=20m, and 1000 RPM

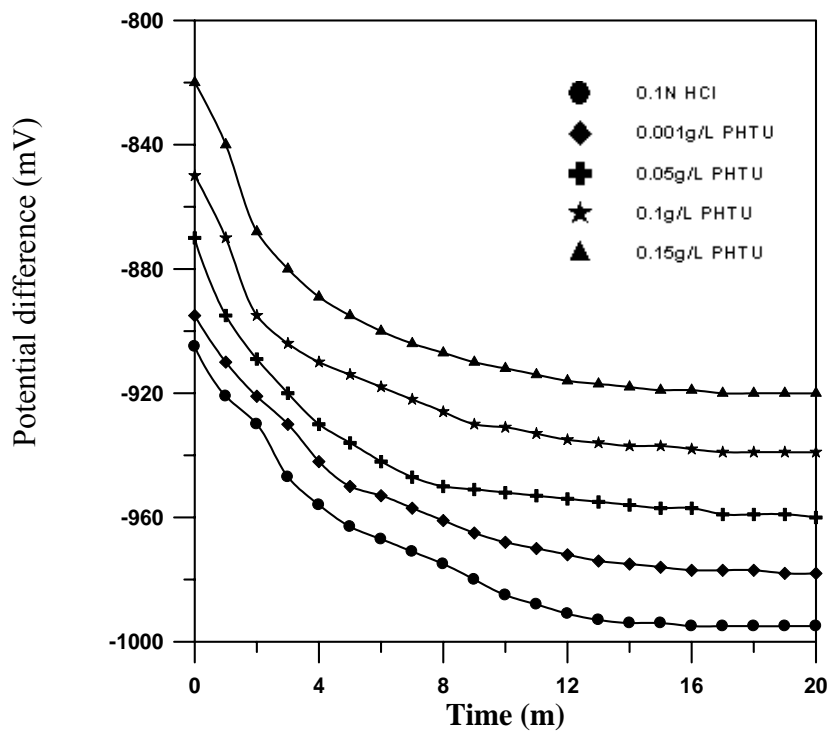


**Figure 5-44a** Potential difference vs. time for iron and zinc metals in 0.1N HCl, AR(Fe/Zn) = 2, T=40 °C, t=20m, and 1000 RPM

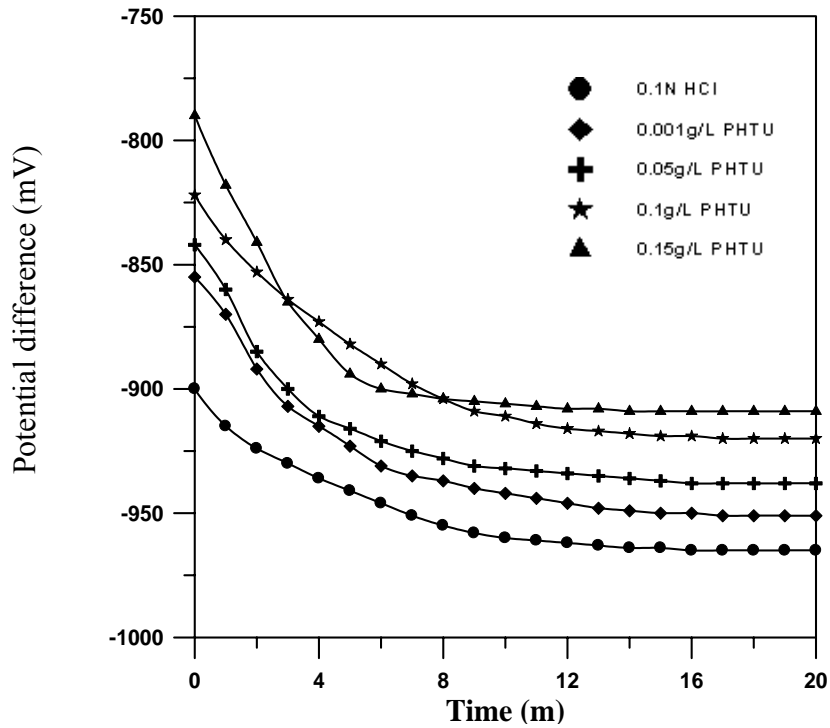


**Figure 5-45a** Potential difference vs. time for iron and zinc metals in 0.1N HCl, AR (Fe/Zn)=0.25, T=40 °C, t=20m, and 1500 RPM

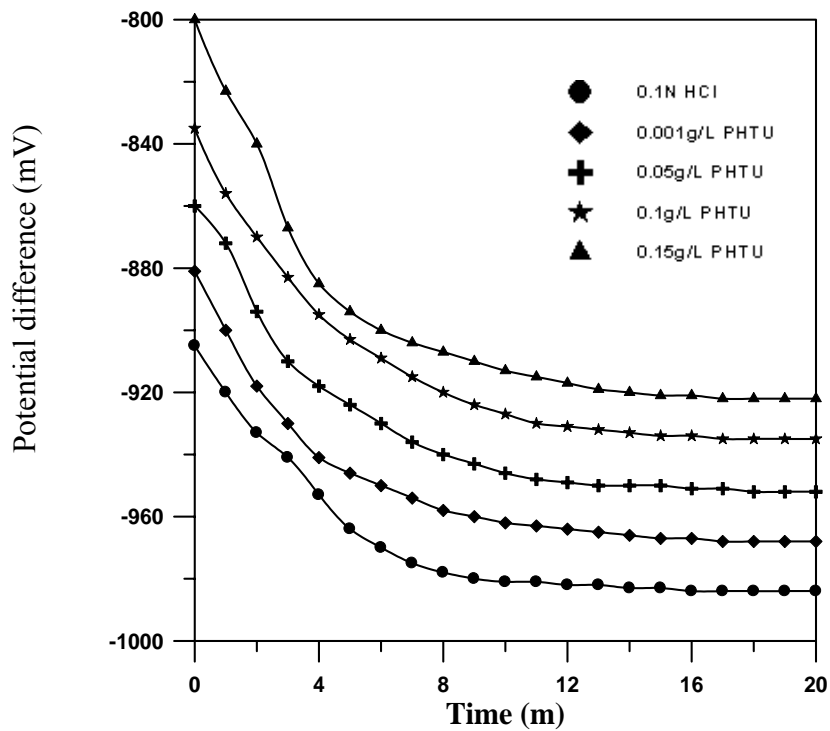


**Figure 5-46a** Potential difference vs. time for iron and zinc metals in 0.1N HCl, AR (Fe/Zn) =0.5, T=40 °C, t=20m, and 1500 RPM

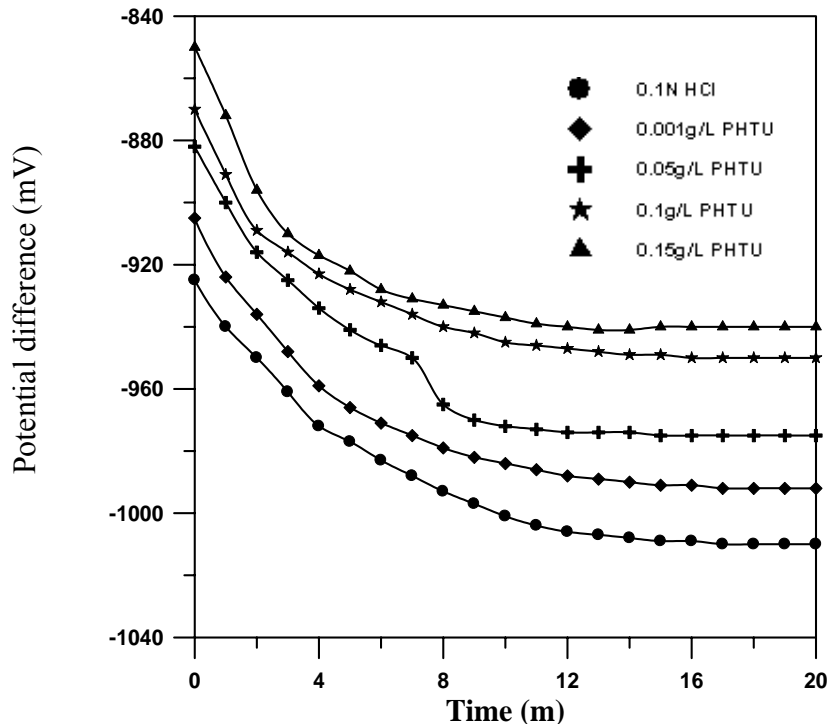


**Figure 5-47a** Potential difference vs. time for iron and zinc metals in 0.1N HCl, AR (Fe/Zn) =1, T=40 °C, t=20m, and 1500 RPM

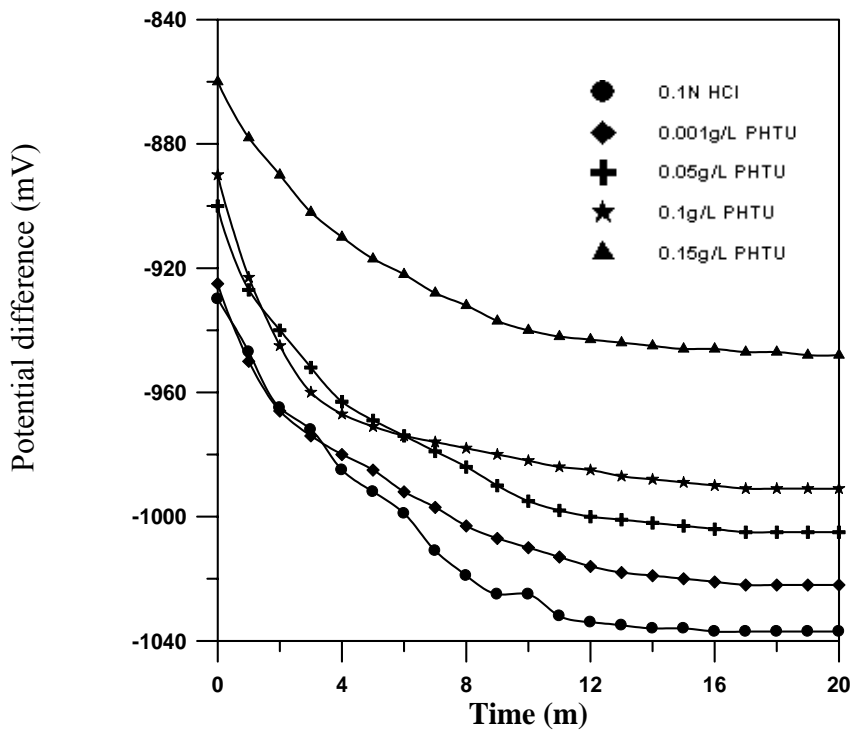


**Figure 5-48a** Potential difference vs. time for iron and zinc metals in 0.1N HCl, AR (Fe/Zn) =2, T=40 °C, t=20m, and 1500 RPM

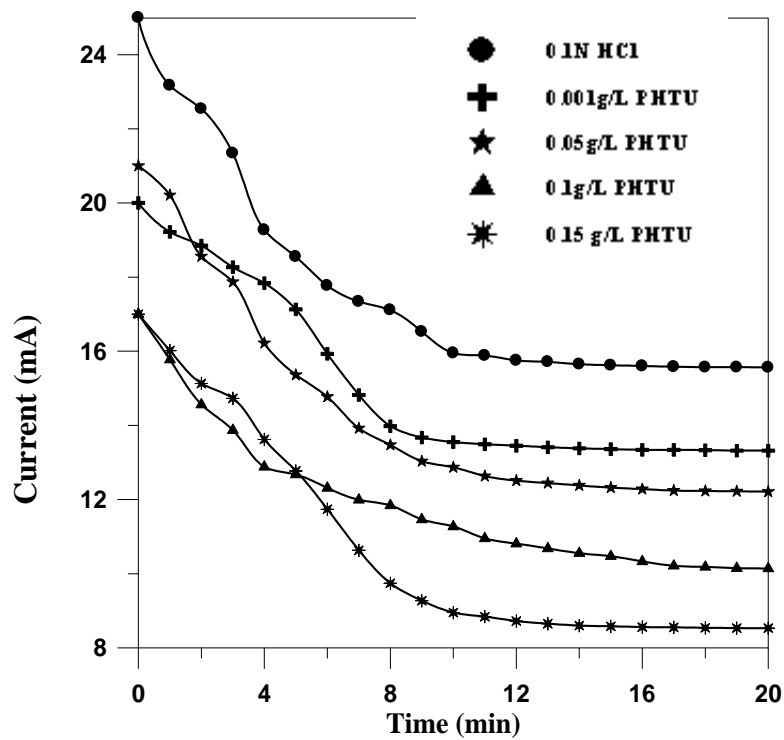


**Figure 5-33b** Current vs. time for a metal couple in 0.1N HCl, AR (Fe/Zn)=0.25, T=40 °C, t=20m, and 0 RPM

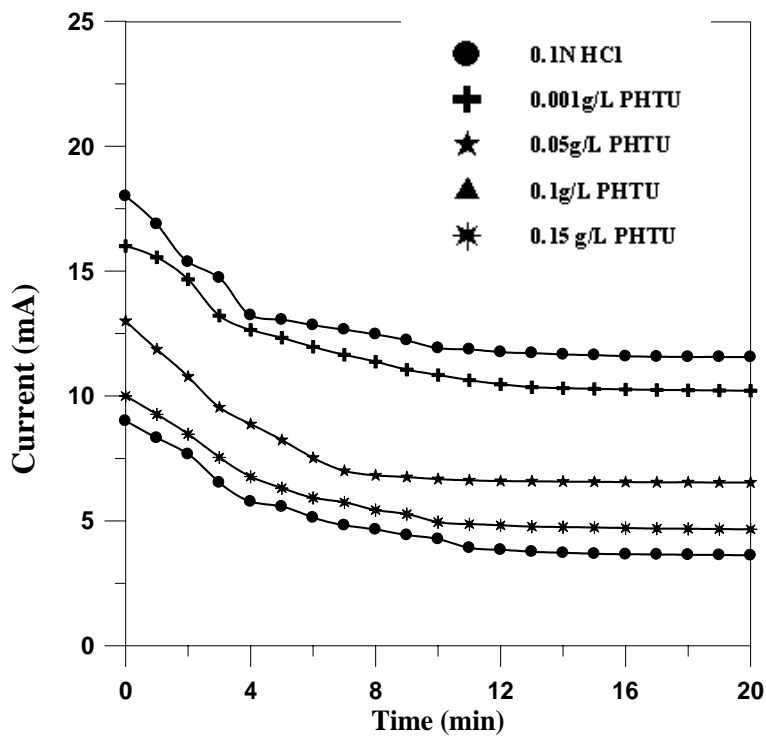


**Figure 5-34b** Current vs. time for a metal couple in 0.1N HCl, AR (Fe/Zn) = 0.5, T=40 °C, t=20m, and 0 RPM

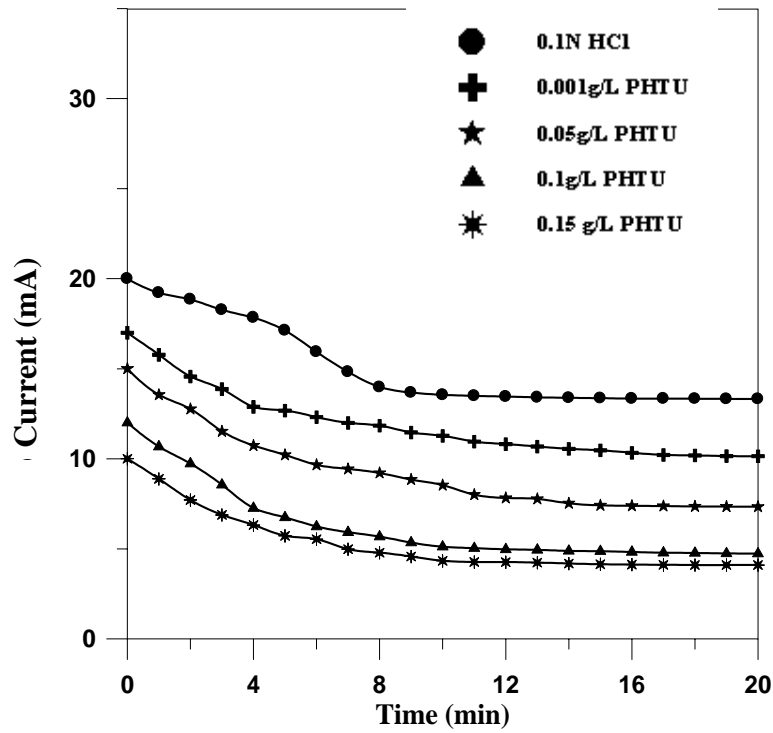


**Figure 5-35b** Current vs. time for a metal couple in 0.1N HCl, AR (Fe/Zn)=1, T=40 °C, t=20m, and 0 RPM

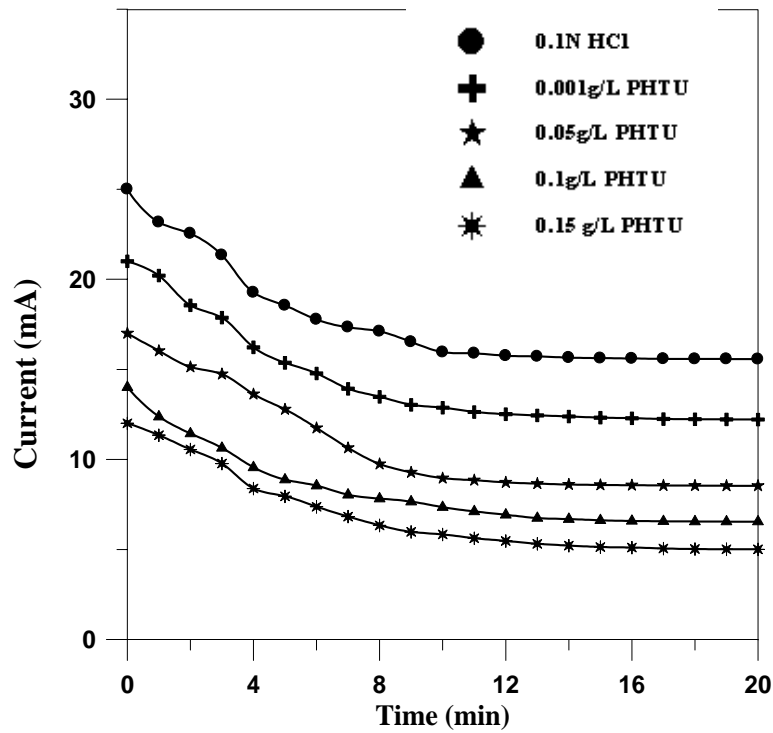


**Figure 5-36b** Current vs. time for a metal couple in 0.1N HCl, AR (Fe/Zn)=2, T=40 °C, t=20m, and 0 RPM



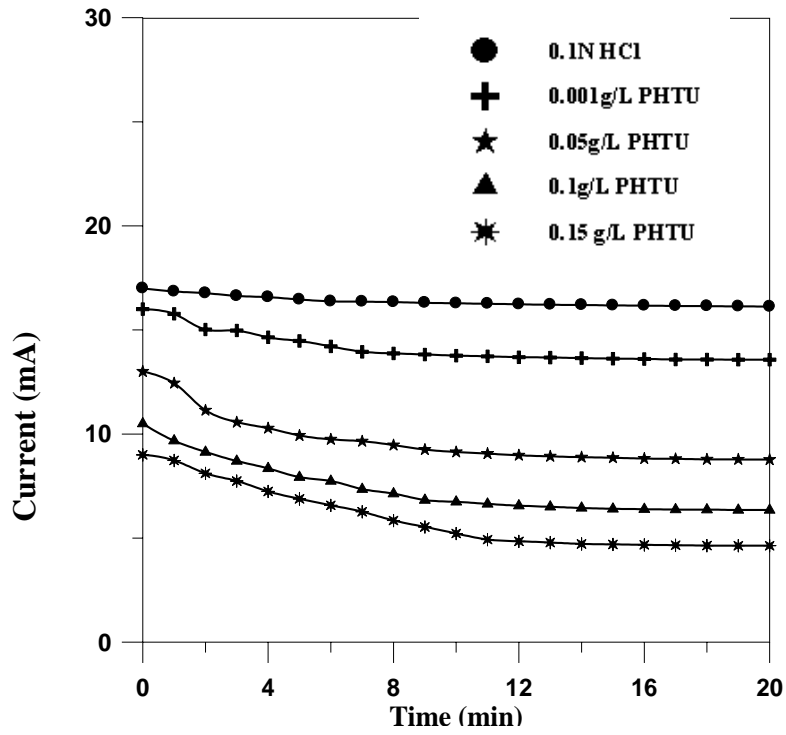


**Figure 5-37b** Current vs. time for a metal couple in 0.1N HCl, AR (Fe/Zn) = 0.25, T=40 °C, t=20m, and 500 RPM

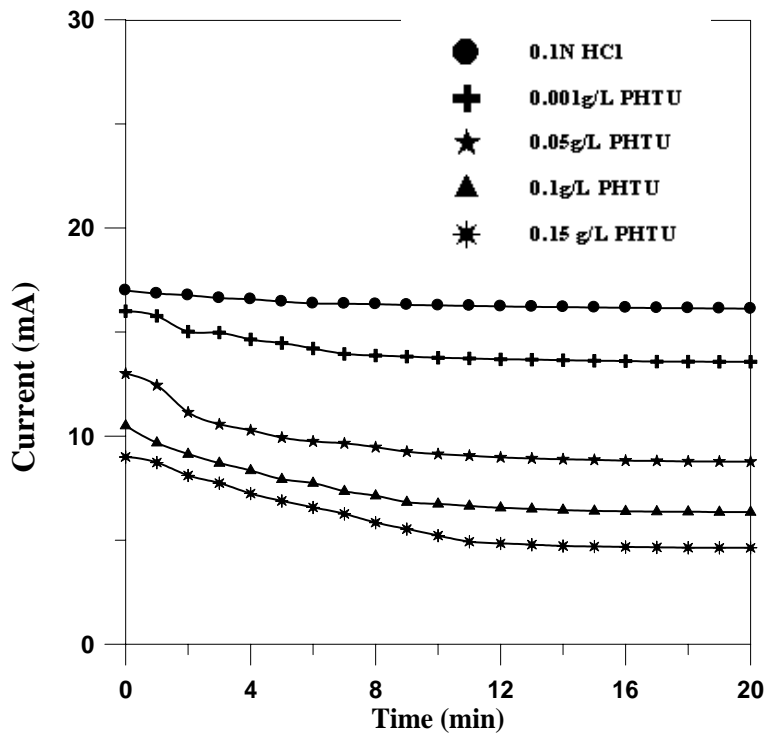


**Figure 5-38b** Current vs. time for a metal couple in 0.1N HCl, AR (Fe/Zn) = 0.5, T=40 °C, t=20m, and 500 RPM

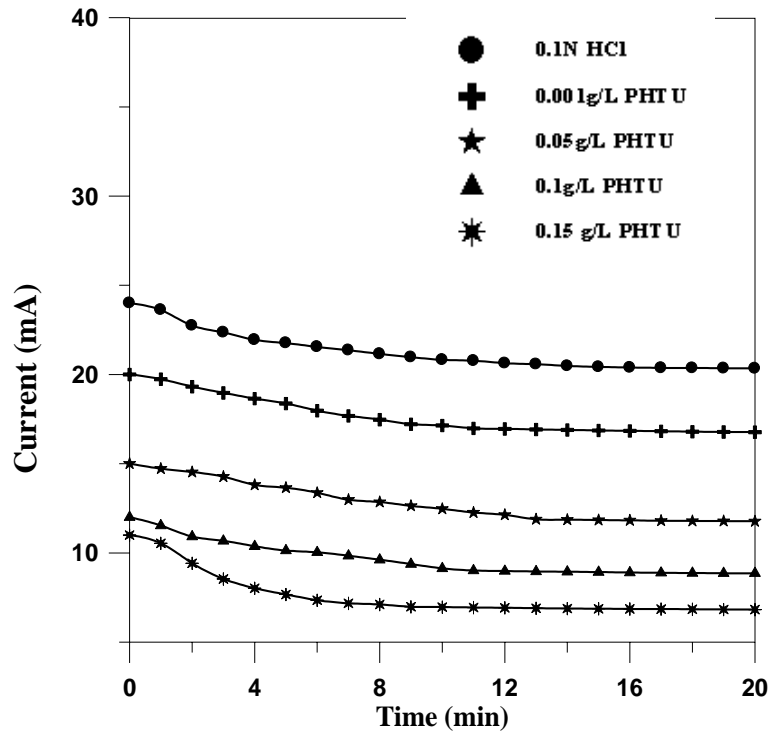


Figure 5-39b Current vs. time for a metal couple in 0.1N HCl, AR (Fe/Zn) =1, T=40 °C, t=20m, and 500 RPM

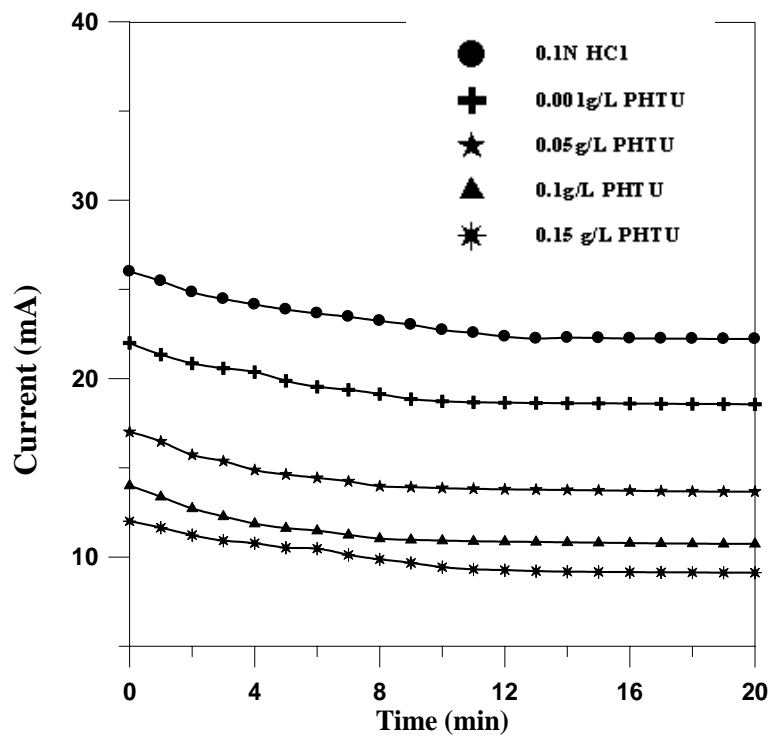
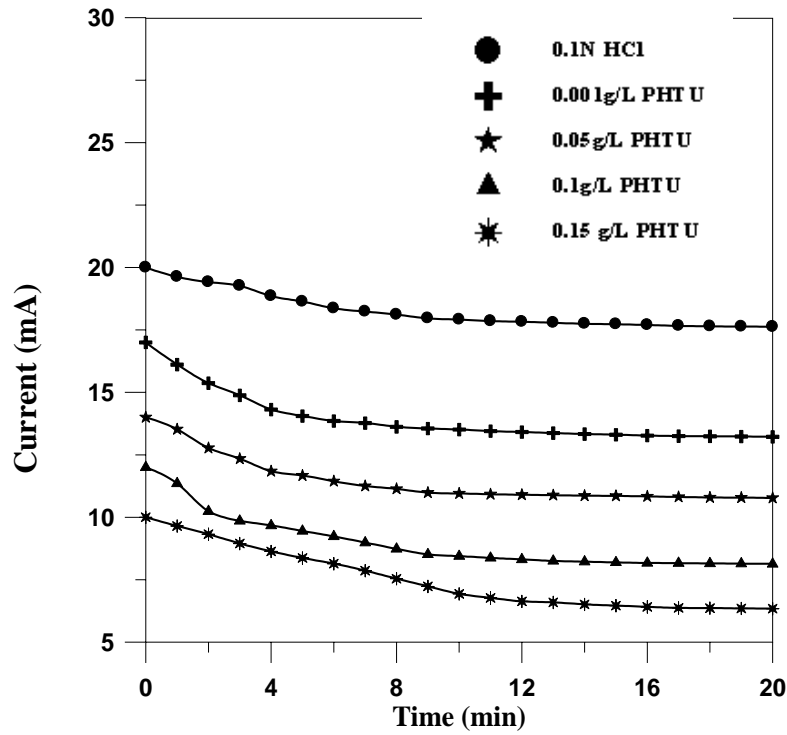
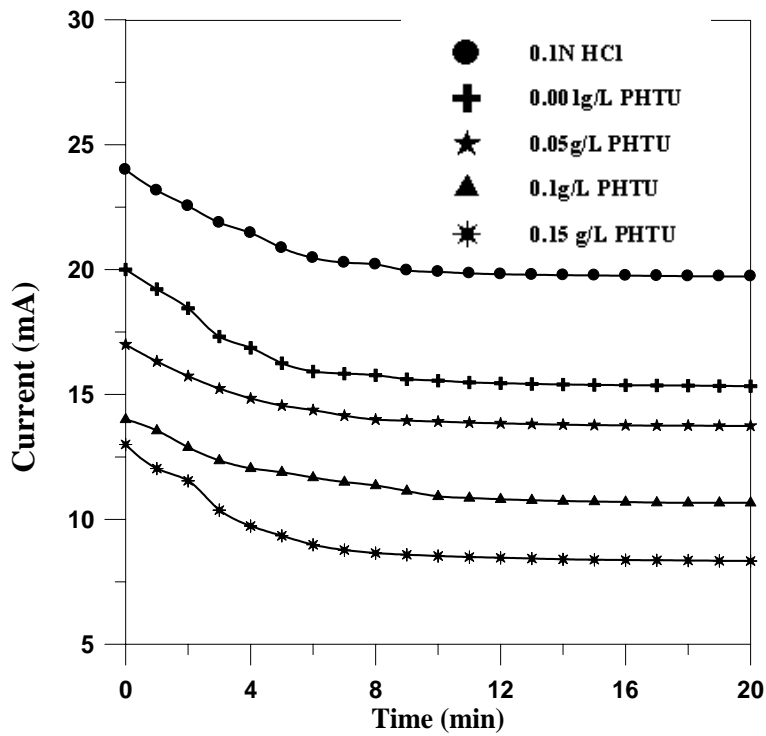


Figure 5-40b Current vs. time for a metal couple in 0.1N HCl, AR (Fe/Zn) =2, T=40 °C, t=20m, and 500 RPM



**Figure 5-41b** Current vs. time for a metal couple in 0.1N HCl, AR (Fe/Zn)=0.25, T=40 °C, t=20m, and 1000 RPM



**Figure 5**-Current vs. time for a metal couple in 0.1N HCl, AR (Fe/Zn)=0.5, T=40 °C, t=20m, and 1000 RPM

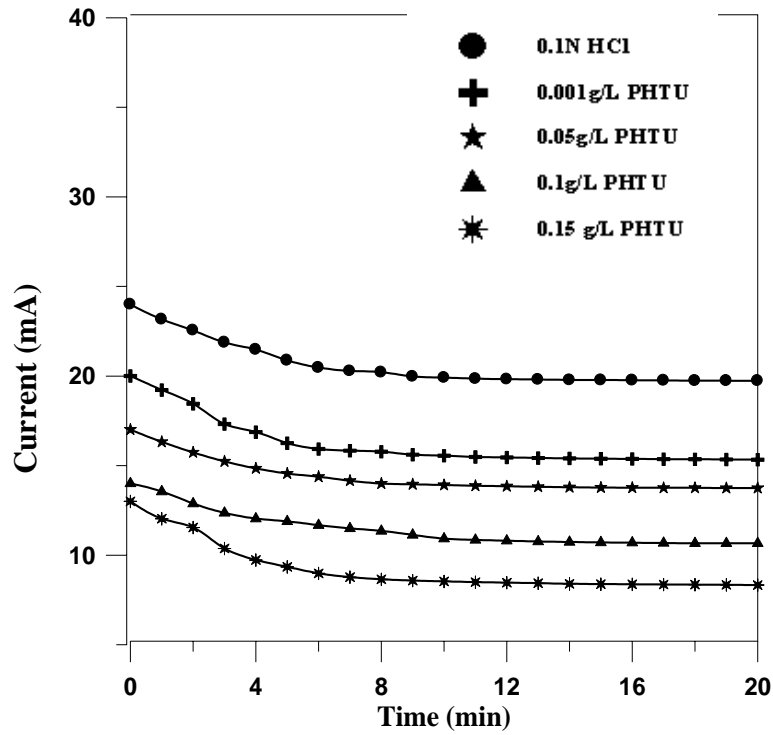


**Figure 5-43b** Current vs. time for a metal couple in 0.1N HCl, AR(Fe/Zn)=1, T=40 °C, t=20m, and 1000 RPM

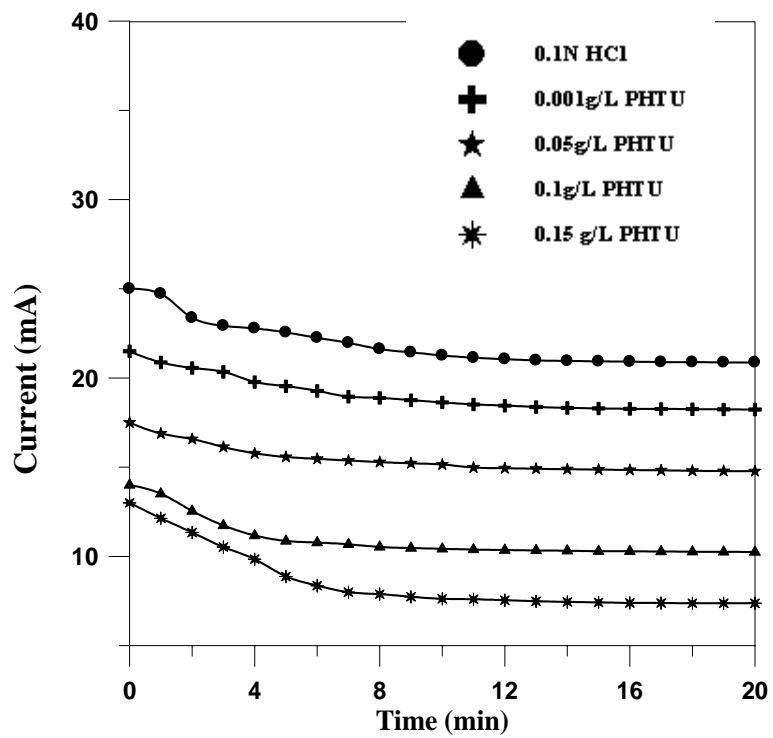


**Figure 5-44b** Current vs. time for a metal couple in 0.1N HCl, AR (Fe/Zn) =2, T=40 °C, t=20m, and 1000 RPM

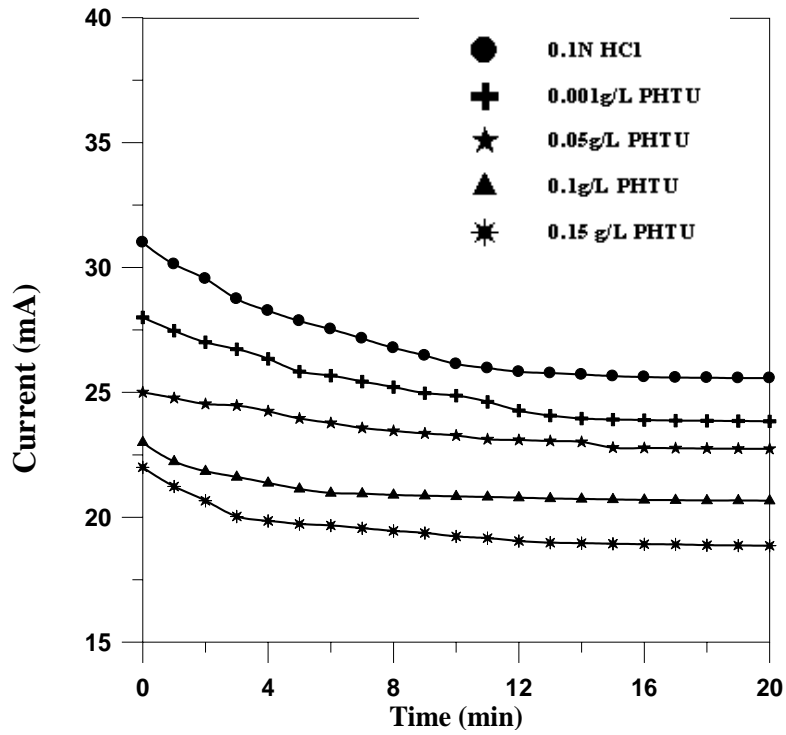


**Figure 5-45b** Current vs. time for a metal couple in 0.1N HCl, AR (Fe/Zn) = 0.25, T=40 °C, t=20m, and 1500 RPM

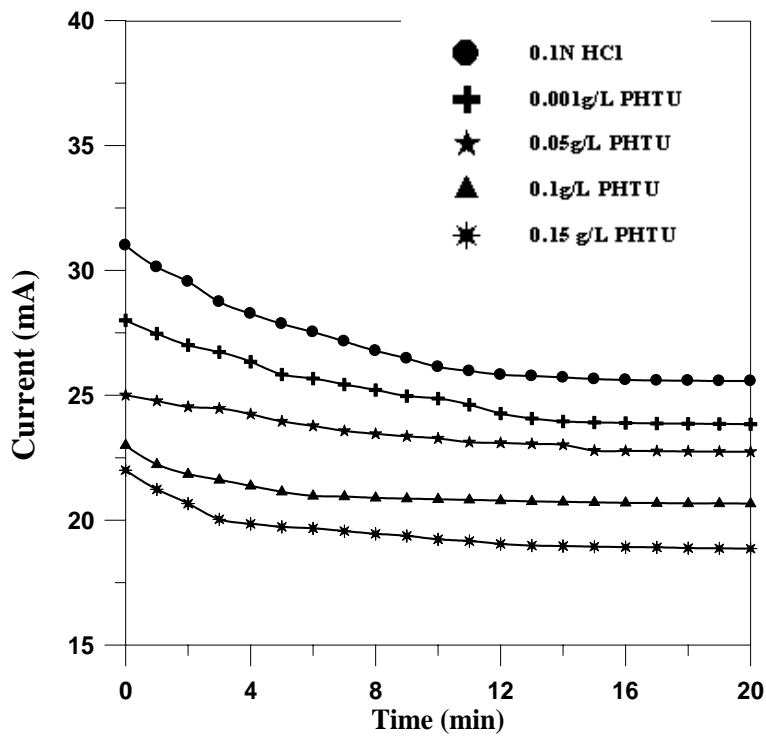


**Figure 5-46b** Current vs. time for a metal couple in 0.1N HCl, AR (Fe/Zn) = 0.5, T=40 °C, t=20m, and 1500 RPM

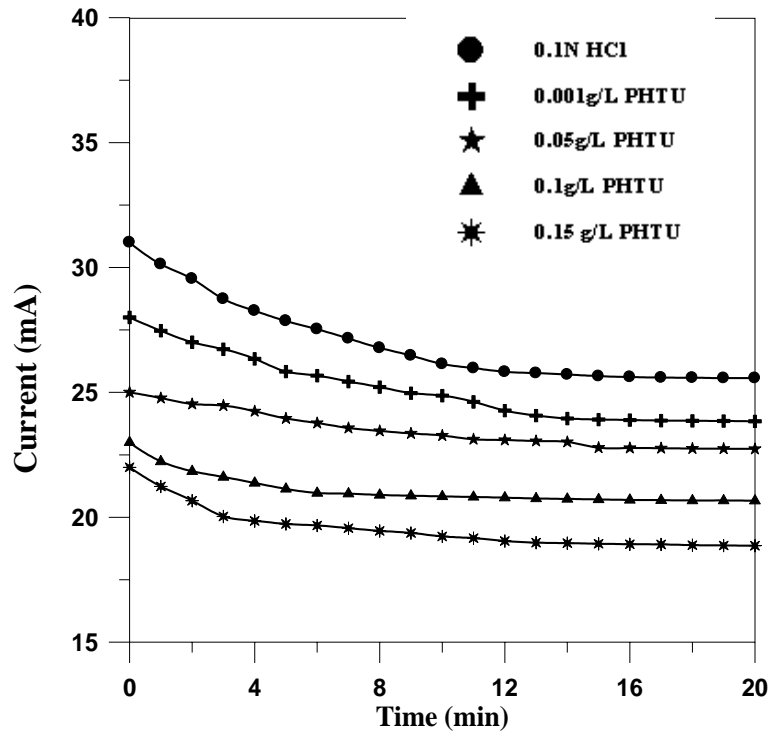


**Figure 5-47b** Current vs. time for a metal couple in 0.1N HCl, AR (Fe/Zn) =1, T=40 °C, t=20m, and 1500 RPM

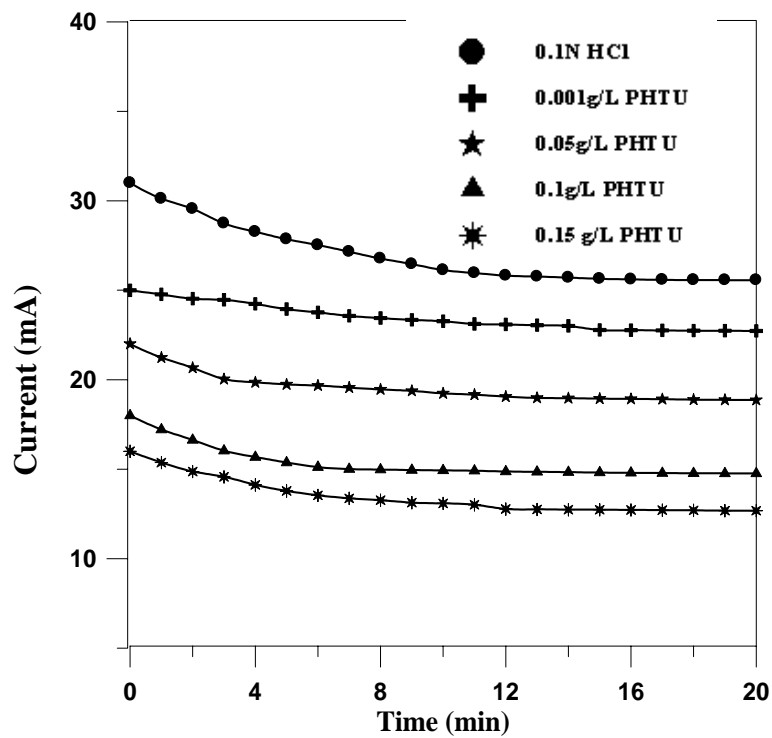


**Figure 5-48b** Current vs. time for a metal couple in 0.1N HCl, AR (Fe/Zn) =2, T=40 °C, t=20m, and 1500 RPM

### 5.4 Measuring the potential and current together for copper and carbon steel couple:

All previous experiments (for copper and carbon steel coupling) have been repeated with the same conditions, but with time 2hrs instead of 20 minutes. Then the potential and current have been measured together. The galvanic potential (at steady state) values are shown in **Figs.(5.49-5.64)**, while **Figs.(5.65-5.80)** show the current of metal couples, see appendix D.

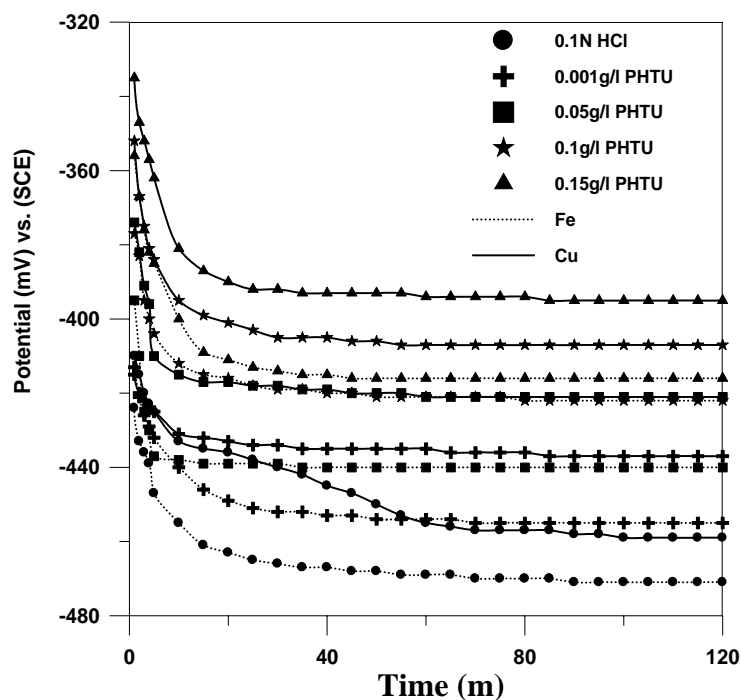


**Figure 5-49** Potential vs. time for a metal couple in 0.1N HCl, AR (Cu/Fe) =2, T=40 °C, t=120m, and 0 RPM

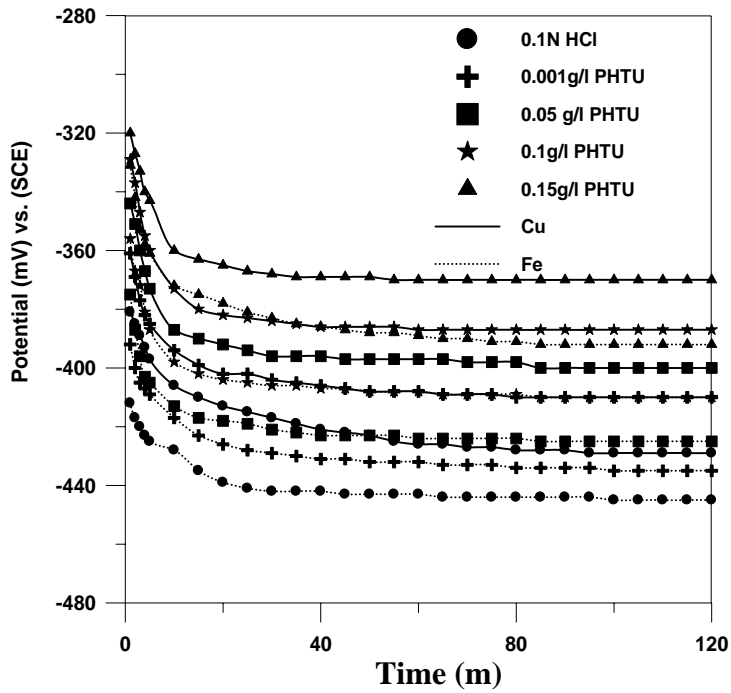


**Figure 5-50** Potential vs. time for a metal couple in 0.1N HCl, AR (Cu/Fe) =1, T=40 °C, t=120m, and 0 RPM

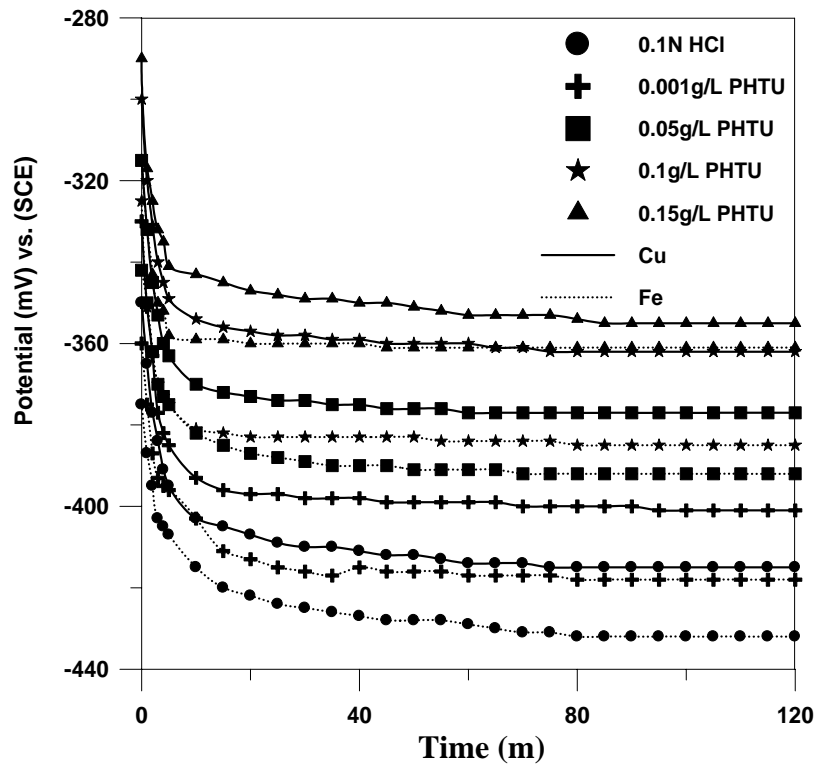


**Figure 5-51** Potential vs. time for a metal couple in 0.1N HCl, AR (Cu/Fe) =0.5, T=40 °C, t=120m, and 0 RPM



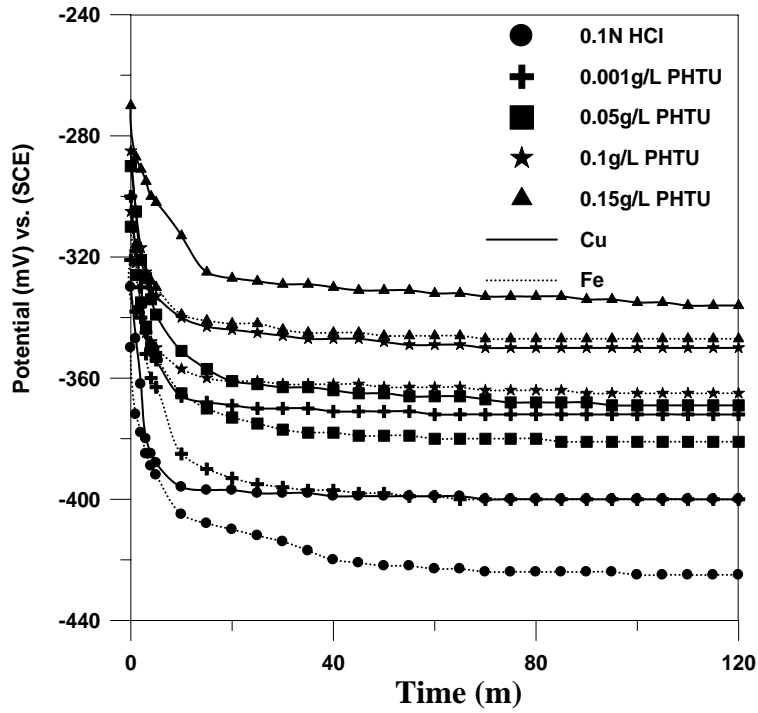


**Figure 5-52** Potential vs. time for a metal couple in 0.1N HCl, AR (Cu/Fe)=0.25, T=40 °C, t=120m, and 0 RPM

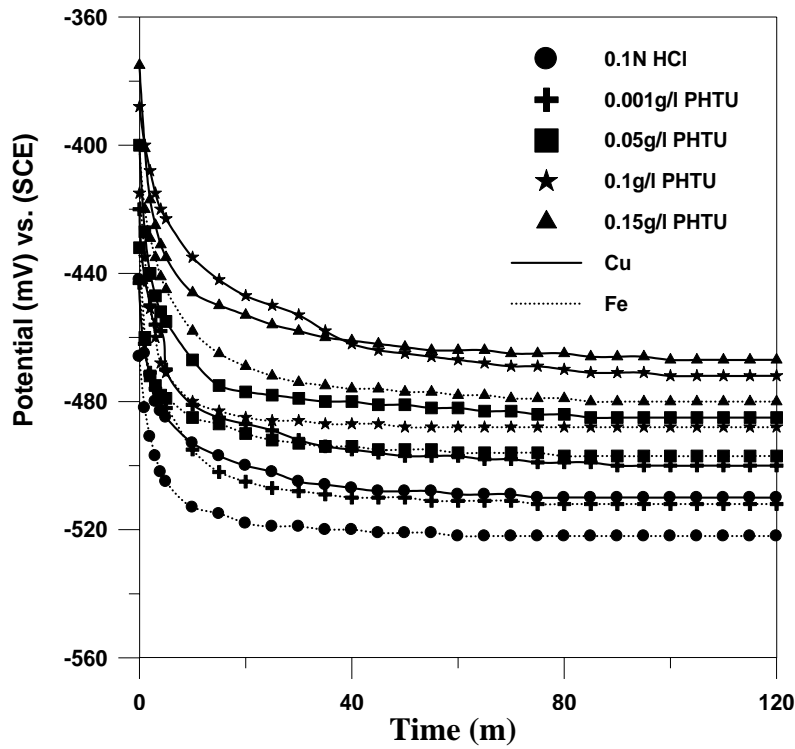


**Figure 5-53** Potential vs. time for a metal couple in 0.1N HCl, AR (Cu/Fe)=2, T=40 °C, t=120m, and 500 RPM

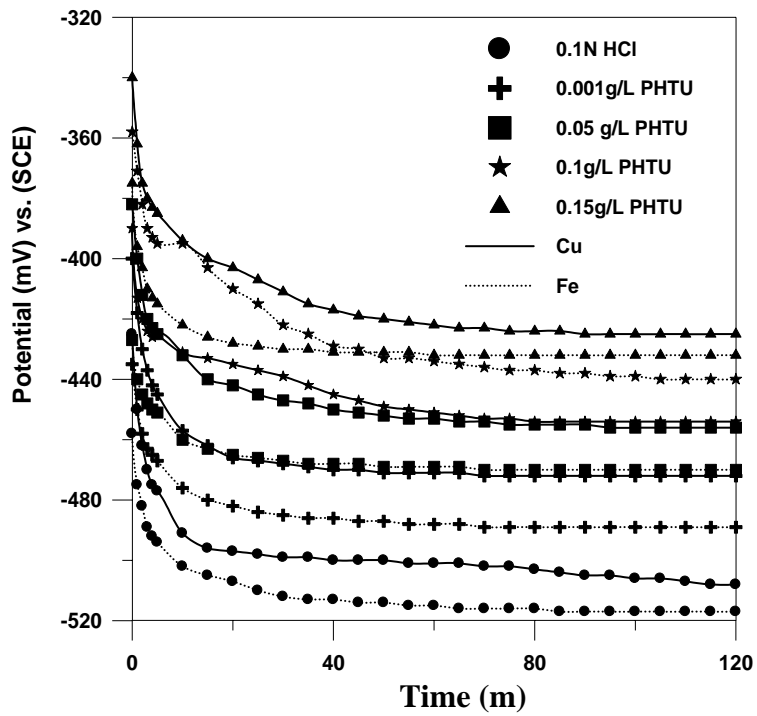


**Figure 5-54** Potential vs. time for a metal couple in 0.1N HCl, AR (Cu/Fe)=1, T=40 °C, t=120m, and 500 RPM

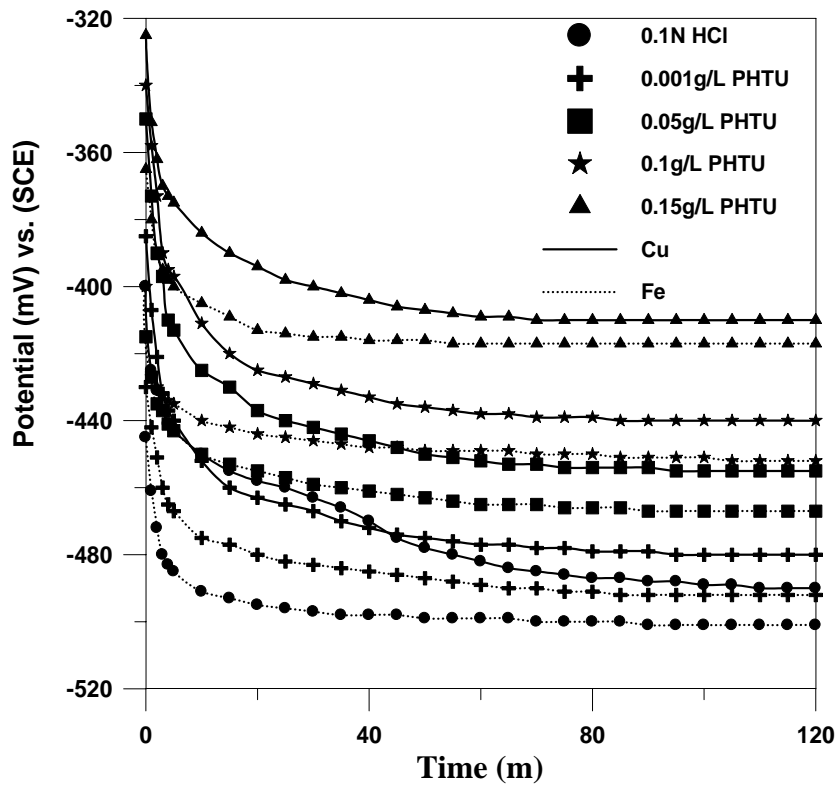


**Figure 5-55** Potential vs. time for a metal couple in 0.1N HCl, AR (Cu/Fe)=0.5, T=40 °C, t=120m, and 500 RPM

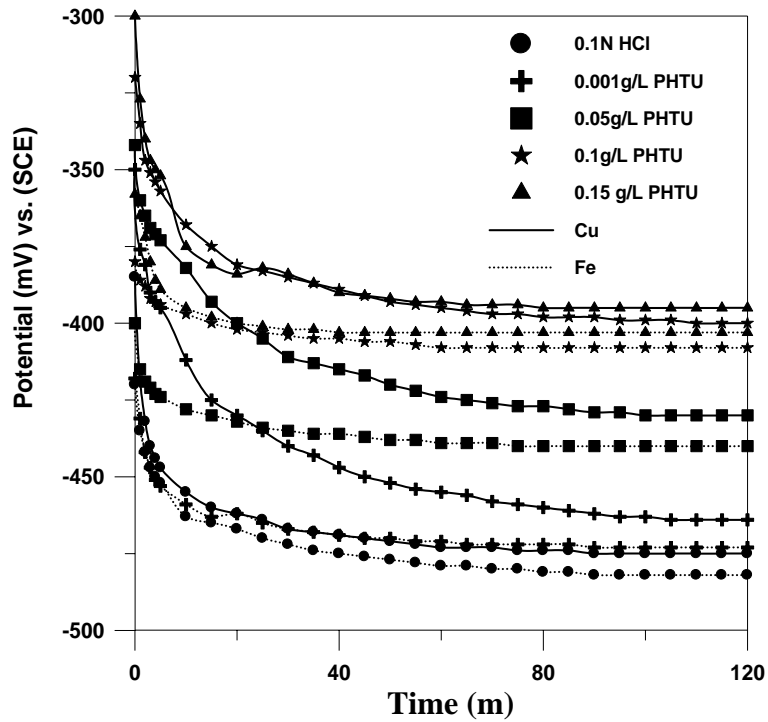


**Figure 5-56** Potential vs. time for a metal couple in 0.1N HCl, AR (Cu/Fe) = 0.25, T = 40 °C, t = 120m, and 500 RPM

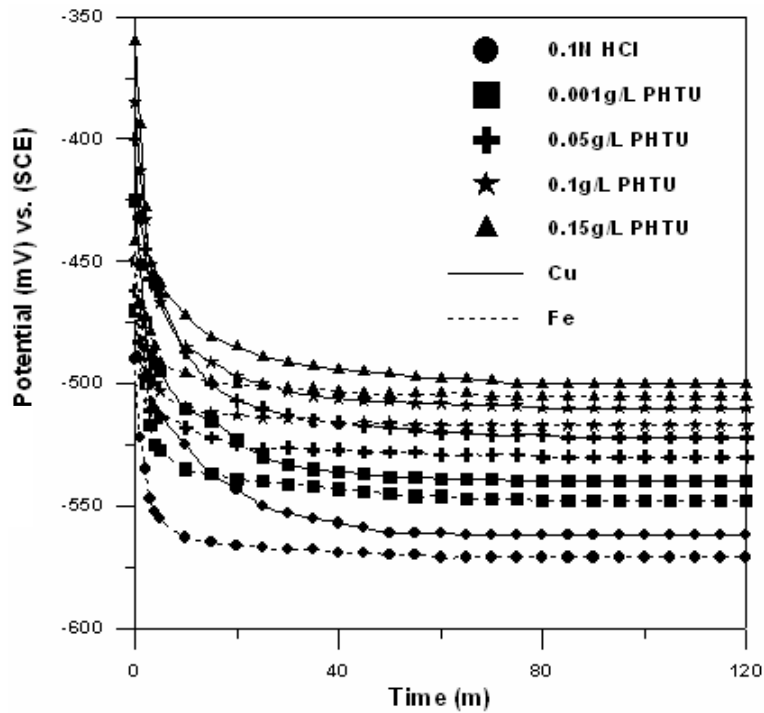


**Figure 5-57** Potential vs. time for a metal couple in 0.1N HCl, AR (Cu/Fe) = 2, T = 40 °C, t = 120m, and 1000 RPM

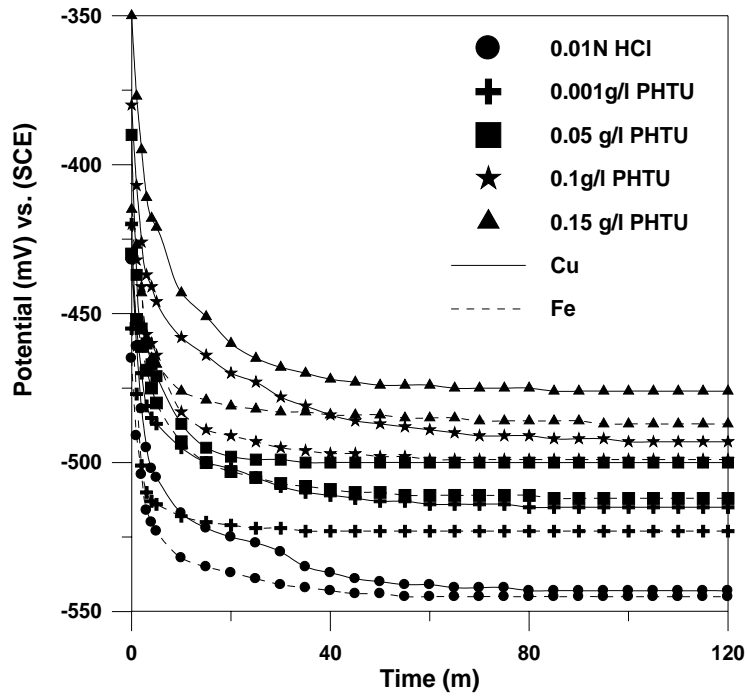


**Figure 5-58** Potential vs. time for a metal couple in 0.1N HCl, AR (Cu/Fe) =1, T=40 °C, t=120m, and 1000 RPM

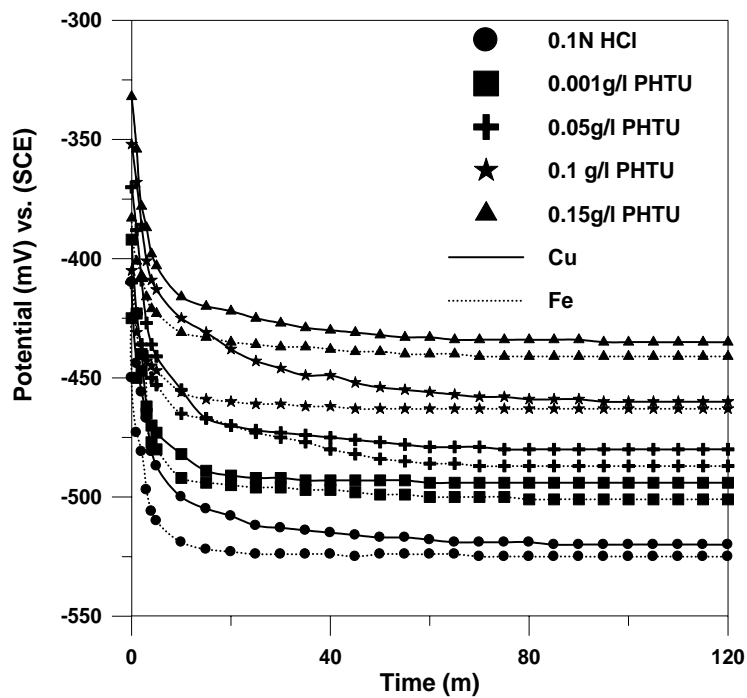


**Figure 5-59** Potential vs. time for a metal couple in 0.1N HCl, AR(Cu/Fe) =0.5, T=40 °C, t=120m, and 1000 RPM

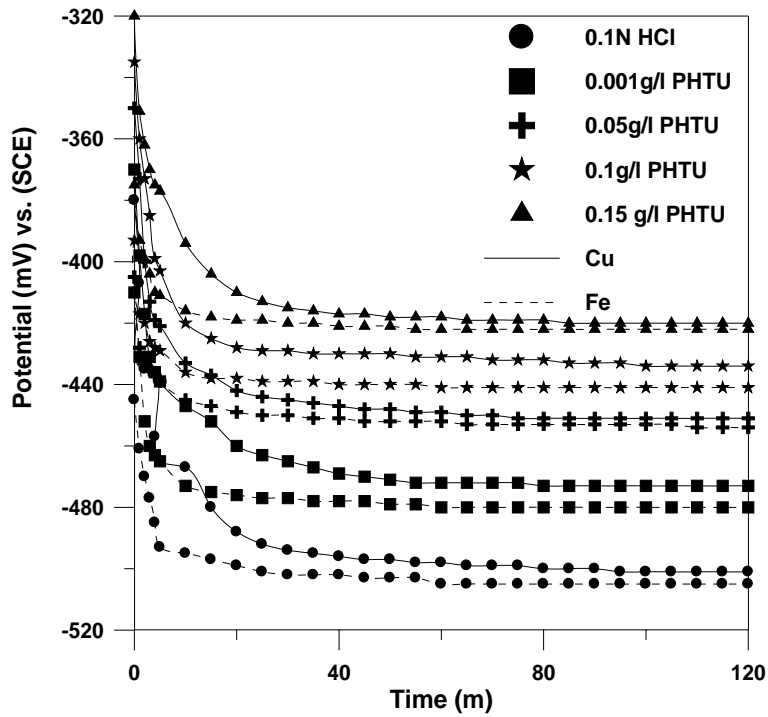


**Figure 5-60** Potential vs. time for a metal couple in 0.1N HCl, AR (Cu/Fe) = 0.25, T = 40 °C, t = 120m, and 1000 RPM

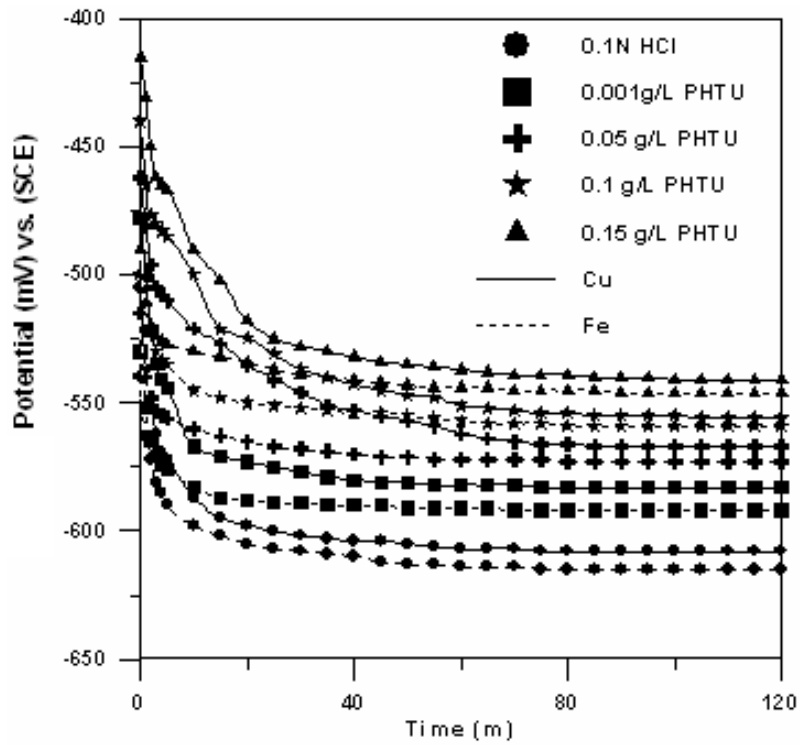


**Figure 5-61** Potential vs. time for a metal couple in 0.1N HCl, AR (Cu/Fe) = 2, T = 40 °C, t = 120m, and 1500 RPM

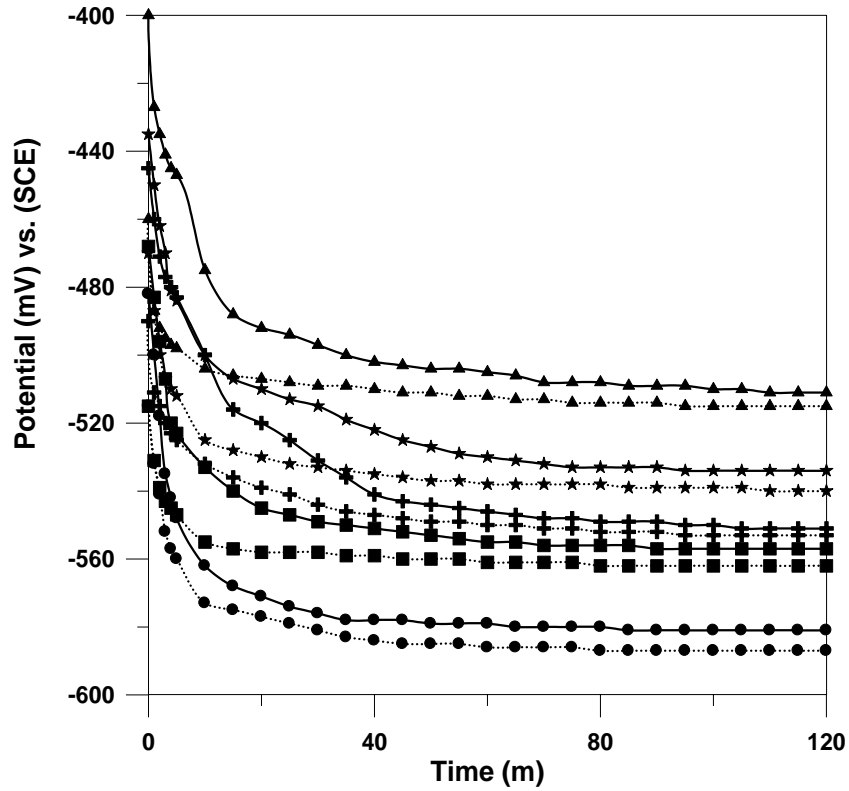


Figure 5-62 Potential vs. time for a metal couple in 0.1N HCl, AR (Cu/Fe)=1, T=40 °C, t=120m, and 1500 RPM

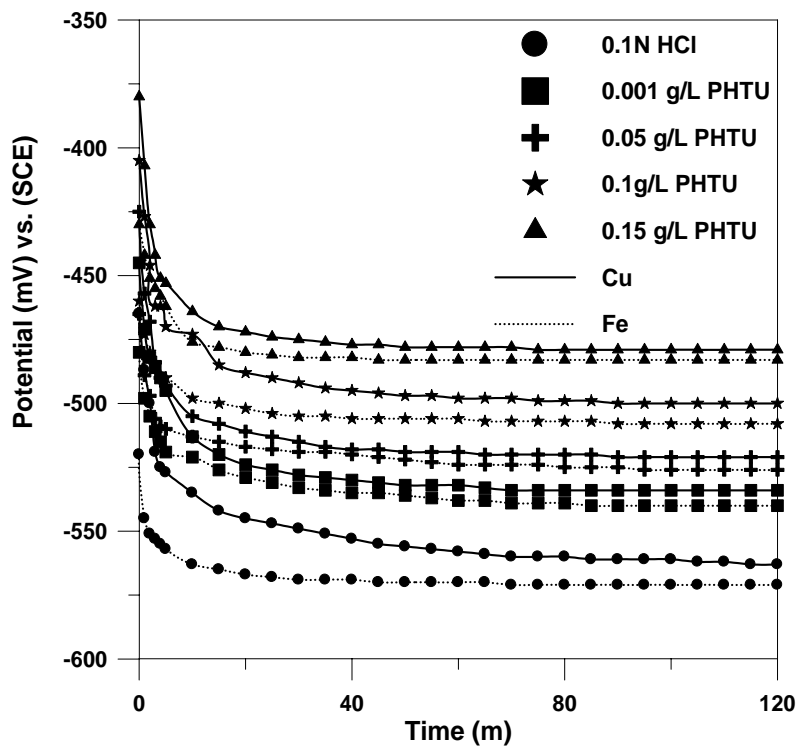
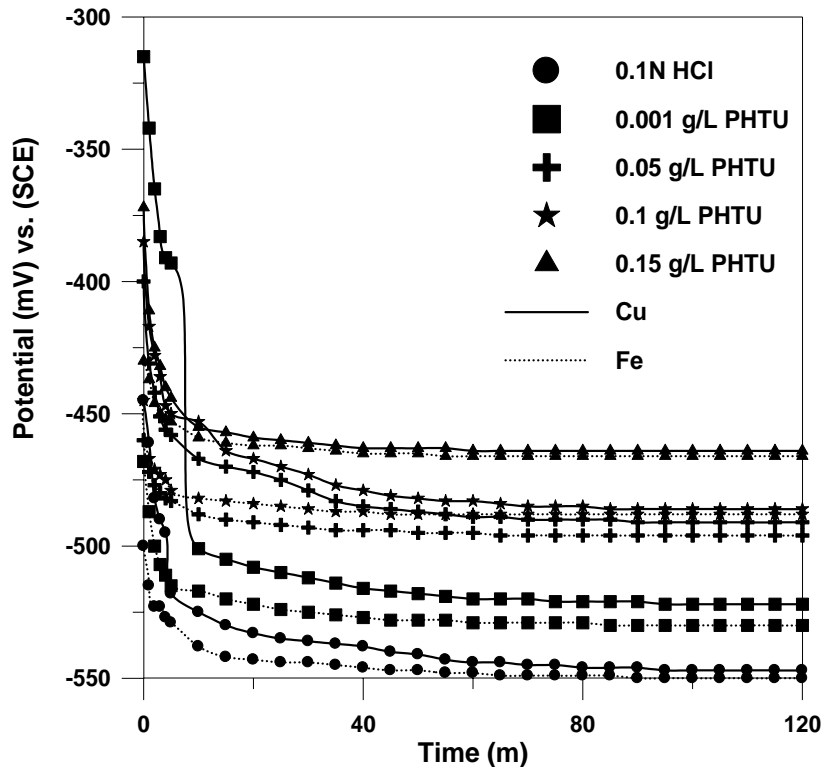
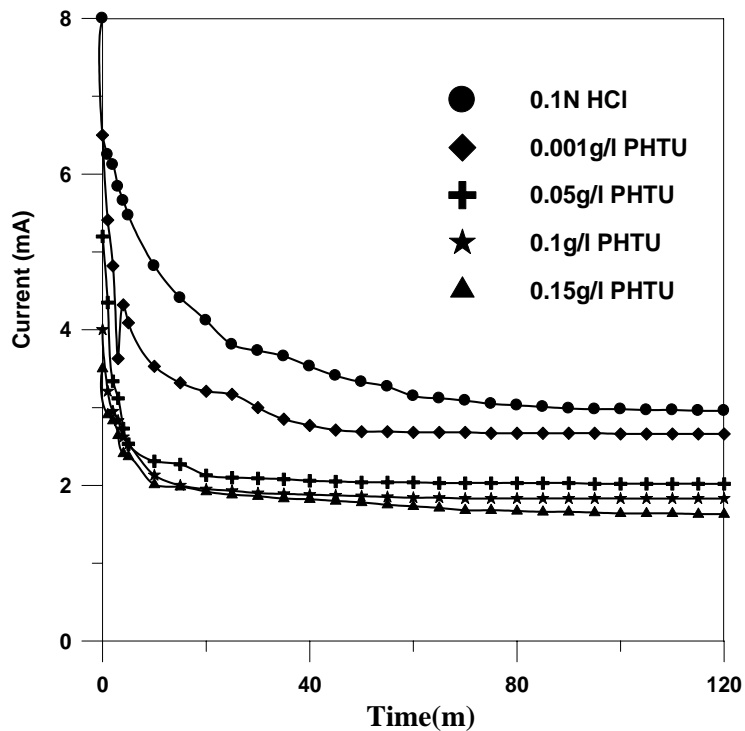


Figure 5-63 Potential vs. time for a metal couple in 0.1N HCl, AR (Cu/Fe)=0.5, T=40 °C, t=120m, and 1500 RPM



**Figure 5-64** Potential vs. time for a metal couple in 0.1N HCl, AR (Cu/Fe)=0.25, T=40 °C, t=120m, and 1500 RPM



**Figure 5-65** Current vs. time for a metal couple in 0.1N HCl, AR (Cu/Fe)=2, T=40 °C, t=120m, and 0 RPM

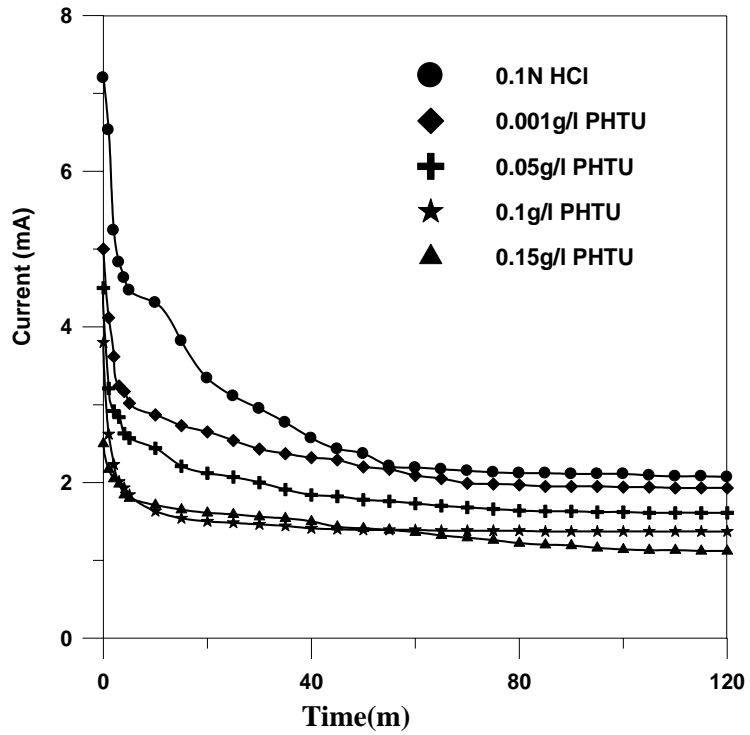


**Figure 5-66** Current vs. time for a metal couple in 0.1N HCl, AR (Cu/Fe)=1, T=40 °C, t=120m, and 0 RPM

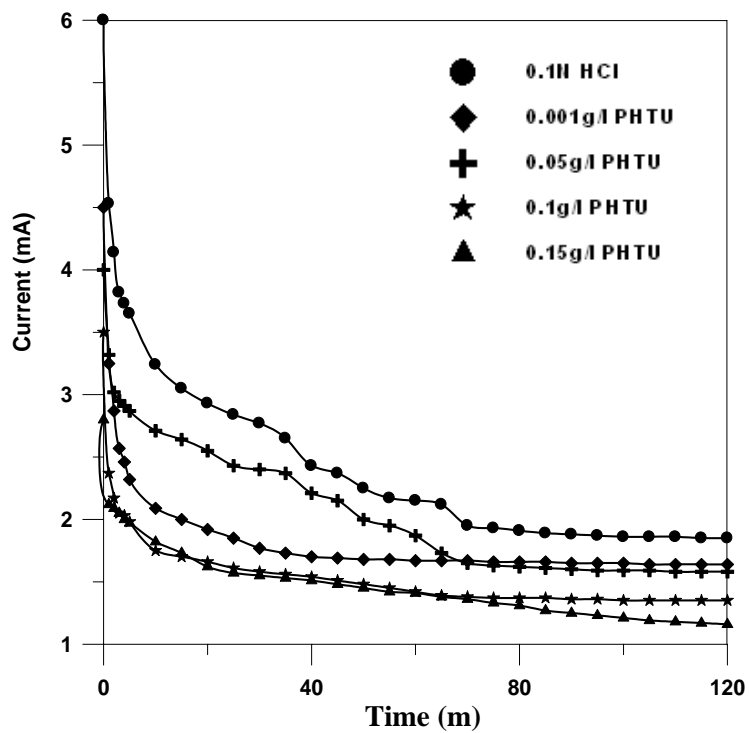


**Figure 5-67** Current vs. time for a metal couple in 0.1N HCl, AR (Cu/Fe)=0.5, T=40 °C, t=120m, and 0 RPM



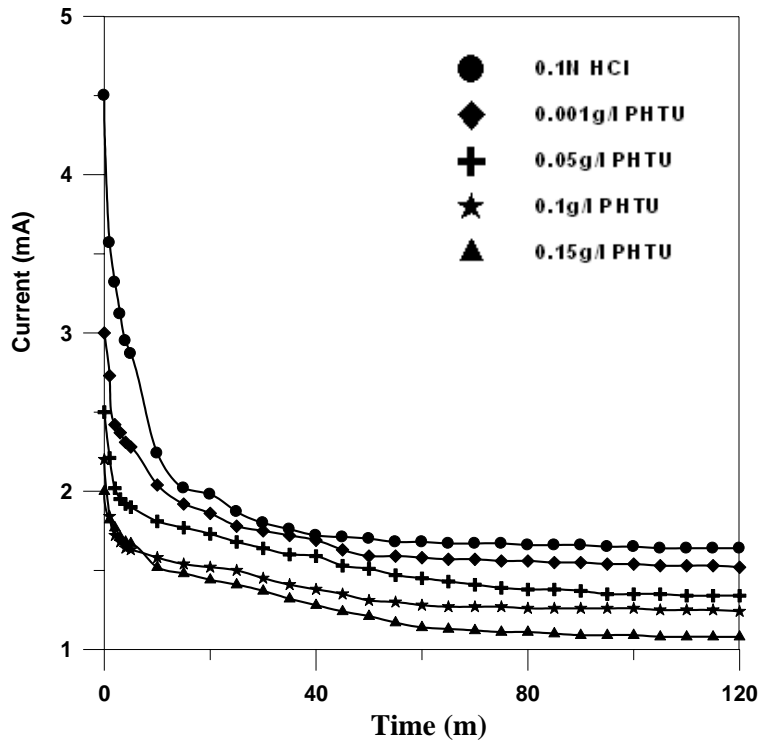


**Figure 5-68** Current vs. time for a metal couple in 0.1N HCl, AR (Cu/Fe) = 0.25, T=40 °C, t=120m, and 0 RPM

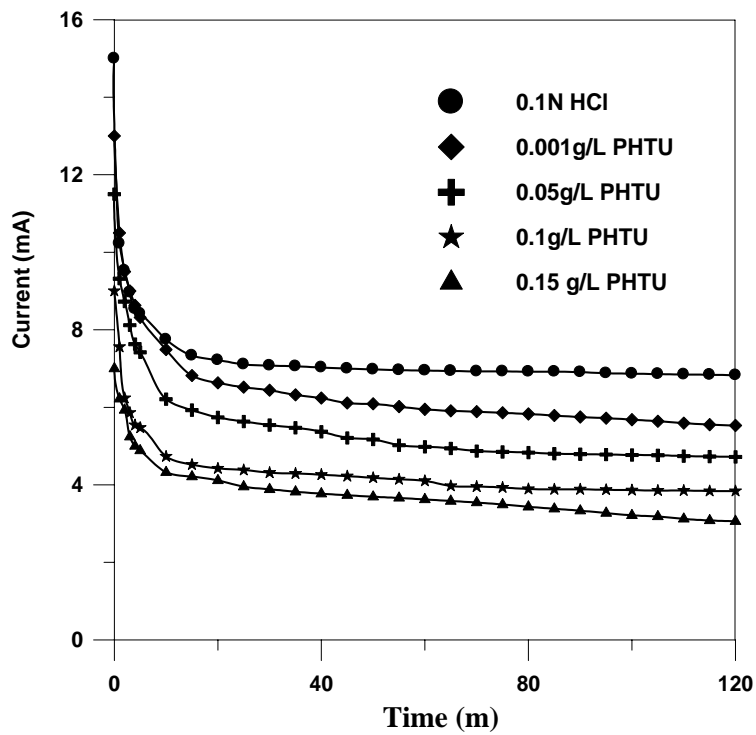


**Figure 5-69** Current vs. time for a metal couple in 0.1N HCl, AR (Cu/Fe) = 2, T=40 °C, t=120m, and 500 RPM

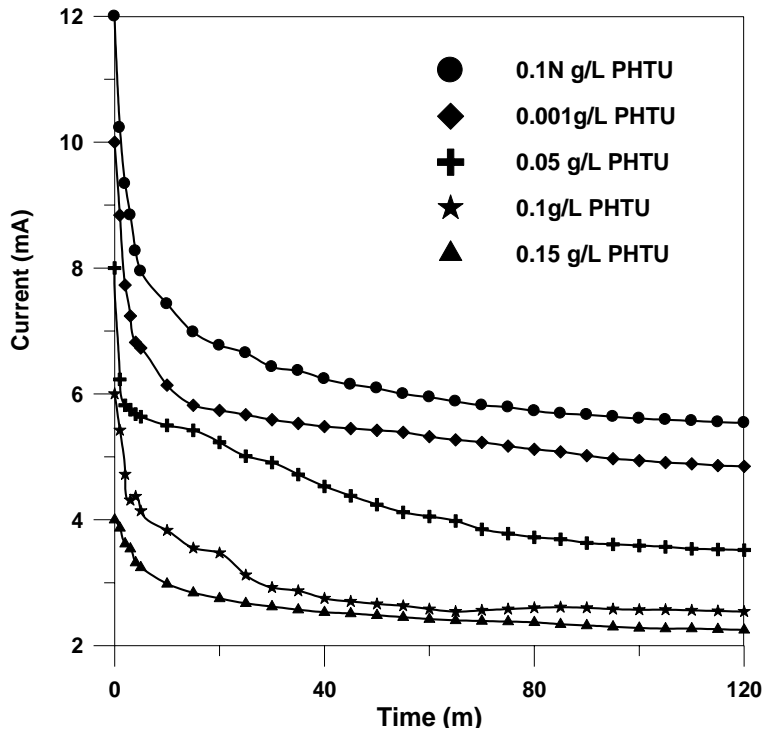


**Figure 5-70** Current vs. time for a metal couple in 0.1N HCl, AR (Cu/Fe)=1, T=40 °C, t=120m, and 500 RPM

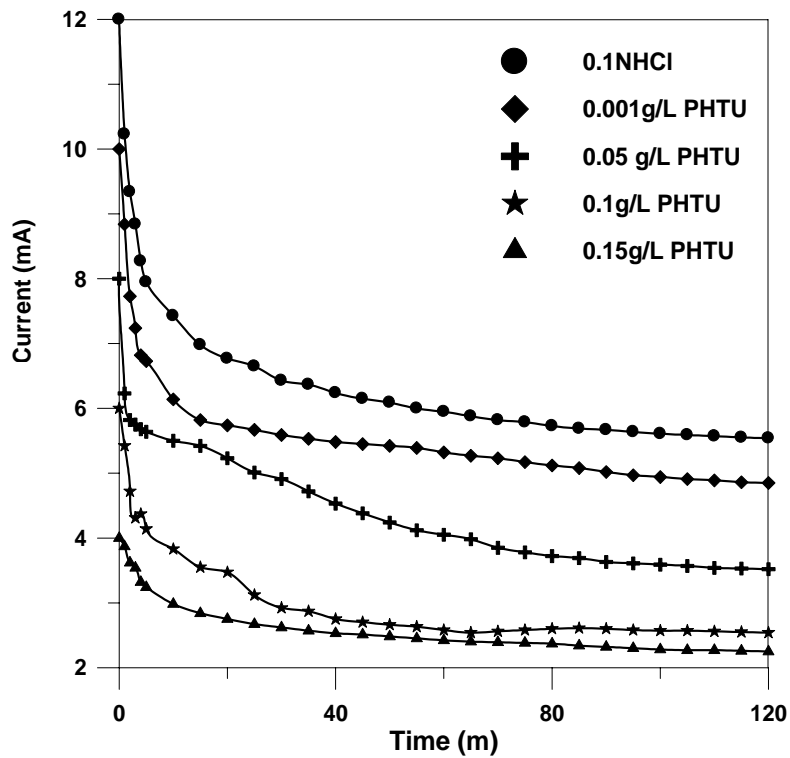


**Figure 5-71** Current vs. time for a metal couple in 0.1N HCl, AR (Cu/Fe)=0.5, T=40 °C, t=120m, and 500 RPM

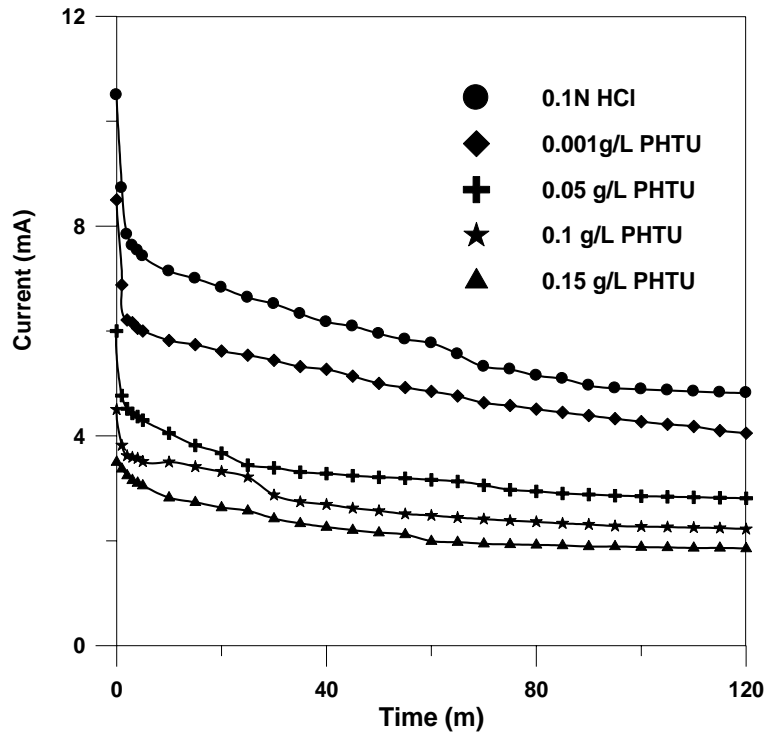


**Figure 5-72** Current vs. time for a metal couple in 0.1N HCl, AR (Cu/Fe)=0.25, T=40 °C, t=120m, and 500 RPM

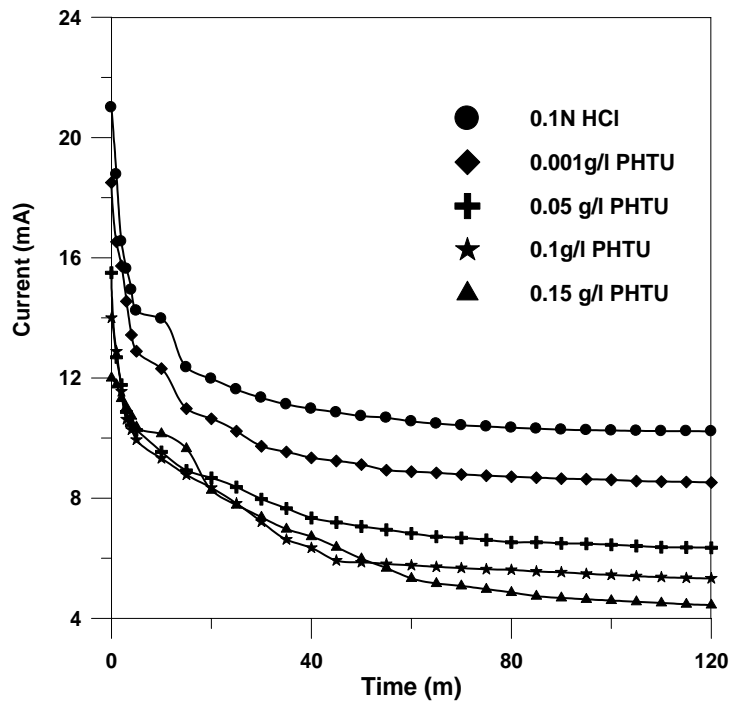


**Figure 5-73** Current vs. time for a metal couple in 0.1N HCl, AR (Cu/Fe)=2, T=40 °C, t=120m, and 1000 RPM

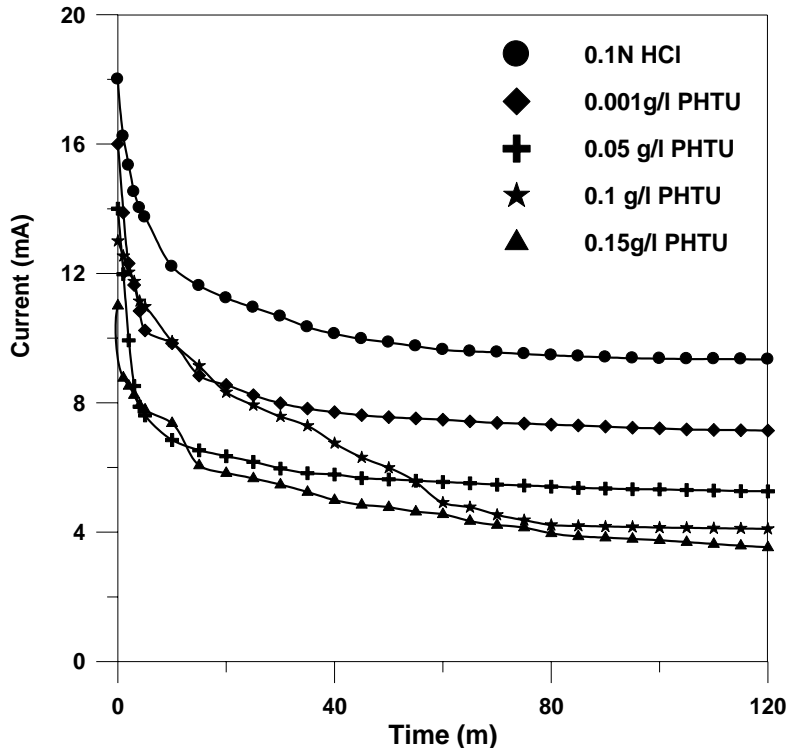


**Figure 5-74** Current vs. time for a metal couple in 0.1N HCl, AR (Cu/Fe)=1, T=40 °C, t=120m, and 1000 RPM

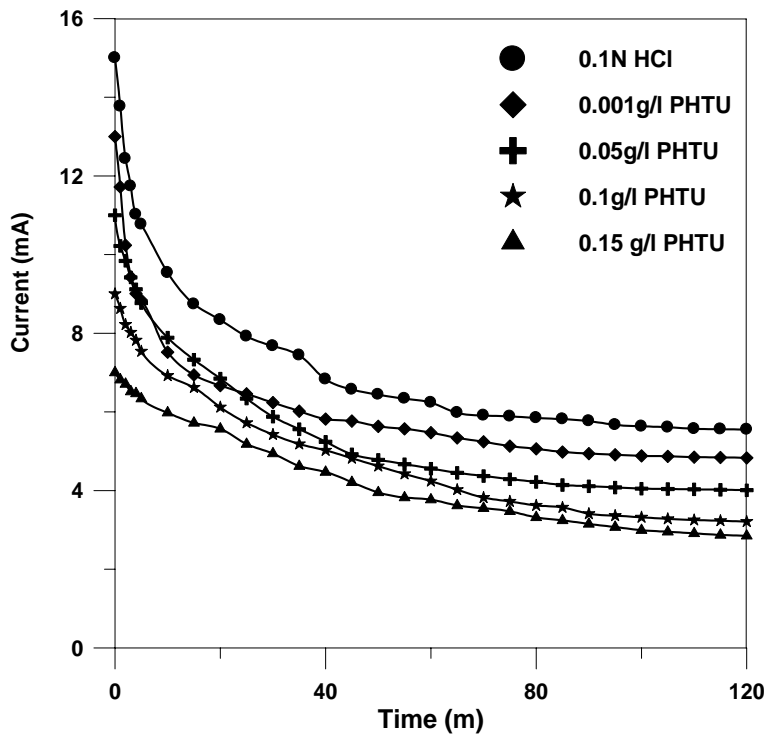


**Figure 5-75** Current vs. time for a metal couple in 0.1N HCl, AR (Cu/Fe)=0.5, T=40 °C, t=120m, and 1000 RPM

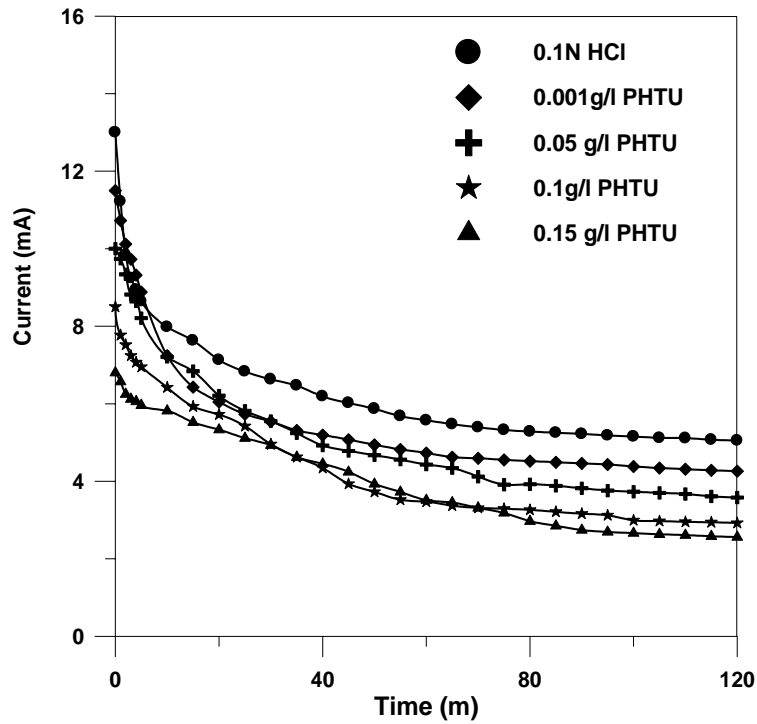


**Figure 5-76** Current vs. time for a metal couple in 0.1N HCl, AR (Cu/Fe) =0.25, T=40 °C, t=120m, and 1000 RPM

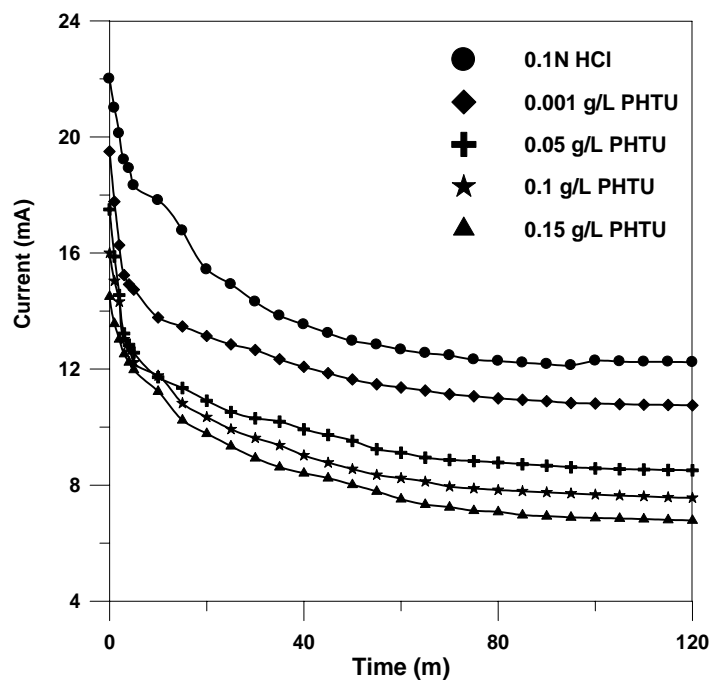


**Figure 5-77** Current vs. time for a metal couple in 0.1N HCl, AR (Cu/Fe) =2, T=40 °C, t=120m, and 1500 RPM

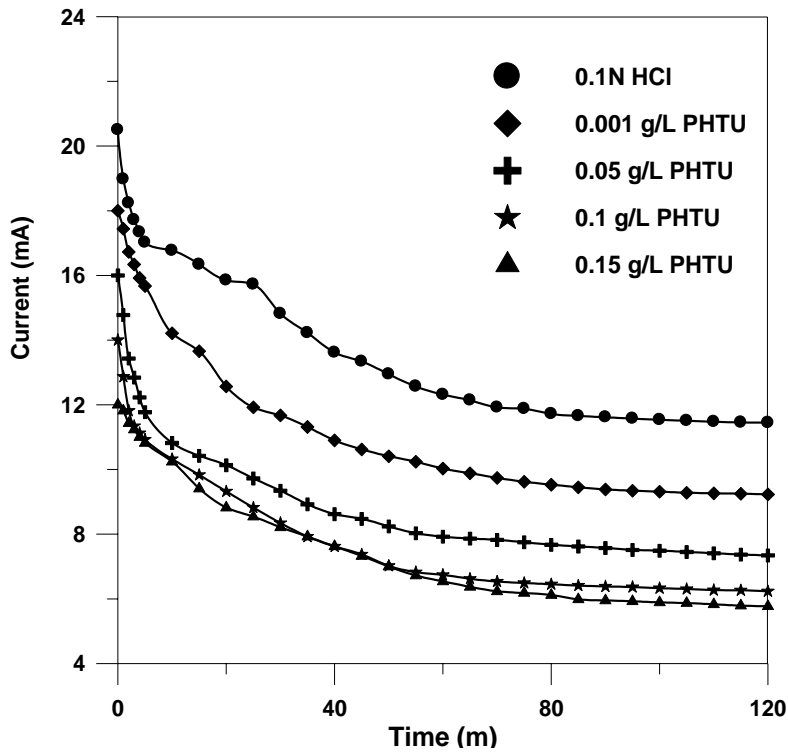


**Figure 5-78** Current vs. time for a metal couple in 0.1N HCl, AR (Cu/Fe)=1, T=40 °C, t=120m, and 1500 RPM

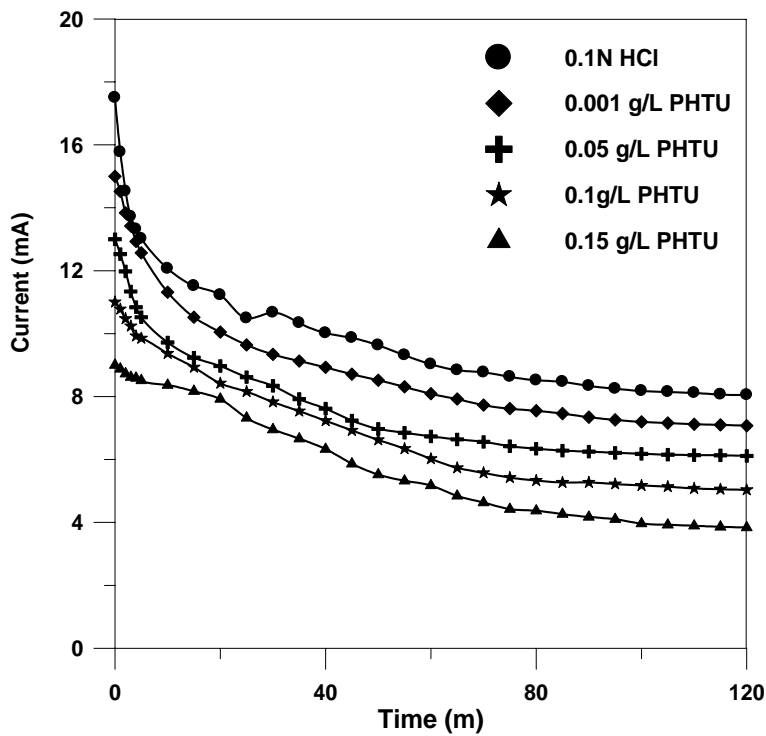


**Figure 5-79** Current vs. time for a metal couple in 0.1N HCl, AR (Cu/Fe)=0.5, T=40 °C, t=120m, and 1500 RPM

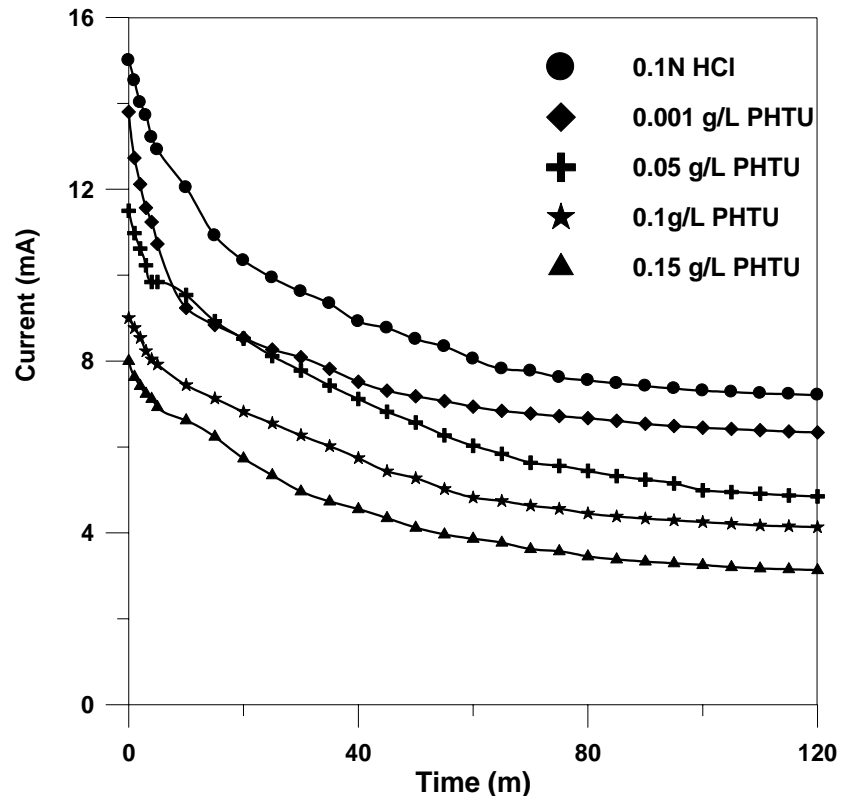


**Figure 5-80** Current vs. time for a metal couple in 0.1N HCl, AR (Cu/Fe) =0.25, T=40 °C, t=120m, and 1500 RPM

### 5.5 Corrosion potential of single metal (Free Corrosion)

The corrosion potential is also monitored experimentally at a variable PHTU concentration and rotating cylinder speed as shown in **Figs.(5.81-5.92)**, and as presented in Appendix E.

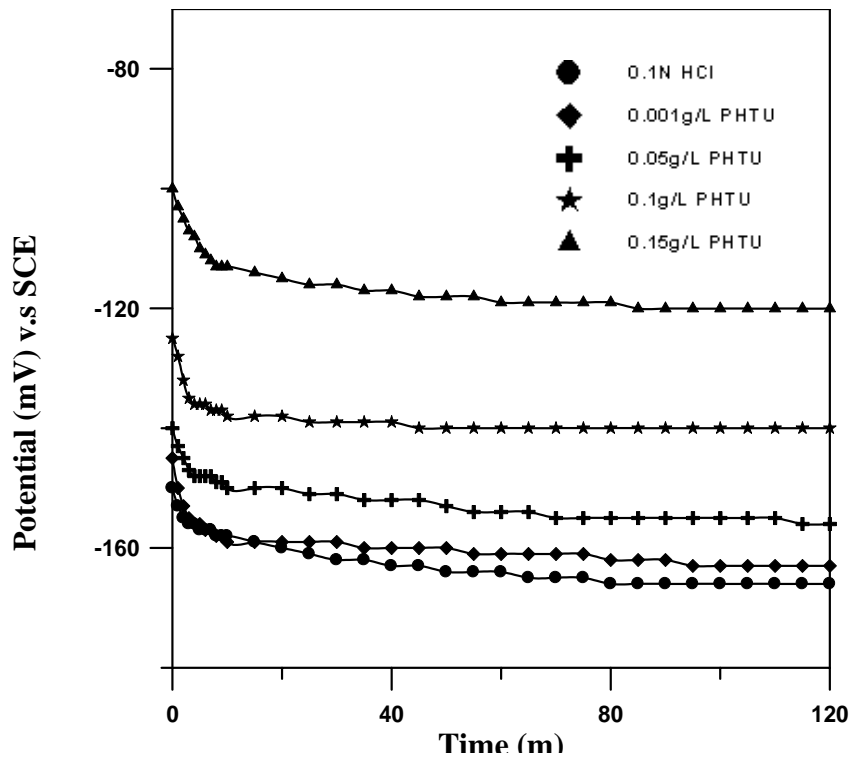


**Figure 5-81** Potential vs. time for copper in 0.1N HCl, T=40 °C, t=120m, and 0 RPM

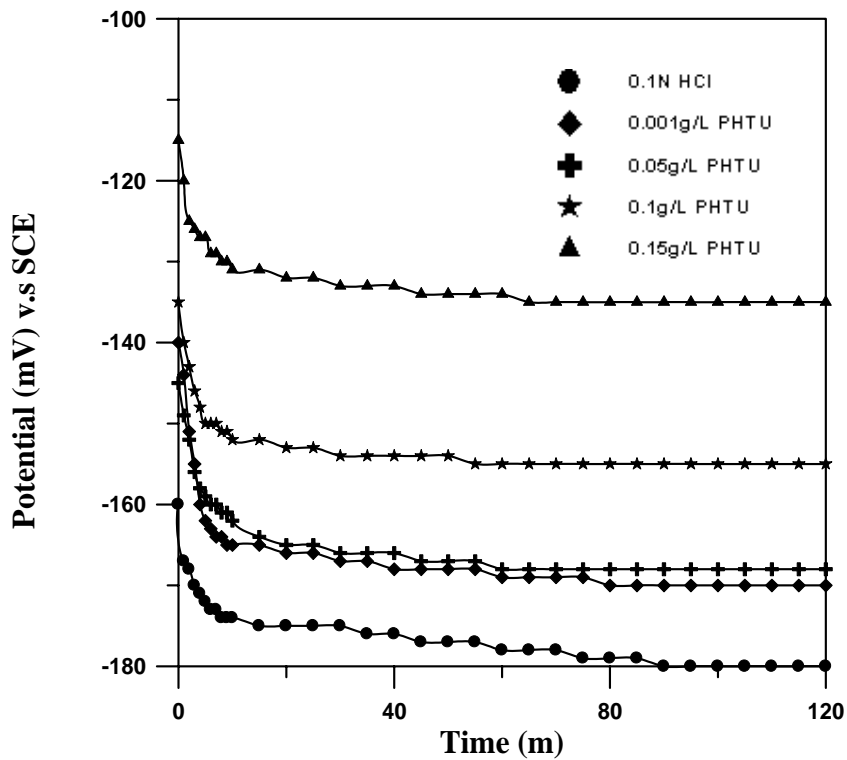


**Figure 5-82** Potential vs. time for copper in 0.1N HCl, T=40 °C, t=120m, and 500 RPM



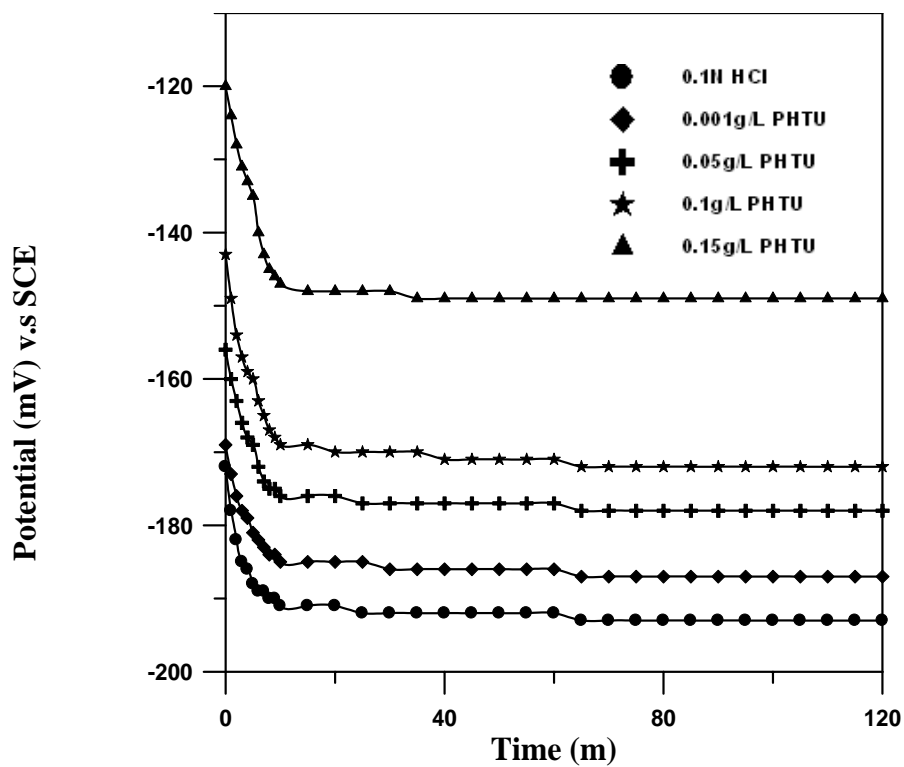


Figure 5-83 Potential vs. time for copper in 0.1N HCl, T=40 °C, t=120m, and 1000 RPM

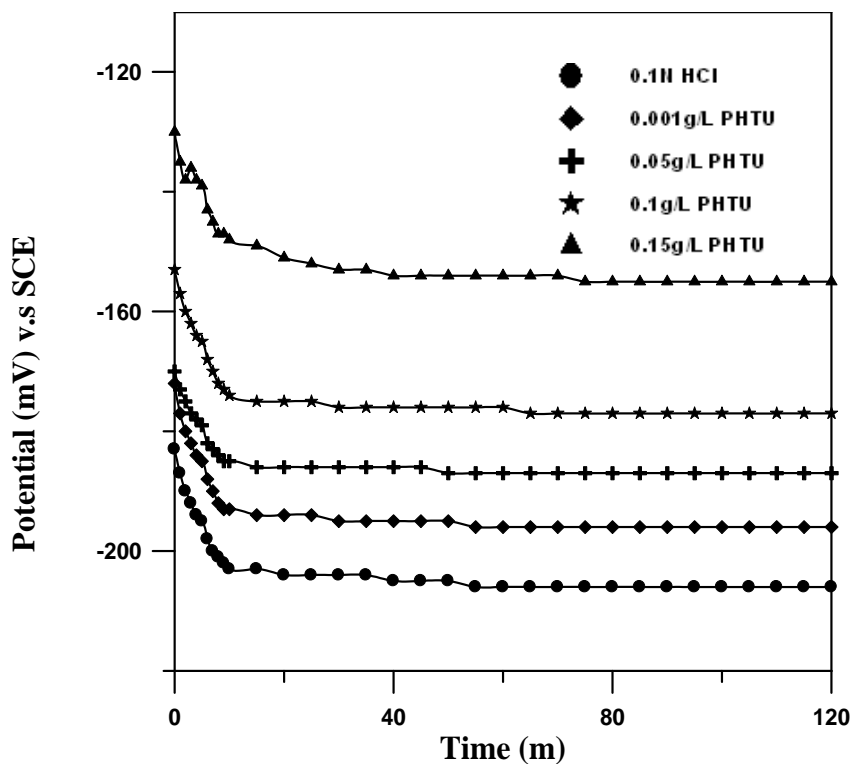
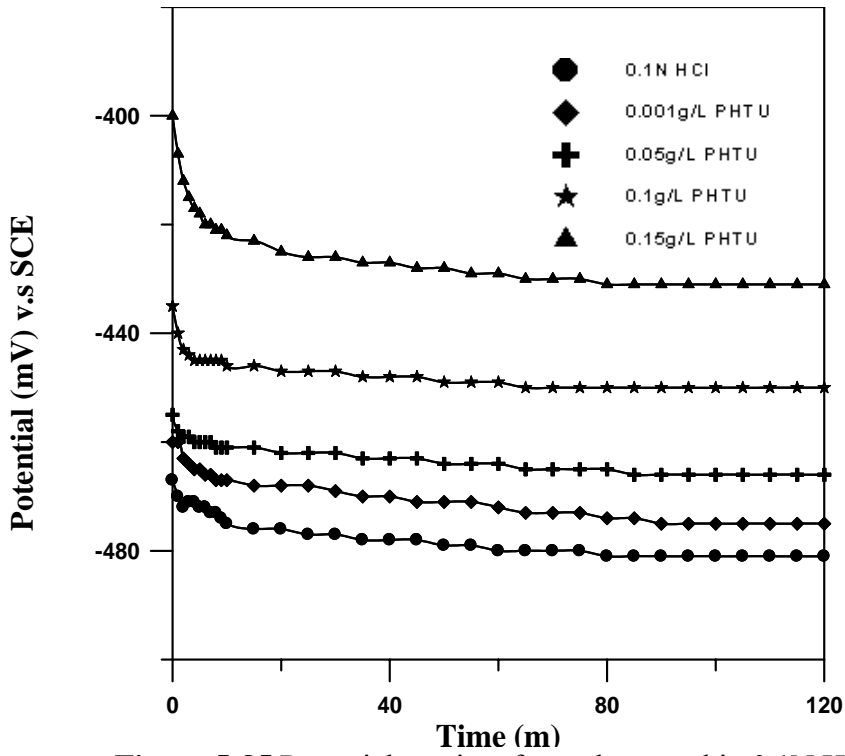
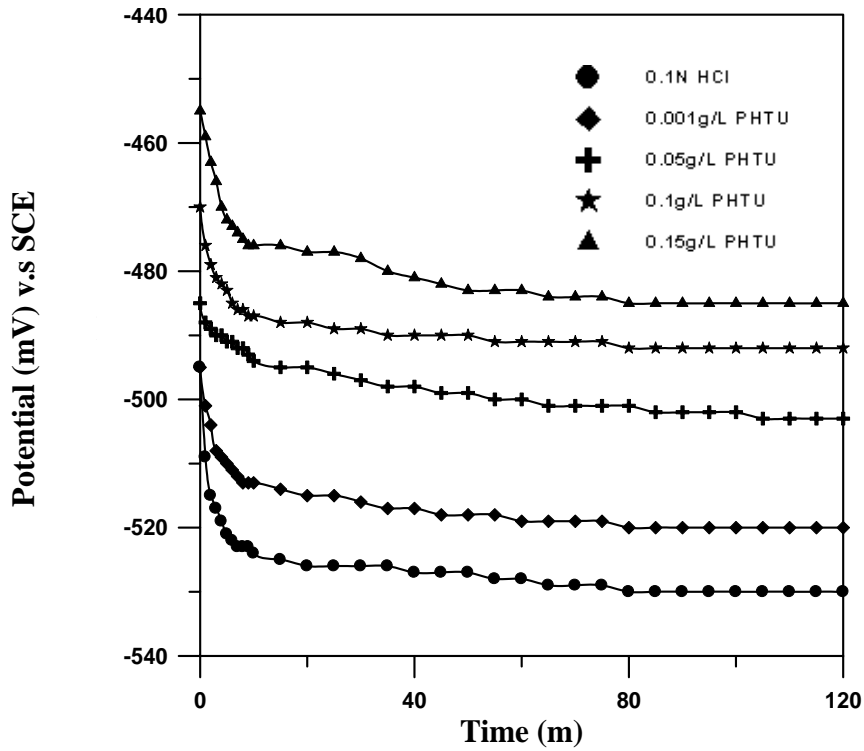


Figure 5-84 Potential vs. time for copper in 0.1N HCl, T=40 °C, t=120m, and 1500 RPM



**Figure 5-85** Potential vs. time for carbon steel in 0.1N HCl, T=40 °C, t=120m, and 0 RPM



**Figure 5-86** Potential vs. time for carbon steel in 0.1N HCl, T=40 °C, t=120m, and 500 RPM

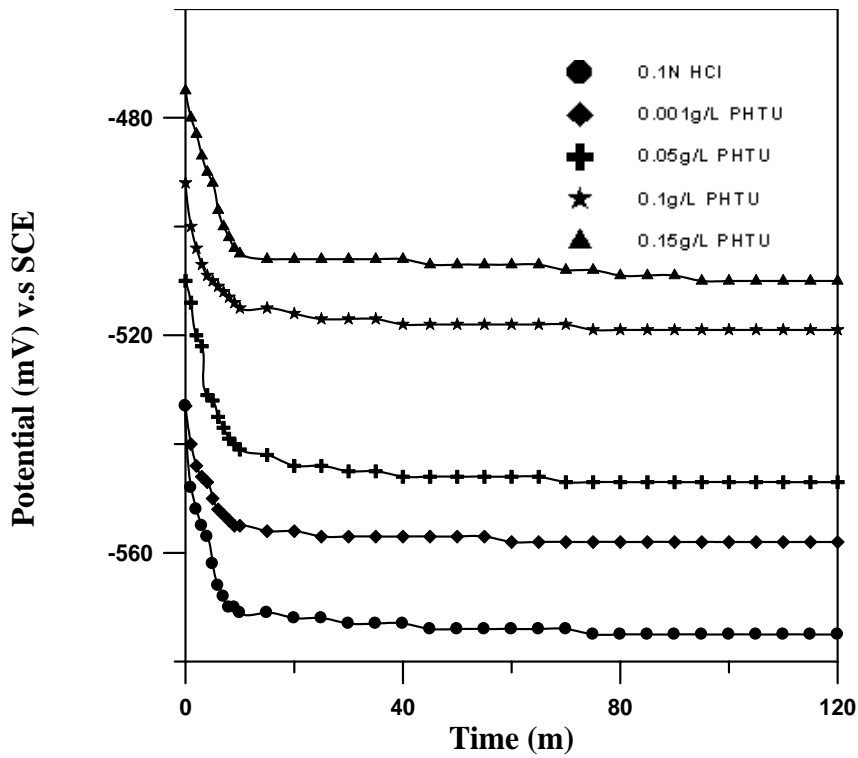


Figure 5-87 Potential vs. time for carbon steel in 0.1N HCl, T=40 °C, t=120m, and 1000 RPM

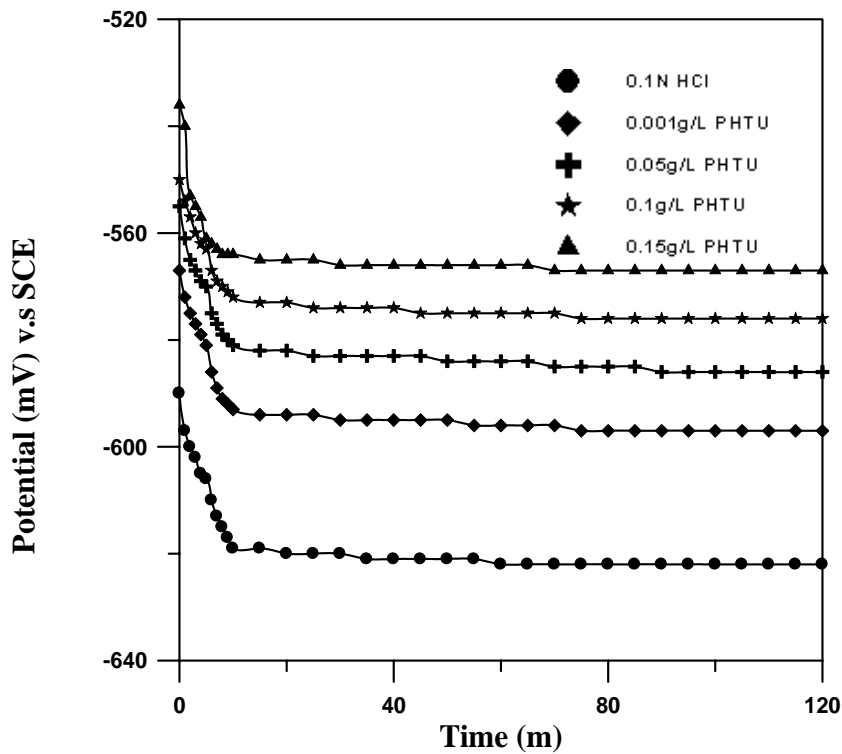


Figure 5-88 Potential vs. time for carbon steel in 0.1N HCl, T=40 °C, t=120m, and 1500 RPM

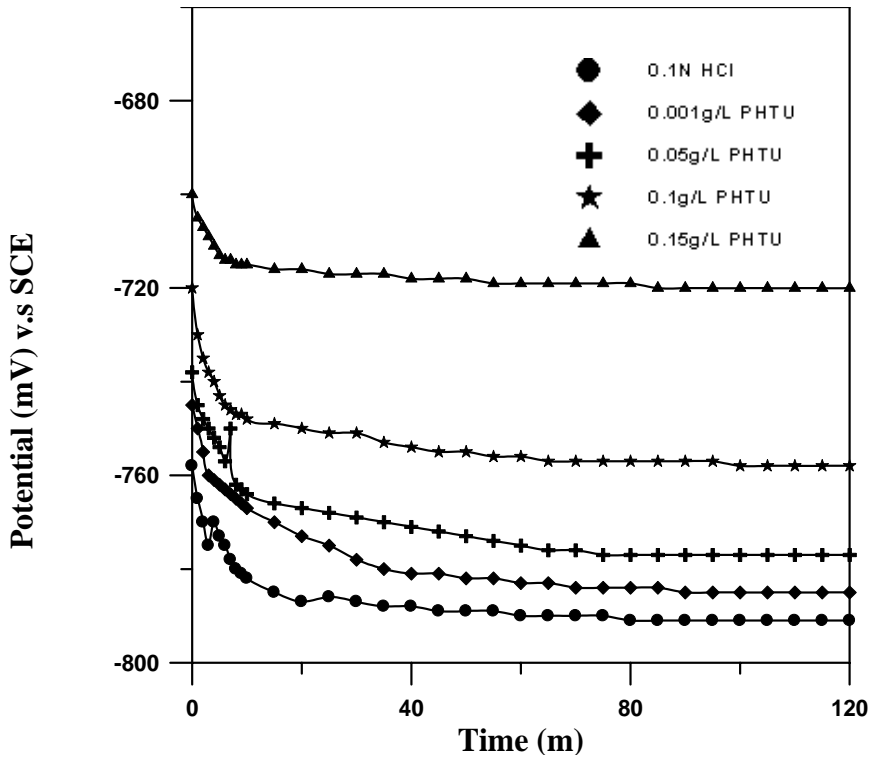


Figure 5-89 Potential vs. time for zinc in 0.1N HCl, T=40 °C, t=120m, and 0 RPM

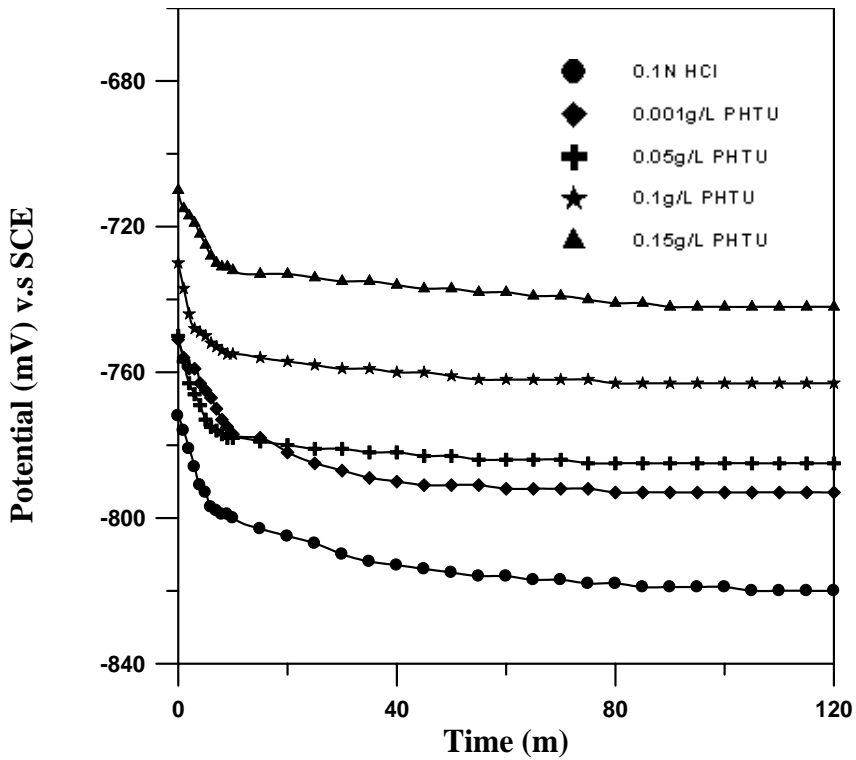


Figure 5-90 Potential vs. time for zinc in 0.1N HCl, T=40 °C, t=120m, and 500 RPM

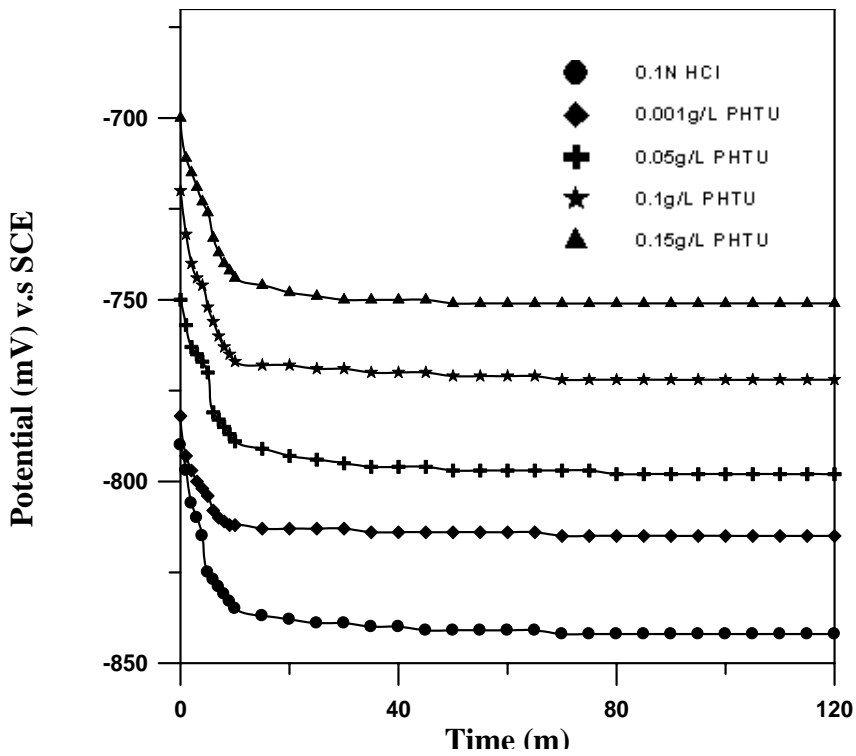


Figure 5-91 Potential vs. time for zinc in 0.1N HCl, T=40 °C, t=120m, and 1000 RPM

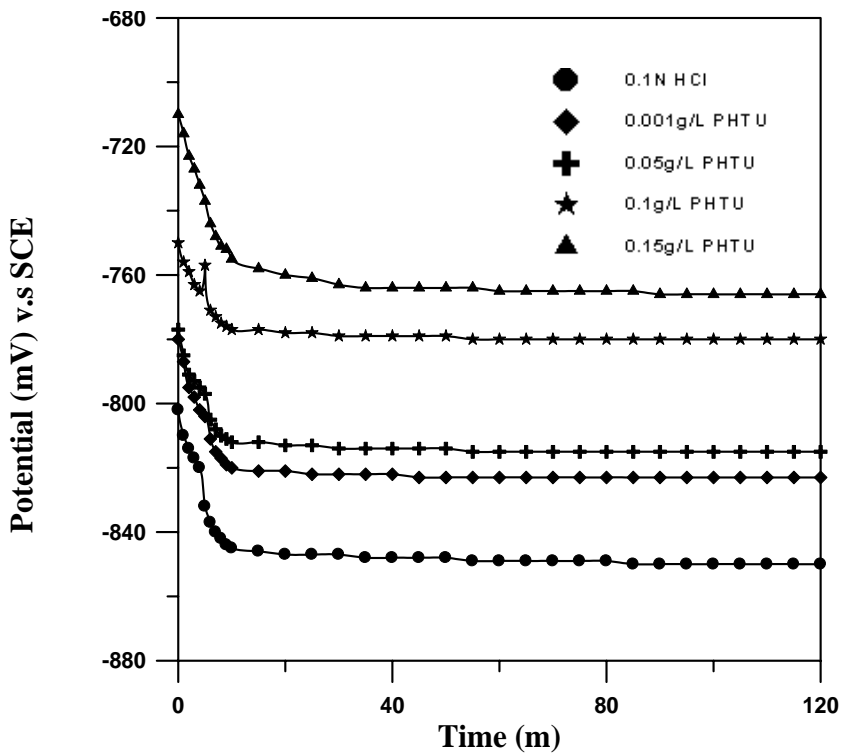


Figure 5-92 Potential vs. time for zinc in 0.1N HCl, T=40 °C, t=120m, and 1500 RPM

### 5.6 Polarization Curves:

The effect of PHTU concentration, rotating cylinder speed and metal type on the polarization curves have been plotted as shown in Figs.(5.93-5.104), and presented in Appendix F.

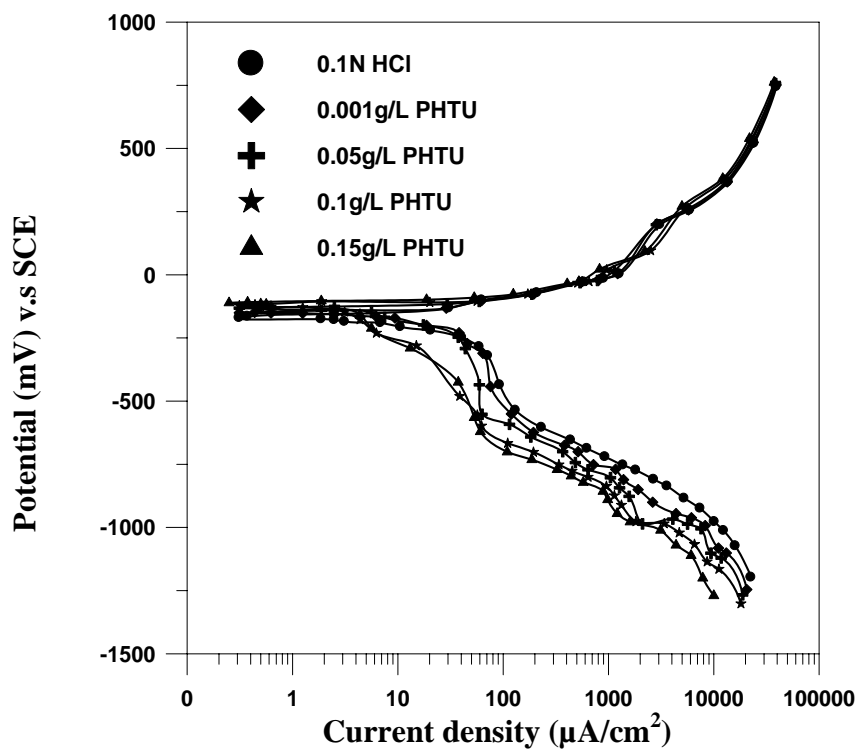
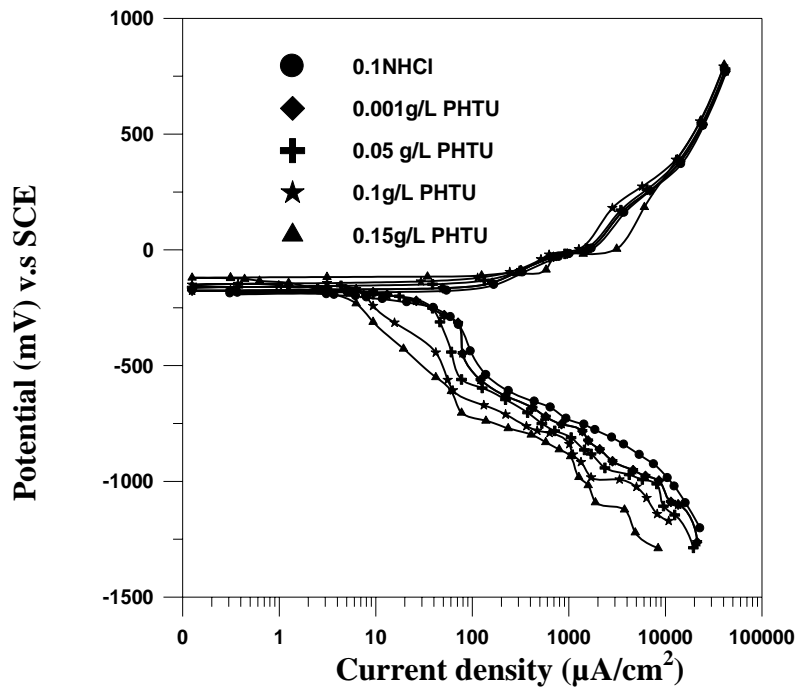
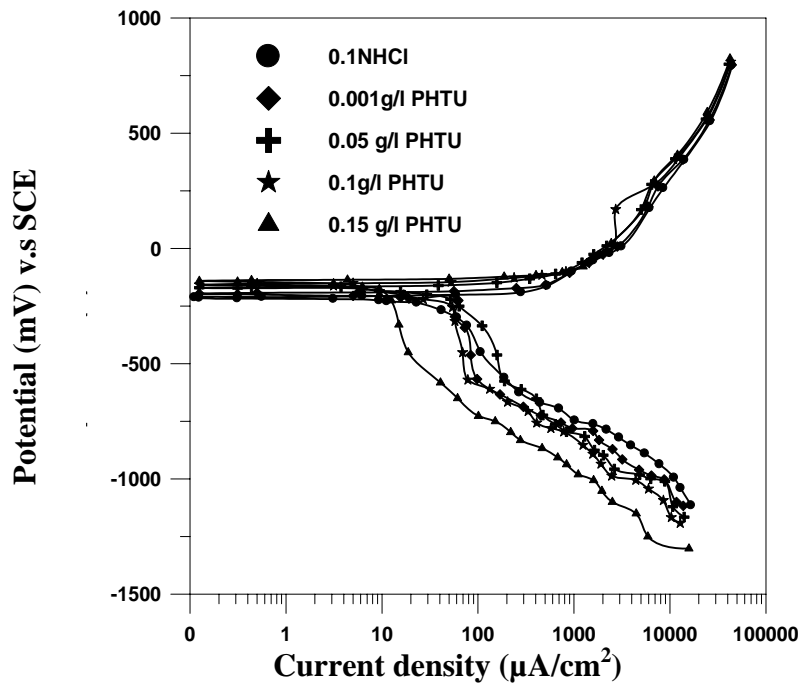


Figure 5-93 Polarization curves on copper metal in 0.1N HCl, T=40 °C, and 0 RPM



**Figure 5-94** Polarization curves on copper metal in 0.1N HCl, T=40 °C, and 500 RPM



**Figure 5-95** Polarization curves on copper metal in 0.1N HCl, T=40 °C, and 1000 RPM

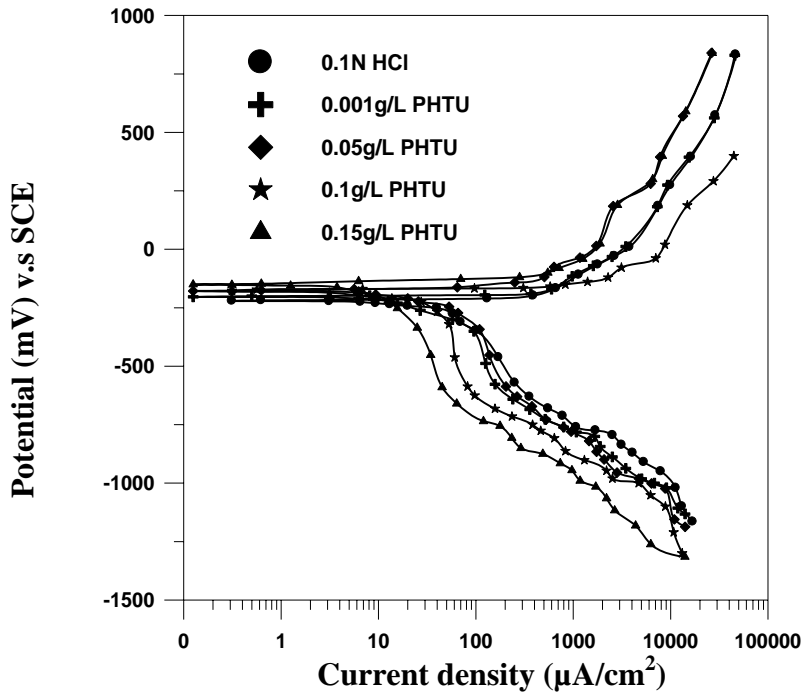


**Figure 5-96** Polarization curves on copper metal in 0.1N HCl, T=40 °C, and 1500 RPM

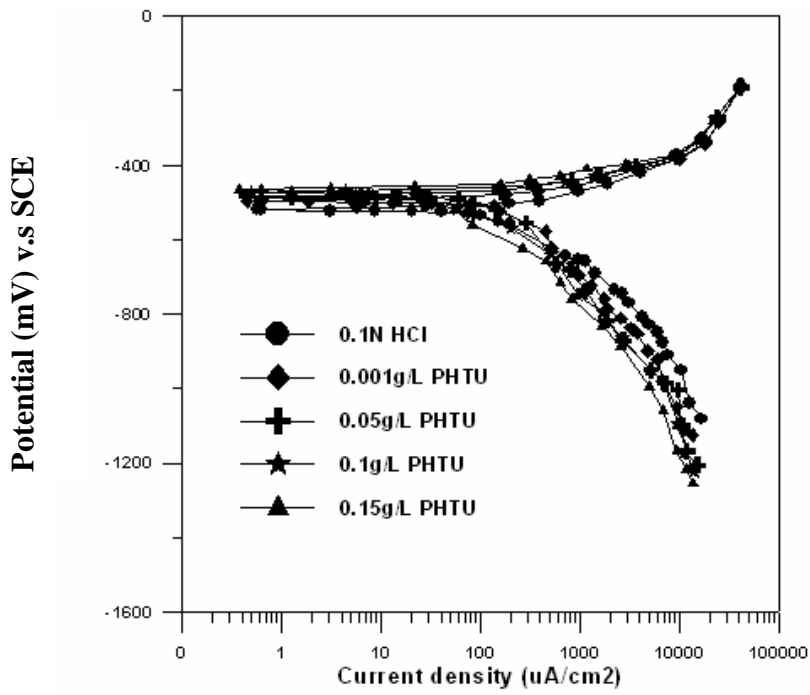


**Figure 5-97** Polarization curves on carbon steel metal in 0.1N HCl, T=40 °C, and 0 RPM



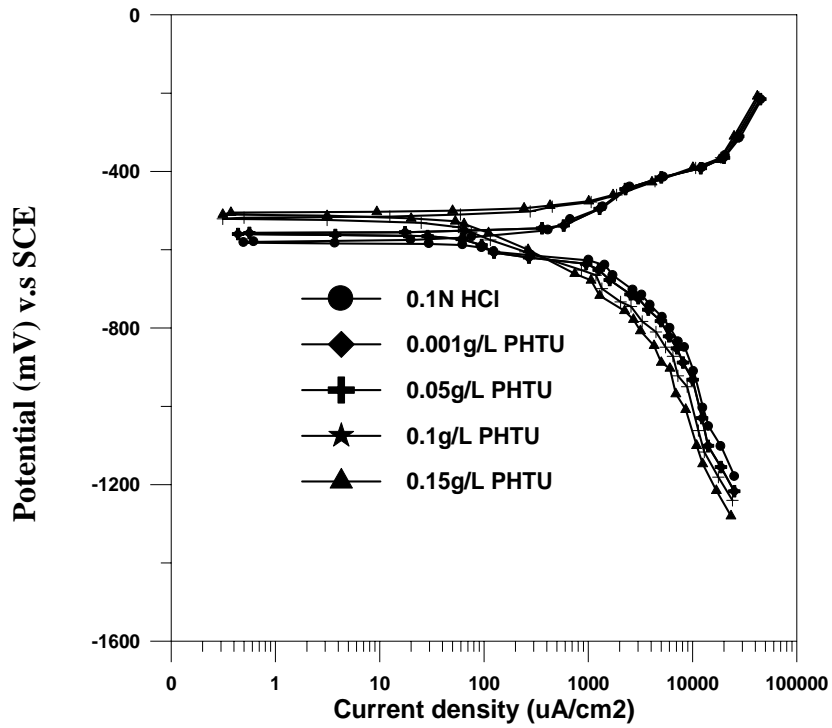


**Figure 5-98** Polarization curves on carbon steel metal in 0.1N HCl, T=40 °C, and 500 RPM

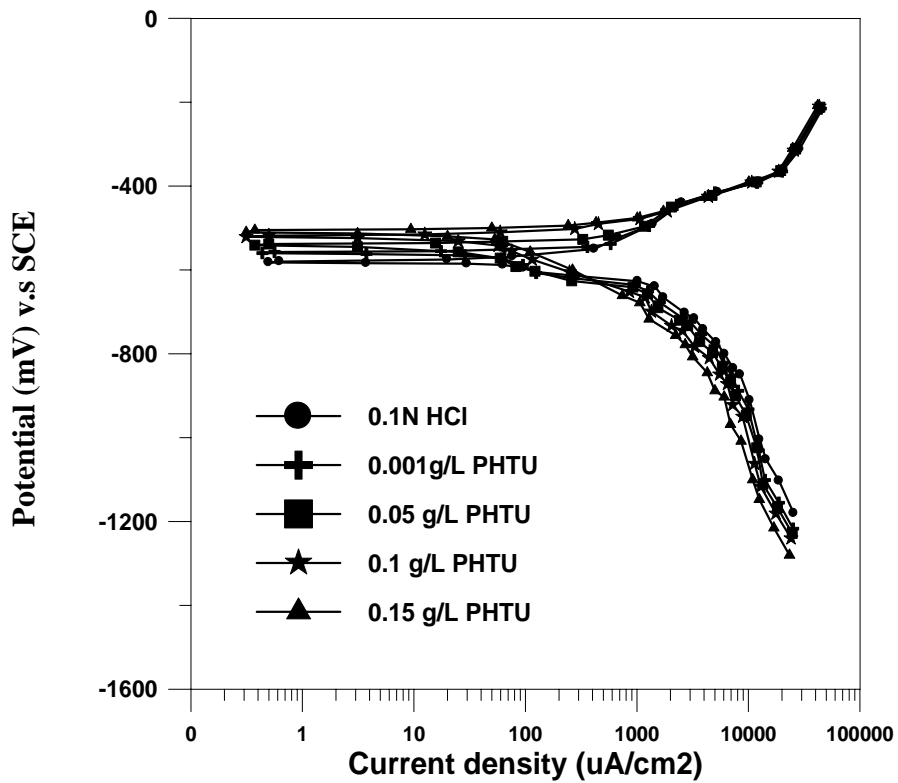


**Figure 5-99** Polarization curves on carbon steel metal in 0.1N HCl, T=40 °C, and 1000 RPM

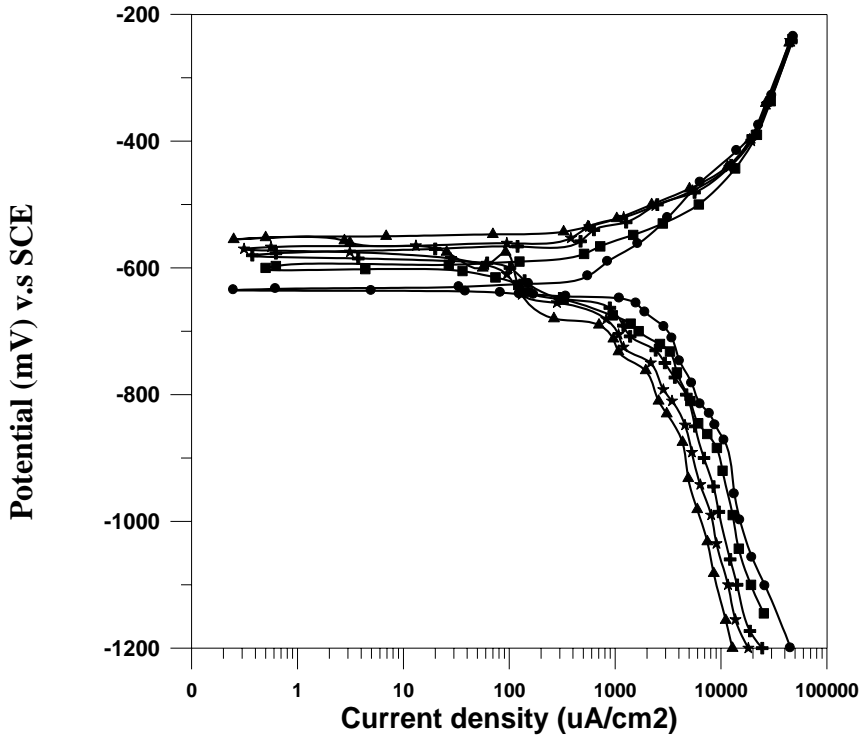


**Figure 5-100** Polarization curves on carbon steel metal in 0.1N HCl, T=40 °C, and 1500 RPM

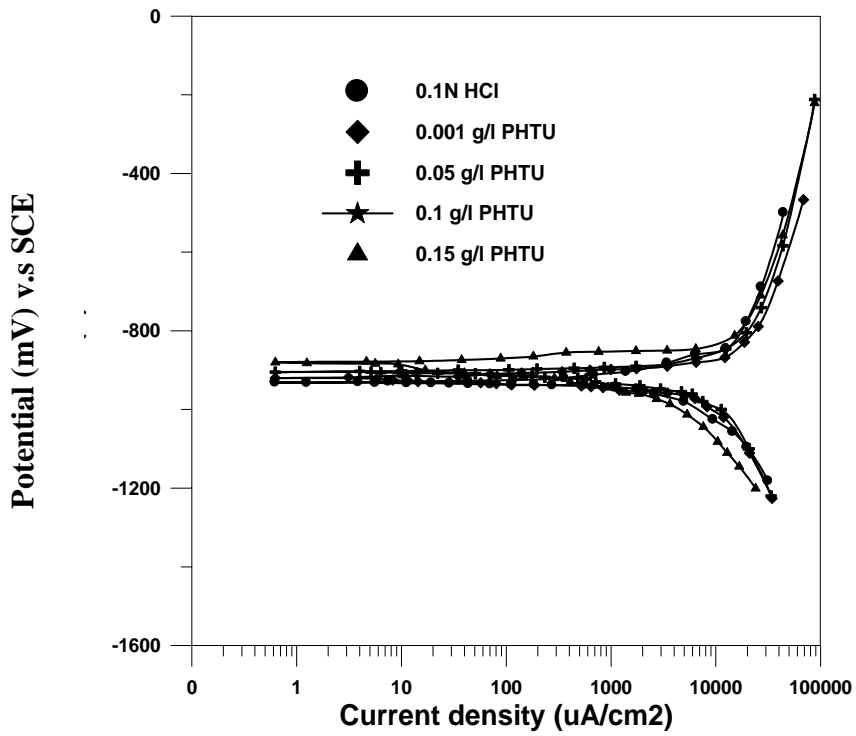


**Figure 5-101** Polarization curves on zinc metal in 0.1N HCl, T=40 °C, and 0 RPM

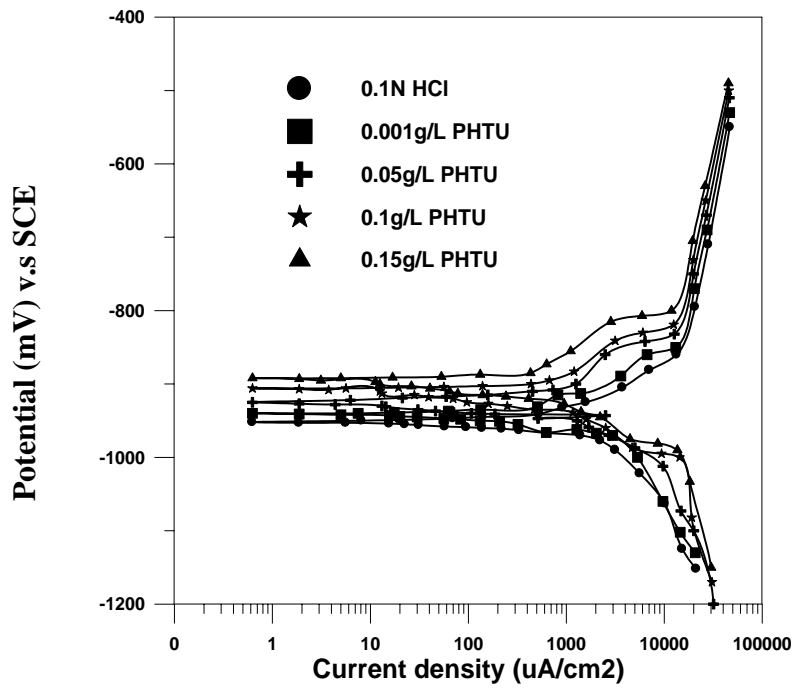


**Figure 5-102** Polarization curves on zinc metal in 0.1N HCl, T=40 °C, and 500 RPM

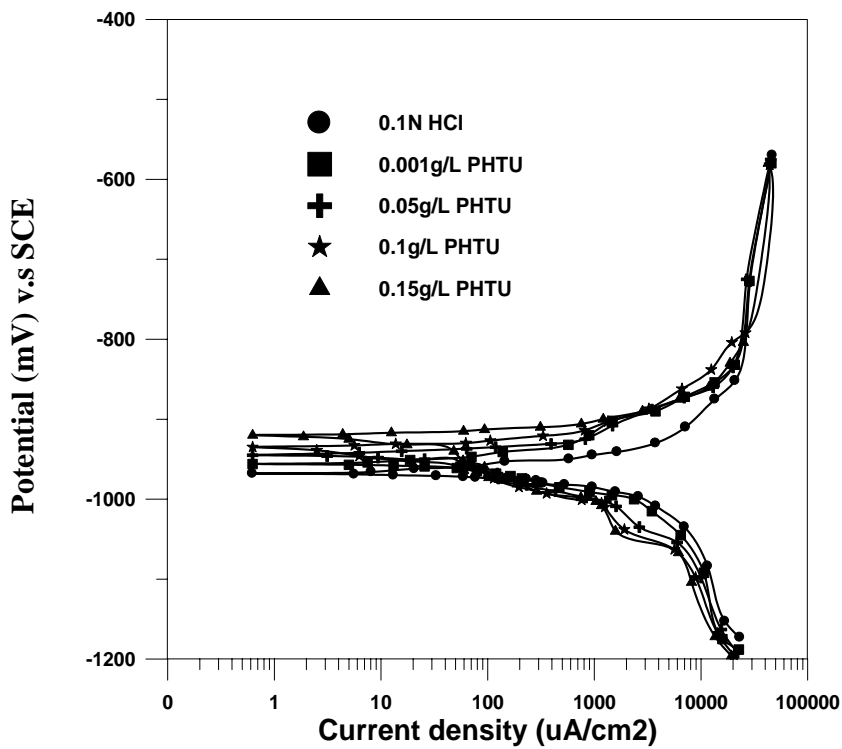


**Figure 5-103** Polarization curves on zinc metal in 0.1N HCl, T=40 °C, and 1000 RPM

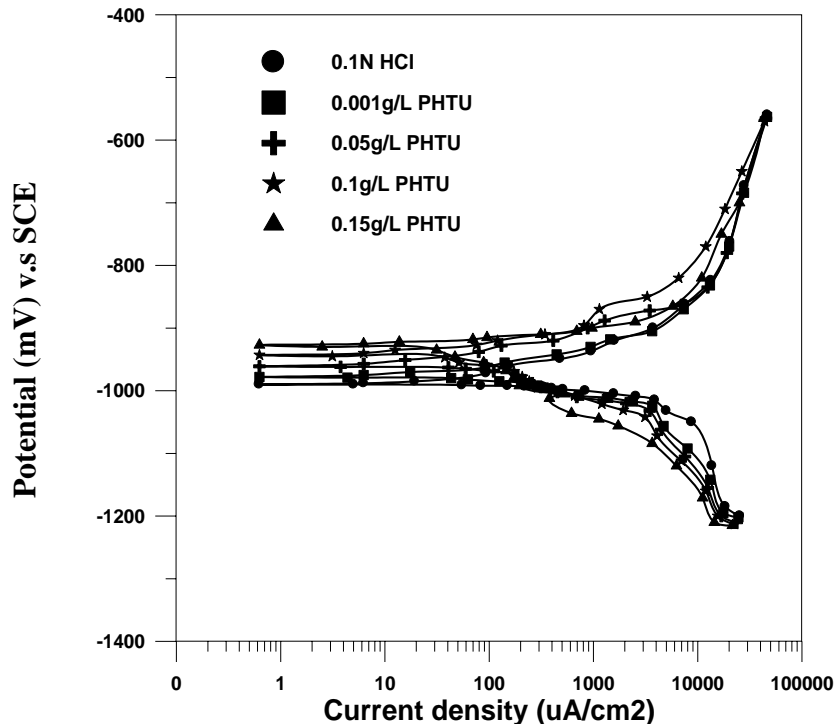


**Figure 5-104** Polarization curves on zinc metal in 0.1N HCl, T=40 °C, and 1500 RPM

### 5.7 Results of cell resistance measurement:

The results as shown in appendix (J) have been obtained from experiments explained in chapter four. This appendix shows the variable resistance (1.3, 2.3, 3.3, 4.3 and 5.3Ω) had been connected between cathodic metal (copper) and anodic metal (carbon steel) to measure potential values to each resistance at each minute for 20minute in air-saturated 0.1N HCl solution and also after adding 0.15g/L PHTU concentration to this solution with 0 and 1500RPM rotational velocities and area ratio AR=1at constant temperature (T=40 °C). The integral current has been calculated from calculating the current according to the following (Ohms law):

$$I = \frac{V}{R}$$

# Chapter Six

## Discussion

### 6.1 Introduction

Chapter five introduces a large amount of experimental results. This is to be expected because of the number of variables involved in the present work, i.e, PHTU concentration, area ratio, rotating cylinder speed and metal types.

### 6.2 Parameters that affect single metal corrosion (Free corrosion):

#### 6.2.1 Rotational velocity:

Corrosion rate experiments were carried out to measure corrosion rates of copper, carbon steel, and zinc specimens as shown in tables (5.1-5.3). Tables (6.1- 6.3) show that the corrosion rate increases with increased rotational velocity (or Re) due to higher transport rate of dissolved oxygen. The Reynolds Number (Re) is obtained by the following equation:

$$Re = \frac{\rho \times D_a^2 \times N_I}{\mu} \quad \dots (6.1)$$

*Where:*

$D_a = OD \text{ of specimen (m)} = 0.00255$

$N_I = \text{Rotational speed of the metal cylinder (Rev/Second)}$

$\rho = \text{Fluid density (kg/m}^3) = 992.04 \text{ kg/m}^3 \text{ (T=40}^\circ\text{C)}$ .

$\mu = \text{Fluid viscosity (kg/m.s)} = 6.556 \times 10^{-4} \text{ kg/ m.s (T=40}^\circ\text{C)}$ .

**Table 6-1** Effect of rotational velocity on corrosion rate (by weight loss) of copper specimen in air-saturated 0.1N HCl solution, T=40C and t=120 min.

<i>Rotational velocities(rpm), U</i>	<i>Re</i>	<i>CR(gmd)</i>
0	0	38.946
500	8199.5	60.666
1000	16399.1	73.399
1500	24598.6	83.135

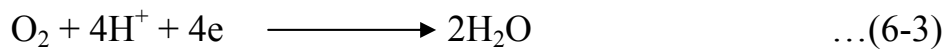
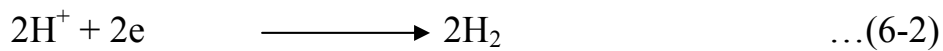
**Table 6-2** Effect rotational of velocity on corrosion rate (by weight loss) of carbon steel specimen in air-saturated 0.1N HCl solution, T=40C and t=120 min.

<i>Rotational velocities(rpm)</i>	<i>Re</i>	<i>CR(gmd)</i>
0	0	121.332
500	8199.5	158.032
1000	16399.1	197.727
1500	24598.6	228.434

**Table 6-3** Effect of rotational velocity on corrosion rate (by weight loss) of zinc specimen in air-saturated 0.1N HCl solution, T=40C and t=120 min.

<i>Rotational velocities(rpm)</i>	<i>Re</i>	<i>CR(gmd)</i>
0	0	327.298
500	8199.5	382.721
1000	16399.1	458.366
1500	24598.6	507.049

The value of  $Re$  in air-saturated HCl acid has no effect on activation controlled  $H_2$  evolution (Eq. 6-2) but affect mass transfer controlled oxygen reduction (Eq. 6-3). Since the corrosion of Cu, Fe and Zn in aerated HCl acid solution is under both mass transfer and activation charge transfer control, therefore increasing  $Re$  (or rotational velocity) will increase the amount of oxygen arriving to the surface and hence leads to a higher corrosion rate.



Increasing  $Re$  leads to decrease in the thickness of diffusion layer that represents the main resistance to oxygen transport<sup>[5]</sup>.

It is clear that the mass transfer coefficient increases with increasing  $Re$ . The increase in  $k$  with  $Re$  can be explained according to the following equation<sup>[30, 112]</sup>:

$$k = \frac{D + \epsilon_D}{\delta_d} \quad \dots (6.4)$$

As  $Re$  increases the convective mass transport of  $O_2$  will increase, i.e., mass transfer by eddy diffusion ( $\epsilon_D$ ) due to the increased turbulence. Increasing turbulence leads to decrease in the thickness of the viscous sub-layer and the diffusion layer that represents the main resistance to momentum and mass transport respectively<sup>[30,112]</sup>, hence the  $O_2$  concentration gradient at the surface will be increased leading to increase in  $k$ .

The corrosion current (or weight loss) increases with increasing  $Re$  so that corrosion potential (**Figs 5-81 to 5-92**) is shifted to more negative values. Also the results reveal that the metals according to their corrosion rate at the investigated rotational velocities (0, 500,

1000 and 1500rpm) were in the following order:

$$\text{Zn} > \text{Fe} > \text{Cu}$$

This fact is obvious in **Fig. 6-1**.

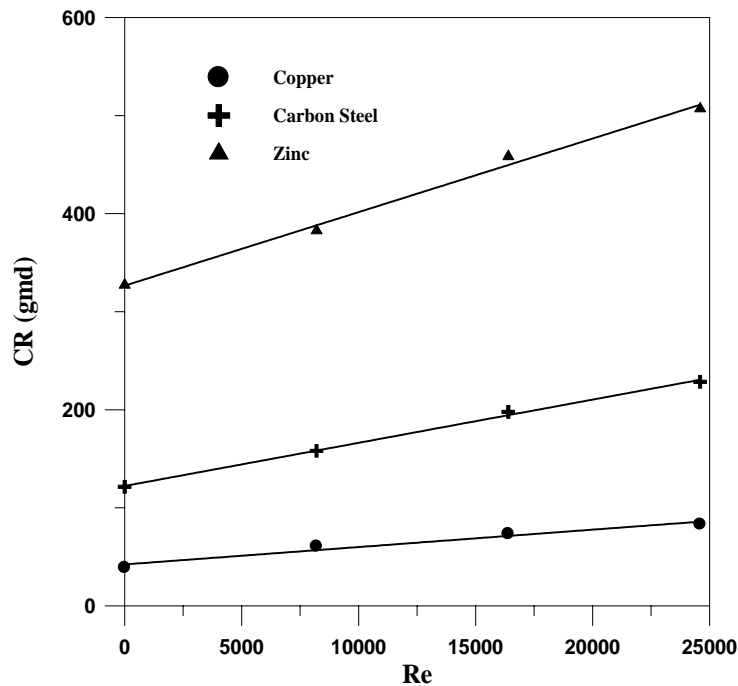


**Figure 6-1** Relationship between Corrosion rate (CR, gmd) and Reynolds Number at T=40°C. (Weight Loss Experiments of Single Metals).

**Fig.6-1** indicates that copper has the lowest corrosion rate, which means it has the highest resistance for this environment, while zinc has the highest corrosion rate, which means that it doesn't resist this environment<sup>[41,93,106]</sup>. Hence the industrially used metals were chosen with greatly different corrosion resistances to be employed for galvanic corrosion investigations.

### 6.2.2 Inhibitor concentration

Tables 5-1 to 5-3 show that efficiency of PHTU inhibitor increases with increasing its concentration leading to decrease in the total cathodic reaction current of oxygen and hydrogen. Hence PHTU leads to a decrease in the corrosion rate. Also anodic current (at the higher



efficiency of PHTU inhibitor) is increasing slightly even at high rotational velocity.

However, in all cases, a preliminary stage of adsorption of the inhibitor can be envisaged and to the extent, the adsorption theory has fulfilled its purpose. Another theory which says those inhibitors are adsorbed on the metal surface forming a protective layer. The adsorption was considered either a physical adsorption or chemisorptions<sup>[113]</sup>.

Most pickling inhibitors function by forming an adsorbed layer on the metal surface, probably no more than a monolayer in thickness, which essentially blocks discharge of  $H^+$  and dissolution of metal ions. Both iodide and quinoline are reported to inhibit corrosion of iron in HCl by this mechanism. Some inhibitors reduce the cathodic reaction (raise hydrogen overvoltage) more than the anodic reaction, or vice versa; but adsorption appears to be general overall the surface rather than at specific anodic or cathodic sites and both reactions tend to be retarded. Hence on addition of an inhibitor to a acid, the corrosion potential of carbon steel is not greatly altered ( $<0.1$  V), although the corrosion rate may be appreciably reduced (**Fig.6.2**)<sup>[24]</sup>.

Compounds serving as pickling inhibitors require, a favorable polar group or groups by which the molecule can attach itself to the metal surface. These include the organic N, amine, S, and OH groups. The size, orientation, shape, and electric charge of the molecule play a part in the effectiveness of inhibition.

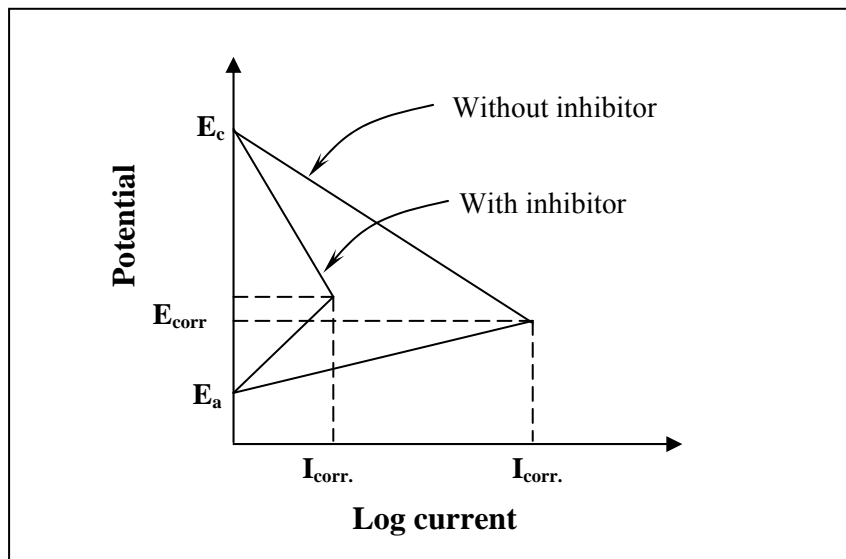


**Figure 6.2**<sup>[24]</sup> Polarization diagram for iron corroding in pickling acid with and without inhibitor (Schematic)

### **6.3 Parameters that affect galvanic corrosion**

In tables 6-4 to 6-6, the potential differences and current have been recorded after 20 min in steady state cases from **Figs. 5-1a,b to 5.48a,b**.

#### **6.3.1 Rotational velocity**

From **Figs.5-1a to 5-48a**, the value of the potential difference is shifted to a more negative value with increasing rotational velocity of the metals. **Figs. 5-1b to 5-48b** show that the value of the current increases with increasing rotational velocity. This is due to the increase in the amount of oxygen transport to the surface. The results of **Figs.5-1a to 5-48a** show that the potential difference is changed with time to more negative values, where the potential difference is recorded at each minute for an experimental run of twenty minute long (each experiment). Precisely the potential difference became rapidly more negative in the first ten minutes, and then the curve converged to slower rate, that is because of the formation of the OH<sup>-</sup> ions in a high rate and grouping on the electrodes<sup>[7]</sup>.

### 6.3.2 Inhibitor concentration

In **Figs.5-1a to 5-48a** and tables 6-7 to 6-9 one can notice that the value of potential difference between two metals will be less negative with increasing value of PHTU concentration which is due to the fact that PHTU inhibitor is a mixed inhibitor. **Figs. 5-1b to 5-48b**, show that the current is decreased with increasing PHTU concentration so that potential difference becomes less negative because of the decreasing cathodic reaction current.

### 6.3.3 Area ratio

Galvanic current increased with increasing area ratio (AR) while potential difference moved in the base direction due to increasing corrosion rate with increasing cathodic area. Area ratio plays an important role in galvanic corrosion as it was found from the results obtained in chapter five. It plays a comprehensive role as shown in **Figs. 5-1a,b to 5-48a,b** and tables 6-7 to 6-9 which show that increase of area ratio ( $A_c/A_a$ ) increases current. Increasing area ratio leads to increase the exposed area to corrosive solution, i.e. the more negative electrode will corrode and the more positive electrode is protected.

The relationship between area ratio, corrosion rate and total surface area of metals is shown in appendix (A):

$$\text{Specimen surface area} = \text{OD} \times \pi \times L \quad \text{OD}=2.55\text{cm}$$

$$\text{Anode surface area which is kept constant } (A_a) = 16.0221\text{cm}^2 \quad L=2\text{cm}$$

Cathode surface areas ( $A_c$ ) are shown in table 6-4 below for varying lengths:

**Table 6-4** Cathodic surface areas

<b>L (cm)</b>	0.5	1	2	4
<b>A<sub>c</sub> (cm<sup>2</sup>)</b>	4.005	8.0111	16.0221	32.0442

The total surface area is equal to the summation of the anode surface area and cathode surface area as shown in table 6-5.

**Table 6-5** Relationship between area ratio (AR) and surface total area ( $A_t$ ).

AR ( $A_c/A_a$ )	$A_c$ (cm <sup>2</sup> )	$A_a$ (cm <sup>2</sup> )	$A_t = A_c + A_a$ (cm <sup>2</sup> )
0.25	4.0055	16.0221	20.0276
0.5	8.0111	16.0221	24.0332
1	16.0221	16.0221	32.0442
2	32.0442	16.0221	48.0663

One can notice from this table that the total area of metals ( $A_t$ ) increased with increasing area ratio (AR) which led to increase total galvanic current  $I_g$  as shown in tables 6-7 to 6-9.

Cathodic current density and anodic current density have been calculated from galvanic current as shown in table 6-6. **Fig.6-3** shows that increasing area ratio leads to decrease the cathode current (Fe) and leads to increase the anodic current (Zn).

This behavior is interpreted as follows: as the cathode area increases the corrosion potential shifted to the base direction reducing the driving force and hence decreasing cathode current and increasing anode current.

The approximate proportionality between galvanic current density and cathode surface area suggests cathodic reduction of hydrogen reduction as the rate determining step. Deviations from their proportionality at higher current densities are due to the increasing anodic polarization of the anode electrode. In addition to the cathodic oxygen reduction a further process, namely anode dissolution, also has an influence on reaction velocity<sup>[105]</sup>.

Also **Fig.6-3** shows that as the velocity increases both anodic and cathodic currents increase. This increase is due to the increase in oxygen transport to the enhancing anodic dissolution of metals (mainly Zn) and the cathodic reduction current.

**Table 6-6** Effect of area ratio AR and rotational velocity on the cathodic current density ( $\mu\text{A}/\text{cm}^2$ ) and anodic current density ( $\mu\text{A}/\text{cm}^2$ ) for different metals couples in air-saturated 0.1N HCl solution,  $t=20$  m and  $T=40$  °C.

<b>Copper and iron couple</b>								
<b>AR</b>	<b>Rotational Velocity (RPM)</b>							
	<b>0</b>		<b>500</b>		<b>1000</b>		<b>1500</b>	
	<b><math>i_c</math></b>	<b><math>i_a</math></b>	<b><math>i_c</math></b>	<b><math>i_a</math></b>	<b><math>i_c</math></b>	<b><math>i_a</math></b>	<b><math>i_c</math></b>	<b><math>i_a</math></b>
<b>0.25</b>	224.690	280.86	270.626	338.28	299.587	374.48	404.442	505.55
<b>0.50</b>	212.206	318.31	248.822	373.23	275.452	413.18	345.356	518.03
<b>1.00</b>	188.489	376.98	234.676	469.352	273.372	546.745	358.879	717.759
<b>2.00</b>	158.531	475.60	219.072	657.22	272.701	830.10	314.566	943.69
<b>Copper and zinc couple</b>								
<b>0.25</b>	472.348	590.43	528.521	660.65	578.202	722.75	593.181	741.48
<b>0.50</b>	433.151	649.73	466.230	699.35	558.602	837.91	547.992	821.99
<b>1.00</b>	353.262	706.52	436.897	873.793	499.310	998.621	546.121	1092.24
<b>2.00</b>	241.021	723.06	411.203	1233.61	417.132	1251.39	469.664	1408.99
<b>Iron and zinc couple</b>								
<b>0.25</b>	515.289	644.11	805.413	1006.73	880.285	1100.36	976.153	1220.19
<b>0.50</b>	480.585	720.88	737.729	1106.59	820.948	1231.42	893.348	1340.02
<b>1.00</b>	415.676	831.35	634.748	1269.5	651.288	1302.58	743.972	1487.94
<b>2.00</b>	323.719	971.16	462.486	1387.46	489.324	1467.97	531.974	1595.92

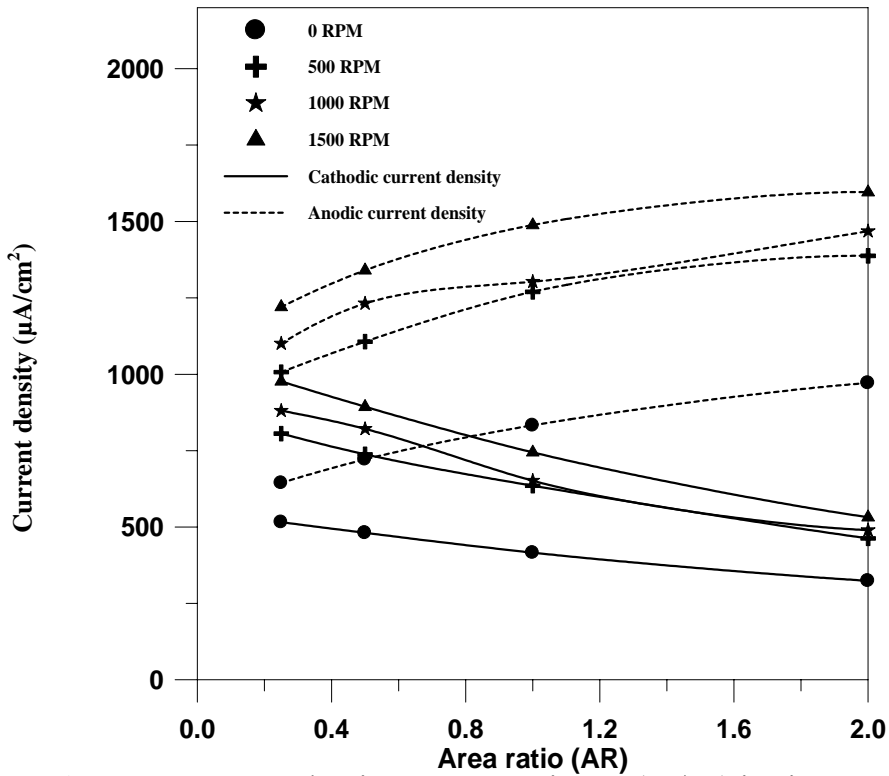


**Figure 6-3** Current density vs. Area ratio AR (Fe/Zn) in air-saturated 0.1N HCl solution,  $t=20$  min and  $T=40$  °C.

Consider the situation in **Fig.6-4** where the area ratio  $f_1/f_2$  is very large, i.e. the noble metal (Fe) greatly exceeds the base (Zn) one in area. The total anodic and cathodic current curves of **Fig.6-4** have been constructed by summing the currents  $f_1i_1$  and  $f_2i_2$  according to the equation (6.5)<sup>[45]</sup>:

$$i_{\text{total}} = f_1i_1 + f_2i_2 \quad \dots (6.5)$$

Clearly, in the absence of Fe, the corrosion of the base metal Zn would be represented by the  $(\bar{E}, f_2i')$ . Now that Fe is also present the overall corrosion situation is represented by the point of intersection of the two total curves at P. At the potential  $E_{\text{couple}}$ , the corrosion rate of Zn is  $f_2i''$ , so that Zn is now corroding at a current density of  $i''$  as against  $i'$  previously. That is, the intensity of attack on the base metal is greatly enhanced (in

the ratio  $i'' / i'$  ) when the metal is coupled to a large area of a more noble metal Fe. In Fig.6-4 the distribution of the various anodic and cathodic reactions is schematically represented. Zn corrodes rapidly (thick arrow) and most of the electrons generated are fed into Fe where cathodic reaction occurs almost exclusively. Zn is said to undergo galvanic attack<sup>[45]</sup>.

Where  $f_1/f_2$  is very small, i.e. the base metal (Zn) greatly exceeds the noble one in area, the situation may be represented by **Fig.6-5**. Again, the total anodic and cathodic curves have been constructed and it may be seen in **Fig.6-5** that these intersect at Q, where the potential  $E_{\text{couple}}$  has now moved in the base direction relative to P in **Fig.6-4**. In these circumstances the presence of Fe makes very little difference to Zn. However, the interest should be directed to Fe. It may be seen that, where Zn is not present, corrosion of Fe would normally take place at a potential  $\bar{E}$  and current  $f_1 i'$ . But because the potential of the couple (viz. at Q) is now below the reversible potential  $E_{\text{Fe}}$ , corrosion of Fe now ceases altogether because there can be no net anodic reaction at the  $\text{Fe} | \text{Fe}^{++}$  interface. As a result, Fe is said to be galvanically protected. **Fig.6-5** shows the distribution of reaction<sup>[25]</sup>. This is also the situation for the couples Cu/Fe and Cu/Zn where Cu is totally protected.

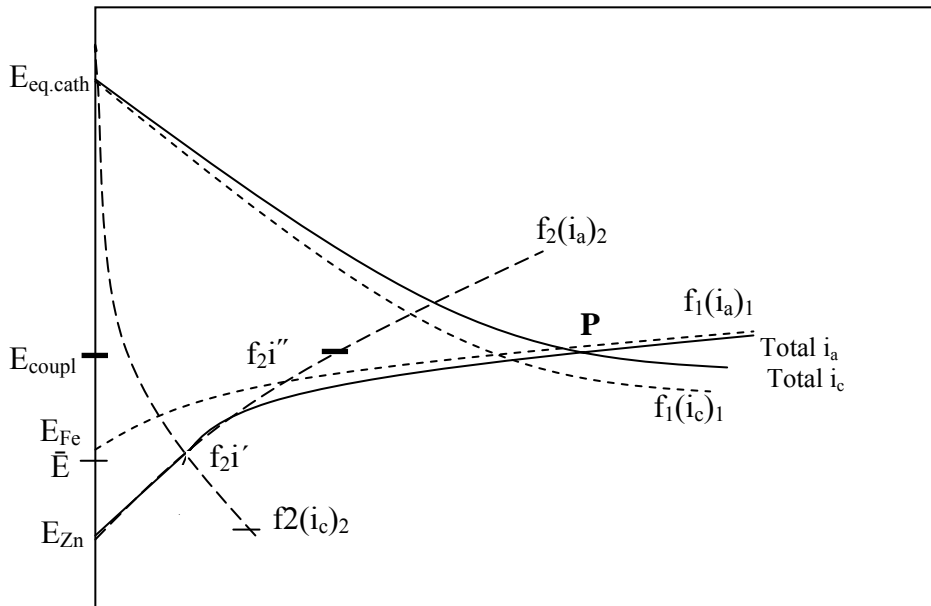


**Figure 6-4** Behaviour of a metal couple Fe-Zn,  $AR \gg 1$  produces galvanic attack of Zn (Schematic)

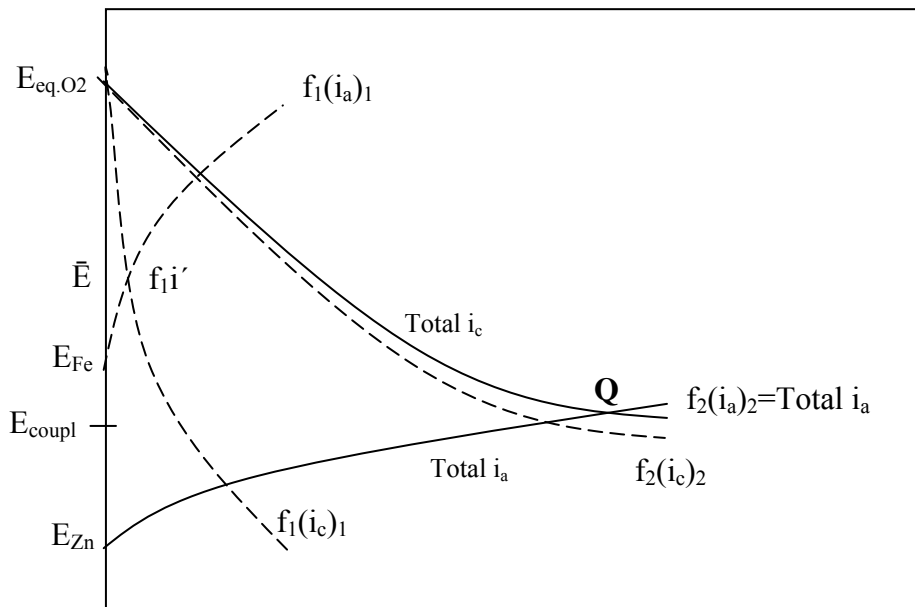


**Figure 6-5** Behaviour of a metal couple Fe-Zn,  $AR \ll 1$  produces galvanic attack of Zn (Schematic)



**Table 6-7** Effect of inhibitor (PHTU) concentration, area ratio AR (Cu/ Fe) and rotational velocity on the current and potential difference (at steady state) in air-saturated 0.1N HCl solution,  $t=20$  m and  $T=40$  °C.

AR	C(g/L) ) PHTU	Rotational Velocity (RPM)							
		0		500		1000		1500	
		I(mA) )	E(mV) )	I(mA) )	E(mV) )	I(mA) )	E(mV) )	I(mA) )	E(mV) )
0.2 5	0.000	4.500	-402	5.420	-502	6.000	-515	8.100	-540
	0.001	2.740	-393	4.000	-491	4.770	-506	6.890	-526
	0.050	1.640	-380	3.510	-484	4.000	-492	6.020	-515
	0.100	1.390	-373	2.600	-470	3.600	-485	5.430	-500
	0.150	0.630	-368	2.110	-465	3.100	-473	4.850	-486
0.5	0.000	5.100	-421	5.980	-516	6.620	-533	8.300	-558
	0.001	4.150	-416	4.350	-503	5.160	-524	7.320	-545
	0.050	2.610	-400	3.710	-492	4.460	-511	6.480	-531
	0.100	1.580	-390	2.950	-480	3.800	-500	5.850	-520
	0.150	0.650	-381	2.500	-472	3.305	-485	5.200	-509
1	0.000	6.040	-438	7.52	-525	8.76	-551	11.50	-585
	0.001	5.490	-422	6.990	-517	8.55	-535	11.33	-578
	0.050	2.100	-405	4.490	-507	8.250	-524	9.820	-566
	0.100	1.185	-394	4.310	-493	6.899	-515	7.610	-550
	0.150	0.950	-385	3.340	-480	5.550	-506	6.550	-541
2	0.000	7.620	-465	10.53	-548	13.30	-570	15.12	-602
	0.001	5.060	-456	7.400	-527	10.95	-561	12.13	-590
	0.050	2.670	-440	5.110	-518	8.410	-549	10.19	-578
	0.100	1.290	-427	4.500	-500	7.120	-535	8.000	-565
	0.150	1.000	-415	3.610	-491	5.825	-522	6.840	-552

**Table 6-8** Effect of inhibitor (PHTU) concentration, area ratio AR (Cu/Zn) and rotational velocity on the current and potential difference (at steady state) in air-saturated 0.1N HCl solution,  $t=20$  m and  $T=40$  °C.

AR	C(g/L) ) PHT U	Rotational Velocity (RPM)							
		0		500		1000		1500	
		I(mA)	E(mV) )	I(mA)	E(mV) )	I(mA)	E(mV) )	I(mA)	E(mV) )
0.2 5	0.000	9.46	-851	10.58 5	-862	11.58	-879	11.88	-930
	0.001	7.84	-838	9.35	-848	11.25	-860	8.185	-913
	0.050	1.82	-826	9.33	-832	5.26	-839	6.475	-894
	0.100	1.175	-823	5.88	-813	4.81	-822	5	-870
	0.150	0.825	-815	4.32	-799	3.96	-812	4.62	-855
0.5	0.000	10.41	-868	11.20 5	-885	13.42 5	-900	13.17	-950
	0.001	7.85	-850	10.56 0	-861	9.670	-886	9.30	-938
	0.050	2.815	-835	9.680	-851	6.235	-864	7.32	-920
	0.100	1.23	-823	6.880	-834	5.160	-845	6.23	-909
	0.150	0.82	-816	5.235	-818	4.12	-826	4.64	-892
1	0.000	11.32	-880	14.00	-900	16.00	-922	17.50	-991
	0.001	7.51	-862	13.73	-882	15.70	-908	17.13	-956
	0.050	2.215	-847	6.75	-861	9.525	-890	10.50	-940
	0.100	1.400	-837	6.275	-840	8.300	-920	8.305	-925
	0.150	1.195	-820	6.255	-831	5.275	-851	6.685	-915
2	0.000	11.58 5	-900	19.76 5	-926	20.05	-957	22.57 5	-990
	0.001	7.66	-886	14.60	-900	16.96	-940	18.21	-975
	0.050	2.366	-865	7.775	-872	10.71	-921	11.50	-958
	0.100	1.63	-850	7.710	-867	9.26	-869	9.53	-945
	0.150	1.35	-830	6.500	-855	6.25	-907	8.915	-915

**Table 6-9** Effect of inhibitor (PHTU) concentration, area ratio AR (Fe/Zn) and rotational velocities on the current and potential difference (at steady state) in air-saturated 0.1N HCl solution,  $t=20m$  and  $T=40^{\circ}C$ .

AR	C(g/L) ) PHTU	Rotational Velocity (RPM)							
		0		500		1000		1500	
		I(mA) )	E(mV) )	I(mA) )	E(mV) )	I(mA) )	E(mV) )	I(mA) )	E(mV) )
0.25	0.000	10.32	-887	16.13	-890	17.63	-924	19.55	-965
	0.001	8.73	-860	13.57	-875	13.22	-910	15.37	-951
	0.050	5.11	-845	8.76	-857	10.77	-897	12.78	-938
	0.100	3.11	-832	6.34	-842	8.13	-880	9.65	-920
	0.150	2.25	-820	4.63	-830	6.34	-871	7.47	-909
0.5	0.000	11.55	-905	17.73	-915	19.73	-950	21.47	-984
	0.001	10.21	890	15.66	-897	15.33	-933	17.47	-968
	0.050	6.53	-875	10.21	-880	13.74	-920	16.02	-952
	0.100	4.66	-850	7.02	-860	10.66	-909	12.56	-935
	0.150	3.62	-832	5.72	-845	8.33	-890	10.76	-922
1	0.000	13.32	-930	20.34	-948	20.87	-973	23.84	-1010
	0.001	10.14	-910	16.77	-930	18.23	-962	20.66	-992
	0.050	7.33	-888	11.77	-912	14.77	-945	15.87	-976
	0.100	4.73	-860	8.86	-895	10.24	-932	12.57	-950
	0.150	4.10	-850	6.82	-880	7.37	-915	9.85	-940
2	0.000	15.56	-950	22.23	-970	23.52	-995	25.57	-1037
	0.001	12.21	-934	18.56	-957	20.77	-978	22.73	-1022
	0.050	8.53	-915	13.66	-940	16.34	-960	18.86	-1005
	0.100	6.54	-915	10.73	-927	12.33	-939	14.76	-991
	0.150	5.00	-890	9.12	-910	10.23	-920	12.68	-974

## 6.4 Parameters that affect galvanic corrosion current

The data of **Figs. 5-1b to 5-48b** is presented in tables 6-10 to 6-13 (see appendix (C)). Table 6-10 shows weight loss values, for both cathode (Cu) and anode (Zn). It can be seen that copper weight loss is equal to zero in **Fig.6-6** because ( $E_{\text{coup.}} < E_{\text{eq,Cu}}$ ) so that the galvanic current is equal to the iron corrosion current ( $I_{\text{corr,Fe}}$ ) after the coupling minus the summation of the oxygen reduction current and hydrogen evolution current [ $I_{\text{LO}_2} + I_{\text{H}^+}$ ] at  $E_{\text{coup.}}$ . This is due to complete protection of copper in Cu/Fe and Cu/Zn couples, also total protection (some cases) of Fe in Fe/Zn couple. Also CR (gmd), CR (mm/y) and  $i_d(\text{uA/cm}^2)$  have been determined and listed in the tables. The results show that weight loss ceased, by the increase of PHTU inhibitor; this may be due to the decreasing of the total cathodic current of oxygen and hydrogen. In galvanic couple between iron and zinc it is clear that the iron corrosion rate isn't zero because  $E_{\text{coup.}} > E_{\text{eq,Fe}}$  i.e. partially protected or partially corroding of iron metal in some Zn/Fe couple as shown in **Fig.6-7** {see appendix (C)}.

Weight loss is increased by increasing cathode /anode ratio (AR). This may be ascribed to the increasing of cathode surface area. This is true for all results for corrosion rate and anodic current density.

In table (6.11), integral current time has been calculated; a suitable equation has been created by using grapher package program (see appendix I). Integration applied for each equation, integral current time for (0-20min) time interval, has been calculated for each case. Anode weight loss has been calculated according to the following equation<sup>[105]</sup>:

$$1\text{Ah} = 1.0418 \text{ g [ Iron (Fe) ]} \qquad 1\text{Ah} = 1.218 \text{ g [ Zinc (Zn) ]}$$

Computer program (Q-Basic language) has been used to calculate corrosion rate, dissolution current density ...etc as shown in tables 6-10 to 6-13, all the rest of tables were shown in the appendix C.

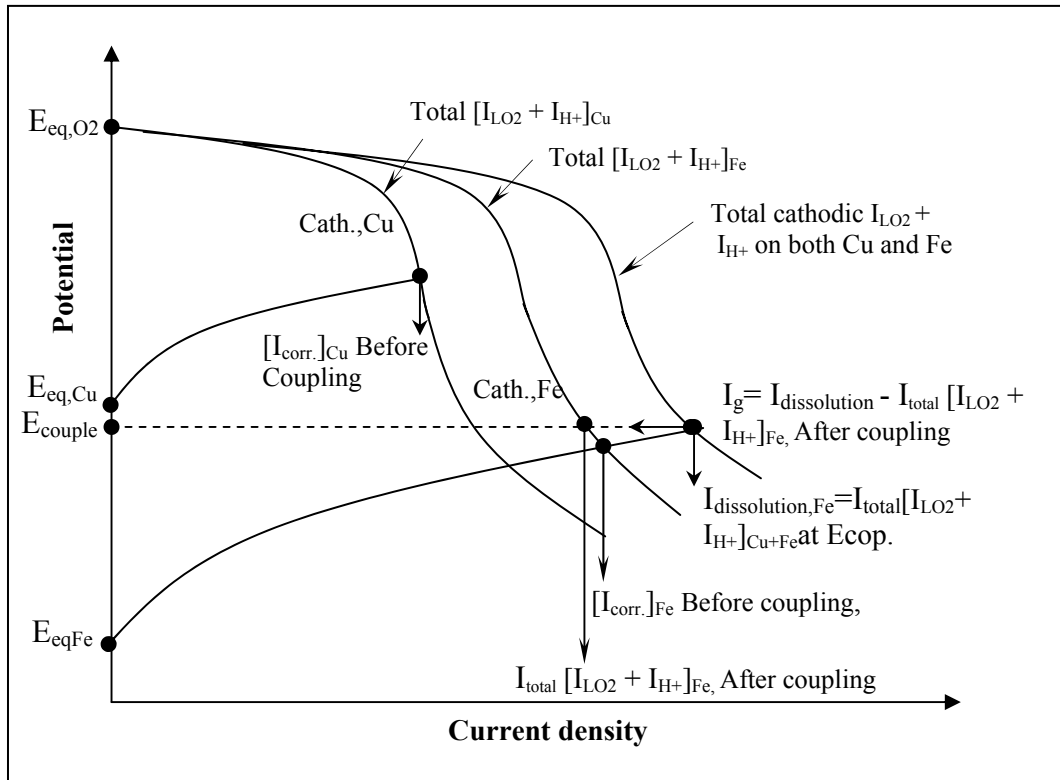


Figure 6-6 Galvanic corrosion couple (complete protection of copper) between copper and iron

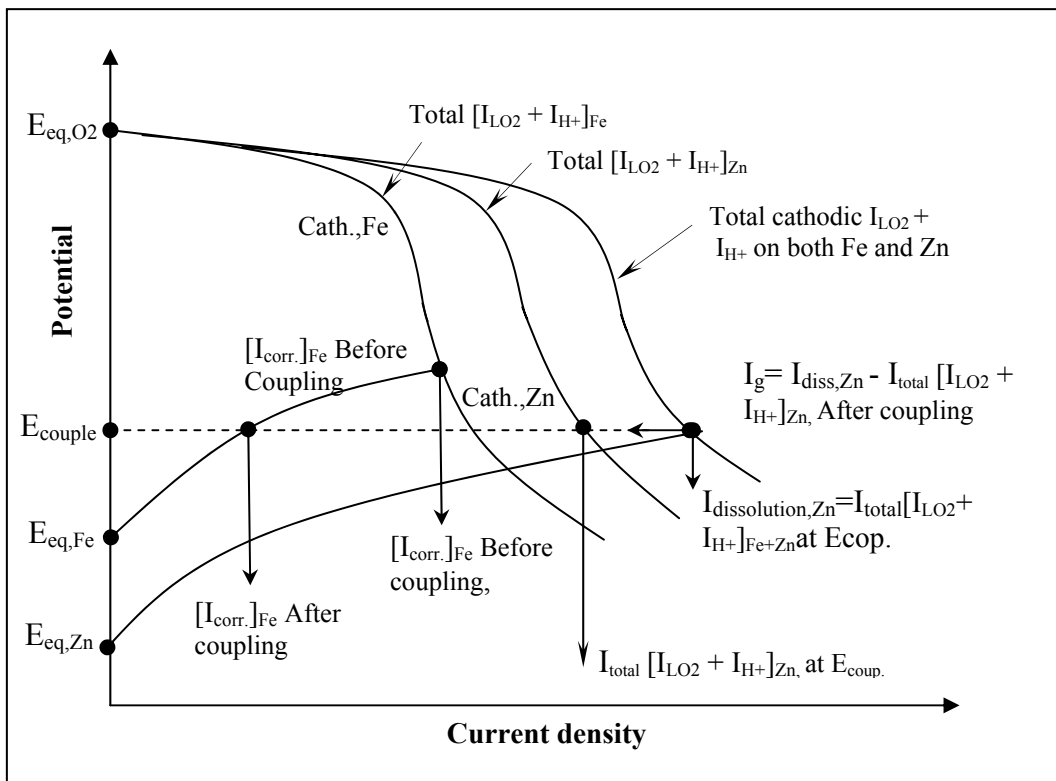


Figure 6-7 Galvanic corrosion couple (partial protection of iron) between iron and zinc

The cell current time integral, the weight loss calculated from cell current and directly from weighing, and the ratio of weight loss from cell current and weighing, is shown in table 6-11. The weight loss equivalent to the cell current is calculated from the relation<sup>[105]</sup>:

$$1\text{Ah}=1.0418\text{ g}$$

The weight loss resulting from the cell current forms only part of the total weight loss. The proportion decreases in the series of coupled metals.

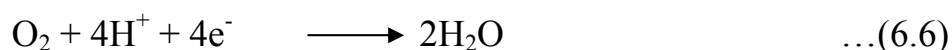
Zinc > Carbon steel > Copper

This is due to the hydrogen overvoltage increasing on the coupled metals in the same order. Since the overvoltage for hydrogen evolution is higher on carbon steel than on copper, the current density of the hydrogen evolution is lower and therefore the cell current is less. The weight loss of Cu in the coupling materials (Cu/Fe and Cu/Zn) is practically zero because it is cathodically protected.

The magnitude of the total corrosion arising from cell current and self-corrosion is given in table 6-12. The self corrosion is the difference between the total corrosion and the corrosion caused by the cell current. The cell current- time integral, the weight loss from the cell current, the weight loss from weighing and galvanic factor (GF) [Weight loss from cell current / weight loss from weighing] have been calculated as shown in table (6-11), see appendix (C). The quantities of total corrosion, corrosion due to cell current and self corrosion are recorded in further tables as current densities.

The results are calculated by using the relation  $1Ah=1.0418\text{ g}$ , the surface area =  $16.022122\text{ cm}^2$  and for time  $t=0.333\text{hr}$ . However, the self corrosion increases as is to be expected. A decrease in the self-corrosion would be expected (the so-called difference effect) as has been observed in long term experiments. The explanation for this unexpected result is supposedly that uncontrolled effects play a role in the initial stages, and thus, in this short term experiment, determine the corrosion phenomena<sup>[105]</sup>. This also leads to a relatively high scatter in the experimental results.

The cathode reaction occurs on both partners of the couple. A result of this is that the corrosion current density is always greater than the cell current density. In addition of the cathodic evolution of hydrogen, the cathodic reduction of oxygen has to be considered:



In table 6-10 weight loss is almost directly proportional to cathode area. For this corrosion system the area principle holds true. The approximate proportionality between weight loss and cathode surface area suggests cathodic reduction of oxygen as the rate determining step. Deviations from their proportionality at higher current densities are due to the increasing anodic polarization of the zinc electrode. In addition to the cathodic oxygen reduction a process, namely iron dissolution, also has an influence on reaction velocity. Variation in the distance between the electrodes does not cause any change in cell current.

In table 6-13 as shown above, average currents, are directly recorded from the ammeter for 0.3333hr time period. Also cathodic current  $I_2$  and anodic current  $I_3$ , estimated from weight loss, have been

calculated. The difference between cathodic and anodic currents which is termed  $I_3$  has been calculated.  $I_3$  is very useful for the calculation the current value which results from the cathodic and anodic potential difference.

$I_4$  which represent the difference between anodic current (weight loss) and the average current ( $I_g$ ) measured for 0.3333hr have been calculated. One can notice that  $I_4$  current, can approach to zero in case of high concentrations of PHTU inhibitor. This is due to close approaching of cathodic current from average current, in high concentrations, so that, current value recorded from ammeter was very low.

By using Q-basic program, the tables where below have been obtained (see appendix H) and area under the curve has been calculated by Mathcade program.



**Table 6-10** Effect of inhibitor (PHTU) concentration and area ratio AR(Cu/Fe) on corrosion rate (by weight loss) of iron specimen in air-saturated 0.1N HCl solution, T=40C , t=20m , and 0 rpm.

AR	C(g/L) PHTU	$\Delta W_{Cu}$ (g)	$\Delta W_{Fe}$ (g)	CR (gmd)	CR (mm/y)	CR (mpy)	$i_d$ ( $\mu A/cm^2$ )
0.25	0.000	0	0.00409	183.796	8.523357	335.5652	735.0579
	0.001	0	0.00219	98.41399	4.563852	179.6792	393.5885
	0.050	0	0.00148	66.50808	3.084247	121.427	265.9867
	0.100	0	0.00092	41.34286	1.917235	75.48167	165.3431
	0.150	0	0.00056	25.16522	1.167012	45.94537	100.6436
0.5	0.000	0	0.00449	201.7711	9.356938	368.3834	806.9463
	0.001	0	0.00263	118.1867	5.48079	215.7791	472.6656
	0.050	0	0.00181	81.33759	3.751111	147.6815	323.4974
	0.100	0	0.00094	42.24162	1.958914	77.12258	168.9375
	0.150	0	0.00067	30.10839	1.396247	54.97035	120.4129
1	0.000	0	0.00594	266.9311	12.37867	487.3491	1067.541
	0.001	0	0.00332	149.1938	6.918716	272.3904	596.6729
	0.050	0	0.00129	57.96988	2.688296	105.8384	231.8398
	0.100	0	0.00086	38.64659	1.806785	71.13328	155.8179
	0.150	0	0.00064	28.76025	1.333728	52.509	115.0213
2	0.000	0	0.00635	285.3556	13.23309	520.9877	1141.227
	0.001	0	0.00345	155.0357	7.18963	283.0563	620.0366
	0.050	0	0.00143	64.26118	2.980049	117.3248	257.0007
	0.100	0	0.00094	42.24162	1.958914	77.12258	168.9375
	0.150	0	0.00086	38.64659	1.792197	70.55896	154.5599

**Table 6-11** Evaluation of galvanic corrosion experiments by cell current time integral, and weight loss of iron specimen in air-saturated 0.1N HCl solution ,T=40 °C , t=20m , and 0 rpm

AR (Cu/Fe)	C(g/L)PHTU	∫Current time mA.h	ΔW <sub>Fe</sub> (mg) Cell current	ΔW <sub>Fe</sub> (mg)	GF
0.25	0.000	1.623	1.691	4.09	0.4134
	0.001	1.417	1.476	2.19	0.6739
	0.050	1.138	1.185	1.48	0.8007
	0.100	0.8	0.833	0.92	0.9059
	0.150	0.53	.552	0.56	0.9857
0.5	0.000	2.069	2.155	4.49	0.4799
	0.001	1.861	1.938	2.63	0.7368
	0.050	1.388	1.446	1.81	0.7989
	0.100	0.806	0.839	0.94	0.8888
	0.150	0.64	0.666	0.674	0.9881
1	0.000	2.224	2.316	5.94	0.3899
	0.001	2.039	2.124	3.32	0.6398
	0.050	0.869	0.905	1.29	0.7016
	0.100	0.702	0.731	0.867	0.8431
	0.150	0.6	0.625	0.64	0.9766
2	0.000	2.897	3.018	6.35	0.4753
	0.001	2.153	2.243	3.45	0.6501
	0.050	1.097	1.143	1.43	0.7993
	0.100	0.803	0.836	0.94	0.8894
	0.150	0.802	0.835	0.86	0.9709

**Table 6-12** Current densities of the total, the cell current and self-corrosion of iron specimen in air-saturated 0.1N HCl solution, T=40C, t=20m, and 0 rpm.

AR (Cu/Fe)	C(g/L)PHTU	$\Delta W_{(total)}(mg)$	$\Delta W_{Fe}(mg)$ Cell current	Current density (mA/cm <sup>2</sup> )		
				Total	Cell current	Self-corrosion
0.25	0.000	4.09	1.691	0.735058	0.303908	0.43115
	0.001	2.19	1.476	0.393589	0.265268	0.128321
	0.050	1.48	1.185	0.265987	0.212969	5.30E-02
	0.100	0.92	0.833	0.165343	0.149779	1.56E-02
	0.150	0.56	.552	0.100644	9.92E-02	1.44E-03
0.5	0.000	4.49	2.155	0.806946	0.387298	0.419648
	0.001	2.63	1.938	0.472666	0.348299	0.124367
	0.050	1.81	1.446	0.323497	0.259876	6.36E-02
	0.100	0.94	0.839	0.168938	0.150786	1.82E-02
	0.150	0.674	0.666	0.120413	0.119694	7.19E-04
1	0.000	5.94	2.316	1.067541	0.416233	0.651308
	0.001	3.32	2.124	0.596673	3.82E-02	0.5585
	0.050	1.29	0.905	0.23184	0.162647	6.92E-02
	0.100	0.867	0.731	0.155818	0.131376	2.44E-02
	0.150	0.64	0.625	0.115021	0.112326	2.70E-03
2	0.000	6.35	3.018	1.141227	0.542397	0.59883
	0.001	3.45	2.243	0.620037	0.403114	0.216923
	0.050	1.43	1.143	0.257001	0.205421	5.16E-02
	0.100	0.94	0.836	0.168938	0.150247	1.87E-02
	0.150	0.86	0.835	0.15456	0.150067	4.49E-03

**Table 6-13** Effect of inhibitor (PHTU) concentration and area ratio AR(Cu/Fe) on galvanic current and corrosion rate (by weight loss) of copper and iron specimens in air-saturated 0.1N HCl solution, T=40C , t=20m , and 0 rpm.

AR(Cu/Fe)	C(g/L)PHTU	$\bar{I}_g$ (mA)	$I_1$ (mA)	$I_2$ (mA)	$I_3$ (mA)=( $I_2 - I_1$ )	$I_4$ (mA)=( $I_2 - \bar{I}_g$ )
0.25	0.000	4.868785	0	11.77717	11.77717	6.908387
	0.001	4.250813	0	6.306114	6.306114	2.055301
	0.050	3.413849	0	4.261666	4.261666	0.847817
	0.100	2.399894	0	2.649144	2.649144	0.24925
	0.150	1.59E+00	0	1.612522	1.612522	2.26E-02
0.5	0.000	6.206726	0	12.92897	12.92897	6.722249
	0.001	5.582753	0	7.573096	7.573096	1.990343
	0.050	4.163816	0	5.183107	5.183107	1.019291
	0.100	2.417893	0	2.706734	2.706734	0.288841
	0.150	1.919915	0	1.929268	1.929268	9.35E-03
1	0.000	6.671705	0	17.10425	17.10425	10.43255
	0.001	6.11673	0	9.559954	9.559954	3.443223
	0.050	2.606885	0	3.714561	3.714561	1.107676
	0.100	2.105907	0	2.49653	2.49653	0.390623
	0.150	1.80E+00	0	1.842883	1.842883	4.30E-02
2	0.000	8.690616	0	18.28485	18.28485	9.594235
	0.001	6.458715	0	9.934289	9.934289	3.475574
	0.050	3.290854	0	4.117691	4.117691	0.826836
	0.100	2.408894	0	2.706734	2.706734	0.29784
	0.150	2.405894	0	2.476373	2.476373	7.05E-02

\*See appendix (C)

The total anodic currents of polyelectrode systems are the sum of the corresponding anodic currents of individual electrodes. If the total area of the system S, made of fraction  $f^A, f^B \dots$  etc..for the various components A,B,....., then the anodic current from the  $j^{\text{th}}$  component is given by<sup>[21,24,106]</sup> :

$$I_a^{\text{system}} = S \cdot \sum f^j i_a^j \quad \dots(6.7)$$

Similarly for the cathodic currents of polyelectrode:

$$I_c^{\text{system}} = S \cdot \sum f^j i_c^j \quad \dots(6.8)$$

At the corrosion potential ( $E_{\text{coupling}}$ ) adopted by the polyelectrode, the total anodic and cathodic currents are equal so that:

$$I_{\text{corr.}}^{\text{system}} = I_a^{\text{system}} = |I_c^{\text{system}}| \quad \dots(6.9)$$

The dissolution current density ( $i_d$ ) is obtained which gives  $I_d$  after multiplying it by the area of the total electrode, while  $I_g$  is obtained from each metal curve given in the galvanic corrosion results in chapter five by using GRAPHER PACKAGE to obtain the area under the curve for each metal from MATHCAD PACKAGE and dividing it by the total time to get  $I_{g(\text{av})}$ ;

$$I_{g(\text{av})}^B = I_d^B - I_c^B \quad \dots(6.10)$$

$$I_{g(\text{av})}^N = I_d^B - I_c^B \quad \dots(6.11)$$

Then according to Eqs. (6.10 and 6.11)  $I_c^N$  and  $I_d^B$  were obtained and shown in tables 6-14 to 6-16 as current densities  $I_{g(\text{av})}$ ,  $i_d$  and  $i_c$ , these tables are part from appendix (G).

**Table 6-14** Effect of inhibitor (PHTU) concentration and area ratio AR (Cu/Fe) on  $i_d$ ,  $i_g$ , and  $i_c$  of noble metal (copper) and base metal (carbon steel) specimens in air-saturated 0.1N HCl solution,  $T=40C$  ,  $t=20m$  , and 0 RPM.

AR	C(g/L) PHTU	Noble metal=Copper			Base metal=Carbon Steel			
		$i_d$ ( $\mu A/cm^2$ )	$i_g$ ( $\mu A/cm^2$ )	$i_{c,n}$ ( $\mu A/cm^2$ )	$i_d$ ( $\mu A/cm^2$ )	$i_g$ ( $\mu A/cm^2$ )	$i_{c,b}$ ( $\mu A/cm^2$ )	GF
0.25	0.000	0	1215.525	1215.525	735.0579	303.879	431.175	0.4134
	0.001	0	1061.244	1061.244	393.5885	265.309	128.279	0.6739
	0.050	0	852.290	852.290	265.9867	213.071	52.916	0.8007
	0.100	0	598.926	598.926	165.3431	149.731	15.612	0.9059
	0.150	0	396.954	396.954	100.6436	99.237	1.407	0.9857
0.5	0.000	0	774.765	774.765	806.9463	387.385	419.561	0.4799
	0.001	0	696.871	696.871	472.6656	348.456	124.209	0.7368
	0.050	0	519.755	519.755	323.4974	259.878	63.619	0.7989
	0.100	0	301.817	301.817	168.9375	150.909	18.028	0.8888
	0.150	0	239.657	239.657	120.4129	119.828	0.585	0.9881
1	0.000	0	416.406	416.406	1067.541	416.406	651.135	0.3899
	0.001	0	381.766	381.766	596.6729	381.766	214.907	0.6398
	0.050	0	162.705	162.705	231.8398	162.705	69.134	0.7016
	0.100	0	131.437	131.437	155.8179	131.437	24.381	0.8431
	0.150	0	112.345	112.345	115.0213	112.345	2.676	0.9766
2	0.000	0	271.207	271.207	1141.227	542.438	598.789	0.4753
	0.001	0	201556	201556	620.0366	403.112	216.925	0.6501
	0.050	0	102.697	102.697	257.0007	205.398	51.603	0.7993
	0.100	0	75.174	75.174	168.9375	150.348	18.590	0.8894
	0.150	0	75.08	75.08	154.5599	150.161	4.398	0.9709

**Table 6-15** Effect of inhibitor (PHTU) concentration and area ratio AR (Cu/Zn) on  $i_d$ ,  $i_g$ , and  $i_c$  of noble metal (copper) and base metal (zinc) specimens in air-saturated 0.1N HCl solution, T=40C , t=20m , and 0 RPM.

AR	C(g/L) PHTU	Noble metal=Copper			Base metal=Zinc			
		$i_d$ ( $\mu\text{A}/\text{cm}^2$ )	$i_g$ ( $\mu\text{A}/\text{cm}^2$ )	$i_{c,n}$ ( $\mu\text{A}/\text{cm}^2$ )	$i_d$ ( $\mu\text{A}/\text{cm}^2$ )	$i_g$ ( $\mu\text{A}/\text{cm}^2$ )	$i_{c,b}$ ( $\mu\text{A}/\text{cm}^2$ )	GF
0.25	0.000	0	2532.143	2532.143	1501.615	633.032	868.583	0.4215
	0.001	0	2202.971	2202.971	872.1033	550.739	321.364	0.6315
	0.050	0	525.128	525.128	170.4286	131.281	39.148	0.7703
	0.100	0	389.714	389.714	115.1545	97.434	17.721	0.8467
	0.150	0	257.321	257.321	66.0219	64.349	1.673	0.9744
0.5	0.000	0	1353.946	1353.946	1817.906	676.977	1140.929	0.3724
	0.001	0	1134.026	1134.026	852.1432	567.017	285.126	0.6654
	0.050	0	422.638	422.638	291.7247	211.321	80.404	0.7242
	0.100	0	206.713	206.713	119.7607	103.413	16.348	0.8641
	0.150	0	160.777	160.777	81.83646	80.414	1.422	0.9887
1	0.000	0	727.096	727.096	1854.755	727.096	1127.659	0.3921
	0.001	0	525.499	525.499	832.1831	525.462	306.721	0.6315
	0.050	0	180.813	180.813	228.7736	180.813	47.961	0.7906
	0.100	0	107.339	107.339	121.2961	107.339	13.957	0.8848
	0.150	0	105.978	105.978	107.4775	106.035	1.443	0.9871
2	0.000	0	430.031	430.031	2140.338	860.062	1280.28	0.4018
	0.001	0	265.274	265.274	789.1921	530.548	258.644	0.6722
	0.050	0	93.215	93.215	241.0567	186.429	546.28	0.7732
	0.100	0	59.655	59.655	135.1146	119.510	15.805	0.8829
	0.150	0	51.334	51.334	104.4067	102.669	1.738	0.9838

**Table 6-16** Effect of inhibitor (PHTU) concentration and area ratio AR (Fe/Zn) on  $i_d$ ,  $i_g$ , and  $i_c$  of noble metal (carbon steel) and base metal (zinc) specimens in air-saturated 0.1N HCl solution, T=40C , t=20m , and 0 RPM.

AR	C(g/L) PHTU	Noble metal= Carbon Steel			Base metal=Zinc			
		$i_d$ ( $\mu\text{A}/\text{cm}^2$ )	$i_g$ ( $\mu\text{A}/\text{cm}^2$ )	$i_{c,n}$ ( $\mu\text{A}/\text{cm}^2$ )	$i_d$ ( $\mu\text{A}/\text{cm}^2$ )	$i_g$ ( $\mu\text{A}/\text{cm}^2$ )	$i_{c,b}$ ( $\mu\text{A}/\text{cm}^2$ )	GF
0.25	0.000	62,9.2 2	2895.519	2832.62	1753.419	723.376	1030.04	0,4128
	0.001	.	2471.527	2471.527	912.0236	617.834	294.19	0,6774
	0.050	.	1609.038	1609.038	512.8214	402.257	110.564	0,7841
	0.100	.	1128.798	1128.798	314.7556	282.173	32.58	0,8966
	0.150	.	813.132	813.132	208.8135	203.282	5.532	0,9730
0.5	0.000	188,7. 6	1590.6681	1401.968	2103.489	795.339	1308.15	0,3781
	0.001	80,874 3	1441.475	1360.61	1102.412	720.255	382.157	0,6038
	0.050	.	952.179	952.179	631.0466	476.092	154.955	0,7040
	0.100	.	720.375	720.375	408.4146	360.128	48.287	0,8819
	0.150	.	604.037	604.037	305.5432	302.020	35.23	0,9884
1	0.000	260,09 0	934.494	673.894	2273.917	934.522	1339.39	0,4110
	0.001	179,72 .	737.756	558.056	12482.75	737.756	1174.45	0,0910
	0.050	104,23 8	572.459	468.260	8275.77	572.441	770.333	0,6916
	0.100	44,93. 1	384.307	339.380	456.0118	384.307	71.705	0,8427
	0.150	.	325.025	325.025	336.2511	325.019	11.232	0,9666
2	0.000	337,87 0	594.507	256.607	2811.305	1189.05	1622.26	0,4229
	0.001	219,20 9	442.295	222.995	1401.814	884.591	517.223	0,6310
	0.050	122,21 .	331.102	208.902	847.537	662.204	185.333	0,7813
	0.100	66,496 6	253.868	187.368	580.3786	507.736	72.643	0,8748
	0.150	.	211.146	211.146	426.8393	422.292	4.547	0,9892



From above tables [tables (6-14 to 6-16)] it can be seen that  $i_d^N$  of Cu/Fe and Cu/Zn couple is equal to zero because complete protection (see **Fig.6-6**) but of Fe/Zn couple do not equal to zero because partial protection i.e.  $E_{\text{coup.}} > E_{\text{eq,Fe}}$ .

After substituting most of the data given in the tables of appendix (G) in Eqn.(3.8), given in chapter three, it was found that both sides of this equation were identical, which shows the accuracy of the results obtained from the experimental work.

$$\frac{i_d^B}{i_d^N} = \frac{A_c}{A_a} \left[ \frac{|i_c^N|}{i_d^N} - 1 \right] + \frac{|i_c^B|}{i_d^N} \quad \dots(3.8)$$

The galvanic factor (GF) is the ratio=(weight loss from cell / weight loss by weighing), i.e., the ratio between the corrosion rate obtained from galvanic current ( $i_{\text{gav}}$ ) and that obtained from the weight loss of coupled metals ( $i_d$ ), which was also studied by Tsujino et al.<sup>[85]</sup> with time in an other environment. In these tables [tables (6-14 to 6-16)] it is found that GF alters with the changes for the same AR in each of the couples given, as well as it changes for the same couple when the temperature is kept constant, variable concentration of PHTU inhibitor (0, 0.001, 0.05, 0.1 and 0.15g/L), variable rotational velocities (0, 500, 1000 and 1500 RPM) and variable AR (0.25, 0.5, 1.0 and 2.0). The alternation of GF could be in an increased or decreased manner because in addition to the mentioned variables (AR, PHTU concentration, and rotational velocities) interaction of these three variables is playing also a role in changing (GF). This effect is clear from the relationships obtained in above tables [tables (6-14 to 6-16)] for the effects of these variables on  $I_{\text{g(av)}}$  and  $I_d$

## 6.5 Measuring the potential and current together for copper and carbon steel couple:

**Figs. 5-49 to 5-64** in chapter five represent results of galvanic potential, which was measured with galvanic current simultaneously as explained in chapter four. With closed circuit a mixed potential results which is near the potential of the iron electrode. The iron electrode is accordingly less polarizable and the copper electrode more strongly. It can be noticed that by increasing PHTU inhibitor concentration, potential became less negative for both copper and carbon steel metals.

There was fast declining in potential curve, until stationary phase is after about 15 minutes. In the first readings, potential values for each metal were very close to the potential value, if there were a single metal, (see appendix F). After while, both curves were very close together, for the couple metals. Galvanic potential values for both copper and carbon steel were between their values in case of single metals. See appendix F.

In **Figs. 5-65 to 5-80** one can notice that the galvanic current in the first few readings, has a fast declining, then it tends to settle down to a steady state phase after about 15 minute. This can be interpreted by the effect of  $\text{OH}^-$  ions formation upon the metal surface. Voltage values for both metals were due to the using of metals (copper and carbon steel).

In case of rotational velocity, one can notice that potentials became more negative, this is the result of increasing transport rate of dissolved oxygen associated with hydrogen evolution, and consequently, metal corrosion rate will be increased. Galvanic current will be increased too.

Free corrosion results were shown in **Figs. 5-81 to 5-92** in steady state (curvature after 15 minutes), potential values were very close to that these of polarization curves at the same conditions, and so this can support, the present results.

## 6.6 Effect of rotational velocity and PHTU concentration on polarization curves behavior

It has been seen in chapter five which shows the results of the polarization curves as given in **Figs.5-93 to 5-104**, (see appendix F) that corrosion potential is less negative with increasing PHTU concentration and more negative with increasing rotational velocities. The corrosion potential is more negative due to the combined influence of hydrogen evolution with increasing transport of bulk oxygen<sup>[49,71,107,108,109]</sup>, as shown in tables 6.17-6.19. The corrosion potential is also monitored experimentally as shown in **Figs.5-81 to 5-92**, and presented in Appendix E. These figures show that  $E_{\text{corr}}$  becomes rapidly more negative reaching steady-state values after about 90 minutes as given also in tables 6-17 to 6-19.

**Table 6-17** Behavior of copper corrosion potential at different rotational velocities and PHTU concentration.

		<i>PHTU Concentrations (g/L)</i>				
		<b>0</b>	<b>0.001</b>	<b>0.05</b>	<b>0.1</b>	<b>0.15</b>
<i>Rotational velocities (RPM)</i>	<b>0</b>	-170!!	-150	-132	-122	-111
		<i>-166€</i>	<i>-163</i>	<i>-156</i>	<i>-140</i>	<i>-120</i>
	<b>500</b>	-189	-176	-162	-150	-120
		<i>-180</i>	<i>-170</i>	<i>-168</i>	<i>-155</i>	<i>-135</i>
	<b>1000</b>	-212	-195	-170	-157	-140
		<i>-193</i>	<i>-187</i>	<i>-178</i>	<i>-172</i>	<i>-149</i>
	<b>1500</b>	-220	-203	-180	-169	-152
		<i>-206</i>	<i>-196</i>	<i>-187</i>	<i>-177</i>	<i>-155</i>

!!  $E_{\text{corr}}$  (V) from polarization curve.

€  $E_{\text{corr}}$  (V) from  $E_{\text{corr}}$  vs. time curve at steady state.

**Table 6-18** Behavior of carbon steel corrosion potential at different rotational velocities and PHTU concentration.

		<i>PHTU Concentrations (g/L)</i>				
		<b>0</b>	<b>0.001</b>	<b>0.05</b>	<b>0.1</b>	<b>0.15</b>
<i>Rotational velocities (RPM)</i>	<b>0</b>	-518!!	-495	-484	-473	-465
		<i>-481€</i>	<i>-475</i>	<i>-466</i>	<i>-450</i>	<i>-431</i>
	<b>500</b>	-528	-510	-497	-488	-473
		<i>-530</i>	<i>-520</i>	<i>-503</i>	<i>-492</i>	<i>-485</i>
	<b>1000</b>	-582	-560	-541	-521	-510
		<i>-575</i>	<i>-558</i>	<i>-547</i>	<i>-519</i>	<i>-510</i>
	<b>1500</b>	-633	-600	-577	-570	-557
		<i>-622</i>	<i>-597</i>	<i>-586</i>	<i>-576</i>	<i>-567</i>

!!  $E_{\text{corr}}$  (V) from polarization curve.

€  $E_{\text{corr}}$  (V) from  $E_{\text{corr}}$  vs. time curve at steady state.

**Table 6.19** Behavior of zinc corrosion potential at different rotational velocities and PHTU concentration.

		<i>PHTU Concentrations (g/L)</i>				
		<b>0</b>	<b>0.001</b>	<b>0.05</b>	<b>0.1</b>	<b>0.15</b>
<i>Rotational velocities (RPM)</i>	<b>0</b>	-931!!	-920	-905	-891	-880
		<i>-791€</i>	<i>-785</i>	<i>-777</i>	<i>-758</i>	<i>-720</i>
	<b>500</b>	-952	-940	-925	-906	-892
		<i>-820</i>	<i>-793</i>	<i>-785</i>	<i>-763</i>	<i>-472</i>
	<b>1000</b>	-968	-956	-945	-935	-920
		<i>-842</i>	<i>-815</i>	<i>-798</i>	<i>-519</i>	<i>-510</i>
	<b>1500</b>	-990	-978	-961	-943	-925
		<i>-850</i>	<i>-823</i>	<i>-815</i>	<i>-780</i>	<i>-766</i>

!!  $E_{\text{corr}}$  (V) from polarization curve.

€  $E_{\text{corr}}$  (V) from  $E_{\text{corr}}$  vs. time curve at steady state.

### 6.7 Effect of rotational velocities and PHTU concentration on potential and current density at regions close to the corrosion potential value:

Current densities ( $\mu\text{A}/\text{cm}^2$ ) and inhibitor efficiency for cathode and anode regions against potential from polarization curves which is near the corrosion potential of copper, carbon steel and zinc metals at variable rotational velocities and PHTU inhibitor concentrations have been calculated as shown in table 6-20.

**Table 6-20** Current densities ( $\mu\text{A}/\text{cm}^2$ ) and inhibitor efficiency for cathode and anode of copper, carbon steel and zinc metals at variable rotational velocities and PHTU concentrations.

<i>Copper metal specimen</i>							
Rotational Velocity (RPM)	Potential (mV)	PHTU concentrations (g/L)					$\eta$
		0	0.001	0.05	0.1	0.15	
0	$E_c=-550$	140	119	63	40	20	0.857
	$E_a=10$	1300	1200	1050	700	600	0.538
500	$E_c=-550$	150	115	77	50	25	0.833
	$E_a=10$	1700	1600	1500	1400	1100	0.353
1000	$E_c=-550$	180	125	100	65	50	0.722
	$E_a=10$	3000	2700	2500	2400	1200	0.600
1500	$E_c=-550$	250	140	110	70	55	0.780
	$E_a=10$	3700	3300	2900	2000	1500	0.595
<i>Carbon steel metal specimen</i>							
Rotational Velocity (RPM)	Potential (mV)	PHTU concentrations (g/L)					$\eta$
		0	0.001	0.05	0.1	0.15	
0	$E_c=-800$	4250	3200	1850	1700	1000	0.765
	$E_a=-400$	4200	3500	3100	3000	1100	0.738
500	$E_c=-800$	4700	3580	3200	2700	2000	0.574
	$E_a=-400$	6000	5000	4500	4300	3000	0.500
1000	$E_c=-800$	6000	5000	4500	4000	3000	0.500
	$E_a=-400$	7000	6000	5000	4300	3500	0.500
1500	$E_c=-800$	6400	5200	4700	4100	3000	0.531
	$E_a=-400$	8000	6200	5500	4500	3700	0.538
<i>Zinc metal specimen</i>							
Rotational Velocity (RPM)	Potential (mV)	PHTU concentrations (g/L)					$\eta$
		0	0.001	0.05	0.1	0.15	
0	$E_c=-1000$	10000	9500	9000	5500	3600	0.540
	$E_a=-800$	18000	16000	15500	14000	13000	0.278
500	$E_c=-1000$	12500	11500	9000	7500	6000	0.520
	$E_a=-800$	20000	19000	16000	14500	14000	0.300
1000	$E_c=-1000$	13000	12000	10000	8000	6500	0.500
	$E_a=-800$	22000	21000	19000	16000	14500	0.341
1500	$E_c=-1000$	15000	12500	11000	8500	7000	0.533
	$E_a=-800$	23000	21000	19500	17000	15000	0.348

## 6.8 Galvanic cell resistance measurement:

It is clear that there is a linear relationship between the current and resistance **Figs.6-8 to 6-9**. From these figures one can notice that current increases with a decreasing resistance, which is due to Ohms law with potential constant. Corrosion rate decreased with increasing PHTU concentration so that current decreased, but current increased with increasing rotational velocities due to increasing corrosion rate. (see appendix J).

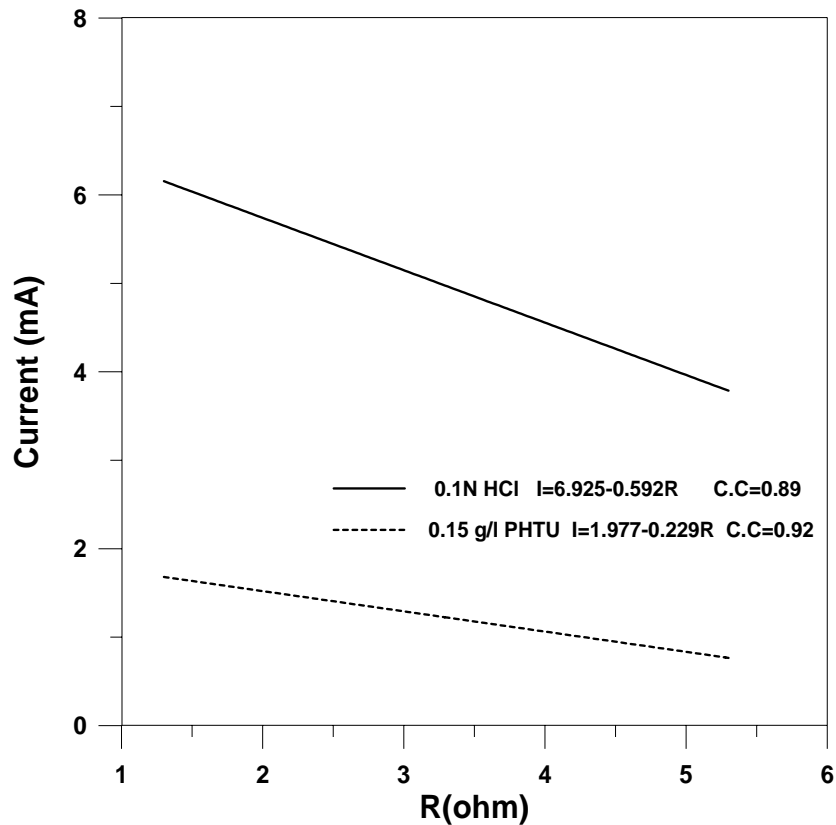


**Figure 6-8** Current vs. resistance of copper and carbon steel specimen in air-saturated 0.1N HCl solution, AR=1, T=40C and 0 RPM

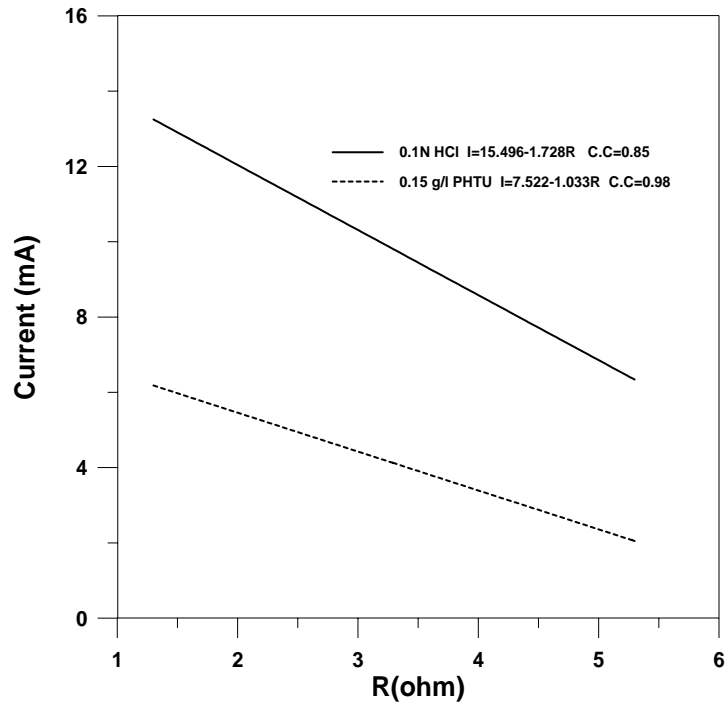


**Figure 6-9** Current vs. resistance of copper and carbon steel specimen in air-saturated 0.1N HCl solution, AR=1, T=40C and 1500RPM

The intercepts from **Figs (6-8 and 6-9)** are representing average galvanic currents when resistance of galvanic cell is equal to zero. The principle of zero ammeter resistance can be applied to this system from knowing these current values at variable conditions. The principle of zero ammeter resistance when ( $IR=0$ ), **Fig. 6-10**, has been obtained.

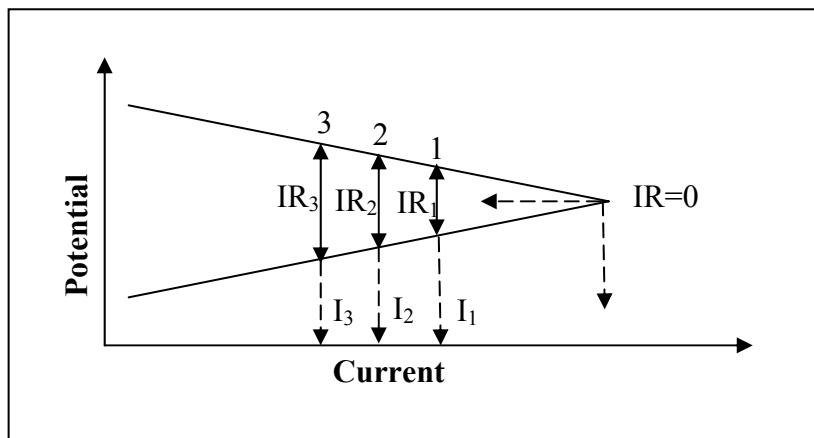


**Figure 6-10** The principle of zero ammeter resistance



## 6.9 Statistical Relationships:

The statistical relationships for potential difference and galvanic current in tables 6-7 to 6-9 are as a function of C, U and AR as follows:

$$E = a + b(C) + d(U) + e(AR).$$

$$I_g = a + b(C) + d(U) + e(AR) + \text{Correction factor}.$$

### For Fe-Zn

$$E = -862.914 + 383.606(C) - 38.737(U) - 0.058(AR).$$

with correlation coefficient C.C=0.979 and mean error=1% .

$$I_g = 10.726 - 71.41(C) + 0.006(U) + 2.032(AR) - 9.208 \left[ \frac{U}{U + C + AR} \right]^{5740.76}$$

with correlation coefficient C.C=0.954 and mean error=3.72% .

### For Cu-Fe

$$E = -418.464 + 276.631(C) - 28.12(U) - 0.087(AR).$$

with correlation coefficient C.C=0.939 and mean error=2.51% .

$$I_g = 4.373 - 32.092(C) + 0.005(U) + 0.553(AR) - 7.517 \left[ \frac{U}{U + C + AR} \right]^{2026.289}$$

with correlation coefficient C.C=0.935 and mean error=5.255% .

### For Cu-Zn

$$E = -831.346 + 376.643(C) - 30.549(U) - 0.055(AR).$$

with correlation coefficient C.C=0.930 and mean error=1.55% .

$$I_g = 9.049 - 65.121(C) + 0.006(U) + 0.633(AR) - 3.457 \left[ \frac{U}{U + C + AR} \right]^{3159.814}$$

with correlation coefficient C.C=0.900 and mean error=9.845% .

Where:

**E** = potential difference (mV) at steady state.

**I<sub>g</sub>** = galvanic current (mA) at steady state.

**C**= PHTU inhibitor concentration (g/L)

**U**=rotational velocity (RPM)

**AR**=area ratio.

These equations have been created depending on Hooke - Jeeves and quasi - Newton method, which is included in statistical program package.

## Chapter Seven

### Conclusions and Recommendations for Future Work

The present work has been mainly aimed to study inhibition of galvanic corrosion of copper, carbon steel and zinc metal couples in air-saturated 0.1N HCl solution at a variable area ratio, rotational velocity at 40°C.

#### 7.1 Conclusions:

- 1- Copper as good cathodes and carbon steel and zinc worked as efficient sacrificial anodes in the environment of air-saturated 0.1NHCl and a variable rotational velocities (0, 500, 1000 and 1500 RPM) at 40 °C.
- 2- PHTU is a good inhibitor with efficiency may reach 99%.
- 3- Galvanic current, total cathodic current density and corrosion rate decrease with increasing PHTU inhibitor concentration in 0.1NHCl solution and increase with increasing rotational velocities.
- 4- Galvanic current, corrosion rate and dissolution current increase with increasing area ratio of metals.
- 5- Potential difference is less negative with increasing PHTU inhibitor concentration in 0.1NHCl solution and it is more negative with increasing rotational velocity.
- 6- Altering the rotational velocity (0, 500, 1000 and 1500 RPM) played an important role in increasing the aggressiveness of the galvanic attack.
- 7- From the weight loss and polarization experiments for single metal, the arrangement of metals to combat corrosion in the

environment of 0.1NHCl solution could be illustrated as follows:

Cu > C.S. > Zn.

- 8- Copper and carbon steel worked as an efficient cathode to zinc in most of the coupling experiments between these two metals.
- 9- In all cases copper was totally protected by zinc and carbon steel.
- 10- Altering AR and rotational velocities played an important role in changing the galvanic factor (GF) and also ( $I_g$  and  $I_d$ ) during the experiments.
- 11- The occurrence of the galvanic corrosion was efficiently verified during the experiments using the following equations:

$$\frac{i_d^B}{i_d^N} = \frac{A_c}{A_a} \left[ \frac{|i_c^N|}{i_d^N} - 1 \right] + \frac{|i_c^B|}{i_d^N}$$

and for each case at  $E_{\text{coupling}}$ ,  $\sum I^c = \sum I^a$  and  $\sum I_g = 0$

12- Statistical Relationships between potential differences and galvanic current as a function of C, U and AR for the various couples are:

### **Fe-Zn**

$$E = -862.914 + 383.606(C) - 38.737(U) - 0.058(AR).$$

$$I_g = 10.726 - 71.41(C) + 0.006(U) + 2.032(AR) - 9.208 \left[ \frac{U}{U + C + AR} \right]^{5740.76}$$

## **Cu-Fe**

$$E = -418.464 + 276.631(C) - 28.12(U) - 0.087(AR).$$

$$I_g = 4.373 - 32.092(C) + 0.005(U) + 0.553(AR) - 7.517 \left[ \frac{U}{U + C + AR} \right]^{2026.289}$$

## **Cu-Zn**

$$E = -831.346 + 376.643(C) - 30.549(U) - 0.055(AR).$$

$$I_g = 9.049 - 65.121(C) + 0.006(U) + 0.633(AR) - 3.457 \left[ \frac{U}{U + C + AR} \right]^{3159.814}$$

## **7.2 Recommendations for Future Work:**

The following suggestions are to be considered or to be examined in greater detail for future work:

1. Investigating galvanic current and potential difference with longer time and greater rotational velocities under different isothermal conditions.
2. Studying the influence of isothermal pipe fluid flow (geometry) on galvanic current and potential system.
3. Investigating the benefit of other types of inhibitors to reduce galvanic corrosion.

## References

1. **“Cost of Corrosion”**, NACE International, July, 2002, <http://www.battlle.org>
2. David Talbot and James Talbot, **“corrosion science and technology”**, CRC press LL.C, 2000, [www.crcpress.com](http://www.crcpress.com).
3. Davis J.R., **“Corrosion understanding the basics”**, ASM international, the materials information society, 1999, [www.ameritech.co.uk](http://www.ameritech.co.uk)
4. Kenneth Trethewey R., **“Corrosion for science and engineering”**, Longman group limited 1995.
5. Shreir L.L, **“Corrosion: Metal / Environment Reactions”**, Newes-Butten Worths, 3<sup>rd</sup> ed., Vol.1, (2000).
6. Uhlig H.H., **“Corrosion Handbook”**, Johen Wiley and Sons, Inc, 1976.
7. Faulkner L.L, S.B.Menkes, **“Corrosion and Corrosion Protection Handbook”**, Marcel Dekker, 1983.
8. **“A short introduction to corrosion and its control”**, Article given on the internet at the web site <http://www.npl.co.uk/>
9. Tomashove N.D., **“Theory of Corrosion and Corrosion and Protection of metals”**, the Macmillan company, 1966.
10. Bahar AL-Kelaby S.S., M.sc. Thesis, **“Cathodic Protection of Simple Structure”**, Chem. Eng. Dept. , Al-Nahrain University ,2002.
11. Howard Rogers T., **“Marine Corrosion”**, William Clowes and Sons, 1968.
12. Jeseeph F. Bosich, **“Corrosion Prevention for Practicing Engineers”**, Barnes and Noble.Inc.1970.
13. Perez N., **“Electrocheistry and Corrosion Science“** ,Kluwer academic publishers 2004, [www://kluweronline.com](http://www.kluweronline.com).
14. Stern M., **“Corrosion”**, Vol.11, No.13,1957.
15. Reeta Agrawal and T.K.G.Namboodhiri, **“The inhibition of sulphuric acid corrosion of 410 stainless steel by thioureas corrosion science”**, Vol.30, No.1, p37-52, 1990.
16. David Talbot and James Talbot, **“Corrosion Science and Technology”**, 1998.
17. **“Science and Reactor Fundamentals. Materials 1 CNSC Technical Training Group. Revision 1”**, January 2003 (Internet).

- 18.Hamm E.R., **“Corrosion control, Naval Facilities Engineering command”**, September, 1992.
- 19.Berry N.E., **“Corrosion”**, Journal Vol.3, No.2, p261-265, 1946.
- 20.schweitzer P.A., **“corrosion and corrosion Protection Handbook”**, Marcel Decker, 1989.
- 21.Fontana and Greene, **“Corrosion Engineering”**, Mc Graw Hill,1984.
- 22.Aung N.N., and Zhou W. ,**”Journal of Applied Electrochemistry”**,32 ,12 , P. 1397-1401 , Dec. (2002).
- 23.Mor E. D. and Beccaria A. M., Corrosion, Vol. 31, No.8, PP.275, Aug, 1975.
- 24.Uhlig.H.H., Winston Revie. R,**”Corrosion and Corrosion Control”**, John Wiley and Sons, 1985.
- 25.Steiger Wald R.F., **“Corrosion”**, NACE, P.1, January, 1968.
- 26.Poulson B., **“Corrosion Science”**, Vol, 23, No.1, P.391, 1983.
- 27.Pohlman S.L., **“Corrosion Journal”**, Vol.5, No.34, P. 157-159. , 1978
- 28.Peabody A. W., **“Control of Pipeline Corrosion”**, NACE, Houston, Texas, 1974.
29. Trethewey K.R., and Chamberlain J., **“Corrosion for Science and Engineering”**, 2<sup>ed</sup> edition ,1996.
- 30.Poulson B. and Robinson R., Corr.Sci. Vol, 26 No.4, P.265, 1986.
- 31.Shreir, L.L, **"Corrosion: Metal / Environment Reactions"**, Newes-Butten Worths, 3<sup>rd</sup> ed., Vol.2, (2000).
- 32.Pots B. F. M., and John Postlethwaite and Nicolas Thevenot, **“Superposition of Diffusion and Chemical Reaction Controlled Limiting Current-Application to Corrosion, Journal of Corrosion Since and Engineering Study for a PhD in corrosion at the corrosion and protection center”**, Vol 1, 1995.
- 33.Scully J.R., Corrosion science, 35, Nos. 1-4 (1993), P. 185-195.
- 34.Wie L.Y, and Westengen H., Magesium Technology, P. 153-160 , Mar.(2000).
- 35.Mickalonis J.I. and Leidheiser J.R., Corrosion Journal, 8, 45, P. 631-636,1989.
- 36.Ulick Evans R., **“The Corrosion and Oxidation of Metals, Scientific Principles and Practical Applications”**, Arnold, London,1<sup>st</sup> ed.,1971.
- 37.Fairman L., and West J.M. Corrosion science, 1963
- 38.Berger F.P.,K.F.F.L.Hau, Int.j. **”heat and mass transfer”**,v.20, p.1185, 1977.
- 39.L. Cifuentes. Anti-corrosion, November, 1987.
- 40.Lee C.D., **“Metals and Materials”**, Vol.6, No.4, P. 351-358, Aug.2002,

41. Shreir L. L., **“Corrosion”**, Volume 1, Newnes-Butterworths, 1976.
42. Yau Y.H., and Streicher M.A., *Corrosion Journal*, 6, 43, P. 60-62, (1987).
43. Scully J.C., **“The Fundamentals of corrosion”**, BPC wheatons Ltd, Exceter, third edition 1990.
44. Astley D.J. and Rowland J.C., *British Journal*, Vol.7, No.20, p971-983, 1985.
45. West J.M., **“Electrodeposition and Corrosion Processes”**, William Clowes and Sons, 1976.
46. Foroulis, Z. A., and Bennete, J.J., *Chem. Soc.*, London, P121, 1922.
47. Yang I.J., *Corrosion Journal*, Vol.7, No.49, p.576-582, 1993.
48. Perry, R. H., and Green, Perry D. W., **“Chemical Engineers Handbook”**, 7<sup>th</sup> ed, McGraw Hill, United states, 1997
49. Foroulis Z.A., **“The Influence of Velocity and Dissolved Oxygen on the Initial Corrosion Behavior of Iron in High Purity Water”**, *Corrosion*, Vol.35, P.340, August, 1979.
50. Pollock W.J., and Hinton B.R., *ASTM STP*, 979, P. 35-50, (1988).
51. Stern M., *“Corrosion-NACE”*, Vol. 13, P.97, 1957
52. **“Corrosion test”**. Article given on the internet at the web site <http://www.gc3.com>
53. Poulson B., **“Corrosion Science”**, Vol, 23, No.1, P.391, 1983
54. Stern M., **“Corrosion-NACE”**, Vol.13, P.97, 1957
55. Selman J.R., **“AICHE”**, Vol.77, No.204, P.88, 1981
56. Steigerwald R. F. **“Corrosion-NACE”**, Vol. , P. 1, 1968
57. Pickett D.J., **“Electrochemical Reactor Design”**, 2<sup>nd</sup> Edition, Elsevier Scientific Publishing Company, Amsterdam, 1979.
58. Sakamoto Y., and Mae T., **“Journal of the Japan Institute of Metals”**, 62, 5, P 436-443, May (1998) .
59. Ellison B.T and Schmeal W. R., **“J. Elerctchem. Soc.”**, Vol. 125, No. 4, P. 524, 1978.
60. Callister D., Williams Jr. **“Materials Science and Engineering”**, An Introduction. 1996. Fourth Edition. Toronto: John Wiley and Sons, Inc.
61. **“Corrosion Theory and Corrosion Protection”**. Article given on the internet at the web site <http://www.usace.army.mil/>. (1995)
62. Cifuentes L. **“Anti-corrosion”**, November, 1987.
63. Hack H.P., **“ATM STP 979”**, (1988), p339-351.
64. Kim. J.G, **“Corrosion”**, 58, 2, PP.(175-181), feb.2002.
65. Eisenberg M., Tobias C. W., and Wike C.R., J., **“Electchem. Soc.”**, Vol. 101, P.306, 1954.
66. West J., **“Electrode position and Corrosion processed”**, V.N.R.Co., 1971.



67. Smith S. W., McCabe K. M., and Black D.W., **“Corrosion-NACE”**, Vol. 45, No. 1, P. 790, 1989.
68. Henry S.D and Scott W.M., **“Corrosion in the Petrochemical Industry”**, 1st Edition , ASM International , USA , (1999).
69. Given on the internet at, **“Corrosion theory and corrosion protection”**, chapter 2, 30 Apr. [www.howtobrew.com](http://www.howtobrew.com). 1995.
70. Bardal E., Johnsen R., **“prediction of galvanic corrosion rates and distribution by means of calculation of corrosion engineers”**, p628-632. 1984.
71. Schweitzer P.A., **“Corrosion and Corrosion protection Handbook”**, Marcel Decker , 2nd ed.,(1989).
72. Copson H.R., **“Industrial and engineering chemistry journal”**, Vol.8, No.38, P721-723, 1945.
73. Kim J.G., **“Corrosion “**,58,2,PP.(175-181), feb.2002
74. Pierre R.Robege, **“Handbook of Corrosion Engineering”**, Mc Graw-Hill,2000
75. Steigerwold R.F., **“Electrochemistry of Corrosion”**, Vol.24,p1-10, 1968.
76. Guang Qiu L. and JianXie A., **”The adsorption and corrosion inhibition of some Cationic Gemini surfactants on carbon steel surface in Hydrochloric Acid”**, Corrosion Science, July 2005, [www.elsevier.com/locate/corsci](http://www.elsevier.com/locate/corsci)
77. Hack H. P.”**Galvanic Corrosion “**,ann Arbor,(1988).
78. Marangozis J., **“corrosion”**, Vol.24, No. 8, P. 255, 1968.
79. Y.H. Yau and M.A.Streicher, **“Galvanic corrosion of duplex FeCu-10%Ni alloys in reducing acids”**, Corrosion (NACE), 1987.
80. French, E. C., Martin, R. L., and Dougherty, J. A., **“Corrosion and Its Inhibition in Oil and Gas Wells, in Raman, A., and Labine, P. (eds.), Reviews on Corrosion Inhibitor Science and Technology”**, Houston, Tex., NACE International, 1993.
81. Banerjee S.N.” **an introduction to science of corrosion and it is inhibitor”**, Oxonian press pvt. LTD., 1985.
82. **“Galvanic corrosion by Stephen C. Dexter, Professor of Applied Science and Marine Biology”**, Article given on the internet at the web sit [www.ocean.udel.edu/seagrant](http://www.ocean.udel.edu/seagrant).(1995).
83. Gilbert, P. T., and Hadden S. E., Vol.77, No. 237, 1960
84. Al-Anbaky H.A., M.Sc thesis, Chemical Engineering Department,

- College of Engineering, Al-Nahrain University, 2006
85. Tsujino B. and T. Oki, **“Measurement of steel and aluminum corrosion rates using the galvanic couple method”**, NACE, Corrosion, December, 1988.
  86. Spataru N. and Gabriel F., **“Catalytic hydrogen evolution in the cathodic stripping voltammetry on a mercury electrode in the presence of cobalt(ii) ion and phenylthiourea or thiourea”**, The royal society of chemistry, 2001, p1907-1911.
  87. Silverman D.C., **“Corrosion NACE”**, Vol. 40, No. 5, P. 220, 1984.
  88. Schmitt G., **“Application of Inhibitors for Acid Media”**, Corrosion, Vol.19, No.4, 1984.
  89. Mickalonis J.I. and Leidheiser H., **“Corrosion Inhibition of steel by lead pigments: the steel-Leed galvanic couple in acetate solutions”**, NACE, Corrosion, Vol.45, No.8, 1989.
  90. Kameswaran L., Gopalakrishnan S., M. Sukumar, (1974). **“Phenylthiocarbamide and Naringin Taste Threshold in South Indian Medical Students”**, Ind. J. Pharmac., 6 (3). 134
  91. Kostic S.Z., **“British corrosion Journal”**, 1, 22, (1987).
  92. Han J.N., Journal of the Korean Institute of Metals and Materials ,
  93. Al-Auasi B.O., Ph.D thesis, **“Heat, mass and momentum analogy to estimate corrosion rate under turbulent flow conditions”**, Al-Nahrain University, 2003.
  94. Holman J.P., **“Thermodynamics”**, forth edition, Mc.Graw.Hill, 1988.
  95. N. D. Tomashov, **“Theory of corrosion and protection of Metals”**, Coller-Macmillan Ltd., London, 1966.
  96. Mahato B. K., Cha C. Y., and Shemlit W., **“Corros. Sci.”**, Vol. 20, P. 421, 1980.
  97. Byan Poulson, **”Electrochemical measurements in flowing solutions”**, corrosion science, Vol.23, No.4, pp391-430, 1983
  98. Silverman D., **“Rotating culinder electrode for velocity sensitivity testing”**, corrosion 1983, paper No.258, NACE, Houston, TX (1983).
  99. Poulson P., Corrosion Sic. 23, 1983.
  100. Eisenberg M., Tobias C.W., C.R. Wilke. J.Electrochem. Soc. 101, 1954
  101. Silverman D., Corrosion J. pp42-49 (1988).

102. Cameron G.R, Chiu. A.S. “**Electrochemical techniques for corrosion inhibitor studies**” pp. 183-189, NACE (1986).
103. Levich V.G. Physico-Chemical Hydrodynamics. Prentice-Hall, Englewood Cliffs, NJ 1962
104. Shirkhan zadeh M., “**A Rotating Cylinder electrode for corrosion studies under controlled heat transfer conditions**”, NACE, Corrosion, 1987.
105. Heitz E., and Henkhaus R., “**Corrosion Science and Experimental Approach**”, Ellis Horwood Limited, 1992.
106. Al-Hadithy, F.F. ,Ph.D. Thesis ,Chemical Engineering Department , College of Engineering , Al-Nahrain University ,(2001).
107. Mansour E.Y., Ph.D. Thesis, “**Heat Transfer Through A Corroding Metal Wall of Concentric Tube Heat Exchanger**”, Al-Nahrain University,2005
108. kadhedm S., M.Sc Thesis, “**Analysis of Activation Controlled Galvanic Corrosion**”, Al-Nahrain University, 2004.
109. Al-Zaidy B.M., Ms.c, Thesis, “**Computer-aided Analysis of Galvanic Corrosion under Simultaneous Charge and Mass Transfer Control**”, 2005.
110. Perry, R. H ,and Green ,D. W ,Perry Chemical Engineers Handbook,7<sup>th</sup> ed, McGraw Hill ,United states ,1997
111. Holman J.P.,”**Heat Transfer**”, McGraw.Hill.Inc, Eighth Edition, 1997.
112. Brodkey R. S. and Hershey H. C., “**Transport Phenomena**”, 2<sup>nd</sup> Printing, Mc Graw Hill, New York, 1989.

:

.( ) -

( ) -

.( , , )

( / ) -

(0.15, 0.1, 0.05, 0.001, 0) Phenylthiourea (PHTU) -

, . /

(GF)

(Id)

/ , (PHTU)

.%

(AR)

(U)

.(PHTU)

:

$$\frac{i_d^B}{i_d^N} = \frac{A_c}{A_a} \left[ \frac{|i_c^N|}{i_d^N} - 1 \right] + \frac{|i_c^B|}{i_d^N}$$

ولكل حالة عند جهد  $E_{\text{coupling}}$  ،  $\sum I^c = \sum I^a$  ، و  $\sum I_g = 0$  .

الربط

قيمت النتائج المخبرية باستخدام تقنية تصحيح المنحنيات اللاخطية للمعادلات بطريقة

هوك-جيفس و كاوس نيوتن باستخدام البرنامج الاحصائي Statistical program

(package) والتي تعطي التيارات وفرق الجهد لكل ثنائي معدنين متأثرة بمتغيرات

:

(C)

(AR)

(U)

• ثنائي الكربون الفولاذي مع الخارصين:

$$E = -862.914 + 383.606(C) - 38.737(U) - 0.058(AR).$$

$$I_g = 10.726 - 71.41(C) + 0.006(U) + 2.032(AR) - 9.208 \left[ \frac{U}{U + C + AR} \right]^{5740.76}$$

• ثنائي النحاس مع الكربون الفولاذي:

$$E = -418.464 + 276.631(C) - 28.12(U) - 0.087(AR).$$

$$I_g = 4.373 - 32.092(C) + 0.005(U) + 0.553(AR) - 7.517 \left[ \frac{U}{U + C + AR} \right]^{2026.289}$$

• ثنائي النحاس مع الخارصين:

$$E = -831.346 + 376.643(C) - 30.549(U) - 0.055(AR).$$

$$I_g = 9.049 - 65.121(C) + 0.006(U) + 0.633(AR) - 3.457 \left[ \frac{U}{U + C + AR} \right]^{3159.814}$$



# شكر وتقدير

الْحَمْدُ لِلَّهِ عَلَى مَا أَنْعَمَ وَلَهُ الشُّكْرُ عَلَى مَا أَلْهَمَ وَالثَّنَاءُ بِمَا قَدَّمَ مِنْ عَمُومٍ نِعَمٍ ابْتَدَاهَا وَسَبَّوْغِ أَلَاءِ أَسْدَاهَا وَتَمَامِ مِنَّةِ أَوْلَاهَا .. وَالصَّلَاةُ وَالسَّلَامُ عَلَى سَيِّدِ الْأَنْبِيَاءِ أَبِي الْقَاسِمِ مُحَمَّدٍ وَآلِهِ الطَّيِّبِينَ الطَّاهِرِينَ وَصَحْبِهِ أَجْمَعِينَ.

أودُّ أن أقدم شكري وأمتناني إلى الأستاذ المشرف الدكتور قاسم جبار محمد سليمان وذلك لأرشاداته وتوصياته واقتراحاته القيمة طوال فترة البحث.

أتقدم بالشكر الجزيل إلى كادر قسم الهندسة الكيماوية التدريسي والأداري لإسهامهم في إظهار هذه الأطروحة بالشكل المناسب.

كما أتقدم بكل اجلالٍ واکرام بفائق الحب والتقدير إلى مرشدي ومعلمي الفاضل الأول والدي العزيز (رحمه الله) رافعاً إلى روحه الطاهرة هذا العمل المتواضع.

ولا أنسى أن أتقدم بفائق الشكر والأمتنان إلى من ساندني طوال فترة البحث بكل الحب والعطف إلى أحب من في الوجود أمي وجميع أفراد عائلتي فلهم جزيل الشكر والتقدير.

أقدم شكري وتقديري واحترامي إلى جميع زملائي لمساعدتهم لي بطريقة أو باخرى لانجاز هذا العمل.

شاكر صالح بحر عيدان الكلابي

نيسان ٢٠٠٧

رسالة

مقدمه إلى كلية الهندسة في جامعة النهرين وهي جزء من متطلبات  
نيل درجة دكتوراه فلسفة في الهندسة الكيمياوية

من قبل

(بكالوريوس ٢٠٠٠)

(ماجستير ٢٠٠٣)

وذلك في

١٤٢٨ هـ

٢٠٠٧ م

ربيع الاول

الموافق نيسان